ENHANCEMENT OF WALKING FOR INDIVIDUALS WITH TRANSFEMORAL AND THROUGH-KNEE AMPUTATIONS

INVERSE AND FORWARD DYNAMIC MUSCULOSKELETAL APPROACHES

Alice M Benton

This thesis is submitted for the degree of Doctor of Philosophy of Imperial College London.

Department of Bioengineering
Imperial College London
United Kingdom
January 2025

Acknowledgments

Thank you to my supervisors, Prof. Anthony Bull and Dr. Pouya Amiri, for their invaluable help and guidance throughout my PhD. I am also grateful to my colleagues in the MSK Mechanics Research Group for their support, encouragement, and collaboration, which made completing the PhD such an enjoyable experience. A special thanks to Diana for her guidance, and to Tiereny and Andra for the support as we completed the final stages of our PhD's together. Finally, thank you to my family and friends for their encouragement and support.

Thank you to all the participants of this study; this research would not have been possible without them. This work was supported by the UK Engineering and Physical Sciences Research Council (EPSRC) Grant EP/S02249X/1 for the Center for Doctoral Training in Prosthetics and Orthotics

Declaration of Originality

I declare that this project is entirely my own work, except where explicit reference is made to the work of others. To the best of my knowledge, the work is not plagiarised.

Copyright Declaration

The copyright of this thesis rests with the author. Unless otherwise indicated, its contents are licensed under a Creative Commons Attribution-Non Commercial 4.0 International Licence (CC BY-NC).

Under this licence, you may copy and redistribute the material in any medium or format. You may also create and distribute modified versions of the work. This is on the condition that: you credit the author and do not use it, or any derivative works, for a commercial purpose.

When reusing or sharing this work, ensure you make the licence terms clear to others by naming the licence and linking to the licence text. Where a work has been adapted, you should indicate that the work has been changed and describe those changes.

Please seek permission from the copyright holder for uses of this work that are not included in this licence or permitted under UK Copyright Law.

Abstract

Reduced muscular capacity increases the demand on the residual musculoskeletal system in individuals with bilateral transfemoral (BTF), bilateral through-knee (BTK), unilateral transfemoral (UTF), and unilateral through-knee (UTK) amputations, contributing to reduced walking endurance. Understanding muscle recruitment is critical for guiding rehabilitation strategies aimed at improving endurance and functionality. This thesis quantified muscle recruitment during walking using inverse dynamic musculoskeletal modelling, predicted gait modifications to reduce muscle demand through forward dynamic modelling, and tested these modifications using a biofeedback gait retraining system.

Two studies examined muscle recruitment during walking. The first involved individuals with BTF/BTK amputations (n=6) and found elevated activation in flexor muscles of the residual limb. The second compared those with UTF amputation (n=11) to able-bodied controls (n=11), identifying significantly greater force, impulse, and activation in the residual limb hip flexors($p \leq 0.05$), particularly in the iliacus and psoas major, indicating increased energy expenditure.

A third study introduced a forward dynamic musculoskeletal model, posed as an optimal control problem and solved via direct collocation. This model predicted gait modifications for individuals with UTF (n=3) and through-knee (n=1) amputations that reduced iliopsoas muscle demand. The most consistent modifications included decreased maximum hip extension, increased maximum hip flexion, and reduced step length.

A fourth study developed and evaluated two biofeedback systems providing audio-visual cues to promote these gait adjustments in individuals with UTF/UTK limb loss (n=6). While the systems successfully altered gait patterns in some cases, they did not consistently reduce iliopsoas recruitment. This suggests that changes in isolated kinematic features may be insufficient without broader gait adaptation. Overall, this thesis provides insight into the muscle recruitment of walking following lower-limb amputation and presents a methodological framework, of modelling-to-experimental implementation, which can guide future rehabilitation strategies.

Contents

1 Context of research **18**
- 1.1 Overview of problem statement and motivation . . . 19
  - 1.1.1 The population . . . 19
  - 1.1.2 Residual limb musculature . . . 20
  - 1.1.3 Rehabilitation and prosthetics . . . 21
  - 1.1.4 Musculoskeletal modelling . . . 22
- 1.2 Thesis aim and significance . . . 23
- 1.3 Thesis objectives . . . 23
- 1.4 Thesis outline . . . 23

2 Muscle recruitment during walking of individuals with bilateral transfemoral and through-knee amputations **25**
- 2.1 Introduction . . . 26
- 2.2 Methods . . . 28
  - 2.2.1 Participants . . . 28
  - 2.2.2 Data collection . . . 28
  - 2.2.3 Anatomical dataset . . . 29
  - 2.2.4 Subject-specific MSK modelling . . . 29
  - 2.2.5 Baseline gait simulations of individuals with BTF / BTK . . . 33
  - 2.2.6 Reduced muscular endurance gait simulations of individuals with BTF / BTK . . . 34
- 2.3 Results . . . 35
  - 2.3.1 Example plot . . . 35
  - 2.3.2 Characterising the muscle overloading . . . 35
  - 2.3.3 Reduced endurance simulation . . . 37
- 2.4 Discussion and conclusion . . . 38

3 Muscle recruitment during gait in individuals with unilateral transfemoral amputations due to trauma compared to able-bodied controls **42**
- 3.1 Introduction . . . 43
- 3.2 Methods . . . 45
  - 3.2.1 Particpants . . . 45
  - 3.2.2 Data collection . . . 46
  - 3.2.3 Musculoskeletal modelling . . . 48
  - 3.2.4 Data analysis and statistical testing . . . 51

3.3 Results . . . 53
3.3.1 Muscle recruitment during gait of individuals with UTF amputations 53
3.3.2 Gait features of individuals with UTF amputations . . . 59
3.4 Discussion and conclusion . . . 60
3.4.1 Muscle recruitment . . . 61
3.4.2 Kinematic and kinetic interpretation . . . 64
3.4.3 Limitations . . . 64
3.4.4 Comparison to the results of Chapter 2 . . . 65
3.4.5 Conclusion . . . 66

4 A forward dynamics model of unilateral transfemoral and through-knee amputations: a tool to propose novel rehabilitation methods 67
4.1 Introduction . . . 68
4.1.1 Motivation . . . 68
4.1.2 Background of modelling technique . . . 68
4.1.3 Aim and objective . . . 70
4.2 Method . . . 70
4.2.1 Participants . . . 70
4.2.2 The generic UTF model . . . 71
4.2.3 Subject specific UTF / UTK models . . . 78
4.2.4 Model adaptations for optimal control (forward dynamic) simulations 79
4.2.5 Data collection . . . 80
4.2.6 Simulations and data processing . . . 81
4.3 Results . . . 87
4.3.1 Inverse kinematics, inverse dynamics and static optimisation . . . 87
4.3.2 Tracking results . . . 91
4.3.3 'Enhanced' walking simulations . . . 99
4.4 Discussion and conclusion . . . 112
4.4.1 Validation of the UTF and UTK model . . . 112
4.4.2 Baseline tracking simulations . . . 112
4.4.3 Emerging walking modifications in the 'enhanced' walking iteration simulations . . . 114
4.4.4 Subject- specific modelling . . . 116
4.4.5 Limitations . . . 116
4.4.6 Future direction . . . 118

5 A biofeedback gait retraining tool for enhanced walking in individuals with unilateral transfemoral and through-knee amputations 119
5.1 Introduction . . . 120
5.1.1 Background . . . 120
5.1.2 Aims and objectives . . . 121
5.2 Method . . . 122
5.2.1 Participants . . . 122
5.2.2 Data collection . . . 123
5.2.3 Data processing and analysis . . . 127

5.3 Results . . . 129
5.3.1 Preliminary Study 1: overground vs. treadmill walking kinematics 129
5.3.2 Preliminary Study 2: EMG validation of Freebody for individuals with unilateral and through-knee amputations . . . 132
5.3.3 Aim 1: could the 'extension goal' and 'step goal' be successfully followed? . . . 137
5.3.4 Aim 2: effect on iliopsoas recruitment . . . 145
5.3.5 Aim 3: kinematic strategies of achieving goals . . . 148
5.3.6 Questionnaire results . . . 158
5.4 Discussion and conclusion . . . 164
5.4.1 Validation of methods . . . 164
5.4.2 Effectiveness of the interface design . . . 164
5.4.3 Clinical significance of the spatial modifications . . . 165
5.4.4 Effect of kinematic and spatial modifications in iliopsoas recruitment 165
5.4.5 Kinematic strategies to achieve goals . . . 167
5.4.6 Interpretation of Chapter 4 results . . . 168
5.4.7 Future direction . . . 169
5.4.8 Limitations . . . 170
5.4.9 Conclusion . . . 171

6 Conclusion 172
6.1 Summary of thesis results . . . 173
6.2 Thesis discussion . . . 174
6.2.1 Discussion of methods . . . 174
6.2.2 Biofeedback development . . . 179
6.2.3 Implication on prosthetic design . . . 180
6.2.4 Alternative methods for rehabilitation improvement . . . 180
6.2.5 Broader context - demographic and access . . . 181
6.2.6 Future work . . . 182
6.2.7 Closing remarks . . . 183

Appendices 184

A Chapter 4: Iteration 1 results 185

B Chapter 5: Biofeedback demonstration slide deck 188

C Chapter 5: Perceived effort questionnaire - extension goal 194

D Chapter 5: Perceived effort questionnaire - step goal 197

E Chapter 5: EMG validation - trial 2-3 200

F Chapter 5: Iliospoas force following 'extension goal' - participants 03 and 05 209

G Chapter 5: Iliospoas force following 'step goal' - participants 03, 05 and 06 **211**

H List of publications and conference presentations **213**
H.1 List of publications 213
H.2 List of conference presentations 213

List of Figures

2.1 Participant with markers attached for data collection 29
2.2 Muscle elements in the FreeBody MSK model of one participant with a through-knee amputation (Toderita et al. 2021) 31
2.3 Anatomy of one participant with bilateral through-knee and transfemroal amputation: left displays the 3D reconstruction of bones and muscles, the right displays the muscles line of action (red line), the centre of hip rotation (yellow dot) and wrapping object (yellow cylinder) (Toderita et al. 2021) 32
2.4 Muscle activations (force normalized to F^i_{max}) over a gait cycle for left limb of participant 02. Muscles are grouped by primary function: flexors, extensors, abductors, and adductors 35
2.5 Maximum muscle activation (force normalized to F^i_{max}) during gait cycle of the 6 individuals with bilateral transfemoral and through-knee amputations. Muscles are categorized as hip flexors, extensors, abductors, and adductors. The box plots show min, max, median, 25 and 75 percentiles, and the outliers. Each participant is plotted in a separate colour, and the left legs are represented by '◁' and right by '▷' (n=12) 36
2.6 Maximum muscle force normalized to body weight (BW) during gait cycle of the 6 individuals with bilateral transfemoral and through-knee amputations. Muscles are categorized as hip flexors, extensors, abductors, and adductors. The box plots show min, max, median, 25 and 75 percentiles, and the outliers. Each participant is plotted in a separate colour, and the left legs are represented by '◁' and right by '▷' (n=12) 36
2.7 Normalized muscle force of the left limb of participant 02 for baseline and reduced endurance (RE) condition gait trial (reduce force capacity of the psoas major and adductor longus) 37
2.8 Maximum muscle activation (force/F^i_{max}) over a gait cycle for the participant limbs where a full solution could be found in the reduced endurance simulations (baseline in red, reduced endurance state in blue). Baseline values are plotted for only legs for which a feasible solution could be found in the reduced endurance state (n=7). A reduced endurance state simulated by a reduction in the maximum capacity of the psoas major and the adductor longus is shown. Muscles are grouped into primary function; p values are presented on a plot for significant difference between the means of baseline and the reduced endurance condition 38

3.1 Participant with markers attached for data collection 48
3.2 Muscle elements lines-of-action in pink, patella ligament in blue and wrapping objects in green defined, for the iliopsoas and gastrocnemius, for the intact and able-bodied limb models (Ding et al. 2019) 50
3.3 Maximum normalised muscle force box plots of major hip muscles grouped by primary function (min, max, median, 25 and 75 percentiles and outliers). Significant p-values displayed. The muscles are grouped by primary function. Red represents the residual limb group (n = 11) of the individuals with UTF ("R"), blue represents the intact limb group (n = 10) of individuals with UTF ("I") and black represents the able-bodied limb group (n = 22) ("AB") 55
3.4 Muscle force normalised to bodyweight of major hip muscles over gait cycle. Red represents the residual limb group (n = 11 ± SD) of the individuals with UTF, blue represents the intact limb group (n = 10 ± SD) of individuals with UTF and black represents the able-bodied limb group (n = 22 ± SD). Arrows and "*" indicate a significant difference in peak value 56
3.5 Left: muscle force normalised to bodyweight of the plantar flexors over the gait cycle. Blue represents the intact limb group (n = 10 ± SD) and black represents the able-bodied limb group (n = 22 ± SD). Right: Statistical parametric mapping results 57
3.6 Muscle impulse box plots of major hip muscles grouped by primary function (min, max, median, 25 and 75 percentiles and outliers). Significant p-values displayed. Red represents the residual limb group (n = 11) of the individuals with UTF ("R"), blue represents the intact limb group (n = 10) of individuals with UTF ("I") and black represents the able-bodied limb group (n = 22) ("AB") 58
3.7 Muscle peak activation box plots of major hip muscles grouped by primary function (min, max, median, 25 and 75 percentiles and outliers). Significant p-values displayed. Red represents the residual limb group (n = 11) of the individuals with UTF ("R"), blue represents the intact limb group (n = 10) of individuals with UTF ("I") and black represents the able-bodied limb group (n = 22) ("AB") 59
3.8 Kinetic and kinematic parameters over gait cycle from initial foot contact (0%–100%) for the residual limb group (red, n = 11 ± SD), the intact limb group (blue, n = 10 ± SD) and the able-bodied control limb group (black, n = 22 ± SD). Solid line represents mean and shaded standard deviation. Arrows and '*' indicate a significant difference in peak value. 60
3.9 The iliopsoas, adductor longus, tensor fasciae latae and pectineus muscles on an able-bodied individual, edited from Schwartzman & Ramamurti (2021) 62

4.1 OpenSim transfemoral amputee model 72
4.2 A Hill- type muscle actuator schematic (De Groote et al. 2016) 72
4.3 Muscle insertion for the unilateral through-knee participant 78
4.4 Muscle- tendon characteristics of 'DeGrooteFregly2016' muscles (De Groote et al. 2016) 79

4.5 Plantar surface of the generic UTF model with contact spheres 80
4.6 Hip, knee and ankle joint angles (left) and torques (right) for residual limb (red) and intact limb (blue) of participant 01 87
4.7 Hip, knee and ankle joint angles (left) and torques (right) for residual limb (red) and intact limb (blue) of participant 02 88
4.8 Hip, knee and ankle joint angles (left) and torques (right) for residual limb (red) and intact limb (blue) of participant 03 88
4.9 Hip, knee and ankle joint angles (left) and torques (right) for residual limb (red) and intact limb (blue) of participant 04 89
4.10 Muscle activations of the main hip muscles of the residual limb (red) and intact limb (blue) of participant 01 89
4.11 Muscle activations of the main hip muscles of the residual limb (red) and intact limb (blue) of participant 02 90
4.12 Muscle activations of the main hip muscles of the residual limb (red) and intact limb (blue) of participant 03 90
4.13 Muscle activations of the main hip muscles of the residual limb (red) and intact limb (blue) of participant 04 91
4.14 Hip, knee and ankle kinematics of the residual limb and intact limb from the tracking simulations (blue) and the inverse kinematics (black- dashed) for particpant 01 92
4.15 Hip, knee and ankle kinematics of the residual limb and intact limb from the tracking simulations (blue) and the inverse kinematics (black- dashed) for particpant 02 92
4.16 Hip, knee and ankle kinematics of the residual limb and intact limb from the tracking simulations (blue) and the inverse kinematics (black- dashed) for particpant 03 93
4.17 Hip, knee and ankle kinematics of the residual limb and intact limb from the tracking simulations (blue) and the inverse kinematics (black- dashed) for particpant 04 93
4.18 Predicted ground reaction force (blue) and recorded ground reaction force (black dashed) for participant 01 94
4.19 Predicted ground reaction force (blue) and recorded ground reaction force (black dashed) for participant 02 94
4.20 Predicted ground reaction force (blue) and recorded ground reaction force (black dashed) for participant 03 95
4.21 Predicted ground reaction force (blue) and recorded ground reaction force (black dashed) for participant 04 95
4.22 Predicted muscle activations of the gluteus maximus, the gluteus medius, hamstrings, iliopsoas, rectus femoris and adductor longus of the residual limb (red) and intact limb (blue) from the tracking simulations (solid) and static optimisations (dashed line) for participant 01 96
4.23 Predicted muscle activations of the gluteus maximus, the gluteus medius, hamstrings, iliopsoas, rectus femoris and adductor longus of the residual limb (red) and intact limb (blue) from the tracking simulations (solid) and static optimisations (dashed line) for participant 02 97

4.24 Predicted muscle activations of the gluteus maximus, the gluteus medius, hamstrings, iliopsoas, rectus femoris and adductor longus of the residual limb (red) and intact limb (blue) from the tracking simulations (solid) and static optimisations (dashed line) for participant 03 97
4.25 Predicted muscle activations of the gluteus maximus, the gluteus medius, hamstrings, iliopsoas, rectus femoris and adductor longus of the residual limb (red) and intact limb (blue) from the tracking simulations (solid) and static optimisations (dashed line) for participant 04 98
4.26 Impulse of iliopsoas muscle of the residual limb in baseline and iterations of 'enhanced walking' for participant 01 100
4.27 Impulse of iliopsoas muscle of the residual limb in baseline and iterations of 'enhanced walking' for participant 02 100
4.28 Impulse of iliopsoas muscle of the residual limb in baseline and iterations of 'enhanced walking' for participant 03 101
4.29 Impulse of iliopsoas muscle of the residual limb in baseline and iterations of 'enhanced walking' for participant 04 101
4.30 The 'normal' gait kinematics exhibited by the baseline tracking simulations (above) and the 'abnormal' gait kinematics that are displayed by kinematics of iteration 1 (below) for participant 02 in the sagittal plane 102
4.31 The 'normal' gait kinematics exhibited by the baseline tracking simulations (above) and the 'abnormal' gait kinematics that are displayed by kinematics of iteration 1 (below) for participant 02 in the frontal plane . 103
4.32 Hip, knee and ankle kinematics of the residual limb and intact limb of baseline, iteration 2 for participant 01 104
4.33 Hip, knee and ankle kinematics of the residual limb and intact limb of baseline, iteration 2, iteration 3.0 , iteration 3.1, iteration 3.2, iteration 3.3 for participant 02 104
4.34 Hip, knee and ankle kinematics of the residual limb and intact limb of baseline, iteration 2, iteration 3.0, iteration 3.1, iteration 3.2, iteration 3.3 for participant 03 105
4.35 Hip, knee and ankle kinematics of the residual limb and intact limb of baseline, iteration 2, iteration 3.0, iteration 3.1, iteration 3.3 for participant 04 105
4.36 Step length in baseline (B), iteration (1), iteration 2 (It 2), iteration 3.0 (It 3.0), iteration 3.1 (It 3.1), iteration 3.2 (It 3.2) and iteration 3.3 (It 3.3) 111
4.37 Step width in baseline (B), iteration (1), iteration 2 (It 2), iteration 3.0 (It 3.0), iteration 3.1 (It 3.1), iteration 3.2 (It 3.2) and iteration 3.3 (It 3.3) 112

5.1 Participant with reflective markers and EMG sensors attached for data collection protocol 124
5.2 Diagram of the visual interface for the 'Extension goal' 125
5.3 Diagram of the visual interface for the 'Step goal' 126

5.4 Kinematics and SPM results of overground baseline walking (black) and treadmill baseline walking (red) at self-selected speeds of the residual limb side of participants with unilateral transfemoral and through-knee amputation (N=6) . . . 130
5.5 Kinematics and SPM results of overground baseline walking (black) and treadmill baseline walking (blue) at self-selected speeds of the intact limb side of participants with unilateral transfemoral and through-knee amputations (N=6) . . . 131
5.6 EMG (grey – dashed) and muscle activation (black – solid) of the intact limb of participant 01, trial 1 . . . 133
5.7 EMG (grey – dashed) and muscle activation (black – solid) of the intact limb of participant 02, trial 1 . . . 133
5.8 EMG (grey – dashed) and muscle activation (black – solid) of the intact limb of participant 03, trial 1 . . . 134
5.9 EMG (grey – dashed) and muscle activation (black – solid) of the intact limb of participant 04, trial 1 . . . 134
5.10 EMG (grey – dashed) and muscle activation (black – solid) of the intact limb of participant 05, trial 1 . . . 135
5.11 EMG (grey – dashed) and muscle activation (black – solid) of the residual limb gluteus maximus of participant 01, trial 1 . . . 136
5.12 EMG (grey – dashed) and muscle activation (black – solid) of the residual limb gluteus maximus of participant 02, trial 1 . . . 136
5.13 EMG (grey – dashed) and muscle activation (black – solid) of the residual limb gluteus maximus of participant 03, trial 1 . . . 137
5.14 The maximum extension angle over a gait cycle for baseline treadmill gait and when following the 'extension goal' of the residual limb of participants with unilateral transfemoral and through-knee amputations (N=6) . . . 138
5.15 The average stride length for baseline treadmill gait and when following the 'step goal' of participants with unilateral transfemoral and through-knee amputations (N=6) . . . 138
5.16 Sagittal hip kinematics of the residual limb (left) and maximum extension angle (right) for baseline treadmill walking (black) and walking while following 'extension goal' (red) over 6 trials for participant 01. P value and difference between means displayed. . . . 139
5.17 Sagittal hip kinematics of the residual limb (left) and maximum extension angle (right) for baseline treadmill walking (black) and walking while following 'extension goal' (red) over 6 trials for participant 02. P value and difference between means displayed. . . . 140
5.18 Sagittal hip kinematics of the residual limb (left) and maximum extension angle (right) for baseline treadmill walking (black) and walking while following 'extension goal' (red) over 6 trials for participant 03. P value and difference between means displayed. . . . 140

5.19 Sagittal hip kinematics of the residual limb (left) and maximum extension angle (right) for baseline treadmill walking (black) and walking while following 'extension goal' (red) over 6 trials for participant 04. P value and difference between means displayed. 141
5.20 Sagittal hip kinematics of the residual limb (left) and maximum extension angle (right) for baseline treadmill walking (black) and walking while following 'extension goal' (red) over 6 trials for participant 05. P value and difference between means displayed. 141
5.21 Sagittal hip kinematics of the residual limb (left) and maximum extension angle (right) for baseline treadmill walking (black) and walking while following 'extension goal' (red) over 6 trials for participant 06. P value and difference between means displayed. 142
5.22 Stride length in baseline treadmill walking and walking while following 'step goal' (6 trials) for participant 01. P-value and difference between means displayed. 142
5.23 Stride length in baseline treadmill walking and walking while following 'step goal' (6 trials) for participant 02. P-value and difference between means displayed. 143
5.24 Stride length in baseline treadmill walking and walking while following 'step goal' (6 trials) for participant 03. P-value and difference between means displayed. 143
5.25 Stride length in baseline treadmill walking and walking while following 'step goal' (6 trials) for participant 04. P-value and difference between means displayed. 144
5.26 Stride length in baseline treadmill walking and walking while following 'step goal' (6 trials) for participant 05. P-value and difference between means displayed. 144
5.27 Stride length in baseline treadmill walking and walking while following 'step goal' (6 trials) for participant 06. P-value and difference between means displayed. 145
5.28 Iliopsoas force (/BW) and impulse (/BW) of the residual limb hip for participant 02, and the maximum iliopsoas force (/BW) over the six trials of baseline treadmill walking and walking while following 'extension goal'. P values displayed. 146
5.29 Iliopsoas force (/BW) and impulse (/BW) of the residual limb hip for participant 01, and the maximum iliopsoas force (/BW) over the six trials of baseline treadmill walking and walking while following 'step goal'. P values displayed. 147
5.30 Iliopsoas force (/BW) and impulse (/BW) of the residual limb hip for participant 02, and the maximum iliopsoas force (/BW) over the six trials of baseline treadmill walking and walking while following 'step goal'. P values displayed. 147

5.31 Iliopsoas force (/BW) and impulse (/BW) of the residual limb hip for participant 04, and the maximum iliopsoas force (/BW) over the six trials of baseline treadmill walking and walking while following 'step goal'. P values displayed. 148
5.32 Kinematics and SPM results of baseline treadmill walking and walking while following 'extension goal' at the same self-selected speed of the residual limb side of participant 02 149
5.33 Kinematics and SPM results of baseline treadmill walking and walking while following 'extension goal' at the same self-selected speed of the intact limb side of participant 02 150
5.34 Kinematics and SPM results of baseline treadmill walking and walking while following 'extension goal' at the same self-selected speed of participant 03 151
5.35 Kinematics and SPM results of baseline treadmill walking and walking while following 'extension goal' at the same self-selected speed of participant 03 152
5.36 Kinematics and SPM results of baseline treadmill walking and walking while following 'extension goal' at the same self-selected speed of the residual limb side of participant 05 153
5.37 Kinematics and SPM results of baseline treadmill walking and walking while following 'extension goal' at the same self-selected speed of the intact limb side of participant 05 154
5.38 Kinematics and SPM results of baseline treadmill walking and walking while following 'step goal' at the same self-selected speed of the residual limb side of participants with unilateral transfemoral and through-knee amputations (N=6) 156
5.39 Kinematics and SPM results of baseline treadmill walking and walking while following 'step goal' at the same self-selected speed of the intact limb side of participants with unilateral transfemoral and through-knee amputatiosn (N=6) 157
5.40 Extension torque force of the residual limb participant 02 in baseline (black), 'extension goal' (red) and 'step goal' (blue) conditions. 166
5.41 Vertical ground reaction force of the residual limb of participant 02 in baseline (black), 'extension goal' (red) and 'step goal' (blue)conditions. . 167

6.1 Schematic of the contact force provided by ischial containment sockets, edited from (Lee et al. 1997) 177

A.1 Iteration 1 results participant 01 for the residual and intact limbs 185
A.2 Iteration 1 results participant 02 for the residual and intact limbs 186
A.3 Iteration 1 results participant 03 for the residual and intact limbs 186
A.4 Iteration 1 results participant 04 for the residual and intact limbs 187

E.1 EMG validation intact limb participant 01 trial 02 200
E.2 EMG validation intact limb participant 01 trial 03 201
E.3 EMG validation intact limb participant 02 trial 02 201

E.4 EMG validation intact limb participant 02 trial 03 202
E.5 EMG validation intact limb participant 03 trial 02 202
E.6 EMG validation intact limb participant 03 trial 03 203
E.7 EMG validation intact limb participant 04 trial 02 203
E.8 EMG validation intact limb participant 04 trial 03 204
E.9 EMG validation intact limb participant 05 trial 02 204
E.10 EMG validation intact limb participant 05 trial 03 205
E.11 EMG validation residual limb participant 01 trial 02 205
E.12 EMG validation residual limb participant 01 trial 03 206
E.13 EMG validation residual limb participant 02 trial 02 206
E.14 EMG validation residual limb participant 02 trial 03 207
E.15 EMG validation residual limb participant 03 trial 02 207
E.16 EMG validation residual limb participant 03 trial 03 208

F.1 Iliopsoas force (/BW) and impulse (/BW) of the residual limb hip for an individual with through-knee amputation (participant 03), and the maximum iliopsoas force (/BW) over the six trials of baseline treadmill walking and walking while following 'extension goal'. P values displayed. 209
F.2 Iliopsoas force (/BW) and impulse (/BW) of the residual limb hip for an individual with through-knee amputation (participant 05), and the maximum iliopsoas force (/BW) over the six trials of baseline treadmill walking and walking while following 'extension goal'. P values displayed. 210

G.1 Iliopsoas force (/BW) and impulse (/BW) of the residual limb hip for an individual with through-knee amputation (participant 03), and the maximum iliopsoas force (/BW) over the six trials of baseline treadmill walking and walking while following 'step goal'. P values displayed. 211
G.2 Iliopsoas force (/BW) and impulse (/BW) of the residual limb hip for an individual with through-knee amputation (participant 05), and the maximum iliopsoas force (/BW) over the six trials of baseline treadmill walking and walking while following 'step goal'. P values displayed. 212
G.3 Iliopsoas force (/BW) and impulse (/BW) of the residual limb hip for an individual with through-knee amputation (participant 06), and the maximum iliopsoas force (/BW) over the six trials of baseline treadmill walking and walking while following 'step goal'. P values displayed. 212

List of Tables

2.1 Participant details, TK = through-knee, TF= transfemoral, *calculated with Eq. 2.1 28
2.2 Optical motion tracking cluster and marker positions and labels 29

3.1 Study participant demographics (* calculated using Eq. 3.5; ** t-test between UTF participants and AB participants) 46
3.2 Optical motion tracking cluster and marker positions and labels 47
3.3 T-test results from the left and the right limbs of the able-bodied participants, significant p-values highlighted in grey 53

4.1 Participant information of the transfemoral (TF) and through-knee (TK) participants, *calculated following Eq.3.5 in Chapter 3 71
4.2 Body segments in the generic UTF model 73
4.3 Joints and joint definitions in the generic UTF model 74
4.4 Muscle in the generic UTF model 75
4.5 Optical motion tracking cluster and marker positions and labels 77
4.6 Interpretation of error margins from the Sprague and Geers metric (Klemt et al. 2019) 83
4.7 Weight given to objective function terms in 'enhanced walking' simulations 85
4.8 Summary of 'enhanced walking' iteration objectives 86
4.9 Combined error for participants 01-04 for the residual (R) and intact (I) limb, where blue indicates 'excellent' similarity, green 'very good', orange 'good', yellow 'moderate' and grey 'none' 98
4.10 Phase error for participants 01-04 for the residual (R) and intact (I) limb, where blue indicates 'excellent' similarity, green 'very good', orange 'good', and yellow 'moderate' 99
4.11 Magnitude error for participants 01-04 for the residual (R) and intact (I) limb, where blue indicates 'excellent' similarity, green 'very good', orange 'good', yellow 'moderate' and grey 'none' 99
4.12 Kinematic modifications from iterations of 2, 3.0, 3.1, 3.2 and 3.3 of enhanced walking with respect to baseline (ext = hip extension, flex = hip flexion, add = hip abduction, abd = hip abduction, int rot = internal hip rotation, ext rot = external hip rotation, k flex = knee flexion, plant flex = ankle planter flexion, dors flex = ankle dorsiflexion) 106

5.1 Participant information 123

5.2 Optical motion tracking cluster and marker positions and labels 124
5.3 Interpretation of error margins from the Sprague and Geers metric (Klemt et al. 2019) 128
5.4 Sprague and Geers measures of error of EMG signal compared to estimated muscle activations for the intact limb of participants with unilateral transfemoral and through-knee amputations (N=5) 132
5.5 Sprague and Geers measures of error of EMG signal compared to estimated muscle activations for the residual limb of participants with unilateral transfemoral and through-knee amputations (N=3) 135
5.6 Question 1 158
5.7 Question 2 159
5.8 Question 3 159
5.9 Question 4 160
5.10 Question 8 160
5.11 Question 1 161
5.12 Question 2 161
5.13 Question 3 162
5.14 Question 4 162
5.15 Question 8 163

List of abbreviations

TF Transfemoral
TK Through-knee
BTF Bilateral transfemoral
BTK Bilateral through-knee
UTF Unilateral transfemoral
UTK Unilateral through-knee
MVC Maximum voluntary contraction
MSK Musculoskeletal
MPK Microprocessor prosthetic knee
RMS Root mean square
RMSE Root mean square error
RMSD Root mean square difference
BW Body weight
GRF Ground reaction force
RoM Range of motion
CoM Centre of mass
Add Adductor
add Adduction
Abd Abductor
abd Abduction
flex Flexion
k flex Knee flexion
int rot Internal rotation
ext rot External rotation
plant flex Plantar flexion
dors flex Dorsiflexion
It Iteration
FES Functional electrical stimulation
SPM Statistical parametric mapping
3D Three dimensional
2D Two dimensional
WHO World Health Organization

Chapter 1

Context of research

This chapter provides the background for this research and outlines the thesis aims, objectives, and overall structure.

1.1 Overview of problem statement and motivation

1.1.1 The population

Traumatic amputation, amputation sustained from accident or injury, is a life changing incident in an individual's life that requires an interdisciplinary team to manage the rehabilitation successfully (Jorge 2020)(Kaur et al. 2021). Traumatic surgeries are more likely to be performed on individuals who are younger and otherwise healthy, compared to amputation associated with diabetes or peripheral artery disease (Milosevic et al. 2024) (NHS-England 2016). Therefore, individuals who have sustained an amputation due to trauma are likely to live longer and more active lives with their amputation (Jorge 2020), incorporating their prosthetic devices into their everyday life and ambitions (Gailey et al. 2008). According to the 2019 Global Burden of Diseases study, there was a reported 25.6 million individuals living with unilateral traumatic lower-limb amputation and 5.97 million with bilateral traumatic lower-limb amputation. There was double the number of male individuals with any type of traumatic amputation than female, and exposure to mechanical force and falls were the leading cause for all traumatic amputation (Yuan et al. 2023). Road injury and accidents are another worldwide leading cause of traumatic amputation (McDonald et al. 2021).

In a military context, advancements in medicine and trauma care have improved survival rates for injuries that were once fatal, although now they may result in amputation (Ladlow et al. 2015). The UK military population sustained a 416 amputations across 265 individuals during the years from 2003 to 2014, with the highest incidence being transfemoral amputation which was sustained by 153 individuals (Edwards et al. 2015). Individuals who have sustained amputation while serving in the UK military will have experienced comprehensive rehabilitation, likely to have high levels of fitness prior to the amputation and access to state-of-the-art prosthetic provision. Jarvis et al. (2021) (2017) have demonstrated how these individuals can be considered a model of 'high-functionality' compared to a more general population (Jarvis et al. 2021) (Jarvis et al. 2017).

Individuals with lower limb amputation are more likely to experience secondary musculoskeletal conditions due to loading conditions induced by the compensatory strategies required for gait. These comorbidities include osteoarthritis, osteopenia / osteoporosis and lower back pain (Gailey et al. 2008) (Farrokhi et al. 2018). Additionally, there are psychological and social challenges associated with societal participation (Keeves et al. 2023), and an increased risk of depression and anxiety in this population (Mckechnie & John 2014) (Lindner et al. 2020). These physical and psychological secondary conditions are detrimental to quality of life for individuals living with traumatic lower limb amputation (Mazzone et al. 2020).

1.1.2 Residual limb musculature

A transfemoral (TF) amputation, also known as an above-knee amputation, and a through-knee (TK) amputation, also referred to as a knee disarticulation, both result in the loss of the ankle and knee joints along with their associated muscles and tendons.

There are two main surgical techniques when managing the soft tissue in TF amputation surgery: myoplasty and myodesis. Myoplasty is where the residual muscles are sutured to their agonistic pair over the end of the residual femur, however, with this method there is a risk of loss in muscle tension. Myodesis, where the residual muscle is directly sutured to the end of the femur, is considered the preferable method as it increases functionality of the residual muscles and therefore reduces muscle atrophy (Jorge 2020). It is essential that the adductor magnus, the rectus femoris and the hamstrings are re-attached to balance motion at the hip. The adductor magnus has been found to be particularly critical in maintaining an adducted position which reduces energy expenditure (Gottschalk 1999)(Gottschalk & Stills 1994). The initial tension of the re-attached muscle directly effects its capacity to generate force which is essential in retaining muscle function (Ranz et al. 2017).

Skeletal muscle tissue adapts to stimulation as to enhance performance of the function most consistently demanded of it. In endurance training hypertrophy occurs; the increased activity levels induce increased strength, mass, and reduced fatigability. In contrast, chronic inactivity will lead to muscle atrophy, manifesting in the opposite effects (Bogdanis 2012). In the residual limb atrophy and hypertrophy induced by changes in muscle recruitment during gait and the direct effects of the re-insertion surgery will lead to changes in tissue quality and volume. For example, the adoption of compensatory strategies leading to hypertrophy in individuals with TK / TF amputation is demonstrated by Henson et al. (2021) who measured volume changes and found an increase in volume in adductor brevis, the iliopsoas and gluteas medius. These muscles are respectively key adductors, flexors and abudctors of the hip and all normally preserved in the TF amputation surgery. This study suggests an increased level of recruitment of these muscles during walking in this group of inviduals with bilateral TF /TK amputations (Henson et al. 2021). Henson et al. (2021) also found reduced volume in the muscles which typically insert distally to the site of TF amputation surgery and therefore are re-attached (ie. the rectus femoris, the sartorius, the gracilis, the vastii, the bicep femoris, the semitendinosus and the semimembranosus). Out of these, the vastii muscles experience the greatest level of volume loss as they are functionaly redundant in the anatomy of the residual limb following transfemoral amputation. The other muscles are somewhat still recruited, though it is apparent that the muscles which are originally biarticular, are recruited to a lesser degree in their monoarticular state with the loss of the knee joint (Henson et al. 2021). In addition to changes in muscle recruitment, the surgical procedure of reattachment to a non-physiological site is another mechanism of atrophy (Fraisse et al. 2008) as there is a loss in tensioning ability (Sherk et al. 2010). Muscle atrophy occurs particularly in the distal end of the residual limb (Putz et al. 2017). MRI imaging can be used to identify the fatty degeneration which occurs in the residual tissue

and is associated with muscle atrophy (Henson et al. 2021). An MRI study concluded that the muscles which have been re-attached or dis-attached are more prone to fatty degeneration (Putz et al. 2017). Muscle atrophy decreases the maximum force potential of a muscle, though the maximum force potential does not change proportionally to muscle volume due to physiological changes in architecture and contractile properties (Sibley et al. 2020). Muscle atrophy therefore makes it harder to predict the maximum force potential of a muscle.

1.1.3 Rehabilitation and prosthetics

Rehabilitation of individuals traumatic TF / TK amputations consists of physical training (walking and strength training), and the use of prosthetic devices. Relative high-functionality can be achieved as demonstrated by Jarvis et al. (2017). Traditionally a TF / TK prosthetic consists of a socket, liner, suspension system, prosthetic knee, pylon and prosthetic foot. Transfemoral sockets tend to be quadrilateral designs where there is a horizontal shelf which induces weight bearing through the ischium bone and gluteus muscles, or ischial containment designs where the socket fits snugly around the ischial tuberosity and ramus (Lee et al. 1997) to increase femur adduction and stabilise the ischium bone in the socket, or sub-ischial designs where the socket ends on the residual limb a few inches distal from the pelvis (Chui et al. 2019) (Brodie et al. 2022). Additionally, through-knee amputations allow for the use of end-bearing sockets which allows the individual to bear weight directly through the distal end of the residual limb. The liner and suspension system improve comfort of the residual limb and secure the socket during swing phase, commonly via suction suspension or belt suspension methods in individuals with TF amputation (Amudhan et al. 2022). Direct fixation of the prosthetic limb to the femur, or osteointegration, is an alternative method of suspension which has exhibited promising benefits (Vandenberg et al. 2023) (Gaffney et al. 2023). 'State-of-the-art' prosthetics referred to earlier in this chapter consist of microprocessor prosthetic knees (MPK) and dynamic response feet. Microprocessor knees such as the Genium (Ottobock, Germany) or the C-leg (Ottobock, Germany) have embedded sensors which inform and actuate variable damping at the knee joint, allowing for natural walking patterns. Dynamic response feet store energy during stance and release at push-off (Amudhan et al. 2022), example of these designs are the Triton (Ottobock, Germany) or Echelon (Blatchford, United Kingdom).

Human gait can be characterised by the transition of the body's centre of mass in a mechanism that has been likened to an inverted pendulum for the able-bodied population (Detrembleur et al. 2005) (Griffin et al. 2003). The partial loss of a lower limb reduces stability and sensory input. The central nervous system compensates for this loss, which manifests as adaptation to kinematics, kinetics (Jarvis et al. 2017) and muscle activity (Tatarelli et al. 2020). The loss of 'push-off' power, provided by the ankle planter flexors and Achilles tendon in an intact limb, increases the burden on the hip muscles for individuals with TF / TK amputation (Wentink et al. 2013) (Au & Herr 2008).

A 6-minute walking test is a measure of walking functionality. A study by Linberg

et al. (2013) compared 6-minute walking test scores between military personnel with and without lower limb amputation. The individuals with lower limb amputation performed significantly worse than the abled-bodied group, with the unilateral transfemoral group scoring 542 m and the bilateral transfemoral group scoring 452 m, compared to the able-bodied group who scored 761 m (Linberg et al. 2013). Jarvis et al. (2017) found that there was a 20% and 60% respective increase in oxygen cost while walking at a self-selected speed for military personnel with unilateral transfemoral (UTF) amputation and bilateral transfemoral (BTF) amputation compared to able-bodied military personnel. The reduced walking functionality, reduced endurance and increased cost of gait demonstrate the increased demand of walking for individuals with transfemoral amputation even for this military population group that can be considered a model of 'high functionality'.

1.1.4 Musculoskeletal modelling

Musculoskeletal modelling is a method to estimate muscle forces and joint loading, aspects of motion which that are not possible to obtain non-invasively. This thesis deals with both inverse dynamic and forward dynamic simulations of motion, ie. the prediction of internal forces from prescribed recorded motion, and the prediction of novel motion and internal forces. There are a variety of musculoskeletal methods that would be valid for these simulations, this is particularly true for the forward dynamic simulations. Two such differing approaches in forward dynamic modelling are trajectory optimisation methods such as optimal control and machine learning methods such as reinforcement learning (Uhlrich et al. 2023*a*), there disadvantages and benefits of both approaches. The optimal control method assumes motion of the musculoskeletal system is the output of an optimisation by the central nervous system and hence solves for parameters and time-varying controls of the musculoskeletal system subject to the dynamics as an optimal control problem. Whereas reinforcement learning is modelling the sensory-motor control of the central nervous system itself (Uhlrich et al. 2023*a*). This allows reinforcement learning models to interact with their environments, as a closed-loop model, and overall be a much more flexible, less constrained, method that can deal with more unknowns in simulations of motion. However, reinforcement learning methods are fundamentally trial and error, and do not utilise our understanding of the physical system. This contrasts to optimal control which works within the constraints of the differential equation. Considering the goals and scope of the forward dynamic's simulations, reinforcement learning was deemed unnecessary due to its higher computational cost and implementation complexity. As a result, an optimal control method was chosen for the purposes of Chapter 4 of this thesis.

OpenSim software is widely used within the biomechanics community, it was chosen for this reason. While widespread use does not necessarily imply it is the best option, it enhances scientific validity due to the volumes of validation studies (Miller & Esposito 2021) (Bianco et al. 2023) (Pariser & Higginson 2022) and the community support available to solve implementation challenges (Uhlrich et al. 2023*a*). OpenSim moco is opensource and customisable tool to implement optimal control simulations, making it appropriate for this project.

1.2 Thesis aim and significance

The broad aim of this thesis was to enhance rehabilitation outcomes and functional capacity for individuals who have undergone transfemoral or through-knee amputations due to trauma. This work specifically focuses on walking, a fundamental element of daily function and social inclusion, with the potential for these findings to be adapted for other forms of motion. While there are various ways to approach this broader aim, such as through epidemiological studies or qualitative investigations of personal rehabilitation experiences, this thesis adopts a biomechanical approach. Given that loading conditions within the musculoskeletal system significantly influence functionality and the risk of secondary conditions, a detailed biomechanical analysis of walking patterns, particularly an in-depth understanding of muscle function, is critical. This approach aimed to contribute to the development of rehabilitation that supports individuals in achieving an active lifestyle without compromising their future musculoskeletal health and overall improving quality of life.

1.3 Thesis objectives

The objectives of this thesis are to:

- quantify muscle recruitment and function in individuals with bilateral and unilateral transfemoral and through-knee amputation due to trauma using established inverse dynamic musculoskeletal modelling methods;
- develop a novel forward dynamic musculoskeletal model that allows for the prediction of motion as a tool to develop potential rehabilitation methods;
- test predictions of the forward dynamic musculoskeletal model utilising biofeedback methods for a potential gait retraining tool to improve walking endurance; and,
- demonstrate a methodological framework where inverse dynamic modelling is utilised to inform forward dynamic modelling to inform experimental rehabilitation methods for clinical translation in this population.

1.4 Thesis outline

This thesis is organised into six chapters.

Chapter 1 outlines the context, aims and objectives of the thesis.

Chapter 2 investigates muscle recruitment, endurance and function of individuals with bilateral transfemoral and through-knee amputation.

Chapter 3 investigates muscle recruitment and function of individuals with unilateral transfemoral amputation compared to able-bodied controls.

Chapter 4 develops and utilises a forward dynamic musculoskeletal model to predict walking patterns for 'enhanced' muscle recruitment for individuals with unilateral transfemoral and through-knee amputation.

Chapter 5 tests the feasibility of a gait retraining system using biofeedback methods informed by predictions made in Chapter 4.

Chapter 6 presents an overall discussion of the thesis, drawing on insights from across the chapters, discusses the limitations of the methods, and proposes the next steps for the research.

Chapter 2

Muscle recruitment during walking of individuals with bilateral transfemoral and through-knee amputations

In order to partly address the first objective of this thesis, this chapter quantified muscle recruitment during walking for individuals with bilateral TF and TK amputations. This chapter utilised subject-specific musculoskeletal modelling to estimate muscle forces and activations during recorded gait trials. To further investigate potential limiting factors of walking in individuals with bilateral TF and TK amputations, the muscles which appeared to be functioning above a 'healthy' level were identified, then walking with a state of reduced muscular endurance was simulated by reducing the maximum force potential of these muscles. If the recorded walking kinematics were still possible in this simulated state of reduced muscular endurance, the impact on the compensatory recruitment of the other muscles of the residual limb was observed.

This work was published in part as: 'Characterization of muscle recruitment during gait of bilateral transfemoral and through-knee persons with limb loss', with authors: Alice M Benton, Pouya Amiri, David P Henson, Biranavan Sivapuratharasu, Alison H. Mcgregor, Anthony MJ Bull. 2023. Frontiers in Bioengineering and Biotechnology, 11, 438.

2.1 Introduction

The partial loss of a lower-limb manifests as a loss in neuromusculoskeletal capacity. The central nervous system will adapt to this loss through the adoption of compensatory strategies which enable an individual with lower limb amputation to ambulate (Su et al. 2007) (Visser et al. 2011) (Hoffman et al. 1997) (Smith et al. 2021). Bilateral lower limb amputation is a less common yet more clinically challenging condition than unilateral. Individuals with bilateral lower limb amputation exhibit slower walking at higher metabolic/physiological cost than able-bodied and individuals with unilateral amputation (Su et al. 2007) (Visser et al. 2011) (Hoffman et al. 1997). Individuals with bilateral lower limb amputations have less ability to compensate for their missing limbs and therefore exhibit less efficient gait (Wright et al. 2008)(Wright et al., 2008). This metabolic inefficiency has been demonstrated by higher oxygen consumption, perceived exertion and 2-minute walk tests (Hoffman et al. 1997) (Wright et al. 2008). Perceived exertion incorporates the sensations of increased muscle fatigue, sweating, breathing rate and heart rate. It is a subjective measure but has been found to provide an adequate indicator of actual exercise intensity (Wright et al. 2008). Perceived exertion has a direct effect on a person's willingness to maintain active. In the general population a higher proportion of individuals with bilateral lower limb amputations resort to a wheelchair than unilateral, which is indicative of the difficulty of daily function (Wright et al. 2008) (Visser et al. 2011).

High levels of functionality for individuals with lower limb amputation is possible and has been observed in the ex-military population when comprehensive rehabilitation interventions were completed and state-of-the-art prosthetics used (Jarvis et al. 2021) (Jarvis et al. 2017) (Ladlow et al. 2015). However, gait remains more functionally demanding for individuals with bilateral transfemoral (BTF) amputations compared to able-bodied individuals (Hoffman et al. 1997), with lower scores found in 6-minute walking tests (Linberg et al. 2013) and higher metabolic cost during gait (Jarvis et al. 2017) in the young ex-military population.

Compensatory gait strategies, emerging as a result of amputation, mean the moment and power of the muscles spanning the hip are therefore higher during gait for individuals with bilateral amputations than in the able-bodied controls (Su et al. 2007) with hip muscle strength being crucial to walking ability (Visser et al. 2011). This will result in high muscle forces that lead to elevated hip joint contact forces (Su et al. 2007) (Wentink et al. 2013). Increased muscle activations place a large physiological demand on the muscle of the residual limb, likely increasing energy expenditure and having detrimental effect on endurance (Fang et al. 2007), rendering individuals with lower limb amputation less able to perform recreational activities and activities of daily living (Wong et al. 2015). However, how the compensatory gait strategies relate to specific muscle recruitment patterns is not known.

Muscular endurance is defined as the ability for a muscle to execute extended repetitions of muscle contractions (Kell et al. 2001). With repeated muscle contractions, as

occurs during walking, there will be a reduction in muscle performance, associated with a reduction in the muscle's ability to produce force (Van Geel et al. 2021). Experiments on isolated muscle cells demonstrate that contractions near maximum capacity induce a reduction in the magnitude of the force of the contractions (Bishop 2012). The reduction in maximum voluntary contraction (MVC) of intact muscles during tasks has been explained by metabolic accumulation and impaired motor control (Bishop, 2012). Muscular endurance of lower limb muscle during gait has been quantified for healthy subjects by an observed reduction in medium frequency of EMG signals (Fidalgo-Herrera et al. 2022). An experiment that implemented "fatigue protocols" on lower limb muscles, consisting of repeated sit- to-stand task, reported that muscle endurance affects spatiotemporal and kinematic features of gait in healthy subjects (Barbieri et al. 2013). These changes in gait characteristics increase the risk of falling (Mohd Safee & Abu Osman 2021) and localised tissue injury (Kumar 2001). High-intensity muscle forces will limit the functionality of individuals with lower-limb amputations, as they negatively affect lower-limb muscular endurance during gait (West et al. 1995).

Musculoskeletal (MSK) modelling enables muscle and articular contact forces to be estimated. Inverse dynamic MSK modelling uses the observed kinematics and ground reaction forces to determine the net forces and moments at the joints and uses an optimisation method to resolve the muscle force sharing. FreeBody is a segment based MSK model (Cleather & Bull 2011) that has been extensively validated for: muscle activations using EMG experimental data for individuals with BTF amputations (Toderita et al. 2021) and unilateral transtibial amputations (Ding et al. 2023); knee joint contact forces for osteoarthritis patients (Ding et al. 2016) and hip joint contact forces using instrumented implants (Amiri & Bull 2022).

Able-bodied walking is an optimised activity that minimises muscle recruitment (Crowninshield & Brand 1981). Therefore, this can provide a gold standard for development of muscle coordination strategies for improved endurance. The muscle activation can be estimated using experimental EMG data and normalized MVC. Healthy walking recruits lower limb muscles generally to below or up to 50 % of their MVC (Elsais et al. 2020) (Nishijima et al. 2010) (Burden et al. 2003) (Franz & Kram 2013) (Guan et al. 2019), with many values in the literature being considerably lower than 50 % . A range between 5 – 64 % has been reported for different muscles with an average value of 27 %. The demand of gait on individuals has also been quantified by net torque actuated across joints as a percentage of maximal torque capacity. Two studies have quantified maximal torque produced in hip flexion and hip extension for self-selected walking, one study quantified this value to be below 30 % in flexion and extension young adults (Anderson & Madigan 2014). The other found the percentage of maximum torque capacity produced during gait to be below 50 % in the hip flexors and below 35 % in the hip extensors for adults (Requiao et al. 2005). Both studies found that this metric of 'functional capacity utilized' increased with increased cadence.

Addressing the first objective of this thesis, which was to quantify muscle recruitment and function in individuals with transfemoral and through-knee amputationzs due to

trauma, the first aim in this chapter was to quantify the muscle forces in individuals with BTF / BTK amputations gait. The second aim was to determine the impact of reduced endurance, simulated by reducing specific muscle force capacities, on this group's ability to actuate their baseline kinematics and to identify potential compensatory muscle strategies. Both of these address the first and final objective of this thesis.

2.2 Methods

2.2.1 Participants

This study is focused on the young ex-military population as a model of highest potential functional outcome (Jarvis et al. 2021): they are young, have had comprehensive rehabilitation and are provided with state-of-the-art prosthetics. As lower limb anatomical and biomechanical factors are different between sexes, a mixed group should include equal numbers. This was not possible as this population has few females. Therefore, this study looked at only male participants. 6 male (aged 27-36 years) individuals with BTF / BTK amputation due to trauma were included in this study. All subjects were fitted with their own state-of-the-art prosthetics; dynamic response energy return prosthetic feet and microprocessor prosthetic knees. Subject details are presented in Table 2.1. Ethical approval was received from the Imperial College Research Ethics Committee and written informed consent obtained from the participants.

Table 2.1: Participant details, TK = through-knee, TF= transfemoral, *calculated with Eq. 2.1

Subject	Sex	Body mass with prosthetic (kg)	Calculated intact mass (kg)*	Age (years)	Height (cm)	Left side level, code	Right side level, code	Prosthetic foot	Prosthetic knee
1	Male	86.0	87.5	32	185	TK, 1L	TF, 1R	Triton	Genium
2	Male	81.2	84.7	27	178	TK, 2L	TF, 2R	Triton	Genium X3
3	Male	90.0	93.9	36	186	TK, 3L	TF, 3R	Triton	Genium X3
4	Male	89.5	96.8	33	182	TK, 4L	TK, 4R	Triton	Genium
5	Male	97.2	102.9	32	185	TK, 5L	TK, 5R	Triton	Genium X3
6	Male	68.8	70.8	31	171	TF, 6L	TF, 6R	Triton	Genium X3

2.2.2 Data collection

Three self-selected gait trials and one static calibration trial were collected per participant in a gait analysis laboratory consisting of a motion capture system with 10 cameras (VICON, Oxford Metrics Group, U.K.) and 2 force plates (Kistler Type 9286B, Kistler Instrumented AG, Winterthur, Switzerland). The marker 3D displacement and ground

reaction forces were sampled at 120, and 960 Hz, respectively. Reflective markers were attached to 14 anatomical landmarks, as listed in Table 2.2, on both the left and the right leg as well as two clusters of markers on the thigh and calf of both limbs as displayed in Figure 2.1.

Table 2.2: Optical motion tracking cluster and marker positions and labels

Marker label	Anatomical location
FCC	Calcaneus
FMT	Tuberosity of the fifth metatarsal
FM2	Head of the second metatarsal
TF	Additional marker placed on foot
FAM	Apex of the lateral malleolus
TAM	Apex of the medial malleolus
C1,C2,C3 (clusters)	Additional markers placed on the shank segment
FLE	Lateral femoral epicondyle
FME	Medial femoral epicondyle
T1,T2,T3 (clusters)	Additional markers placed on the thigh segment
RASIS	Right anterior superior iliac spine
LASIS	Left anterior superior iliac spine
RPSIS	Right posterior superior iliac spine
LPSIS	Left posterior superior iliac spine

includegraphics[]images/2.1.1.png

Figure 2.1: Participant with markers attached for data collection

2.2.3 Anatomical dataset

Anatomical datasets of all participants have previously been published (Toderita et al. 2021). In summary, these datasets were built from MRI scans acquired with a 3.0T MRI scanner (MAGNETOM Verio, Siemens, Germany) with a 3D T1-weighted spoiled gradient echo sequence set at a 450×450 mm^2 field of view, 1 mm slice thickness and 1.17×1.17 mm axial plane resolution. The scans were completed from the iliac crest to the distal end of the longest residuum, so an anatomical atlas could be constructed of the left and the right residual limb of each of the 6 participants (Toderita et al. 2021).

2.2.4 Subject-specific MSK modelling

The FreeBody v2.1 model (Cleather & Bull 2011) was utilised to quantify the muscle forces during the gait trials. FreeBody consists of four segments: the foot, shank, thigh, and pelvis, which are connected through the ankle, hip, and knee joints. The residuum, socket and liner are modelled as the thigh segment.

Anthropometric and body segment parameters

The anthropometric and body segment parameters were estimated using the following methods (Toderita et al. 2021). Mass, centre of mass and moments of inertia were derived with DeLeva calculations (De Leva 1996) for the pelvis using the estimated intact weight following Eq.2.1, where W_I is the estimated intact mass, w_a is the weight without the prosthetic device, $\sum \frac{\triangle W}{W_I}$ is an estimate of the percentage of bodyweight lost due to amputation derived from residuum lengths (Tzamaloukas et al. 1994). The residual limb length was measured from the MRI scans, from centre of hip rotation to the distal end of the residual limb. The mass of the residual limb was then obtained by quantifying the residual limb volume from the 3D geometry of the MRI scan, volume of soft tissue and bone were multiplied by the assumed density of soft tissue (1.03 g/cm^3) and bone (1.42 g/cm^3) (White et al. 1987). The residual limb length and mass was used to obtain the centre of mass and inertial properties of the residual limb with DeLeva calculations. The mass of the prosthetic components, socket (including liner), prosthetic knee and prosthetic foot, was measured. The centre of mass and inertial properties were measured with the reaction board method with moment of equilibrium (Smith et al. 2014). The mass of the composite socket-and residuum thigh segment was calculated by adding the mass of the residual limb and the mass of socket. The inertial properties of the composite socket-and-residuum thigh segment was calculated with the Huygens-Steiner parallel axis theorem using the measured socket values and the De Leva derived residuum values (from estimated residuum mass and length).

$$W_I = \frac{W_a}{1 - \sum \frac{\triangle W}{W_I}} \tag{2.1}$$

Musculature model

The MSK model of an individual with TF / TK contains 92 muscle elements, representing 21 muscles. The muscle elements are displayed in Figure 2.2 for one participant. The subject-specific geometry of muscle and bones were obtained from the MRI images, the details of which are outlined elsewhere (Toderita et al. 2021) and is described here briefly. For each leg, the MRI scans of the subject were used to render 3D shapes of bones and muscles. The 3D reconstruction of the pelvis, femur and muscles from the MRI scans are displayed in Figure 2.3 (left) for an example participant. Subsequently, following the methodology of Horsman et al. (2007), the muscle origins, insertion and via points, as well as hip joint rotation centre, and a cylindrical wrapping surface (to represent iliopsoas muscle elements actions along superior pubic ramus of pelvis) were digitized. The muscles line of action, the centre of hip rotation and the cylindrical wrapping surface are displayed in Figure 2.3 (right) for an example participant.

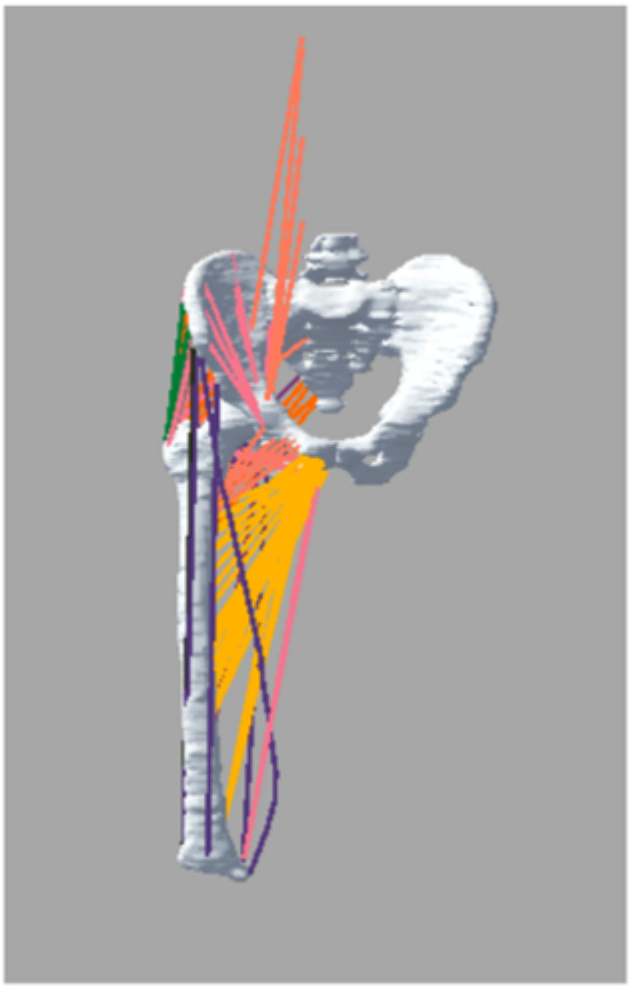


Figure 2.2: Muscle elements in the FreeBody MSK model of one participant with a through-knee amputation (Toderita et al. 2021)

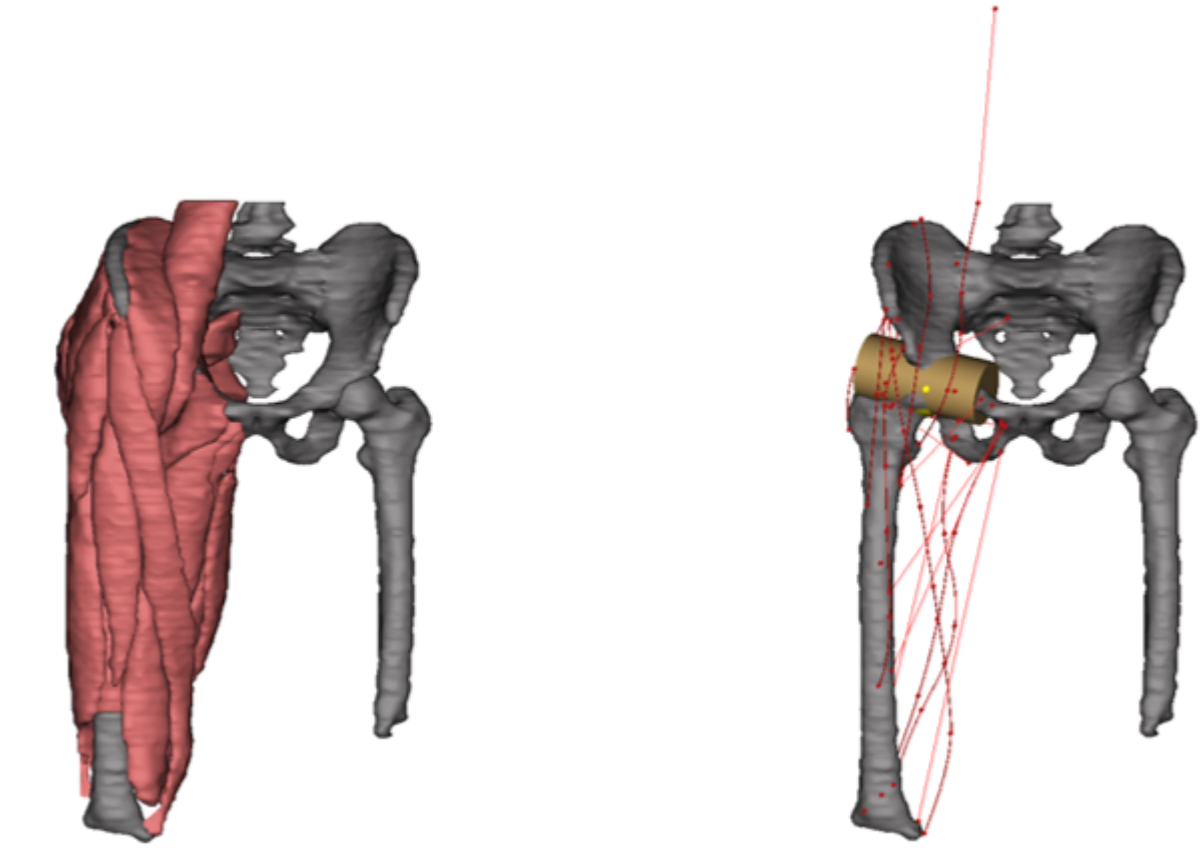


Figure 2.3: Anatomy of one participant with bilateral through-knee and transfemroal amputation: left displays the 3D reconstruction of bones and muscles, the right displays the muscles line of action (red line), the centre of hip rotation (yellow dot) and wrapping object (yellow cylinder) (Toderita et al. 2021)

The physiological cross-sectional area (PSCA) of each muscle was calculated using the following equation 2.2, where muscle volume (V_m) was acquired from rendered 3D geometry of the muscles, muscle length to its length ratio ($\frac{L_f}{L_m}$), pennation angle (θ) and optimal sarcomere length (L_s) were taken from in vivo cadervic studies in the literature. In the cases where there were no values found in the literature θ was set to 0, $\frac{L_f}{L_m}$ to 1 and L_s to 2.7μm (Toderita et al. 2021).

$$PCSA = \frac{V_m \times cos\theta}{L_m \times \frac{L_f}{L_m} \times \frac{2.7}{L_s}} \tag{2.2}$$

The maximum force potential (F^i_{max}) of each muscle was calculated from the multiplication of its PCSA (which is subject specific as per the anatomical atlas), and an assumed fixed maximum muscle stress (31.39 N/cm^2), following equation 2.3 (Yamaguchi 2005):

$$F^i_{max} = PSCA \times M_i \times \theta \tag{2.3}$$

Where F^i_{max}, M_i, and θ represent the maximum force potential, multiplier, and maximum muscle stress, respectively. The multiplier (M_i) was used to modify F^i_{max} to account for

changes in muscle structure that are known that occur due to atrophy and hypertrophy in the residual limb post-surgery TF amputation and rehabilitation (Yamaguchi 2005) (Henson et al. 2021). There are two contributing factors to the progression of atrophy and hypertrophy observed: firstly, changes in muscle recruitment in the monoarticular function assumed by muscles which have a biarticular function of the knee and hip in their intact state (Henson et al. 2021). Secondly, the direct effects of the surgery can produce atrophy in muscles which have been re-attached to a non-physiological site (Fraisse et al. 2008) (Putz et al. 2017). Therefore, M_i of the muscles which are distally inserting from the site of surgery was set to less than 1, with muscles more affected by the surgery set lowest. As per these observations, M_i was reduced to the following: 0.12 for rectus femoris, 0.33 for bicep femoris and gracilis, 0.50 for the adductor magnus and semimembranosus, and 0.80 for the tensor fascia latae and sartorius. As adductor brevis, illiacus, pectineus and gluteus medius have a greater function in the compensatory gait of a individuals with TF / TK (Henson et al. 2021), M_i of these muscles was set to 1.20. The adaptations of F^i_{max} account for the physiological / structural changes that occur in an atrophied / hypertrophied muscle which affect force capacity but are not represented by the changes in muscle volume (Henson et al. 2021).

Inverse kinematics, inverse dynamics and static optimisation

Quaternion algebra was used to perform inverse kinematic calculations and inverse dynamics simulations were carried out using a wrench formulation to estimate the net forces and moments during the captured motion (Dumas et al. 2004). The model then ran a one-step constraint static optimisation to estimate muscle and articular contact forces over the captured gait cycle. The load sharing optimisation minimised the sum of the cubed muscle activations as shown in Eq.2.4, while satisfying the equations of motion of the MSK system and constraining the muscle forces to their maximum force potentials:

$$J = \sum_{92}^{i=1} (\frac{F_i}{F^i_{max}})^3 \tag{2.4}$$

where J and F_i are the sum of cubed muscle activations and force of muscle element i, respectively.

Two sets of simulations were performed: first to identify overburdened muscles during gait (baseline) and then to quantify the consequences of the reduced muscular endurance of the overburdened muscles (reduced endurance).

2.2.5 Baseline gait simulations of individuals with BTF / BTK

Captured gait kinematics and kinetics along with the subject specific MSK geometry were used to estimate muscles forces. Muscles whose mean activations (F_i/F^i_{max}) across the 3 trials for all legs were above the maximal level in healthy gait were identified as the overburdened muscles. The threshold for healthy muscle activation during gait was taken as 50% force capacity (0.5 F^i_{max}) as reported in previous EMG (Elsais et al. 2020)

(Nishijima et al. 2010) (Burden et al. 2003) (Franz & Kram 2013) (Guan et al. 2019) and maximal torque studies (Anderson & Madigan 2014) (Requiao et al. 2005). The term 'overburdened' will be used throughout this chapter to refer to muscles that have activations higher than this threshold.

2.2.6 Reduced muscular endurance gait simulations of individuals with BTF / BTK

Muscular endurance is defined by the ability of a muscle to maintain a level of muscle contraction over extended repetitions (Kell et al. 2001). A reduced muscular endurance can therefore be quantified by a reduced force production capacity during a task of repeated contractions (ie. Gait); a reduced muscular endurance was therefore simulated by re-running the optimisations with reduced maximum force potentials (F^i_{max}) of the muscles which were identified as overburdened from the results of the baseline gait simulations. The F^i_{max} of these muscles were reduced to 50% of their original level. It is hypothesized that inhibitory senses preserve a level of critical reduced muscular performance from occurring, meaning that task failure (i.e. the inability to maintain baseline kinematics in this case) will occur before a subject specific critical level of reduction in MVC is reached (Amann & Dempsey 2008). In the practise of modelling reduced muscular endurance, this suggests that modelling a reduction of MVC to a point beyond 50% may risk being physiologically irrelevant due to a protective mechanism of the body.

The reduced endurance simulations were carried out on one gait trial per subject; the trial selected was the trial with the highest maximum force of the 'overburdened' muscles from the baseline gait optimisation. It was investigated whether the optimisation was able to find a feasible solution (i.e. whether the reduced muscle capacity can reproduce the experimentally collected baseline kinematics). If a feasible solution could be found it would likely be due to a compensatory muscle recruitment strategy (van der Kruk et al. 2021). It was hypothesised that muscles with a similar function would indicate a significantly greater muscle recruitment force in the reduced endurance condition compared to baseline.

A two-way repeated measures ANOVA was performed with SPSS software between the maximum muscle activations (force / F^i_{max}) for each muscle of reduced endurance simulations (for the legs where a solution could be found in the reduced endurance simulations) and baseline (only including the baseline trials used in the reduced endurance simulations, for the legs where a solution could be found). The nominal variables were muscle type and condition (baseline and reduced endurance); the test included 13 main muscles (excluding the muscles with simulated reduced force capacities) and alpha was adjusted with Bonferroni correction for the pairwise comparisons. Each leg was treated as independent in the statistical analysis due to the variable, trauma-induced, anatomy. An ANOVA test was selected as the appropriate statistical test to control for the risk of type I error and due to it's robustness to violations of normality.

2.3 Results

2.3.1 Example plot

The baseline muscle activations (F/F^i_{max}) are plotted over the gait cycle (1-100%). An example plot for one trial of one subject is displayed in Figure 2.4. The baseline gait trial was plotted for the left leg of participant 2 (2L) as this was a typical example of muscle activation. The main muscles are shown grouped by primary function (flexors, extensors, abductors, and adductors). For this example, it can be observed that the psoas major, the rectus femoris, the sartorius and the tensor fascia latae become saturated (activation reaches 1.0, meaning that they have reached the limit of their theoretical load-generating capacity as defined by the physiological cross-sectional area and maximum muscle stress). Additionally, the iliacus, gluteus medius and adductor longus muscles are functioning at greater than 0.5 activation.

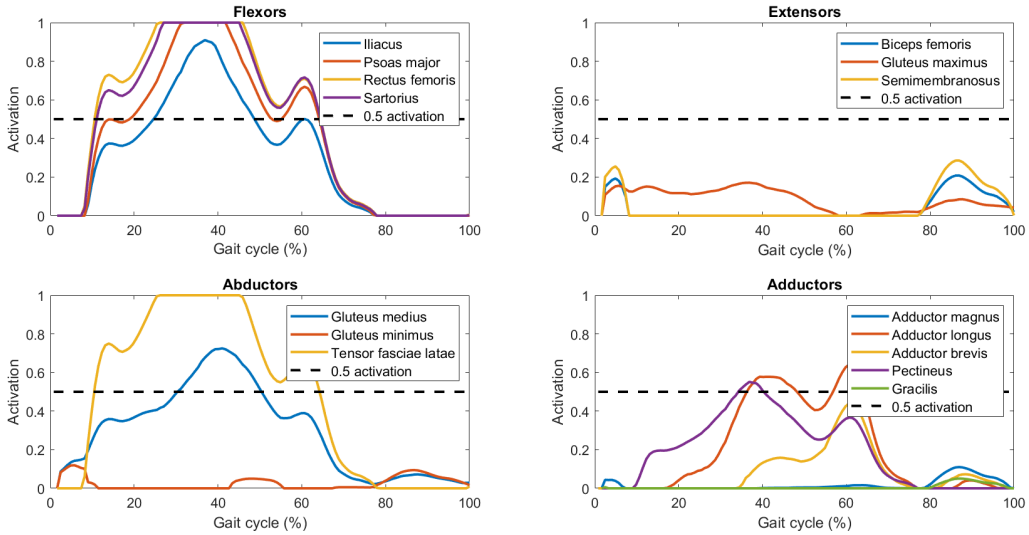


Figure 2.4: Muscle activations (force normalized to F^i_{max}) over a gait cycle for left limb of participant 02. Muscles are grouped by primary function: flexors, extensors, abductors, and adductors

2.3.2 Characterising the muscle overloading

The maximum force generated by the muscles of the residual limb have been normalised to F^i_{max} (ie. muscle activation) in Figure 2.5 and subject specific body weight (BW) in Figure 2.6. The muscles are grouped by primary functions. The median activation of the flexor muscle group is high (above 0.5) and this is also true for the tensor fascia latae and adductor longus (Figure 2.5). For the muscles which have an average maximum muscle activation above 0.5 (psoas major = 0.7, adductor longus = 0.7, rectus femoris = 0.9, sartorius = 0.8, tensor fascia latae = 0.9), the adductor longus and psoas major also have larger normalised magnitudes (Figure 2.6), suggesting that their force contributions are instrumental in creating the moments required by gait.

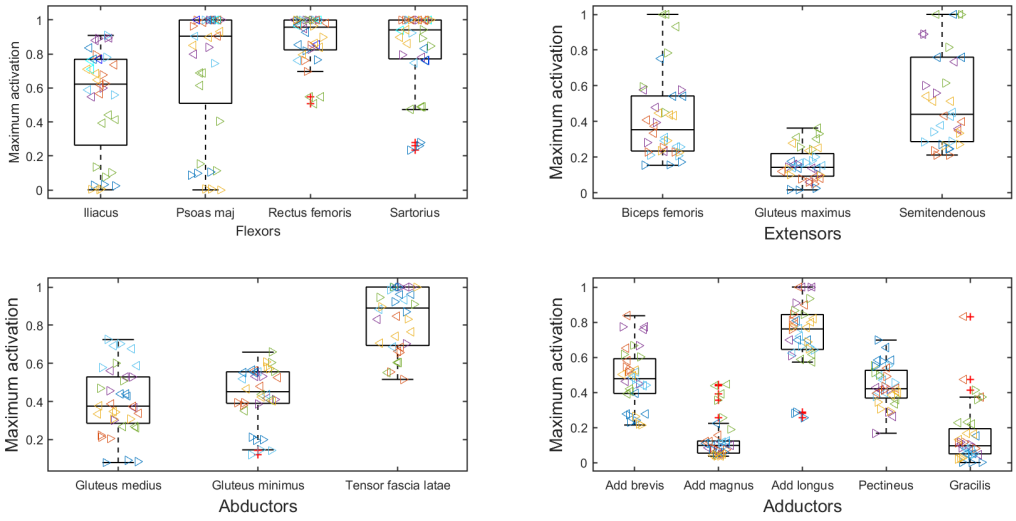


Figure 2.5: Maximum muscle activation (force normalized to F^i_{max}) during gait cycle of the 6 individuals with bilateral transfemoral and through-knee amputations. Muscles are categorized as hip flexors, extensors, abductors, and adductors. The box plots show min, max, median, 25 and 75 percentiles, and the outliers. Each participant is plotted in a separate colour, and the left legs are represented by '◁' and right by '▷' (n=12)

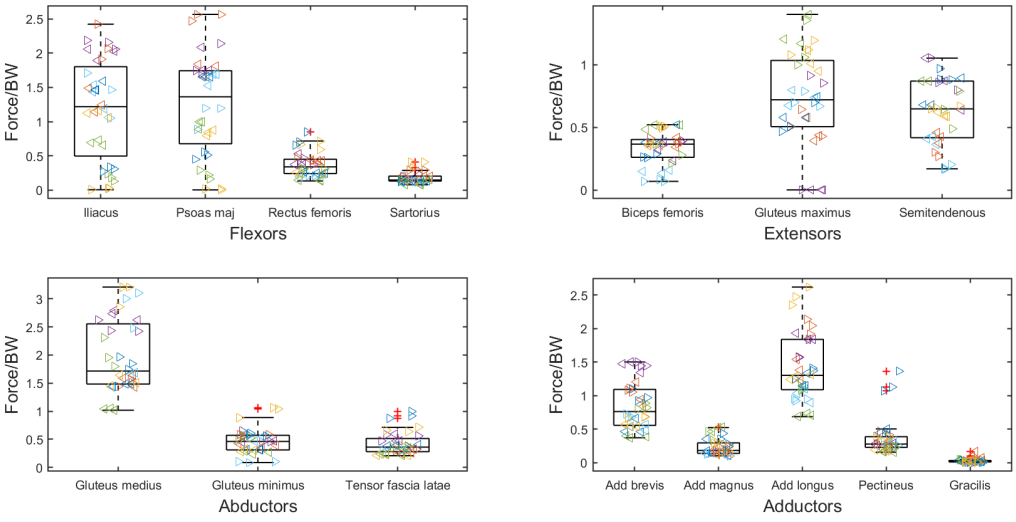


Figure 2.6: Maximum muscle force normalized to body weight (BW) during gait cycle of the 6 individuals with bilateral transfemoral and through-knee amputations. Muscles are categorized as hip flexors, extensors, abductors, and adductors. The box plots show min, max, median, 25 and 75 percentiles, and the outliers. Each participant is plotted in a separate colour, and the left legs are represented by '◁' and right by '▷' (n=12)

2.3.3 Reduced endurance simulation

Following the baseline characterisation, the psoas major and the adductor longus were identified as muscles which would be particularly susceptible to experiencing a reduced endurance (as they have high activations and high magnitudes); their F^i_{max} was reduced to 50%. In the reduced endurance condition, it can be predicated that 3 out of the 6 participants could not retain their baseline kinematics, as the optimisation could not find a solution for 5 out of 12 legs studied. This was true for both the sides of subject 1 and 5, and the right limb of subject 6. For the following legs a solution could be found in the reduced endurance state: 2L, 2R, 3L, 3R, 4L, 4R, 6R. In the legs where a solution could be found (7/12), there was a consistent increase in total maximum muscle activation of the muscles over the gait cycle, with an increase ranging from 3.3 to 30.4% in total maximum activation in the reduced endurance condition (average increase was 19.7%). Total maximum muscle activation is the sum of the maximum muscle activation reached over the gait cycles by all 21 muscles modelled. An example plot of the reduced endurance condition is presented in Figure 2.7, the leg plotted in this example is the left side of participant 2 (2L). This example shows that the simulated reduced force capacity of the psoas major and the adductor longus increases the force contributions of the remaining muscles of the same primary function.

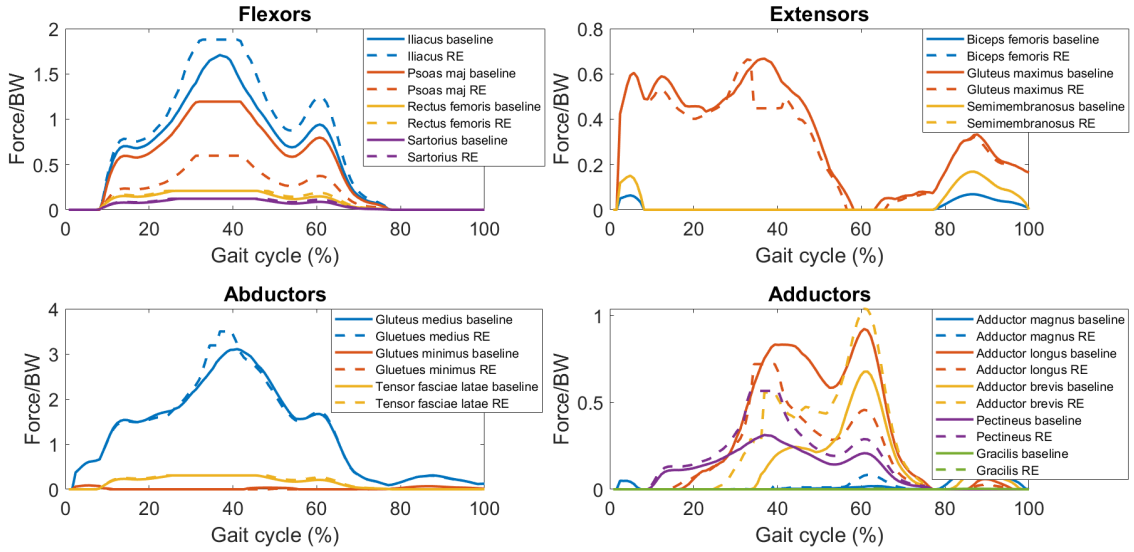


Figure 2.7: Normalized muscle force of the left limb of participant 02 for baseline and reduced endurance (RE) condition gait trial (reduce force capacity of the psoas major and adductor longus)

Figure 2.8 presents the overall effect of the reduced endurance condition on the maximum activations (force normalised to F^i_{max}) of the remaining muscles when the psoas major and the adductor longus have reduced force capacities. The muscles are grouped by primary function. All legs where a full solution could be found in the reduced endurance optimisations were included in this plot for baseline and the reduced endurance (2L,2R,3L,3R,4L,4R,6R), all legs where a full solution could not be found were excluded

(1L,1R,5L,5R,6L); The maximum activations (force normalised to F^i_{max}) are plotted for the baseline (red) and the reduced endurance simulation (blue). In the simulations of reduced muscular endurance of the psoas major and adductor longus, the maximum activations (force normalised to F^i_{max}) of the iliacus, adductor brevis, and pectineus are increased ($p \leq 0.003$). This is indicative of the increased burden on these muscles when the psoas major and the adductor longus have reduced endurance.

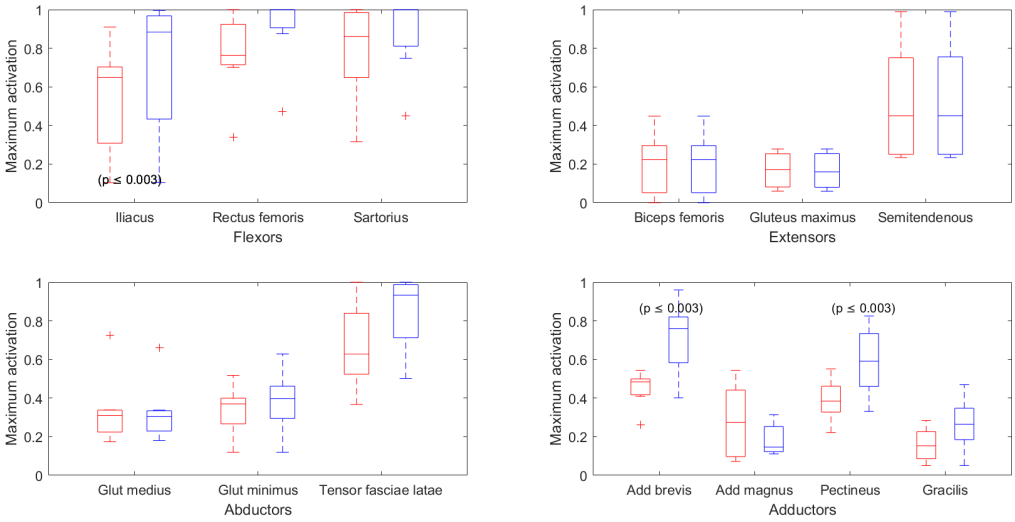


Figure 2.8: Maximum muscle activation (force/F^i_{max}) over a gait cycle for the participant limbs where a full solution could be found in the reduced endurance simulations (baseline in red, reduced endurance state in blue). Baseline values are plotted for only legs for which a feasible solution could be found in the reduced endurance state (n=7). A reduced endurance state simulated by a reduction in the maximum capacity of the psoas major and the adductor longus is shown. Muscles are grouped into primary function; p values are presented on a plot for significant difference between the means of baseline and the reduced endurance condition

2.4 Discussion and conclusion

In agreement with the literature, this study has shown gait for individuals with BTF / BTK results in highly burdened flexor muscles due to the loss of ankle propulsion (McNealy & Gard 2008). Although not their primary function, the adductor longus and the tensor fascia latae provide some flexor action (Neumann 2010) and these also have high activations in this study. This study has highlighted the high cost of gait on the residual MSK system of this young traumatic BTF / BTK amputation population, highlighting the importance of the preservation of all residual flexor action capacity in surgery and flexor functionality in rehabilitation, as well as its consideration with ageing. This high cost is particularly significant for the psoas major and adductor longus, as their critical role in function is demonstrated in the reduced endurance simulation in this study, with 5 out of the 12 simulations not being able to find a feasible solution and preserve baseline kinematics with the reduced capacity of these two muscles. Their function should

therefore be an emphasis in rehabilitation protocols.

The estimations of muscle force found the average activation of the flexor muscles to be above 50% of their maximum force potential. Individuals with lower limb amputation experience a loss in muscular capacity, therefore daily tasks are executed close to their functional capacity (van der Kruk et al. 2021). The effect of this specific loss in capacity on muscular endurance seems unexplored in published studies in the context of individuals with lower limb amputation, however, this is comparable to the loss in muscular capacity of the elderly population, which has been much more comprehensively studied. In studies of the elderly population, muscle activation (EMG/MVC) has been taken as a measure of work relative to capacity. It is concluded that the elderly population have greater difficulty with performing daily activities due to experiencing early onset fatigue because the activities require performance that is closer to their functional capacity than the younger population (Hahn et al. 2005) (Hortobágyi et al. 2011) (Hortobágyi et al. 2003). For example, through an EMG experimental set up, one study found that level walking required 80.2% MVC in the elderly group compared to 37.5% MVC in the younger group when quantifying the sum of muscle activation for the vastus lateralis, biceps femoris, tibialis anterior and the lateral gastrocnemius (Hortobágyi et al. 2011). Another study by the same author highlights how this difference in muscle activity with respect to muscle capacity between the old and the young is true for other activities of daily living, for example, similar differences were found in ascending (62% and 28% MVC) and descending (79% and 33% MVC) stairs between the elderly and younger participants respectively when just studying the vastus lateralis (Hortobágyi et al. 2003). This chapter has used a similar method of analysing the comparative relative demands of walking. These studies consolidate the need for a rehabilitation method that relieve the flexor muscles with respect to their capacity and reduce the risk of detriment to muscular endurance. Additionally, the former study reflects how our findings may be applicable to other activities of daily living.

High inter-subject variability within muscle forces, and high inter-subject variance in kinematics, and therefore resultant loading, has been reported previously in the bilateral population (Wentink et al. 2013) (Wright et al. 2008). In this study this is particularly evident when looking at the maximum muscle activations of psoas major and illiacus (Figure 2.5). For some participants, the muscles appear to become saturated and in other participants they are only minimally recruited. This variation suggests the need for patient specific prescription of interventions and highlights potential underlying differences in gait biomechanics.

The baseline gait simulations here found that the psoas major and the adductor longus function at comparatively high activations and magnitude. High intensity muscle contractions will induce a reduced muscular performance (Westerblad & Allen 2002) (Kumar 2001), so when selecting muscles that may experience a reduced endurance, the muscles with both high activations and high absolute forces were chosen as these will have a larger contribution to the moments of gait. Muscles which function at high activation, but low relative absolute magnitude may experience a decline in performance, but this

will be less detrimental to gait. The simulations of reduced endurance of the psoas major and adductor longus demonstrated two scenarios. The first, which was true for half the participants, is that the original kinematics were not possible with the reduced contribution of psoas major and adductor longus. This confirms our findings that these muscles are essential for maintaining gait of individuals with BTF / BTK amputation and, in these cases, a kinematic adaptation is required. The second, is where a full solution could be found despite the simulated reduced capacity of the adductor longus and psoas major. This occurred in 7 out of 12 simulations, highlighting redundancy in the MSK system and therefore robustness to the decline in functionality of overburdened muscles, as shown previously with the able-bodied MSK system (Komura et al. 2004). This was achieved by compensating for the impaired muscles by the recruitment of muscles with similar function. Muscle recruitment in the reduced endurance state requires high forces of the compensating muscles which in turn increases the acute functional demand on these muscles.

This study included participants with BTF and BTK amputations. It is interesting to observe that the distribution of TF and TK between the legs which could find a solution in the reduced endurance state (TF = 3, TK = 4) and the legs which could not find a solution (TF = 3, TK = 2) was fairly even. This is unexpected, as the TF legs will have a lower residual muscular capacity, suggesting that the properties of the more proximal flexor muscles (such as the iliacus and psoas major) are responsible for this distinction between the legs which could maintain kinematics in the reduced endurance state and the legs which could not.

There are limitations to this study, notably that the inverse dynamics model is limited to the recorded kinematics. This means that any kinematic changes that may occur due to the simulated reduction in force capacity in the reduced endurance condition were not included. A forward dynamics model could predict the changes in kinematics due to potential reduced endurance of certain muscles. A forward dynamics model could also predict optimal kinematics for reduced muscle activation and improved load sharing. Predicted optimal kinematics could be employed as a quantified aim in the design of a novel rehabilitation intervention. Forward dynamics could also be used to identify the cause of the variability in muscle activations observed in this study by modelling differences in anatomy (due to surgery, training or natural variation) and biomechanics. Other limitations include the inherent assumptions and estimates of the MSK model. For example, although the muscle volumes were subject specific, the fibre length to muscle length ratio, pennation angle, and sarcomere length were obtained from in vivo cadaveric studies (Toderita et al. 2021) as it is not possible to acquire these values from MRI imaging. Muscle force capacities are sensitive to such properties. F^i_{max} has been used throughout this study as an indication of force capacity; these values were also adapted to account for atrophy and hypertrophy, as previously described, in a subjective manner. As the static optimisation takes place time frame to time frame it cannot account for the excitation-contraction dynamic properties of muscles with respect to length and velocity (Porsa et al. 2016). Although the methods of this chapter did not include the dynamic properties of muscle activation and contraction, this limitation is mitigated by the slow

nature of the task studied here. The literature shows that inclusion of these properties results in similar magnitudes of muscle force for gait when compared to the static optimisation used here (Anderson & Pandy 2001) (De Groote et al. 2016).

This study has developed a new approach to analyse muscular endurance using inverse dynamics modelling. It has highlighted the critical muscles that are likely to have reduced endurance and so limit the ability to walk for an individual with BTF/ BTK amputations. Research on clinical interventions to address this reduced endurance may focus on gait retraining, such as changing the kinematics, or modifying the balance of muscle forces required to achieve a proscribed gait pattern. The next chapter will continue this research by addressing muscle recruitment during walking for individuals with unilateral transfemoral amputations. Subsequently, this thesis will present a forward dynamic MSK modelling method that could be used to simulate potential clinical interventions for individuals with bilateral transfemoral amputations in future work.

Chapter 3

Muscle recruitment during gait in individuals with unilateral transfemoral amputations due to trauma compared to able-bodied controls

Chapter 3 continues on from Chapter 2 in addressing the first objective of this thesis by quantifying and characterising muscle recruitment in individuals with unilateral transfemoral amputations. Unilateral traumatic amputation is more prevalent than bilateral in the global population of individuals with traumatic amputations. The intact limb introduces differing compensatory strategies; hence these two groups (bilateral and unilateral) have been investigated separately. This chapter utilised inverse dynamic musculoskeletal modelling and includes an able-bodied control group to allow for comparison of the intact limb's knee and ankle muscles.

This work was published in part as: 'Muscle recruitment during gait in individuals with unilateral transfemoral amputation due to trauma compared to able-bodied controls', with authors: Alice M Benton, Diana Toderita, Natalie Egginton, Sirui Liu, Kate Sherman, Pouya Amiri, Anthony MJ Bull. 2024. Frontiers in Bioengineering and Biotechnology, 12, 1429574.

3.1 Introduction

In 2019 there was an estimated 25.6 million people living globally with unilateral lower limb amputations due to traumatic causes (Yuan et al. 2023). The physiological demand of gait is greater in this population compared to able-bodied individuals, which leads to reduced endurance as evidenced by a 29% reduction in the 6-min walking test (Linberg et al. 2013). Ex-military individuals with transfemoral amputation are likely to be the gold standard of functional ability, as they are young, experience comprehensive rehabilitation, have high levels of fitness pre-injury and are fitted with state-of-the-art prosthetics (Ding et al. 2021). However, even with these positive factors, the oxygen cost of gait at self-selected speeds is 20% higher for ex-military personnel with unilateral transfemoral amputations (n = 10, average age = 29 years) compared to able-bodied controls (n = 10, average age = 30 years) (Jarvis et al. 2017). These findings are supported by another study which controlled for walking speed and found an 24.1%–24.2% increase in oxygen consumption for young, fit, individuals with traumatic unilateral amputations donning micro-processor knees (n = 8, six male, two female, average age = 22.5 years) compared to an able-bodied control group (Chin et al. 2003). This elevated oxygen cost has been found to be even more extreme, 55%, when observing a population of older civilian individuals with transfemoral amputation (n = 60, average age = 51.1 years) donning mechanical knees compared to their age-matched able-bodied control group (n = 10, average age = 51 years) (Carse et al. 2020). Oxygen cost during gait in individuals with lower limb amputation has been found to be higher in transfemoral compared to trans-tibial amputation (Göktepe et al. 2010).

Co-morbidities such as lower back pain and osteoarthritis are prevalent in individuals with unilateral transfemoral limb amputations (Silverman et al. 2023): 47.7%–76.6% of individuals with unilateral amputations experience lower back pain, compared to 1%–37% in an able-bodied population (Sivapuratharasu et al. 2019). These comorbidities are detrimental to quality of life (Silverman et al. 2023).

Unilateral transfemoral limb loss, muscle loss, and loss of control mechanisms result in compensatory strategies in gait biomechanics, including kinematics, kinetics (Seroussi et al. 1996) (Jarvis et al. 2021) (Silverman et al. 2023), and muscle activation timing (Mehryar et al. 2021)(Wentink et al. 2013) which may lead to muscular loading conditions associated with loss of muscular endurance (Fang et al. 2007), functional deficit (Slater et al. 2022) and the risk of developing secondary conditions (Ding et al. 2021). Individuals with unilateral amputation experience asymmetrical gait resulting in increased weight bearing on the intact side (Sangeux 2019) (McNealy & Gard 2008).

Though it is evident that there is a need to improve these rehabilitation outcomes, muscle recruitment in the residual limb and intact limb, compared to an able-bodied control group has not been quantified in this young, fit, military cohort. Inverse dynamic musculoskeletal modelling is a non-invasive method of estimating muscle and joint contact forces from motion data, providing insight into pathological and non-pathological gait. Within research of biomechanics of individuals with lower limb amputation, musculoskele-

tal modelling has been used for several applications, such as, to assess prosthetic device function (Pickle et al. 2017), understand the progression of musculoskeletal pathologies (Ding et al. 2021) and evaluate surgical technique (Ranz et al. 2017). One study utilised musculoskeletal modelling to quantify muscle forces during walking to identify the contribution to centre of mass acceleration for the intact and residual limb of individuals with unilateral transfemoral amputations and found significant differences in force magnitude between the limbs, as well as compensatory mechanism adopted by the muscles in the intact limb to accelerate the centre of mass. However, this study was looking at a small sample size (n = 6) donning a mix of microprocessor and non-microprocessor knees, and did not include a control group in their analysis. Additionally, it was also solely looking at the stance phase of gait (differences in muscle recruitment have been found during the swing phase in transtibial amputees (Ding et al. 2023)) and scaled all subjects from a generic musculoskeletal model (Harandi et al. 2020).

The aim of this chapter, addressing the first objective of this thesis, was to quantify muscle recruitment, with force magnitude and metrics associated with endurance, during the whole gait cycle in the intact and residual limb of individuals with traumatic unilateral transfemoral (UTF) amputation who have received high quality intensive rehabilitation and advanced prosthetics, and compare this to able-body equivalents, using validated musculoskeletal modelling methods (Toderita et al. 2021) (Ding et al. 2023). This investigation will contextualise muscle recruitment into known kinematic and kinetic adaptations of this population (Jarvis et al. 2021) to inform future rehabilitation research aimed to improve walking endurance, functional ability, alleviate the risk of comorbidities and therefore improve quality of life. This chapter builds on Chapter 2 and investigates the unilateral condition, which is more globally prevalent.

3.2 Methods

3.2.1 Particpants

This study focused on 11 male young /middle-aged individuals with unilateral transfemoral (UTF) amputation due to traumatic injuries donning state-of -the-art prosthetics following intensive rehabilitation. 9 of the 11 participants were ex-military personnel. This demographic can be taken as a model of high-functionality in persons with UTF limb loss (Jarvis et al. 2021). This study considered male participants only due to the lack of availability of anatomical datasets for female persons with UTF amputation. 11 able-bodied (AB) participants were selected as a control group, matched to the UTF group for gender, age and height (Table 3.1). The able-bodied dataset has been previously published (Ding et al. 2019)(Long et al. 2017). The able-bodied group were significantly lighter (body mass) than individuals with UTF amputations, which is consistent with the literature in this predominantly military group (McMenemy et al. 2023). Ethical approval was received from the Imperial College research ethics committee and written informed consent obtained from the participants.

Table 3.1: Study participant demographics (* calculated using Eq. 3.5; ** t-test between UTF participants and AB participants)

Group	Participant code	Sex	Age (years)	Body mass with prostheses (kg)	Calculated intact mass (kg)*	Height (m)	Level	Prosthetic knee
UTF (n=11)	1	M	47	93.8	95.4	1.76	UTF	Ottobock Genium X3
	2	M	57	91.8	97.8	1.76	UTF	Ottobock C-leg
	3	M	58	64.4	65.5	1.64	UTF	Endolite Orion
	4	M	52	91	94.2	1.78	UTF	Ottobock C-leg
	5	M	32	88.7	94.6	1.74	UTF	Ottobock Genium X3
	6	M	49	82.7	86.4	1.77	UTF	Ottobock Genium X3
	7	M	47	94.1	95.5	1.77	UTF	Ottobock Genium
	8	M	31	74.3	77.3	1.75	UTF	Ottobock Genium X3
	9	M	36	109.3	114.3	1.89	UTF	Ottobock Genium X3
	10	M	39	133.3	139.4	1.90	UTF	Blatchford KX06
	11	M	36	91.1	96.3	1.83	UTF	Ottobock Genium X3
	Mean	-	44.0	92.2	96.0	1.78	-	-
	SD	-	9.7	17.9	18.9	0.07	-	-
AB (n=11)	Mean	M -	42.2	79.5		1.79	-	-
	SD	-	11.0	93		0.07	-	-
	P-value	-	0.74	0.04**	0.02**	0.85	-	-

3.2.2 Data collection

As in Chapter 2, reflective markers were attached to anatomical landmarks of the pelvis, the left and right lower limbs as well as marker clusters on the thighs and shanks (Table 3.2), as exhibited in Figure 3.2. Three gait trials at a self-selected walking speed and one static trial were collected for each participant in a motion capture system. For UTF participants 1 to 4 this motion capture system consisted of ten cameras (VICON, Oxford Metrics Group, United Kingdom) and two force plates (Kistler Type 9286B, Kistler Instrumented AG, Winterthur, Switzerland). The marker 3D displacement and ground reaction forces were sampled at 120 and 960 Hz, respectively. For participants 5 to 11 this consisted of twenty cameras (VICON, Oxford Metrics Group, United Kingdom) and six Optima force plates (AMTI Force and Motion, Massachusetts, USA). The marker 3D

displacement and ground reaction forces were sampled at 100 and 1000 Hz, respectively. For the previously published able-bodied trials this consisted of ten cameras (VICON, Oxford Metrics Group, United Kingdom) and two force plates (Kistler Type 9286B, Kistler Instrumented AG, Winterthur, Switzerland), sampled at 100 Hz and 1000 Hz respectively (Long et al. 2017).

Table 3.2: Optical motion tracking cluster and marker positions and labels

Marker label	Anatomical location
FCC	Calcaneus
FMT	Tuberosity of the fifth metatarsal
FM2	Head of the second metatarsal
TF	Additional marker placed on foot
FAM	Apex of the lateral malleolus
TAM	Apex of the medial malleolus
C1,C2,C3 (clusters)	Additional markers placed on the shank segment
FLE	Lateral femoral epicondyle
FME	Medial femoral epicondyle
T1,T2,T3 (clusters)	Additional markers placed on the thigh segment
RASIS	Right anterior superior iliac spine
LASIS	Left anterior superior iliac spine
RPSIS	Right posterior superior iliac spine
LPSIS	Left posterior superior iliac spine

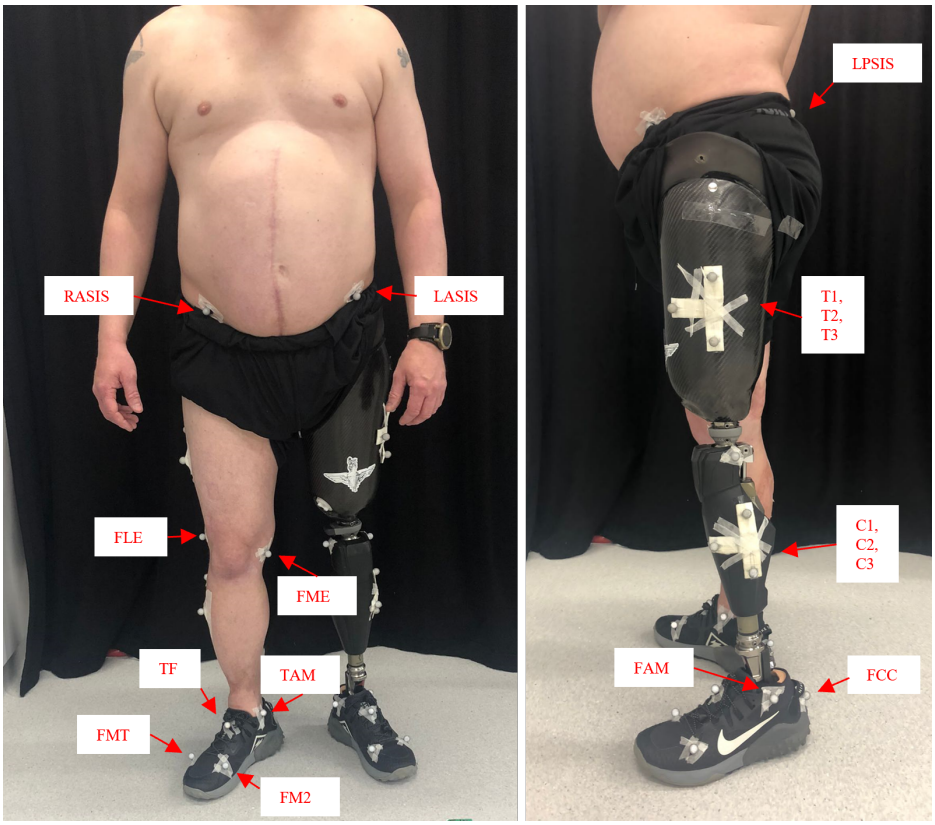


Figure 3.1: Participant with markers attached for data collection

3.2.3 Musculoskeletal modelling

General modelling method

The FreeBody musculoskeletal model (Cleather & Bull 2015) was utilised to quantify the muscle forces for the participants with UTF amputation and the able-bodied group. FreeBody v2.1 has been validated against in-vivo knee contact forces for able-bodied individuals Ding et al. (2016) and for muscle activations against EMG for individuals with bilateral transfemoral amputation (Toderita et al. 2021) and unilateral transtibial amputation (Ding et al. 2023). FreeBody v2.1 is a segment based musculoskeletal model with four rigid bodies including the foot, shank, thigh and pelvis. FreeBody v2.1 uses quaternion algebra to perform inverse kinematics to calculate joint kinematics, inverse dynamics with wrench formulations to estimate net forces and moments, and then a one-step static optimisation to predict muscle forces and joint loading for the captured gait trial. The static optimisation minimises the sum of cubed muscle activations following the objective function Eq.3.1 (Crowninshield & Brand 1981), where J is the sum of the cubed muscle activations, F_i is the instantaneous force of muscle element i, F^i_{max} is the maximum force potential of the muscle element i, and n is the number of muscle elements of the model. Ligament force contribution is assumed insignificant to net moments.

$$J = \sum_{92}^{i=1} (\frac{F_i}{F_{max}^i})^3 \tag{3.1}$$

The maximum force potential of each muscle element is calculated following Eq.3.2 which is a multiplication of the physiological cross-sectional area (PCSA) of the muscle element i and the assumed maximum muscle stress (θ) which is 31.39 N/cm^2 (Yamaguchi 2005).

$$F_{max}^i = PSCA \times M_i \times \theta \tag{3.2}$$

The PCSA was calculated following Eq.3.3 where muscle volume (V_m) was acquired from rendered 3D geometry of the muscles (details described below), fibre length to muscle length ratio (L_f/L_m), pennation angle (θ) and optimal sarcomere length (L_s) were taken from the literature. In the cases where there were no values found in the literature, θ was set to 0, L_f/L_m to 1 and L_s to 2.7μm (Lieber et al. 1994) (Ding et al. 2019).

$$PCSA = \frac{V_m \times cos\theta}{L_m \times \frac{L_f}{L_m} \times \frac{2.7}{L_s}} \tag{3.3}$$

Able-bodied limb and intact limb model

FreeBody is a unilateral model, so the individual limbs of a participant are modelled separately. The limbs of the able-bodied participants and the intact limbs of the participants with transfemoral amputations are modelled in an identical manner. This model consists of 163 muscle elements representing 38 muscles. The muscles are modelled as an ideal force generator, where the force is proportional to the maximum force potential. The anatomical measures (muscle and joint geometries) required for the static optimisation, as previously described, are acquired from a previously published anatomical able-bodied atlas of anatomical datasets (Ding et al. 2019). Each dataset contains origin, insertion and via points of the 163 muscle elements. The dataset defines the centres of joint rotation, bone geometries, and the wrapping surfaces of the muscles with curved lines of actions. The muscle lines-of-action and wrapping surfaces for the able-bodied and intact limb models are displayed in Figure 3.2. This information was originally digitised from MRI scans of able-bodied participants, following the methodology of (Horsman et al. 2007). The method of Ding et al. (2019), was used to select an appropriate anatomical dataset from the atlas and scale for each participant's dimensions following the regression model in Eq.3.4 to minimize error in hip contact forces, where RMSD represents the root mean square difference, $\triangle$LL the difference in limb length, $\triangle$mass the difference in body mass and $\triangle$sex the difference in sex.

$$RMSD = 9.60 + 0.38 \times \triangle LL + 0.10 \times \triangle mass + 2.64 \times \triangle sex \tag{3.4}$$

The segment parameters (mass, centre of mass location and moment of inertia) were calculated from De Leva's method (De Leva 1996). For the intact limb, the segment parameters were calculated using the adjusted intact weight of the participant if they did not have the transfemoral amputation. The adjusted intact weight was estimated using Eq.3.5 (Tzamaloukas et al. 1994) where W_I is the estimated intact mass, W_a is the weight

without the prosthetic device, $\sum \frac{\triangle W}{W_I}$ is an estimate of the percentage of bodyweight lost due to amputation derived from residuum length.

$$W_I = \frac{W_a}{1 - \sum \frac{\triangle W}{W_I}} \tag{3.5}$$

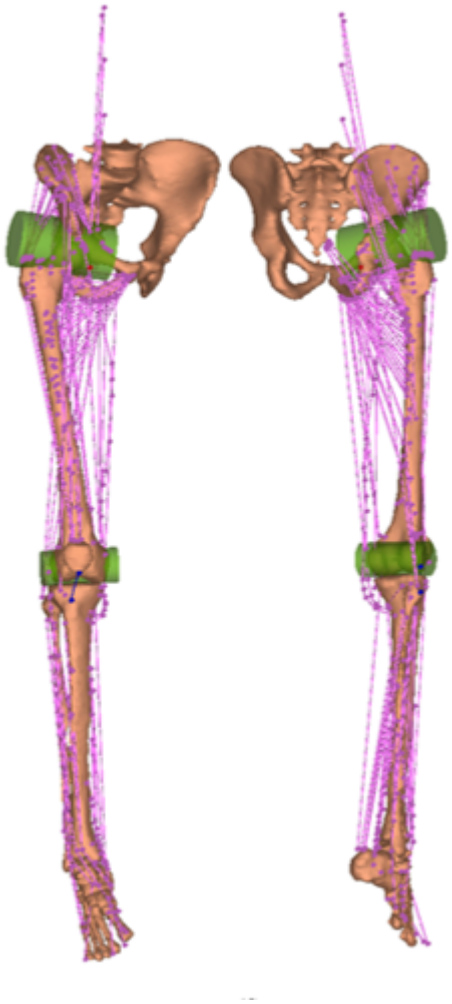


Figure 3.2: Muscle elements lines-of-action in pink, patella ligament in blue and wrapping objects in green defined, for the iliopsoas and gastrocnemius, for the intact and able-bodied limb models (Ding et al. 2019)

Residual and prosthetic limb model

As with the residual limb models in Chapter 2, the UTF residual limb model consists of 92 muscle elements, representing 21 muscles. The anatomical geometries for the residual limb models were acquired from a previously published atlas of datasets of residual limbs of participants with bilateral transfemoral amputations (Toderita et al. 2021). These are the same datasets used in Chapter 2. As described in Chapter 2, the method to acquire these muscle and bone geometries is the same as the intact and able-bodied

limbs. Anatomical dataset selection and scaling followed Eq.3.6 (Toderita et al. 2021), where RMSD represents the root mean square difference, △ PW difference in pelvis width, △ BMI difference in body mass index (from the adjusted body mass, Eq.3.5), and △ ratio residual limb length to pelvis ratio.

$$RMSD = 36.82 + 6.55 \times \triangle PW + 2.85 \times \triangle BMI + 0.28 \times \triangle \text{ratio} - 0.38 \times \triangle BMI \times \triangle PW \quad (3.6)$$

The inertial and mass properties of the residual limb model represent the residual and prosthetic limb configuration. The mass of the of the prosthetic foot, knee and socket (with liner) had been previously measured and the inertial properties have been previously determined using the reaction board method with moment of equilibrium (Smith et al. 2014) (Toderita et al. 2021). For the prosthetic foot and the prosthetic knee, these values are directly in-putted into the model for the foot and shank segment respectively. The socket and the residual limb are modelled as one rigid component. The mass of the residual limb was calculated from the estimated mass of the participant's intact thigh from the De Leva equations using the adjusted intact mass, this was multiplied by the ratio of residual limb length to intact limb length. The mass of the composite thigh segment was the sum of the estimated residual limb mass and the measured mass of the socket and liner. The inertial properties of the residual limb was assumed to be proportional to De Leva and calculated using the residual limb length. The moments of inertia of composite residual limb and socket segment was calculated using Huygens-Steiner parallel axis theorem.

3.2.4 Data analysis and statistical testing

The limbs were grouped into: the residual limb of the participants with UTF group (R), the intact limb of the participants with UTF group (I), and the limb of the able-bodied participants control group (AB).

The hip muscle (iliacus, psoas major, rectus femoris, sartorius, biceps femoris, gluteus maximus, semitendinosus, adductor brevis, adductor magnus, adductor longus, pectineus, gracilis, gluteus medius, gluteus minimus, tensor fascia latae) and plantar flexor muscle (gastrocnemius, soleus) forces of the residual, intact and able-bodied limb groups were compared. For each muscle, the force was calculated by summing the F^i of its muscle elements and was normalised to measured body weight plus weight of the prosthetic components (BW). This force was plotted over the gait cycle (initial foot contact to subsequent foot contact); this output will be referred to as 'force over gait cycle' throughout this chapter. The maximum value of force over gait cycle was calculated; this parameter will be referred to as maximum muscle force. Additionally, as muscular endurance is negatively associated with intensity of force production with respect to maximum voluntary contraction (West et al. 1995), activation was estimated by normalising the total F^i of the muscle by the maximum force capacity (total F^i_{max} of that muscle), following Eq.3.2. The maximum value of activation over the gait cycle was calculated; this will be

referred to as peak activation throughout this chapter and is an estimation of contraction intensity. Additionally, force impulse was calculated by finding the area under the 'force over gait cycle' curve as an indication of the total muscular energy expended (Bemben et al. 1996). This parameter will be referred to as impulse throughout this thesis.

A three-way comparison was made of the kinematics and kinetics to assist the interpretation of the muscle recruitment comparison. Kinetics were normalised to BW. The inverse kinematic, inverse dynamic were plotted over the gait cycle. The maximum values of kinematic and kinematic features of gait were calculated. These gait features include maximum anterior pelvic tilt, maximum hip flexion and extension angles, maximum hip abduction and adduction angles, maximum hip extension and flexion torques, the 1st and 2nd peak of hip abduction torque, and the 1st and 2nd peak of vertical ground reaction force. The self-selected gait speed of the gait cycle was also calculated.

A preliminary Student's t-test was conducted between the left and the right limb of the able-bodied control group. This test showed no significant difference between the two sides in any of the variables (maximum muscle forces, peak activation, impulse and gait features) apart from one account, which was the adductor magnus activation. The results from the t-test is presented in Table 3.3. So, the right and left limb of the able-bodied controls were treated as one group for comparison. For the three-way comparison of maximum muscle force, peak activation, impulse and gait features, generalized estimation equations were used to compare the means of the variables described between the residual limb group, the intact limb group, and the able-bodied limb group (control group), with significance set at 0.05. The generalized estimation equation method was chosen as the appropriate statistical test as it accounts for the potential correlation between variables of limbs from the same participant by adjusting the estimation of standard error (Wang 2014) and does not assume normality. For the two-way comparison of force over gait cycle (between the plantar flexors of the intact and able-bodied limb group), data normality was checked using the Shapiro-Wilk statistical test and then statistical parametric mapping was used with a Student's T test with significance set at 0.05 (Pataky et al. 2013). Statistical parametric mapping was selected as the appropriate statistical test as this test allows for a two-way comparison of a continuous signal. A student's t-test was conducted between self-selected gait speed of the UTF participants and the able-bodied control group with significance set at 0.05.

Table 3.3: T-test results from the left and the right limbs of the able-bodied participants, significant p-values highlighted in grey

Parameter	p-value for maximum muscle force	p-value for peak activation	p-value for impulse
Adductor Brevis	0.56	0.77	0.11
Adductor Longus	0.36	0.92	0.10
Adductor Magnus	0.61	0.39	0.04
Biceps Femoris	0.25	0.09	0.11
Gluteus Maximus	0.30	0.67	0.20
Gluteus Medius	0.20	0.21	0.06
Gluteus Minimus	0.17	0.32	0.13
Gracilis	0.17	0.38	0.46
Iliacus	0.19	0.50	0.21
Pectineus	0.39	0.80	0.13
Psoas Major	0.19	0.50	0.21
Rectus Femoris	0.28	0.38	0.06
Sartorius	0.15	0.48	0.35
Semitendenous	0.59	0.19	0.13
Tensor Fascia Latae	0.18	0.84	0.12
Parameter	p-value		
Maximum anterior tilit	0.71		
Maixmum saggital torque	0.20		
Minimum saggital torque	0.26		
Frontal torque 1st peak	0.13		
Frontal torque 2nd peak	0.19		
Maximum extension angle	0.47		
Maximum flexion angle	0.43		
Maximum abduction angle	0.14		
Maximum adduction angle	0.50		

3.3 Results

The able-bodied limb group consists of 22 limbs, the residual limb group 11 limbs and the intact limb group 10 limbs due to an error identified in the motion capture data of the intact side of participant 6. These trials have been excluded from the analysis. The residual limb from this participant was included in the analysis as the generalized estimation equation method accounts for participants and all values were normalised.

3.3.1 Muscle recruitment during gait of individuals with UTF amputations

Maximum muscle force

Hip muscles are grouped by primary function and maximum muscle forces are presented in Figure 3.3, with significant p-values labelled. Figure 3.3 displays that the largest values of maximum muscle force were exhibited by the residual limb's gluteus medius, iliacus, and psoas major, which had mean values of 1.49 ±0.67 N/BW, 1.40 ± 0.72 N/BW, and 1.50 ± 0.72 N/BW, respectively, followed by the able-bodied and intact groups' gluteus medius at 1.20 ± 0.39 N/BW and 1.14 ± 0.25N/BW, respectively.

From the comparison between the residual limb group and the intact limb group, twelve out of fifteen maximum muscle forces were significantly different. Six muscles (iliacus, psoas major, adductor longus, pectineus, gluteus minimus and tensor fasciae latae) were recruited to significantly higher levels in the residual limb group compared to the intact limb group. Six other muscles (rectus femoris, sartorius, biceps femoris, gluteus maximus, semitendinosus, and adductor magnus) exhibited significantly higher maximum muscle force in the intact limb group compared to the residual.

From the residual limb group to able-bodied limb group comparison, ten out of fifteen of the major muscles were recruited to significantly different maximum muscle forces. Five muscles (iliacus, psoas major, adductor longus, pectineus and tensor fasciae latae) had significantly greater maximum muscle force in the residual limb group compared to the able-bodied limb group. Five muscles (adductor magnus, biceps femoris, rectus femoris, sartorius, and semitendinosus) were recruited to higher maximum force in the able-bodied limb group than the residual limb group.

From the intact limb group to able-bodied limb group comparison, only the pectineus exhibited a significantly higher maximum muscle force in the able-bodied limb group, Figure 3.3.

The force over gait cycle for the 15 hip muscles are displayed in Figure 3.4, with the significant differences in maximum muscle force labelled.

Statistical parametric mapping identified significant differences in the force over gait cycle of the plantar flexors of the intact limb group and the able-bodied limb group, Figure 3.5. The plantar flexors were recruited to significantly higher levels in the intact limb group than the able-bodied limb group during 50-60% and 70-80% of gait.

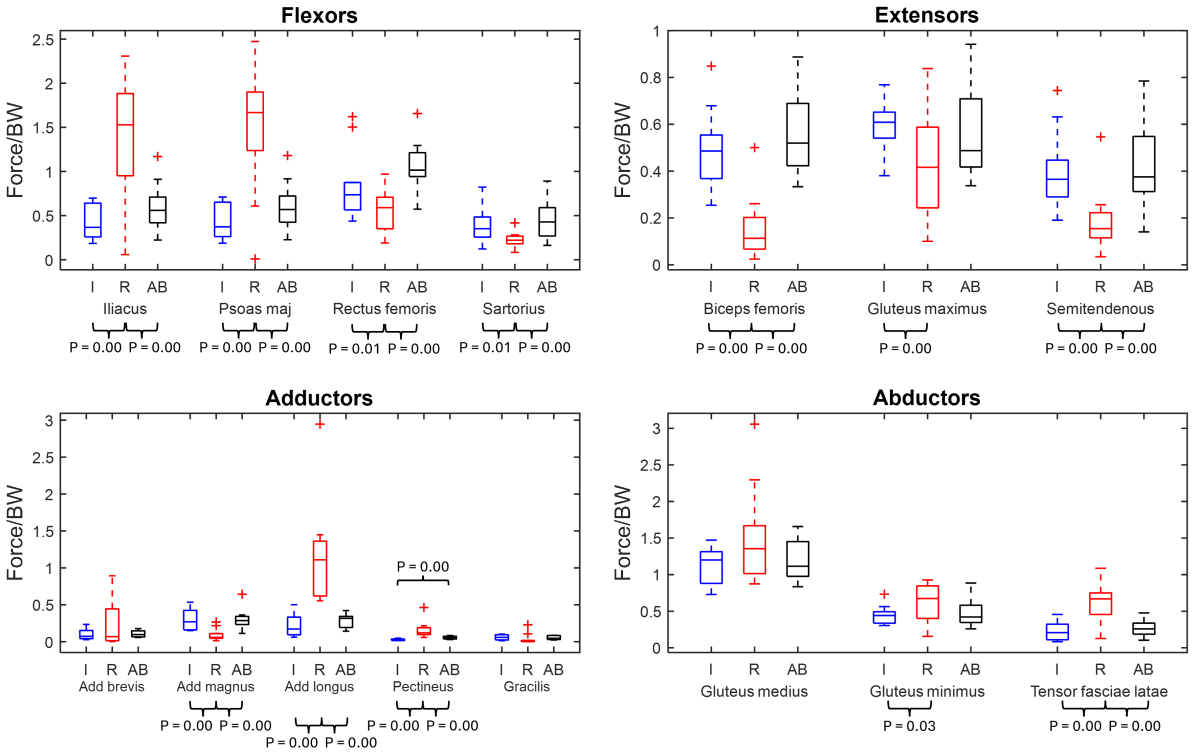


Figure 3.3: Maximum normalised muscle force box plots of major hip muscles grouped by primary function (min, max, median, 25 and 75 percentiles and outliers). Significant p-values displayed. The muscles are grouped by primary function. Red represents the residual limb group (n = 11) of the individuals with UTF ("R"), blue represents the intact limb group (n = 10) of individuals with UTF ("I") and black represents the able-bodied limb group (n = 22) ("AB")

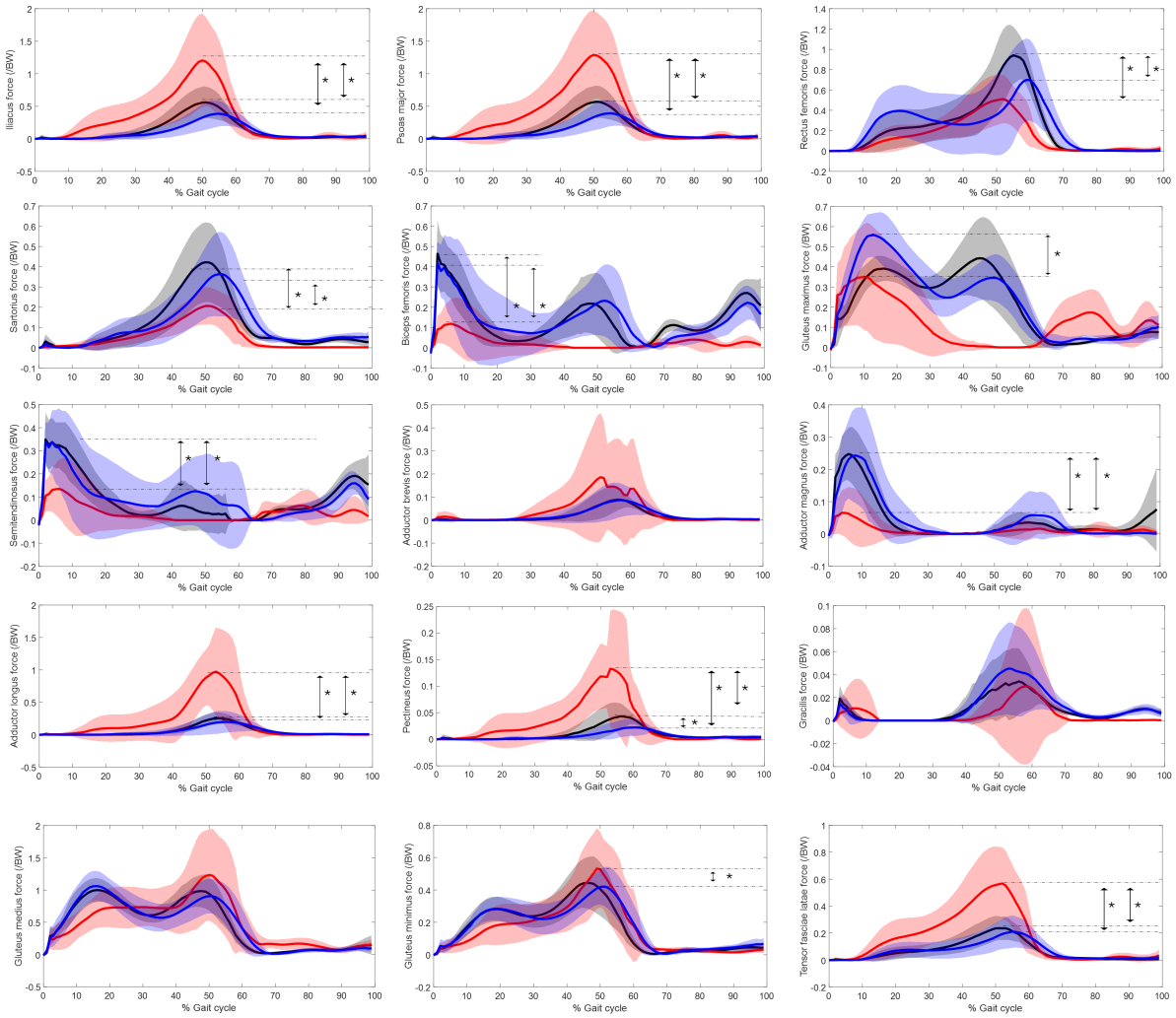


Figure 3.4: Muscle force normalised to bodyweight of major hip muscles over gait cycle. Red represents the residual limb group (n = 11 ± SD) of the individuals with UTF, blue represents the intact limb group (n = 10 ± SD) of individuals with UTF and black represents the able-bodied limb group (n = 22 ± SD). Arrows and "*" indicate a significant difference in peak value

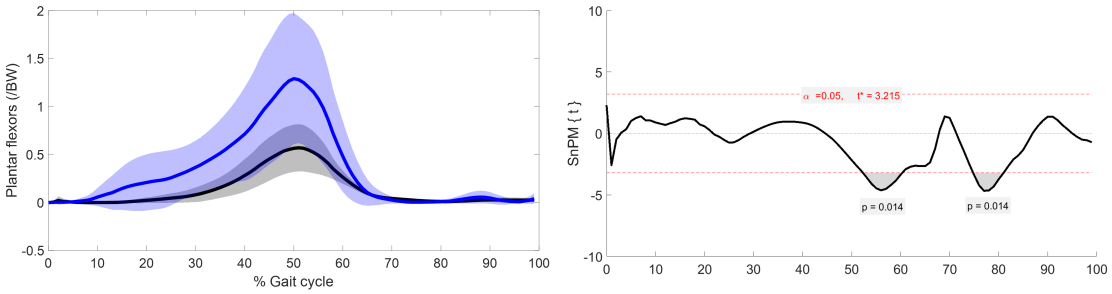


Figure 3.5: Left: muscle force normalised to bodyweight of the plantar flexors over the gait cycle. Blue represents the intact limb group (n = 10 ± SD) and black represents the able-bodied limb group (n = 22 ± SD). Right: Statistical parametric mapping results

Impulse

Figure 3.6 displays the impulse for the main fifteen hip muscles of the residual limb, intact limb, and able-bodied limb groups. From the residual limb to intact limb group comparison, ten out of the fifteen of the impulse values were significantly different. Five muscles (iliacus, psoas major, adductor longus, pectineus and tensor fasciae latae) showed significantly higher values of impulse in the residual limb group compared to the intact limb group. While five muscles (sartorius, biceps femoris, gluteus maximus, semitendinosus and adductor magnus) had higher values of impulse in the intact limb group compared to the residual limb group.

From the residual and able-bodied limb group comparison there were nine out of the fifteen significant differences. Eight muscles (iliacus, psoas major, adductor brevis, adductor longus, pectineus, gluteus medius, gluteus minimus and tensor fasciae latae) had a greater impulse in the residual limbs compared to the able-bodied limbs. The biceps femoris had a greater impulse in the able-bodied limbs than the residual.

From the intact limb group to able-bodied limb group comparison all muscles, apart from the adductor longus, exhibited a significantly greater impulse in the intact limb group than the able-bodied limb group.

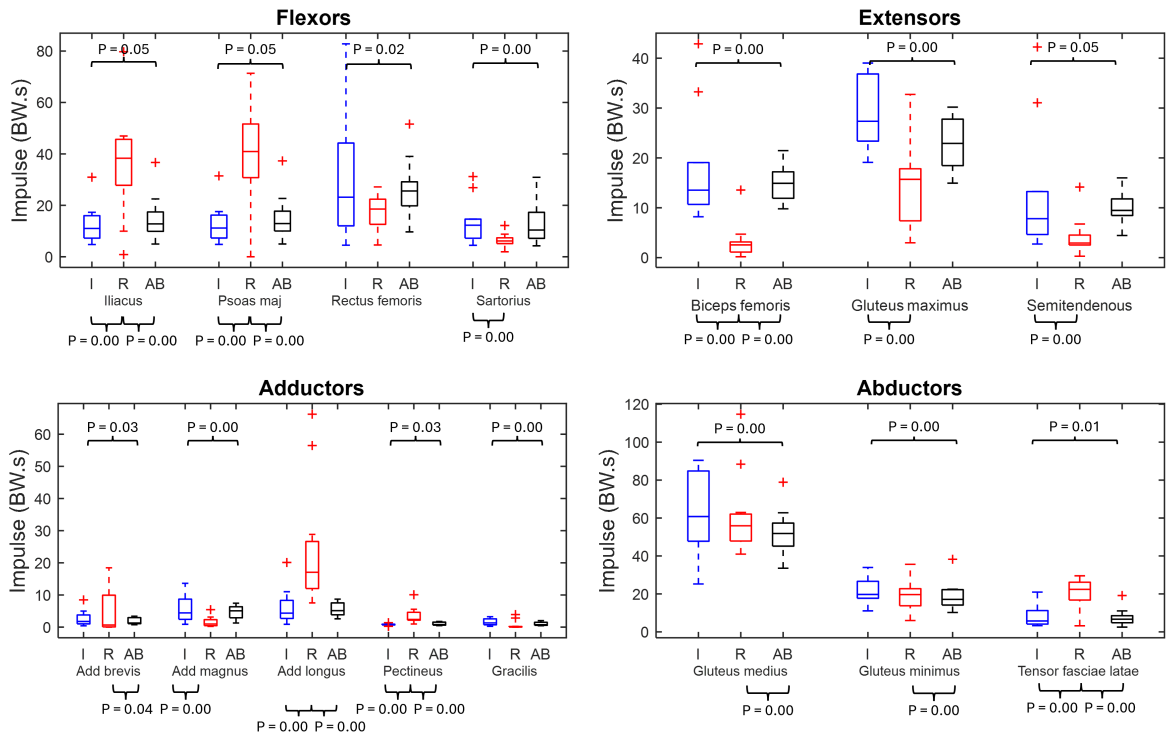


Figure 3.6: Muscle impulse box plots of major hip muscles grouped by primary function (min, max, median, 25 and 75 percentiles and outliers). Significant p-values displayed. Red represents the residual limb group (n = 11) of the individuals with UTF ("R"), blue represents the intact limb group (n = 10) of individuals with UTF ("I") and black represents the able-bodied limb group (n = 22) ("AB")

Peak muscle activation

Figure 3.7 displays the peak muscle activations for the main hip muscles for the residual, intact and able-bodied limb group. From the residual to intact limb group comparison, nine (iliacus, psoas major, rectus femoris, sartorius, adductor longus, pectineus, gluteus medius, gluteus minimus and tensor fasciae latae) of the fifteen muscles were recruited to significantly higher peak activation in the residual limb group compared to the intact.

From the residual limb to able-bodied limb group comparison, the same nine (iliacus, psoas major, rectus femoris, sartorius, adductor longus, pectineus, gluteus medius, gluteus minimus and tensor fascia late) of the fifteen muscles were recruited to significantly higher peak activation in the residual than the able-bodied limb group.

From the intact limb group to able-bodied limb group comparison, the gluteus minimus had significantly greater peak activation in the intact limbs compared to the able-bodied limbs.

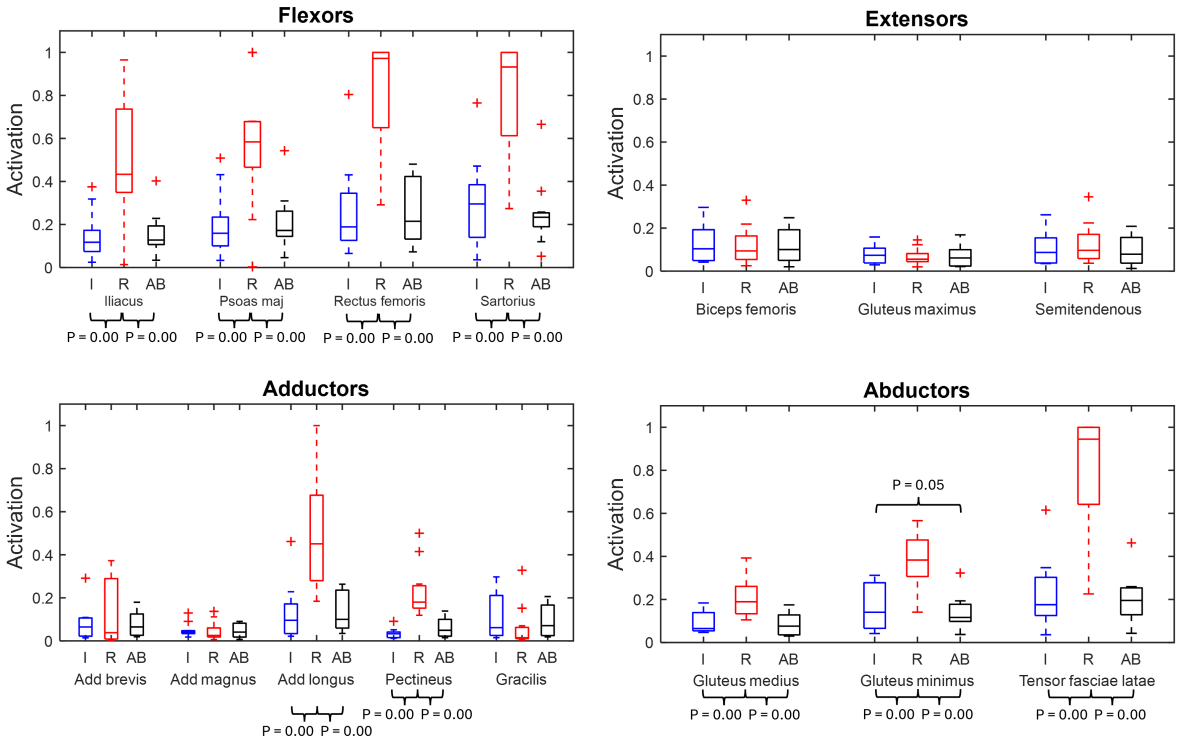


Figure 3.7: Muscle peak activation box plots of major hip muscles grouped by primary function (min, max, median, 25 and 75 percentiles and outliers). Significant p-values displayed. Red represents the residual limb group (n = 11) of the individuals with UTF ("R"), blue represents the intact limb group (n = 10) of individuals with UTF ("I") and black represents the able-bodied limb group (n = 22) ("AB")

3.3.2 Gait features of individuals with UTF amputations

Figure 3.8 displays the anterior pelvic tilt, the vertical ground reaction force, and the sagittal and frontal hip kinematics and moments over the gait cycle for the residual, intact and able-bodied limbs. The significant differences in gait features are labelled. The angle of maximum anterior pelvis tilt was greater in the residual than the able-bodied (p=0.00). Maximum hip extension torque was significantly greater in the intact and able-bodied limbs than the residual limbs (p=0.00 and p= 0.04 respectively). The maximum hip flexion torque was lower in the intact limbs compared to the residual and able-bodied limbs (p=0.00 and p=0.04 respectively). For the hip kinematics in the frontal plane, the maximum abduction angle was significantly greater (p=0.00) in the intact and able-bodied limbs compared to the residual limbs. The hip abduction torque was significantly smaller (p=0.00) in the residual limbs compared to the intact and able-bodied for both peaks. There was no significant difference in self-selected gait speed between the UTF participants and the able-bodied participants which was 1.08 m/s and 1.23 m/s respectively (p=0.20).

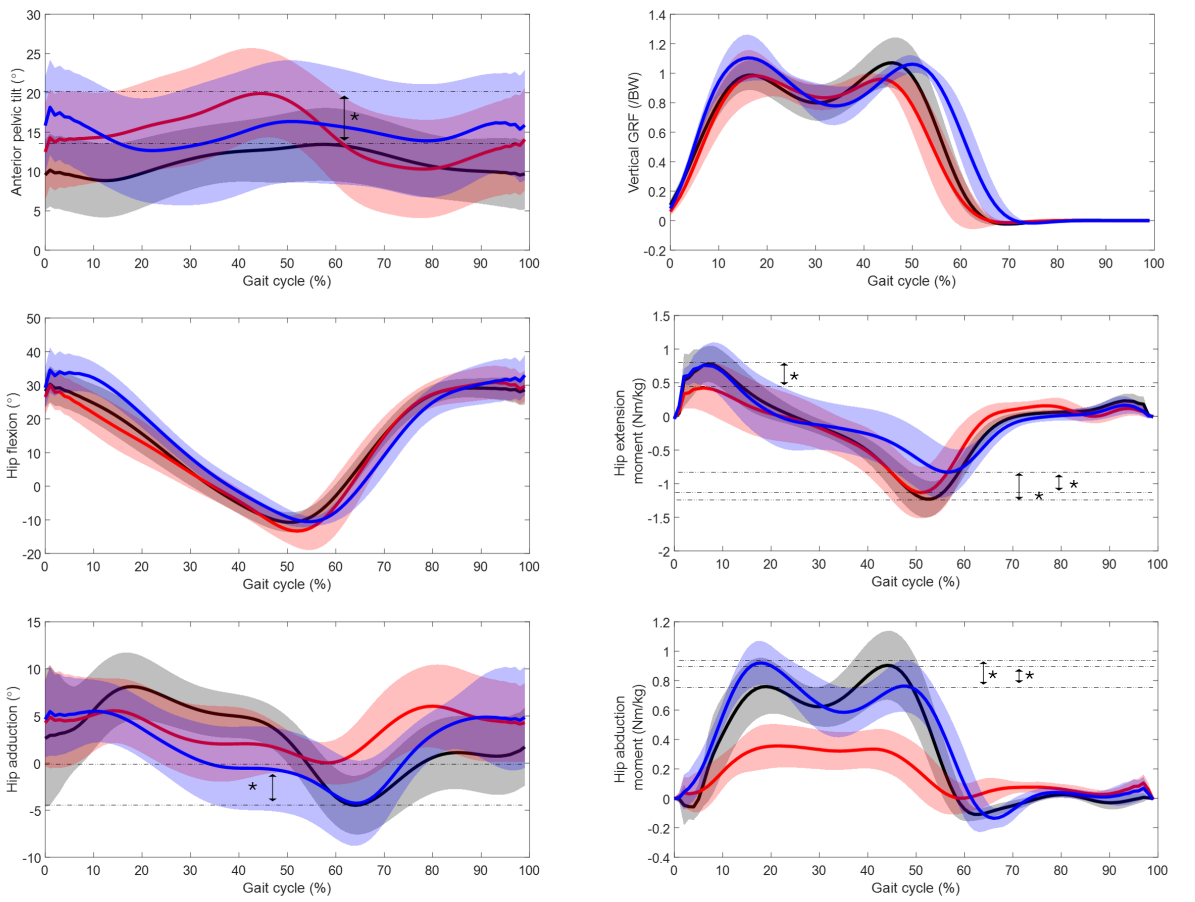


Figure 3.8: Kinetic and kinematic parameters over gait cycle from initial foot contact (0%–100%) for the residual limb group (red, n = 11 ± SD), the intact limb group (blue, n = 10 ± SD) and the able-bodied control limb group (black, n = 22 ± SD). Solid line represents mean and shaded standard deviation. Arrows and '*' indicate a significant difference in peak value.

3.4 Discussion and conclusion

This is the first study to have quantified normalised muscle force, impulse, and peak activation during gait of individuals with transfemoral amputations of a 'high-functioning' demographic due to their comprehensive rehabilitation, high levels of fitness prior to surgery and state-of the-art prosthetics. Comparable self-selected walking speeds of the UTF participants to the matched able-bodied controls demonstrate this 'high-functionality' (Jarvis et al. 2017).

3.4.1 Muscle recruitment

Force magnitude

The muscle recruitment strategies with respect to maximum muscle force of the major hip muscles in able-bodied limbs and the intact limbs of individuals with UTF are broadly similar, with only a significant difference in pectineus force. However, there are significant differences in the plantar flexor muscle forces, Figure 3.5. The increased recruitment in the intact limb of individuals with transfemoral amputations during 50 -60% gait is in agreement with EMG studies (Mehryar et al. 2021) (Wentink et al. 2013) which show increased recruitment of the plantar flexors in the intact limb of individuals with unilateral amputations to compensate for the amputated side.

It appears that muscle recruitment strategies in the residual limb group differs from the intact limb group and able-bodied limb group. Evidently, the psoas major and iliacus of the residual limb in individuals with UTF are heavily relied upon to actuate gait, with the first and third largest values of maximum muscle force across all muscles of all groups at 1.50 N/BW and 1.40 N/BW, these values appear to be abnormal (ie. significantly larger than the able-bodied controls). This is indicative of the loss of the forward propulsion from the plantar flexors with the amputation, that has been reported as a reduced torque of the ankle on the prosthetic side (Seroussi et al. 1996). Therefore, the demand on these intact proximal hip flexors increases. It appears the adductor longus, tensor fasciae latae and pectineus may also be recruited to flex the hip in the residual limb for this reason. As shown in Figure 3.4, these muscles of the residual limb peak similarly to the iliacus and psoas major, at terminal stance phase / pre-swing phase of gait (40-60%) when flexion action is required. These muscles have secondary flexor function (Neumann 2010). This coincides with the increased peak in hip flexion moment of the residual limb group compared to the intact limb group, Figure 3.8. One study which recorded electromyography (EMG) of the residual limb during gait, found that more muscles were active and for longer periods during this 'pre-swing' phase of gait in the residual limb compared to able-bodied controls (Wentink et al. 2013). The rectus femoris and sartorius, which are primary hip flexors in the intact anatomy / able-bodied anatomy, are compromised by the amputation surgery (Henson et al. 2021). This may increase the demand on the iliopsoas, adductor longus, tensor fasciae latae and pectineus. The anatomical location of these muscles in an able-bodied individual are pictured in Figure 3.9 (Schwartzman & Ramamurti 2021). The force reached by these muscles in the residual limb group appears to be abnormal, as it is significantly higher than in the able-bodied group. This abnormal force requirement may have an effect on muscular endurance and therefore gait endurance (Fang et al. 2007).

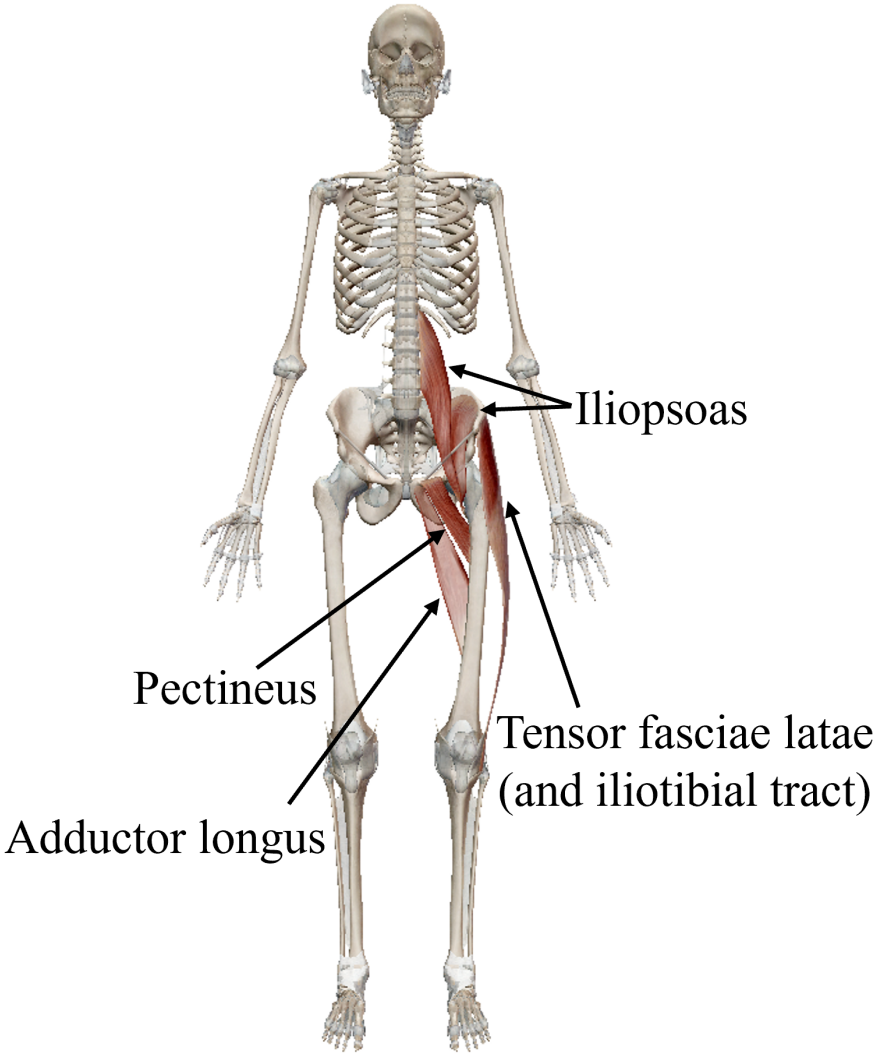


Figure 3.9: The iliopsoas, adductor longus, tensor fasciae latae and pectineus muscles on an able-bodied individual, edited from Schwartzman & Ramamurti (2021)

The imbalanced recruitment of the iliopsoas between the bilateral limbs of individuals with UTF has not been reported in the literature. In fact, a study by Harandi et al. (2020) estimated the opposite conditions with slightly higher levels of force in the iliacus on the intact side, yet comparisons are hard to make, because they included non-microprocessor knees and older participants in their study. As Jarvis et al. (2021) highlights, this is a group representing a high functioning demographic compared to a more general UTF population. So, perhaps they exhibit a higher functionality which is demanding more of the iliopsoas. Due to the position of the iliopsoas, it is challenging to validate its activation with EMG data. Asymmetry in the lumbopelvic region has been associated with the increased levels of lower back pain in the transfemoral amputation population as an 'mal-adaptive' impairment in this population's gait (Devan et al. 2014), therefore

the asymmetry found in the magnitude of iliopsoas contraction may have implications on secondary conditions such as lower back pain.

The elevated magnitudes of muscle force of the iliopsoas, adductor longus, tensor fasciae latae and pectineus in the residual limb may be unexpected due to the atrophy that is known to occur in the residual limbs post transfemoral amputation (Henson et al. 2021). However, when using normalisation methods which correct for thigh length, the maximum isometric extension, flexion, and abduction torque potential of the residual limbs of individuals with unilateral amputations is significantly greater than the intact, and equal to able-bodied control limbs (Sawers & Fatone 2023). Furthermore, Sawers and Fatone (2023) found the hip adduction strength to be significantly greater in the residual compared to the intact and the control group, and suggested that this may be due to increased activation of the adductor muscles during gait. It may be that the increased recruitment of the adductor longus during gait found in our study contributes to the increased strength of hip adduction torque in this population.

Unlike the iliopsoas and other flexor muscles, the major extensor muscles in the residual limb appear to be recruited to a lesser magnitude than in both the controls and the intact side, Figure 3.3. The hamstrings are biarticular muscles in the intact state, yet they take a monoarticular function when cleaved and re-inserted in a transfemoral amputation (Henson et al. 2021). Due to this loss in function, they are found to be atrophied in the transfemoral residual limb Jaegers et al. (1995). Although the gluteus maximus only articulates the hip, being the main hip extensor in the intact anatomy, it has also been found to be atrophied in the residual limb (Jaegers et al. 1995). The gluteus maximus inserts via the iliotibial tract which tends to require re-insertion in transfemoral amputation. So, although the individual's residual limb anatomy will depend on the residual limb length, specifics of the traumatic injury and detailed surgical procedure used, the main hip extensors in the residual limb are all potentially functionally compromised by the surgery, which may explain their reduced recruitment compared to the intact and able-bodied limb groups. This imbalanced recruitment of the extensor/flexors on the residual limb side may impact pelvis stabilisation, and therefore pelvis kinematics. There is a peak in average anterior pelvis tilt at roughly 50% of the gait cycle for the residual limb group (Figure 3.8) which may be associated the recruitment of iliacus and the psoas major muscles (Figure 3.2) as their peak force and peak anterior pelvic tilt coincide.

The increased burden on the plantar flexors of the intact limb and of the hip flexors of the residual limb reinforces the theoretical need for powered prosthetic knee, which generate energy to compensate for the power lost with the absent muscles in lower limb amputation. However, currently powered yellow prosthetic knees tend to be heavier than a microprocessor or mechanical prosthetic knee, increasing loading on the residual limb which limits their use, particularly for those with transfemoral amputation (Gehlhar et al. 2023).

Impulse and peak activation

Together peak activation - force relative to maximum capacity - and impulse - an index of muscular energy expenditure - give an indication of the endurance implications of muscle recruitment (West et al. 1995) (Bemben et al. 1996). The peak activation and impulse are abnormally high (ie. greater than the controls) for the flexor residual limb muscles highlighted previously: iliopsoas, adductor longus and tensor fasciae latae. This indicates a potential cause for reduced gait endurance. It has previously been shown that an exoskeleton on the residual limb providing external torque (flexion and extension) in the sagittal plane reduces the metabolic cost of gait by 15.6 % for individuals with transfemoral amputations (Ishmael et al. 2021). The peak power injected in by the exoskeleton occurred at 60% of gait cycle assisting hip flexion with hip flexion torque (Ishmael et al. 2021). Considering the apparent increased energy expenditure of the hip flexors this may relate to the increased physiological cost of gait. Therefore, gait endurance could be improved if a similar functional ability was possible with reduced requirements on the flexor muscles (Ishmael et al. 2021). The estimations of peak activation tend to be higher in the residual limb which is indicative to the loss in muscular capacity (through atrophy and amputation).

Although the recruitment and function of the intact and able-bodied limbs appears to be similar, the impulse in the intact limb is significantly greater than the able-bodied for all main hip muscles apart from the adductor longus, Figure 3.6. This indicates that the intact limb is having to expend significantly greater energy to actuate gait compared to the able-bodied group and agrees with higher oxygen cost (Jarvis et al. 2017) and lower walking endurance (Linberg et al. 2013).

3.4.2 Kinematic and kinetic interpretation

The participants with UTF amputations exhibited higher levels of anterior pelvic tilt compared to the controls and a significantly higher hip extension torque and a lower hip flexion torque in the intact limb compared to the residual limb, Figure 3.4. This is in agreement with a study of a similar population (Jarvis et al. 2021). This is consistent with the respective increased flexor muscle recruitment and lower extensor muscle recruitment in the residual limb. The frontal torque exhibits significant differences between the residual and the intact limb, with the hip abduction torque on the residual limb being significantly smaller. This does not seem to be explained simply by differences in hip frontal kinematics, Figure 3.8, further investigation into the relationship between differences in external loading (GRF) and differences limb kinematics is required.

3.4.3 Limitations

There are several limitations to this study. Firstly, in terms of musculoskeletal modelling, the residual limb and prosthetic limb configuration was modelled as a rigid body composite 'thigh' segment, neglecting pistoning and swivelling. The effect of this assumption is not known, yet a study with transtibial amputations found that including this relative

motion had little effect on modelled metabolic costs, derived from muscle forces (Miller & Esposito 2021). The anatomical geometries of the individuals with UTF were scaled from datasets of able-bodied participants and participants with bilateral transfemoral amputations for their intact and residual limbs respectively. Using anatomical datasets from the intact limb and residual limb of participants with UTF would have been more accurate. There may be some patterns in atrophy/ hypertrophy that occur due to muscle recruitment patterns in gait in the UTF population that are not accounted for in this current model. Additionally, variations in surgical technique will impact the recruitment capabilities. There are two main methods of muscle stabilization, myodesis, where the muscles are sutured directly to the bone, and myoplasty, where the agonistic and antagonistic muscles are sutured together (Fabre et al. 2024). This variation was not considered in the anatomical dataset selection. Using anatomical geometries derived from participant specific MRI scans would have reduced error in muscle force estimations (Toderita et al. 2021). Finally, the experimental data was obtained from two motion capture laboratories. Typically studies will present data from one laboratory only for reasons of consistency. However, in order to maximise participant recruitment and participation, a regional approach was taken by providing two laboratory locations. The laboratory technicians ensured a standardised calibration protocol was completed at each location and a consistent data collection protocol was followed.

3.4.4 Comparison to the results of Chapter 2

In Chapter 2, the muscle activations of the residual limbs of individuals with BTF / BTK amputations were identified as 'overburdened' muscles if they were recruited to over a mean value of 0.5 activation. This was based on values gathered from the literature of muscle activity from able-bodied walking. This follows the assumption that baseline walking for able-bodied individuals is an optimised motion that minimises muscle activation / muscular effort to preserve energy. This threshold of 0.5 activation for 'normal' muscle activations during walking for able-bodied individuals is supported by the results of this chapter as the maximum activations of the able-bodied control group were below this threshold, Figure 3.7. This supports the assumption that muscle activations above this threshold may lead to reduced muscular endurance.

The pattern in muscle recruitment is similar, in some respects, for the residual limbs of individuals with BTF / BTF amputations in Chapter 2 and the residual limbs of individuals UTF in this chapter. It seems that the muscles with flexor action are recruited to relatively high muscle activations and magnitudes in both groups (bilateral TF / TK and unilateral TF). This suggests that the loss of plantar flexor torque increases the demand on the residual limb in both the bilateral and unilateral conditions and potentially in a similar manner for the TF and TK conditions. However, there appears to be differences in other aspects, for example recruitment of the extensors. It appears the biceps femoris and semitendenous muscles of the residual limb of individuals with BTF / BTK amputations, in Chapter 3, are recruited to higher magnitudes and activations than in the residual limb of individuals with UTF amputations. Perhaps in the unilateral condition the intact limb compensates for the residual limb side, relieving the force required of

the extensors. This exhibits how walking with bilateral amputation is more functional demanding than with unilateral amputation.

3.4.5 Conclusion

This chapter found individuals with unilateral transfemoral amputations to have similar muscle recruitment strategies in their intact limb compared to the limbs of the able-bodied controls. However, muscle recruitment in the residual limb group varies significantly from the intact and able-bodied group, this is particularly true for the iliacus, the psoas major, the adductor longus and the tensor fasciae latae. The demand on these muscles for flexor action appears to be elevated in the residual limb function due to the loss in forward propulsion from the loss of the plantar flexors. Although this group (fairly young, majority donning a microprocessor prosthetic knee, and majority ex-military) is likely to be of high functionality compared to a more general UTF population, there is room for improvement in their rehabilitation. To increase gait endurance and reduce the asymmetry in loading of the lumbo-pelvic region, which may be related to lower back pain, rehabilitation strategies to reduce this demand (on the residual and intact limbs) and to correct the asymmetry between muscle groups in the residual and intact limb of individuals with UTF should be developed. Chapter 2 and 3 addressed the first objective of this thesis, to quantify muscle recruitment and function during walking for individuals with unilateral and bilateral transfemoral and through-knee amputations. The subsequent chapters will address the final three objectives, focusing on developing rehabilitation strategies to improve walking endurance. This will be achieved through forward dynamic MSK modeling and the implementation of biofeedback gait retraining tools, building on the conclusions drawn from this chapter.

Chapter 4

A forward dynamics model of unilateral transfemoral and through-knee amputations: a tool to propose novel rehabilitation methods

Chapter 3 highlighted the elevated demand on the hip flexors of the residual limb during walking for individuals with unilateral transfemoral amputations. To address the second objective of this thesis, a forward dynamic musculoskeletal model of individuals with unilateral transfemoral and through-knee amputations was developed to allow the prediction of novel motion that reduces the burden on the iliopsoas muscle group. The iliopsoas muscle group was selected as a point of focus from the analysis in Chapter 3 as they are the primary flexors in the residual limb, demonstrated by the relatively high magnitudes of force compared to the other hip flexors. The elevated energy expenditure, as demonstrated by the elevated impulse and elevated intensity of muscle contractions compared to the able-bodied controls in Chapter 3 indicated that the recruitment patterns of the iliopsoas muscle in the residual limb may be a source of reduced walking endurance. As unilateral amputation due to trauma is globally more common than bilateral amputation due to trauma (Yuan et al. 2023), a musculoskeletal model of unilateral amputation was taken as the first step in this research. Addressing the fourth objective of this thesis, this model can be used as part of a methodological pipeline to develop rehabilitation research for increased functionality, specifically walking endurance, in this population.

4.1 Introduction

4.1.1 Motivation

The results of Chapter 3 suggest it may be beneficial to walking endurance to reduce the demand on the iliopsoas muscle of the residual limb during walking for individuals with unilateral transfemoral amputations.

The inverse musculoskeletal modelling methods that have been applied in Chapter 2 and 3 are restricted to prescribed motion (the motion data captured experimentally of marker co-ordinates and ground reaction force), as they utilise this data to calculate the joint angles and the net joint moments, and then solve the indeterminate problem of muscle redundancy / joint moments, using static optimisation to estimate the load sharing. Although inverse dynamics models are an efficient and effective estimation of muscle forces for slow motion such as walking (De Groote et al. 2016)(Anderson & Pandy 2001), inverse dynamic musculoskeletal modelling inherently cannot predict novel motion, or any motion that deviates from the recorded motion data. However, forward dynamic musculoskeletal modelling utilises the dynamics of the musculoskeletal model itself to predict forward simulations of muscle (actuator) forces / torques and body motion according to goals.

To predict a solution of walking with reduced recruitment of the iliopsoas muscle, a forward dynamic musculoskeletal model is required to predict kinematics that deviate from recorded motion. Therefore, the aim of this chapter was to develop a forward dynamic musculoskeletal modelling approach for predicting walking motion of individuals with unilateral transfemoral (UTF) and through-knee (UTK) amputations, which can be applied to predicting walking kinematics which are less demanding of the iliopsoas of the residual limb. Detailed aims are defined later on after the background section.

4.1.2 Background of modelling technique

OpenSim Moco to solve optimal control problems

In forward dynamic MSK modelling it is assumed that motion and coordination of the musculoskeletal system is naturally an optimal control problem, ie. the control of the musculoskeletal system is executed to minimize energy consumption, or another movement goal. Mathematically optimal control problems find the continuous states and controls of a system that minimise a cost subject to the system dynamics (equations describing how the system moves, which are differential). Optimal control finds the 'best' feasible (ie. satisfies the problems conditions) trajectory. An objective function defines the 'best' trajectory (Kelly 2017). Forward dynamic MSK modelling has been implemented previously using a variety of methods. For example, OpenSim SCONE (Simulated Controller Optimization Environment) which uses shooting-based methods to solve these optimal control problems. Shooting-based simulations tend to have long convergence times, whereas an alternative method, direct collocation, has been shown to result in shorter simulations (De Groote et al. 2016). OpenSim Moco (Dembia et al.

2020) facilitates forward dynamic simulations solved with direct collocation. Direct collocation discretizes the optimal control problem, this process is called transcription, by approximating the continuous functions in the problem into polynomial splines over a mesh of time points (Dembia et al. 2020) (Kelly 2017). Hermite- Simpson transcription (Kelly 2017) is used in Moco. The optimiser solves for the knot points that satisfy the system dynamics; the time derivatives of the state splines are enforced to match the system differential equations at that time (Dembia et al. 2020) and solved simultaneously as a non-linear programming problem (De Groote et al. 2016). 'Goals' can be added to Moco problems in the form of cost terms that are minimised in the objective function or boundary constraints. Weights are applied to these goals. Tracking simulations are a subset of optimal control problems that can be implemented in OpenSim Moco. Tracking simulations have a 'cost' term in the objective function that minimises the error between experimental data (for example, marker coordinates or ground reaction force) and the simulated values. Tracking simulations can be used to solve optimal control problems that recreate motion based on experimental motion data (Miller & Esposito 2021). Alternatively, OpenSim Moco has been used to predict novel motion thereby overcoming the constraints of experimental data collection (Dembia et al. 2020).

OpenSim Moco has been used to predict gait for a variety of applications, for example to predict gait modifications that may reduce the progression of knee osteoarthritis in patients (Gupta et al. 2022), to simulate the effects of exoskeletons (Bianco et al. 2023) (Ostraich & Riemer 2024) and to assess the impact on metabolic cost of a transtibial amputation (Miller & Esposito 2021). Gupta et al (2022) highlighted the importance of subject specific modelling in their study, which predicted gait modifications required for reduced knee adduction moment, as although they observed a generalisable modification in gait patterns (an increased step width), the four participants they simulated achieved this modification with differing kinematic strategies (Gupta et al. 2022). These differing strategies may be important in the clinical application of their findings, as highlighted by Uhlrich et al (2022), who demonstrated experimentally the importance of personalisation when prescribing gait modifications to individuals with knee osteoarthritis.

Modelling of microprocessor knee

Inverse dynamic modelling enables the torque and forces at the prosthetic knee to be calculated based on kinematic and external force inputs. However, when forward dynamic modelling is used, the way that the prosthetic knee and ankle joints respond to the dynamics of the motion cannot be inferred directly and a model of the dynamics of the prosthetic knee and ankle joints are required. Microprocessor prosthetic knees (MPK) implement dynamic damping to allow for natural gait kinematics. Integrated sensors in MPK's inform the implementation of variable damping throughout the gait cycle, which adapts to different gait speeds and is calibrated to the wearer. The algorithms that produce the damping based on sensor inputs are proprietary to the prosthetic manufacture and so are not known. In order to implement a model of this, some inferences are required. A study by Miller (2023) modelled an MPK in OpenSim Moco with a generalised spring force, and additional torque actuator which supplemented the spring model

(Miller et al. 2023). Another study which built an OpenSim model of an individual with a prosthetic knee applied ideal actuators to the joint, as the kinematics were prescribed (Raveendranathan et al. 2023). More complex mathematical models of the MPK dynamics have been proposed, derived from bench test experiments and estimations of the dynamics of the variable damping of an MPK, though these have not been implemented into forward dynamic modelling (Chien et al. 2014) (van den Bogert et al. 2012).

4.1.3 Aim and objective

The aim of this study was to develop a model that can be used for forward dynamic subject specific musculoskeletal modelling to predict walking in individuals with UTF / UTK amputations, and to use this model to predict gait modifications that reduce the demand on the iliacus and psoas major muscle in the residual limb. The objective of this study is to use the predictions of forward dynamics musculoskeletal model to propose gait modifications that could be incorporated in a gait retraining protocol for individuals with UTF / UTK amputations to reduce the demand on the iliopsoas muscle group in the residual limb, and therefore improve walking endurance.

4.2 Method

4.2.1 Participants

This study took a subject specific approach to musculoskeletal modelling and focused on three individuals with transfemoral amputation and one individual with through-knee amputation. Participant information, including their prosthetic devices displayed in Table 4.1. Although, the findings of Chapter 3 were based on a group of individuals with unilateral transfemoral amputations, this study includes an individual with a unilateral through-knee amputation to increase the translation potential of this study. For an individual with a through-knee (TK) amputation, the loss of plantar-flexor function likely places a comparable demand on the iliopsoas muscle. This assumption is supported by the muscle recruitment patterns exhibited by the mixed group of individuals with TK and TF amputations in Chapter 2. Ethical approval was received from the Imperial College Research Ethics Committee and written informed consent obtained from the participants. These participants are a subset of participants from other studies, so cannot self-identify from these results.

Table 4.1: Participant information of the transfemoral (TF) and through-knee (TK) participants, *calculated following Eq.3.5 in Chapter 3

Participant code	01	02	03	04
Amputations level	TF	TF	TK	TF
Age (years)	46.9	47.0	47.0	57.0
Sex	M	M	M	M
Height (m)	1.77	1.76	1.77	1.76
Body mass with prosthetic (kg)	94.1	93.8	79.9	91.8
Estimated intact body mass (kg)*	95.5	95.4	82.2	97.8
Residual limb length (cm)	37.8	37	31	34
Intact thigh length (cm)	45	42	31	38
Prosthetic knee type	Ottobock Genium X3	Ottobock Genium X3	Ottobock Genium X3	Ottobock C-leg 4
Prosthetic foot type	Ottobock Triton	Ottobock Triton	Ottobock Triton	Ottobock Triton

4.2.2 The generic UTF model

A generic model of an individual with a unilateral transfemoral amputation (UTF) was created by adapting an able-bodied model published by Rajagopal et al (2016). The generic model is presented in Figure 4.1. As per the original able-bodied model, the muscles are represented by massless muscle-tendon units with a line of action from origin to insertion. Muscles with larger attachment areas are represented by multiple muscle-tendon units. The Hill-type muscle model (Zajac 1989) is used as shown in Figure 4.2 (De Groote et al. 2016). The Hill – type muscle actuator is represented by a contractile element of the muscle (CE) in parallel with the passive element of the muscle (PE), which are in series with the tendon (T). In this diagram (Figure 4.2) l_M is muscle length, l_T is tendon length, l_{MT} is muscle tendon length and α is muscle pennation angle.

The muscle architecture in the able-bodied Rajagopal model was built combining MRI acquired muscle volumes from young adults (Handsfield et al. 2014) and cadaver acquired pennation angles and optimal fibre length (Ward et al. 2009). Optimal force was calculated from the muscle volumes, acquired from MRI (Handsfield et al. 2014). The total muscle mass was calculated from the model mass and height, and the individual muscle mass was calculated using muscle volume fraction following Handsfield et al. (2014). PCSA was calculated and multiplied by muscle tension, taken as 60 N/cm^2 (Rajagopal et al. 2016), to estimate the maximum isometric fiber force.

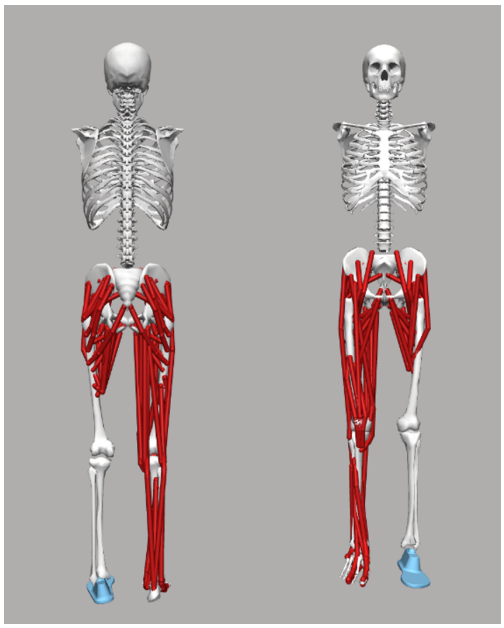


Figure 4.1: OpenSim transfemoral amputee model

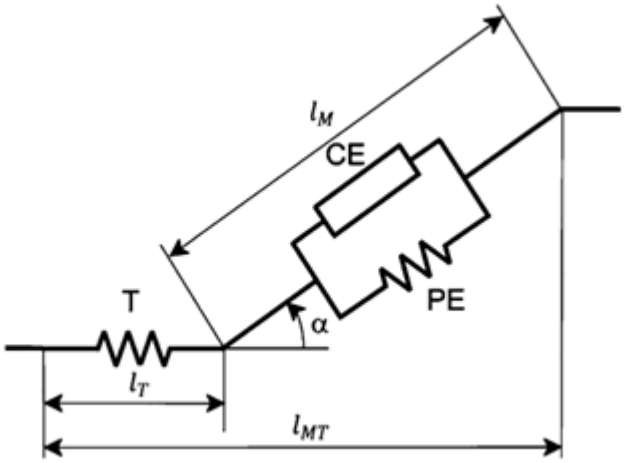


Figure 4.2: A Hill- type muscle actuator schematic (De Groote et al. 2016)

Body and joint adaptations for the generic UTF model

The original able-bodied Rajagopal model was made up of 22 articulating rigid bodies. To represent an individual with a UTF amputations of the left side, the left foot bodies (talus, calcaneus and toes) and the left patella, and associated joints and constraints, were removed. The foot segment was replaced with a prosthetic foot, the geometry of which was taken from a published transtibial model (Willson et al. 2022). On the side of the amputations, the left tibia remained, as this rigid body was an adequate representation of the shank segment, or pylon, of a prosthetic. The left femur also remained as the socket and the residual limb were modelled as a singular rigid body. Pistoning of the

residual limb in relation to the socket is not accounted for in this model as a previous study found that modelling the pistoning in an individual with transtibial amputation had a minimal effect on the modelled metabolic cost derived from muscle forces, which is the focus of this study, and did not affect the quality of kinematic tracking (Miller & Esposito 2021). The mass, the centre of mass (COM) and moment of inertia of the prosthetic foot and pylon bodies were adapted to values from previously collected experimental data as used in Chapter 3 (Toderita et al. 2021), which were acquired through the reaction board with moment of equilibrium method (Smith et al. 2014). The mass properties of the femur body (representing a composite of the socket and residual limb) were adapted on a subject specific basis, detailed below. The 'prosthetic' knee and ankle joints on the side of amputations were configured as pin-joints with one degree of freedom (DoF) which was flexion. The prosthetic 'ankle' represents the impression of articulation given with the dynamic response foot. The range of motion of the 'prosthetic' ankle joint was reduced to 20°plantar flexion and 20 °dorsiflexion to represent the reduced range of motion of the prosthetic ankle compared to the intact ankle exhibited in previous inverse kinematic analysis (Jarvis et al. 2021). The 'intact' limb metatarsophalangeal and subtalar joints were locked pin joints in the original able-bodied Rajagopal model, so these were replaced with weldjoint (no range of motion) to be compatible with the optimal control simulations. The upper limb bodies (ulna, radius, humerus and hand) were removed from the model to simplify the model and reduce computational expense of the forward dynamic simulations, as the upper limb kinematics are out of the scope of this study, and it was assumed that the participants would preserve normal upper limb dynamics in the forward dynamic solutions. This method has been used in a previous study, which achieved good results in direct collocation tracking simulations of the 3D dynamics of walking for able bodied participants (Lin & Pandy 2017). The mass of the upper limb bodies was added to the torso. The UTF model therefore consisted of 11 articulating rigid bodies which are listed in table 4.2. The corresponding joints and joint definitions are listed in table 4.3.

Table 4.2: Body segments in the generic UTF model

Segment	BodySet name
Pelvis	pelvis
Right thigh	femur_r
Right calf	tibia_r
Right patella	patella_r
Right talus	talus_r
Right calcaneus	calcn_r
Right toes	toes_r
Left residual limb and socket	femur_l
Left prosthetic pylon	tibia_l
Left prosthetic foot	talus_l
Torso	torso

Table 4.3: Joints and joint definitions in the generic UTF model

Joint	JointSet name	Type	Coordinates (DOF)
	ground_pelvis	CustomJoint	-90 to 90° pelvic tilt, list, rotation and X,Y,Z translation with respect to ground
Lumbopelvic	back	CustomJoint	-90 to 90° lumbar extension, bending, and rotation
Right hip	hip_r	CustomJoint	30° extension to 120° flexion, 50° abduction to 30° adduction, and 40° external rotation to 40° internal rotation
Right knee	walker_knee_r	CustomJoint	0 to 120° flexion
Right Patellofemoral	patellofemoral_r	CustomJoint	
Right ankle	ankle_r	PinJoint	40° plantarflexion to 30° dorsiflexion
Right subtalar	subtalar_r	WeldJoint	0
Right metatarsophalangeal	mtp_r	WeldJoint	0
Left hip	hip_l	CustomJoint	30° extension to 120° flexion, 50° abduction to 30° adduction, and 40° external rotation to 40° internal rotation
Left knee	walker_knee_l	PinJoint	0° to 120° flexion
Left ankle	ankle_l	PinJoint	20° plantarflexion to 20 ° dorsiflexion

Muscle and actuator adaptations for the generic UTF model

All distally inserting muscles from the knee joint on the amputated side (left) were removed to represent the amputations. The vastus muscles were also removed as they become functionally redundant in the transfemoral state and are atrophied accordingly (Henson et al. 2021). The distal segment of the rectus femoris was removed, the biceps femoris, the gracilis, the tensor fascia latae, the sartorius, the semimembranosus, the semitendinosus, and the ischial segment of the adductor magnus, were re-inserted to a more proximal site. The residual limb consisted of 26 remaining muscles and intact limb consisted of 40 muscles. All muscles included in the generic UTF model are listed in table 4.4. The model represents a transfemoral amputated limb with surgery following the Myodesis technique as this approach is recommended over the Myoplasty technique due to its advantage in preserving muscle tension (Jorge 2020). Myodesis involves suturing

the re-inserted straight onto the femur under tension (Ranz et al. 2017). In the anterior-posterior axis and the transverse axis, the insertion of the re-inserted muscles was set to be in-line with the femur body origin, as to represent attachment to the centre of the femur. In longitudinal axis of the residual limb and socket segment the re-insertion for the general model was based on average residual limb length. This was calculated from the average residual limb / femoral length ratio reported from 26 traumatic unilateral transfemoral amputees. This average residual limb length was found to be 0.58 of the intact limb length (Bell et al. 2014). This longitudinal axis attachment site was then adapted for each participant as detailed below, the anterior-posterior axis and the transverse axis attachment coordinates remained consistent to the generic model for all participant. The muscle representation of the residual limb in the generic OpenSim model of an individual with transfemoral amputation is displayed posteriorly and anteriorly in Figure 4.1. A 'CoordinateActuator', which provides a generalized force in the direction of the coordinates of the joint it is assigned to, was added to the prosthetic (left) knee and ankle for static optimisation (the 'inverse dynamic') simulations of this study. The lumbopelvic 'back' joint was actuated by a 'CoordinateActuator' in 3 DoF as per the original model.

Table 4.4: Muscle in the generic UTF model

Muscles		**Muscle actuator name**
Right adductor brevis		addbrev_r
Right adductor longus		addlong_r
Right adductor magnus	Distal	addmagDist_r
	Ischial	addmagIsch_r
	Middle	addmagMid_r
	Proximal	addmagProx_r
Right biceps femoris	Long head	bflh_r
	Short head	bfsh_r
Right extensor digitorum longus		edl_r
Right extensor hallucis longus		ehl_r
Right flexor digitorum longus		fdl_r
Right flexor hallucis longus		fhl_r
Right gastrocnemius lateral head		gaslat_r
Right gastrocnemius medial head		gasmed_r
Right gluteus maximus	Superior	glmax1_r
	Middle	glmax2_r
	Inferior	glmax3_r
Right gluteus medius	Anterior	glmed1_r
	Middle	glmed2_r
	Posterior	glmed3_r

Right gluteus minimus	Anterior Middle Posterior	glmin1_r glmin2_r glmin3_r
Right gracilis		grac_r
Right iliacus		iliacus_r
Right peroneus brevis		perbrev_r
Right peroneus longus		perlong_r
Right piriformis		piri_r
Right psoas		psoas_r
Right rectus femoris		recfem_r
Right sartorius		sart_r
Right semimembranosus		semimem_r
Right semitendinosus		semiten_r
Right soleus		soleus_r
Right tensor fascia latae		tfl_r
Right tibialis anterior		tibant_r
Right tibialis posterior		tibpost_r
Right vastus intermedius		vasint_r
Right vastus lateralis		vaslat_r
Right vastus medialis		vasmed_r
Left adductor brevis		addbrev_l
Left adductor longus		addlong_l
Left adductor magnus	Distal Ischial Middle Proximal	addmagDist_l addmagIsch_l addmagMid_l addmagProx_l
Left biceps femoris	Long head Short head	bflh_l bfsh_l
Left gluteus maximus	Superior Middle Inferior	glmax1_l glmax2_l glmax3_l
Left gluteus medius	Anterior Middle Posterior	glmed1_l glmed2_l glmed3_l

Left gluteus minimus	Anterior Middle Superior	glmin1_l glmin2_l glmin3_l
Left gracilis		grac_l
Left iliacus		iliacus_l
Left piriformis		piri_l
Left psoas		psoas_l
Left rectus femoris		recfem_l
Left sartorius		sart_l
Left semimembranosus		semimem_l
Left semitendinosus		semiten_l
Left tensor fascia latae		tfl_l

Marker adaptations for the generic UTF model

32 virtual markers were added to the generic UTF model at the anatomical locations listed in table 4.5. For the prosthetic foot and ankle these anatomical locations were estimated to have a symmetrical position to the intact limb side, as is done with experimental motion capture protocols in this population.

Table 4.5: Optical motion tracking cluster and marker positions and labels

Marker label	Anatomical location
FCC	Calcaneus
FMT	Tuberosity of the fifth metatarsal
FM2	Head of the second metatarsal
TF	Additional marker placed on foot
FAM	Apex of the lateral malleolus
TAM	Apex of the medial malleolus
C1,C2,C3 (clusters)	Additional markers placed on the shank segment
FLE	Lateral femoral epicondyle
FME	Medial femoral epicondyle
T1,T2,T3 (clusters)	Additional markers placed on the thigh segment
RASIS	Right anterior superior iliac spine
LASIS	Left anterior superior iliac spine
RPSIS	Right posterior superior iliac spine
LPSIS	Left posterior superior iliac spine

Following publication, a digital version of the generic Open Sim will be submitted to the OpenSim online repository allowing for open access.

4.2.3 Subject specific UTF / UTK models

The model was scaled to represent 4 participants with UTF (N=3) and UTK (N=1) amputations using the static trial and the estimated intact bodyweight. The same method of estimated intact weight was followed as detailed in Chapter 3, following Eq.3.5. For the UTF models, the muscle attachments of the 're-inserted' muscles of the residual limb were adapted to represent the residual limb length in the longitudinal axis, ie. the longitudinal axis attachment coordinates were the length of the residual limb. The anterior-posterior axis and the transverse axis attachment coordinates were the same as the generic model. For the UTK model the original distal insertions at the femur from the able-bodied model were preserved in all three axis, as displayed in Figure. 4.3. Apart from muscle attachment site, the UTF and UTK muscles were identical, but scaled to the individual participant with the static trial and estimated intact bodyweight.

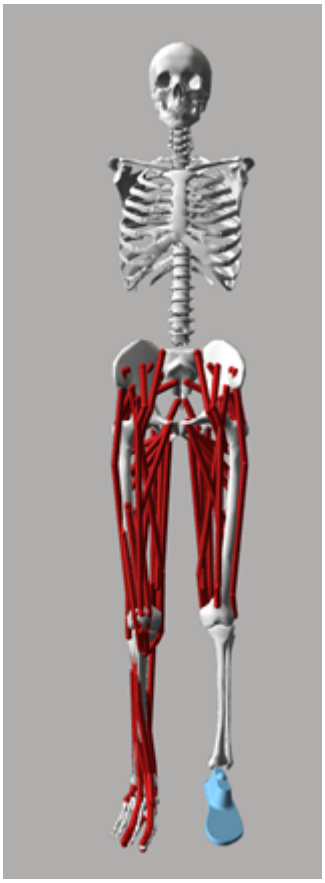


Figure 4.3: Muscle insertion for the unilateral through-knee participant

The composite thigh (residual limb and socket) inertial properties were calculated. Firstly, the mass of the residual limb was estimated from the ratio of the intact thigh length / residual limb length multiplied by the OpenSim scaled 'intact' femur mass. The mass of the composite thigh (residual limb and socket) was calculated by the addition of the estimated residual thigh mass and the experimental values of the socket mass used in Chapter 3. The inertial properties of the composite thigh segment were estimated using

the parallel axis theorem with the experimental values of the socket used in Chapter 3 and the De Leva's estimates (using the residual limb length and estimated intact mass) (De Leva 1996). The residual limb length was used to acquire the centre of mass (CoM) of the residual limb using De Leva's estimates (De Leva 1996). Experimental data of the socket CoM was used, as in Chapter 3. The CoM of the composite was calculated with Eq. 4.1.

$$CoM_{composite} = \frac{CoM_{residual} \times Mass_{residuum} + CoM_{socket} \times Mass_{socket}}{Mass_{socket} + Mass_{residuum}} \tag{4.1}$$

4.2.4 Model adaptations for optimal control (forward dynamic) simulations

Muscle adaptations

The muscles were swapped for the 'DeGrooteFregly2016' type muscles, which are hill-type models with smooth dynamic properties of activation and contraction that are compatible with the optimal control problems of Moco (continuous and differentiable). The muscle tendon dynamics are described in Figure 4.4 (De Groote et al. 2016), where f_t is tendon force, l_t is normalised tendon length, f_{act} is active muscle force (solid line in the graph), f_{pas} is passive muscle force (dashed line in the graph), l_M normalised muscle length, f_v is muscle force / velocity relationship and is $\tilde{v}M$ normalised muscle velocity.

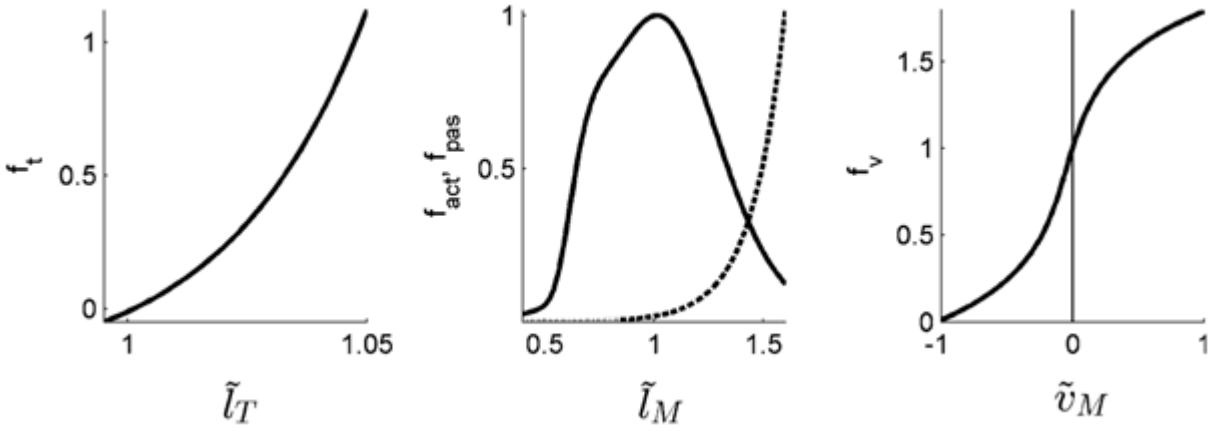


Figure 4.4: Muscle- tendon characteristics of 'DeGrooteFregly2016' muscles (De Groote et al. 2016)

Adaptions of the prosthetic joints for forward dynamic simulation

All participants donned a MPK knee and energy return foot. As discussed in the introduction, assumptions had to be made to model the prosthetic joints in the forward dynamic simulations as the control of the variable damping of an MPK is unknown. Both the knee and the ankle were actuated with a 'SpringGeneralizedForce'. This actuator provides a generalised force with spring characteristics, the stiffness and viscosity were

determined with moco in an 'parameter optimisation' simulation. The optimisation of parameters was completed for participant 04 to gain values for stiffness and viscosity. It was assumed these values were representative of all MPKs and energy return feet, so this stiffness and viscosity was used for all participants. In addition to the spring force, there were reserve actuators of 'CoordinateActuator', the torques of which were limited to 10 Nm. These actuators accounted for any force that was not accounted for by the spring actuators. The 'SpringGeneralizedForce' at the ankle is a representation of the dynamics of the 'energy return' feature of the dynamic response foot, but 'SpringGeneralizedForce' at the knee is a simplified model of the MPK.

Foot contact model

Foot- ground contact was modelled by 6 sphere-shaped Hunt-Crossley contact elements on the plantar surface of each foot (Sherman et al. 2011), Figure 4.5. The contact force parameters were taken from a previous study by Miller (2021) who obtained good ground reaction force tracking. Contact elements had an elastic modulus of 3.06 MPa and damping coefficient of 2.0 s/m so the deformation and elastic return replicates that of a human foot in a sports shoe (Aerts & Clercq 1993). The friction was modelled as a Stribeck function with static coefficient of 0.8, a dynamic coefficient of 0.8 and a viscous coefficient of 0.5 with a transition velocity of 0.2 m/s (Sherman et al. 2011) (Miller & Esposito 2021).

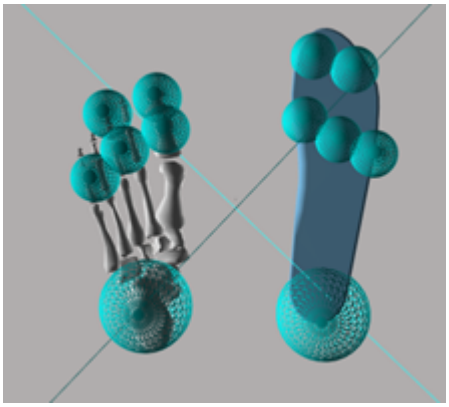


Figure 4.5: Plantar surface of the generic UTF model with contact spheres

4.2.5 Data collection

For each participant one static trial and one gait trial at a self-selected walking speed was collected. The gait trial consisted of at least one full gait cycle per leg (heel strike to heel strike). The collection of this data is described in Chapter 3, and briefly described here. Motion data (marker coordinates and external forces) were collected with a ten camera (VICON, Oxford Metrics Group, United Kingdom) and two force plate system (Kistler Type 9286B, Kistler Instrumented AG, Winterthur, Switzerland). The marker 3D displacement and ground reaction forces were sampled at 120 and 960 Hz, respectively.

4.2.6 Simulations and data processing

Inverse dynamics model validation

The first step was to validate the musculoskeletal model of the four individuals with UTF / UTK amputations with static optimisation to estimate muscle activations. To do so, inverse kinematics, inverse dynamics, and static optimisation simulations were completed with the OpenSim GUI. The static optimisation minimised the objective function, equation 4.2, subject to equation 4.3, where a_m is the activation of muscle m, F_m^0 is the maximum isometric force of muscle m, $r_{m,j}$ is moment arm of muscle m about the j^{th} joint, T_j joint torque acting about the j^{th} joint.

$$J = \sum_{m=1}^{n} (a_m)^3 \tag{4.2}$$

$$sum_{m=1}^{n} (a_m F_m^0) r_{m,j} \tag{4.3}$$

Forward dynamics simulations

The forward dynamics simulations were implemented with OpenSim Moco tools and scripted in MATLAB.

Tracking simulations of baseline gait for initial guess

When predicting novel motion in forward dynamic simulations it is useful to have an initial guess to guide the optimiser into a solution that resembles gait. An 'initial guess' of baseline gait was created from tracking simulations of the experimental and inverse kinematics data. This 'initial guess' was then used as a baseline comparison in subsequent simulations when observing the kinematic adaptations produced when solving to reduce the recruitment of the iliopsoas.

Open Moco utilises direct collocation to solve optimal control problems with a tracking element, that minimises the cost function (j_{track}) following Eq.4.4. The objective function (j_{track}) included cost terms of marker tracking, kinematic tracking and contact force tracking goals, as well as a muscular effort goal. The tracking elements minimize deviations from the experiment data of ground reaction force, marker coordinate data, and the results of inverse kinematics for the 3 DoF at the hip joints and 1 DoF at the knee and ankle joints. The muscular 'effort' term function is the excitation of the actuators (muscular and coordinate actuators) per unit distance. Deviations of the trunk from an upright position were minimised, to account for the lack of upper body markers in the experimental data (Miller & Esposito 2021). The 'weight' assigned to the objective function elements dictates how 'costly' this term is to the objective function. Equation 4.4 describes the tracking objective function where t_i is the initial time, t_f is final time , $d(t)_i^{exp}$ the marker (i) position in the experimental data at time(t), $d(t)_i^{sim}$ is the marker (i) position in the simulation at time(t), $d(t)_i^{exp}$ model joint angle (i) from experimental data at time (t), $q(t)_i^{sim}$ model joint angle (i) from simulated solution at

time (t), $O(t)_i^{neutral}$l is torso orientation (i) in natural upright position, $O(t)_i^{sim}$ is torso orientation (i) in simulation solution, $x(t)_i$ is simulated actuator control value at time (t), $GRF_{exp}(t)$ is experimental ground reaction force at time (t) and $GRF_{sim}(t)$ is simulated ground reaction force at time (t), w_m weight of the marker tracking term, w_k weight of the ankle, knee and hip joint kinematic tracking term, w_t weight of the torso orientation tracking term, w_e weight of the effort term (control excitations) and w_g is the weight of the contact tracking of the ground reaction force.

$$
\begin{aligned}
j_{track} = \min \int_{t_i}^{t_f} \Bigg[& w_m \cdot \sum_{i=1}^{32} \left(d(t)_i^{exp} - d(t)_i^{sim} \right)^2 \\
& + w_k \cdot \sum_{i=1}^{10} \left(q(t)_i^{exp} - q(t)_i^{sim} \right)^2 \\
& + w_t \cdot \sum_{i=1}^{3} \left(O(t)_i^{neutral} - O(t)_i^{sim} \right)^2 \\
& + w_e \cdot \sum_{i=1}^{85} \left(x(t)_i \right)^2 \\
& + w_g \cdot \sum_{i=1}^{6} \left(GRF_{exp}(t) - GRF_{sim}(t) \right)^2 \Bigg] dt
\end{aligned} \tag{4.4}
$$

In order to create 'normal' walking, speed was defined to be the self-selected walking speed from the experimental data. Walking speed was calculated for each participant from their recorded gait trial; the tracking simulations and subsequent simulations were constrained at this speed. The simulations were very sensitive to the weight given to the ground reaction force goal (w_g) and effort goal (w_e). To achieve a simulation that converged the following steps in simulation were taken, the initial weights were selected on a trial and error basis to achieve convergence, each solution of the steps was used as the first guess for the subsequent step:

1. a first tracking simulation just tracking the markers (w_m =10) and effort weight low (w_e =0.00001);
2. a tracking simulation tracking markers (w_m=10) and with recorded ground reaction force added to the model as a force (not tracked) and effort weight low (w_e =0.00001);
3. a tracking simulation with marker (w_m=10), ground reaction tracking of low weight (w_g = 0.00001) and effort weight low (w_e =0.00001); and
4. a tracking simulation with marker (w_m=10) and ground reaction tracking of low weight (w_g = 0.00001) and kinematic tracking (w_k=10) of inverse kinematic results and effort weight low (w_e =0.00001).

After this process had been followed the solution was iteratively improved. The w_g was increased incrementally until there was adequate tracking of ground reaction force, this was analysed visually from plotting results. The final weights for the ground reaction force were w_g= 0.01. The w_e was increased incrementally to the point where the kinematics were still being adequately tracked as assessed from plotting results, this was w_e = 0.01. A mesh refinement was then performed; the mesh density of the simulations was increased incrementally from N = 5 to N = 20 where N is the number of intervals. With the Hermite-Simpson transcription, the problem is evaluated at 2*N+1 nodes. It was observed that from N=5 to N=20 the tracking results improved (ie. improved in replicating the experimental data), but beyond N= 20 the results did not improve, yet significantly increased simulation time.

Data analysis of tracking results

The predicted kinematics and ground reaction forces were plotted against the results of the inverse kinematics and recorded ground reaction forces. The predicted muscle activations were cut and normalised to gait cycle, to aid comparison with previously published muscle activations for walking in this population.

The root mean square (RMS) error was calculated between the tracking results of joint kinematics and ground reaction force and the inverse kinematic results of joint angles and the recorded values of ground reaction force. The magnitude (M), phase (P) and combined (C) errors of the estimated muscle activations the tracking simulations and the muscle activations from the static optimisation results were quantified using the Sprague and Geers metric (Schwer 2007) for the key hip adductors, abductors, flexors and extensors of the intact and residual limb. The interpretations of these errors between the static optimisation muscle activations and the tracking muscle activations are defined in Table 4.6 (Klemt et al. 2019).

Table 4.6: Interpretation of error margins from the Sprague and Geers metric (Klemt et al. 2019)

Error margin	Similarity
0 – 0.15	Excellent
0.15 – 0.30	Very good
0.30 – 0.45	Good
0.45 – 0.60	Moderate
>0.60	None

Resultant kinematic modifications of 'enhanced walking'

The results of the tracking simulation were used as the first guess for the simulations that simulated reduced recruitment of the residual limb iliopsoas muscle. Walking with a goal of reduced muscle recruitment of the iliopsoas muscle force will be referred to as 'enhanced' walking in this study, following from recommendations in Chapter 3. The

predictive simulations of enhanced walking included a tracking element; this was done to predict novel kinematics that did not deviate too far from the participants natural gait to increase the likelihood of achieving the kinematics in a clinical setting, and for them to be learnt and retained by the participant. Walking speed was calculated from the inverse kinematic results and was preserved in the predictions of 'enhanced' gait to preserve the functionality / performance of gait. The first 'guess' of the 'enhanced' walking simulations was the final baseline tracking solution.

The key element of the 'enhanced' walking predictions was the addition of Equation 4.5 into the objective function. This element ($j_{activation.iliopsoas}$) will be referred to as the activation goal, which minimised the squared activation of the residual limb iliopsoas muscle elements, where $a(t)_i$ is the activation of the residual limb iliopsoas muscle elements at time (t) and w_a is the weight given to the activation goal in the objective function. The overall objective function of the enhanced walking conditions ($j_{enhanced}$) is show in equation 4.6.

$$J_{activation.iliopsoas} = min \int_{t_i}^{t_f} \left[w_a \cdot \sum_{i=1}^{2} (a(t)_i)^2 \right] dt \tag{4.5}$$

$$\begin{aligned} j_{enhanced} = \min \int_{t_i}^{t_f} \Bigg[& w_m \cdot \sum_{i=1}^{32} \left(d(t)_i^{exp} - d(t)_i^{sim} \right)^2 \\ & + w_k \cdot \sum_{i=1}^{10} \left(q(t)_i^{exp} - q(t)_i^{sim} \right)^2 \\ & + w_t \cdot \sum_{i=1}^{3} \left(O(t)_i^{neutral} - O(t)_i^{sim} \right)^2 \\ & + w_e \cdot \sum_{i=1}^{85} \left(x(t)_i \right)^2 \\ & + w_g \cdot \sum_{i=1}^{6} \left(GRF_{exp}(t) - GRF_{sim}(t) \right)^2 \\ & + w_a \cdot \sum_{i=1}^{2} (a(t)_i)^2 \Bigg] dt \end{aligned} \tag{4.6}$$

The enhanced walking predictions were done with varying weights on the marker and kinematic tracking terms, to allow varying levels of deviation from baseline, and with varying weight on the activation goal. These varying conditions will be referred to as different 'iterations' of the enhanced walking. The first iteration was a 'loose' tracking simulation, with low marker tracking and no kinematic tracking to allow for substantial deviations from baseline walking and priority of the activation goal, it was hypothesized that this solution would not be a clinically advisable walking pattern for a participant but may give some insight into exaggerated walking modifications that lead to reduced activation of the iliopsoas muscle in the residual limb. The second iteration enforced greater

tracking of the marker positions while reducing the activation of the residual limb iliopsoas; it was thought this would give a solution that could be more easily adopted by a participant in gait retraining. There were four versions of iteration 3 (3.0, 3.1, 3.2 and 3.3). Iteration 3.0 included marker tracking, and kinematic tracking of the knee and ankle. The motivation of this iteration was to encourage a simulation that found a solution of walking with reduced iliopsoas activation by kinematic deviations of the hip, not the knee and ankle, as an individual donning a prosthetic knee and ankle will have limited control of the knee and ankle kinematics, hence hip kinematic modifications would be more easily implemented in a gait retaining protocol.

Iterations 3.1, 3.2 and 3.3 also included marker tracking, and kinematic tracking of the knee and ankle for the reasons just stated, additionally these iterations included hip kinematic tracking but each version excluded the tracking of the hip kinematics in the sagittal, frontal and transverse plane in order. This iteration intended to isolate hip kinematic modifications on a plane-by-plane basis to be implemented with gait retaining. Isolating kinematic modifications on a plane-by-plane basis was done for ease of clinical translation. All iterations of the 'enhanced' walking included symmetrical tracking elements on the residual and intact limb, this was done to encourage symmetrical kinematic adaptations to reduce the risk of increasing loading to the intact limb. There was low ground reaction force tracking for all iterations, to allow for adaptations. The effort term was kept the same as baseline. The breakdown of the weights for each 'enhanced walking' iteration is displayed in Table 4.7. All iterations were completed at a mesh of 20 nodes. w_k is broken down into the kinematic tracking weights of the hip, knee, and ankle coordinates. A weight of 0 indicates this term is not included in the objective function.

Table 4.7: Weight given to objective function terms in 'enhanced walking' simulations

	Iteration 1	Iteration 2	Iteration 3	Iteration 3.1	Iteration 3.2	Iteration 3.3
w_m	0.01	1	1	1	1	1
w_k - sagittal ankle	0	0	1	1	1	1
w_k - sagittal hip	0	0	1	1	1	1
w_k - sagittal hip	0	0	0	0	1	1
w_k - frontal hip	0	0	0	1	0	1
w_k - transverse hip	0	0	0	1	1	0
w_t	1	1	1	1	1	1
w_e	0.01	0.01	0.01	0.01	0.01	0.01
w_g	0.0001	0.0001	0.0001	0.0001	0.0001	0.0001
w_a	1	1	1	1	1	1

A summary of the hypothesised implications of the 'enhanced walking' iterations objective functions is provided in Table 4.8.

Table 4.8: Summary of 'enhanced walking' iteration objectives

Iteration	Description
1	Goal of minimising the activation of the iliospoas, with a 'loose' marker tracking, ie. allows large deviations from baseline kinematics
2	Goal of minimising the activation of the iliospoas, with a marker tracking, ie. allows some deviations from baseline kinematics
3.0	Goal of minimising the activation of the iliospoas, with a marker tracking and tracking of knee and ankle kinematics, ie. allows deviations from baseline of hip kinematics
3.1	Goal of minimising the activation of the iliospoas, with a marker tracking and tracking of knee, ankle, frontal hip and transverse hip kinematics, ie. allows deviations from baseline of hip sagittal kinematics
3.2	Goal of minimising the activation of the iliospoas, with a marker tracking and tracking of knee, ankle, sagittal hip and transverse hip kinematics, ie. allows deviations from baseline of hip frontal kinematics
3.3	Goal of minimising the activation of the iliospoas, with a marker tracking and tracking of knee, ankle, sagittal hip and frontal hip kinematics, ie. allows deviations from baseline of hip transverse kinematics

Data analysis of 'enhanced gait' simulations

With each iteration it was observed whether the simulation could converge, whether this solution achieved walking forward (translation of pelvis in the X axis) and whether the solution was achieved without a fall (observed with the visualiser and plotting of pelvis height). For each converged solution, the activation impulse of the iliospoas muscle elements (area under the curve) was calculated to see if the iteration has successfully reduced the activation of the iliopsoas. Activation impulse was selected as the metric of success to represent the minimisation of activation throughout the whole motion, which was the aim of the added cost function in the 'enhanced gait' simulations. Activation impulse can be taken as a measure of energy expenditure, as force impulse was in Chapter 3. For the solutions that achieved a reduction in activation impulse, the kinematic deviations from baseline (tracking solution) were plotted, to observe the kinematic adaptations predicted to reduce the activation of the iliacus and psoas. The gait modifications in kinematics were quantified by calculating differences in maximum joint angle values, changes in range of motion (increase in maximum joint angle in both directions) and changes in joint angle throughout the gait cycle (ie. of non-maximum angle features). Additionally, for the solutions that achieved a reduction in activation impulse, step length and step width were calculated and plotted against step length and step width from baseline (tracking solution). These gait parameters were selected as features that could easily be implemented in a gait retraining rehabilitation protocol if required. No statistical analysis was completed due to small sample size and trial repeats.

4.3 Results

4.3.1 Inverse kinematics, inverse dynamics and static optimisation

Figures 4.6 4.7 4.8 and 4.9 display the joint angles (left) and torques (right) of the hip, knee and ankle joints from the inverse kinematics and inverse dynamics for participants 01-04. The inverse kinematics all solved with a RMS error of 2 cm or less, suggesting the model was able to replicate the experimental data adequately (Hicks 2018). The sagittal joint range of motion angle and torque are comparable to kinematic and kinetic data published by Jarvis et al (2021) of 10 high functioning individuals with UTF amputations, however the sagittal hip joint angle is offset by around 10 degrees, this is because flexion angle is 0 in neutral, whereas it is around 12-13 degrees in other clinical studies (Bovi et al. 2011). The same pattern was found by Carloni et al. (2024) in their OpenSim model of an individual with unilateral transfemoral amputation (Carloni et al. 2024). Jarvis et al (2021) calculated kinematics with visual 3D, this 'shift' in the definition of flexion / extension when comparing Visuals 3D and OpenSim results has been reported previously (Wei Tech 2023) but does not affect torque calculations.

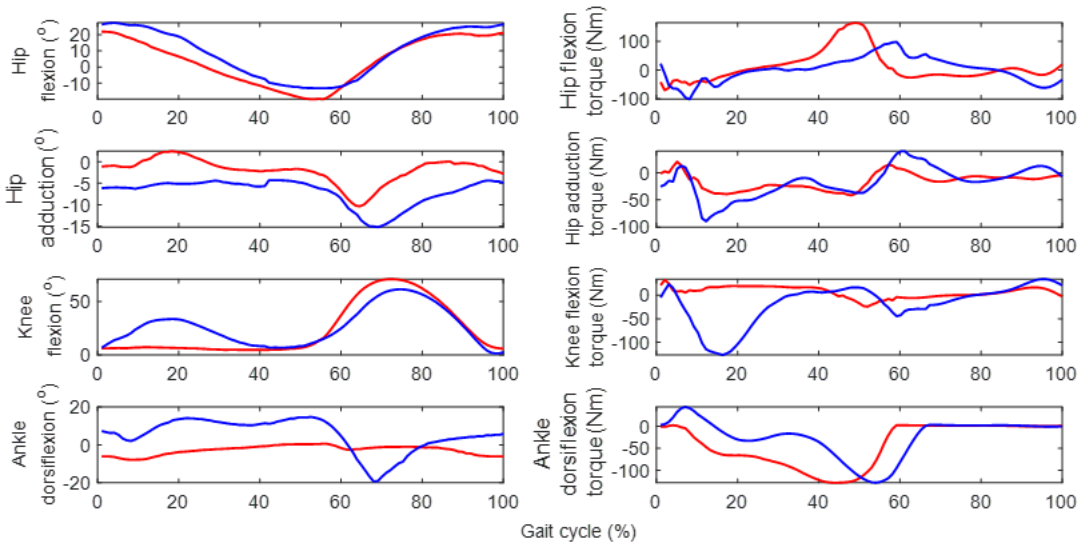


Figure 4.6: Hip, knee and ankle joint angles (left) and torques (right) for residual limb (red) and intact limb (blue) of participant 01

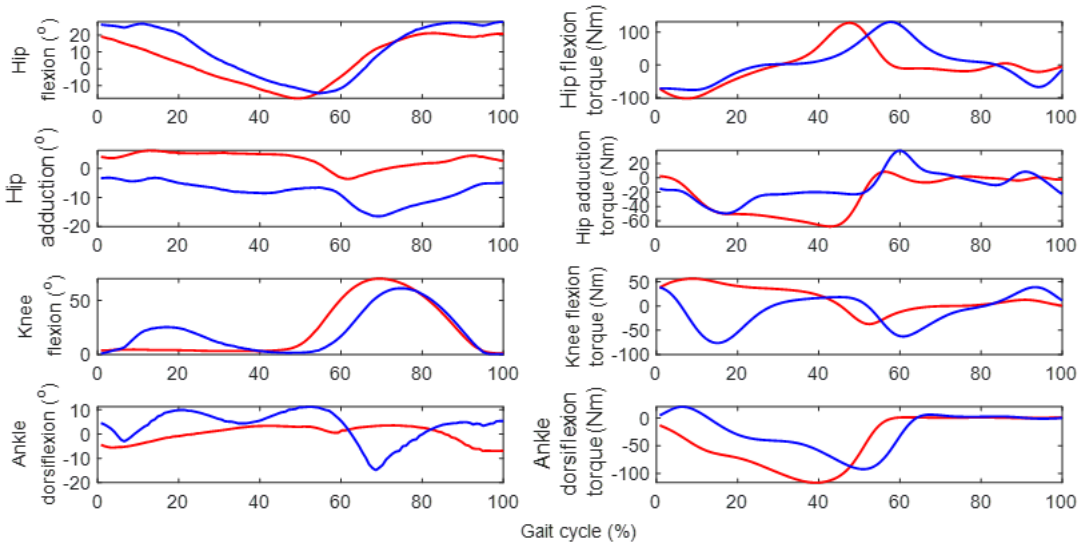


Figure 4.7: Hip, knee and ankle joint angles (left) and torques (right) for residual limb (red) and intact limb (blue) of participant 02

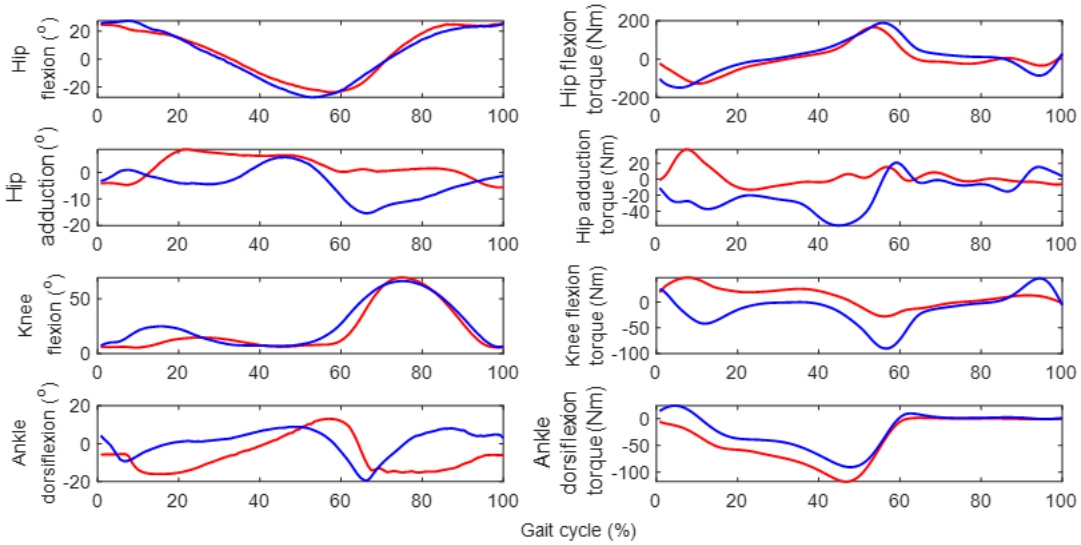


Figure 4.8: Hip, knee and ankle joint angles (left) and torques (right) for residual limb (red) and intact limb (blue) of participant 03

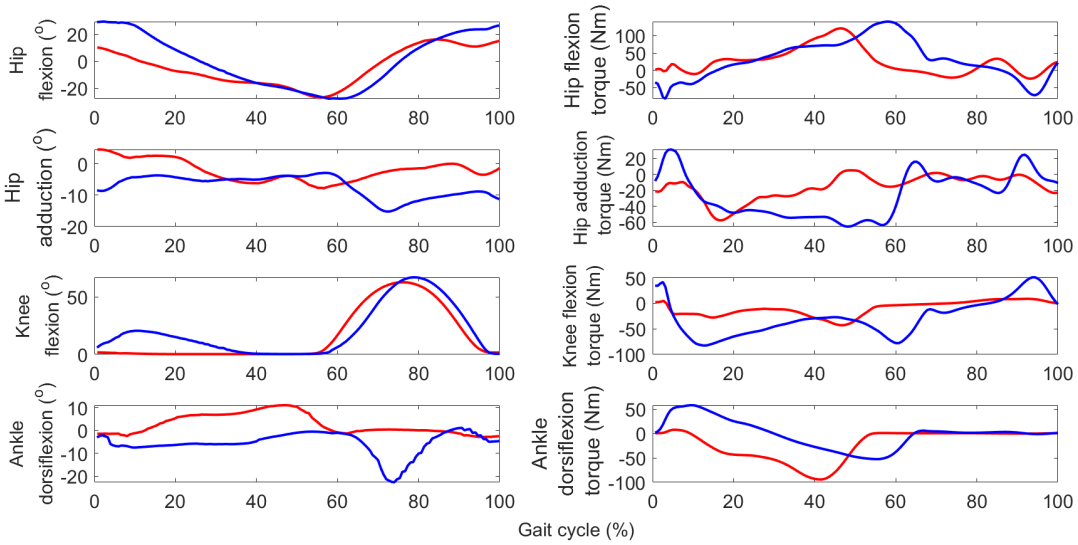


Figure 4.9: Hip, knee and ankle joint angles (left) and torques (right) for residual limb (red) and intact limb (blue) of participant 04

Figure 4.10 4.11 4.12 and 4.13 display the muscle activations of the main hip muscles predicted in the static optimisation for participant 01 - 04. These results are in accordance with the mean muscle activations found in Chapter 3 which predicted muscle activations of the intact and residual limb of individuals with UTF with a validated musculoskeletal model Freebody.

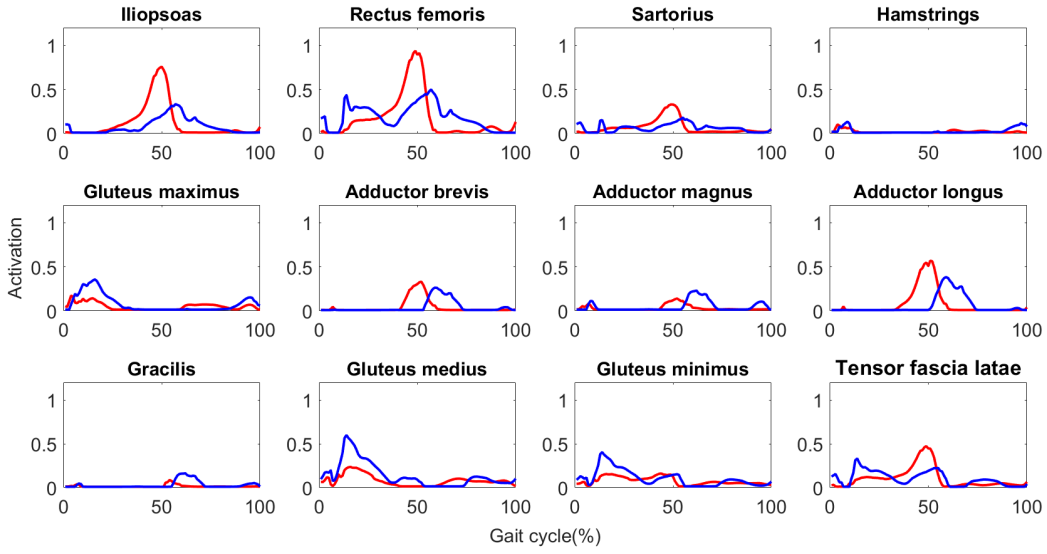


Figure 4.10: Muscle activations of the main hip muscles of the residual limb (red) and intact limb (blue) of participant 01

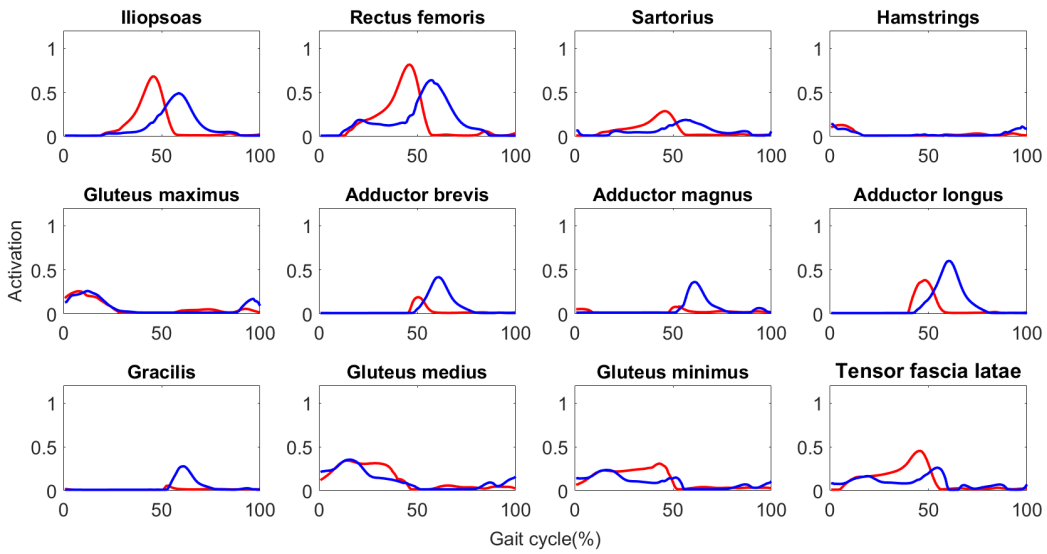


Figure 4.11: Muscle activations of the main hip muscles of the residual limb (red) and intact limb (blue) of participant 02

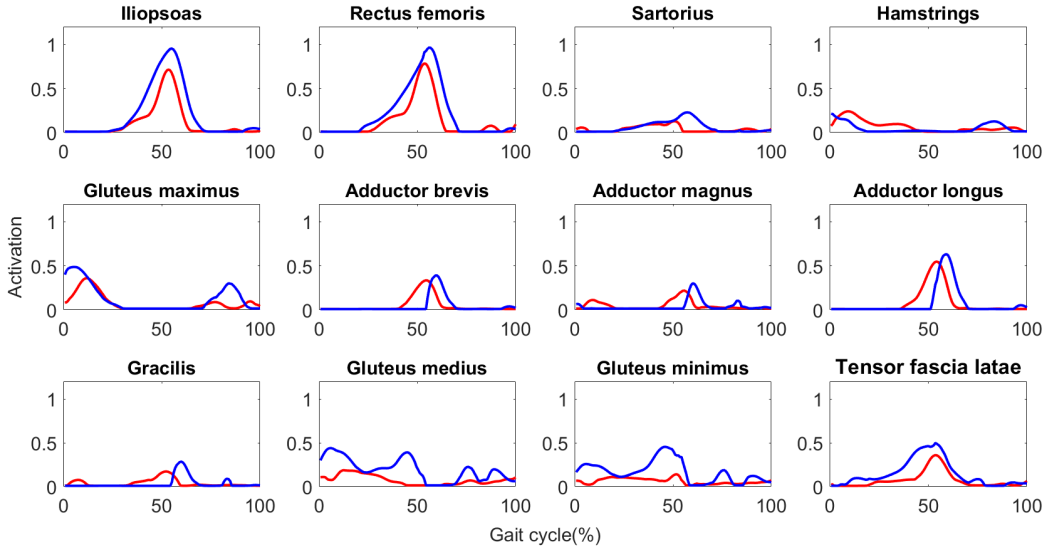


Figure 4.12: Muscle activations of the main hip muscles of the residual limb (red) and intact limb (blue) of participant 03

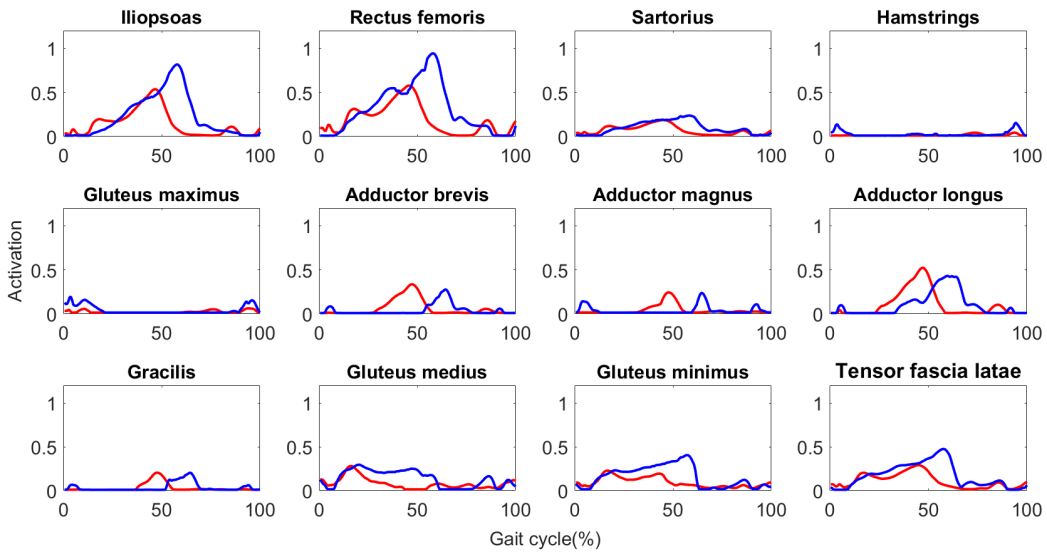


Figure 4.13: Muscle activations of the main hip muscles of the residual limb (red) and intact limb (blue) of participant 04

4.3.2 Tracking results

Tracking kinematics

Figures 4.14 4.15 4.16 and 4.17 display the hip, knee and ankle kinematics from the tracking simulations plotted with the results from the inverse kinematics for particpcants 01-04. From visual inspection the tracking of the invers kinematics results were considered adequate and comparable to the kinematics of this population in the literature (Jarvis et al. 2021). However, the ankle tracking appears to be poorer compared to the sagital hip and knee tracking, especially for partipant 02. The average RMS error range from 4.0 – 5.1°across the four particpants for the joint angles displayed in Figures 4.14 4.15 4.16 and 4.17, with an average of 4.8°.

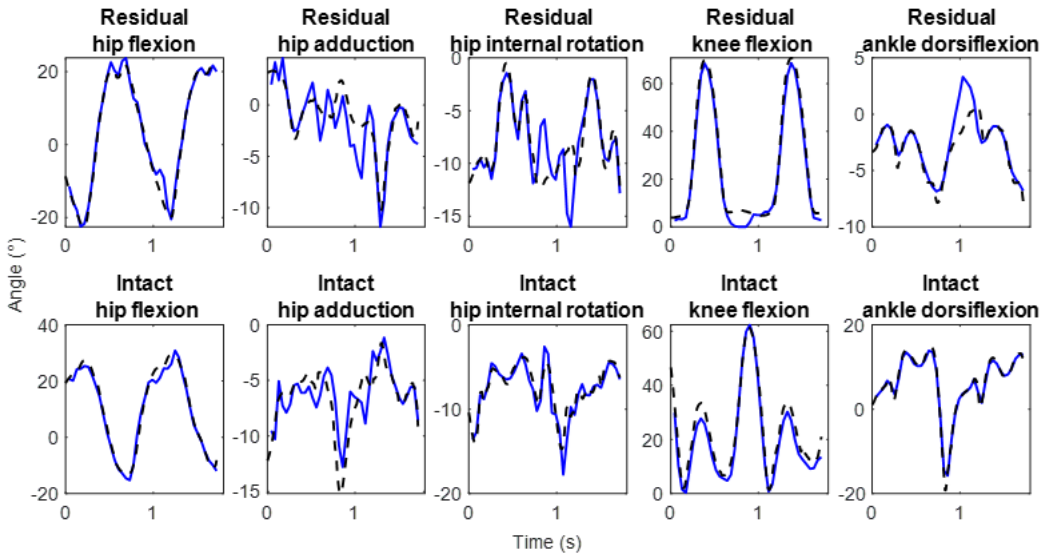


Figure 4.14: Hip, knee and ankle kinematics of the residual limb and intact limb from the tracking simulations (blue) and the inverse kinematics (black- dashed) for particpant 01

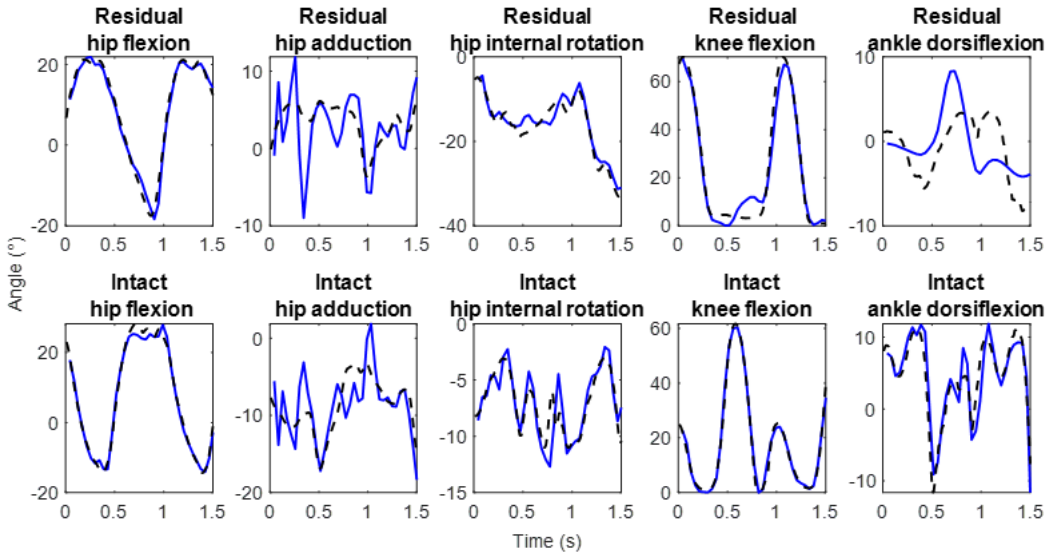


Figure 4.15: Hip, knee and ankle kinematics of the residual limb and intact limb from the tracking simulations (blue) and the inverse kinematics (black- dashed) for particpant 02

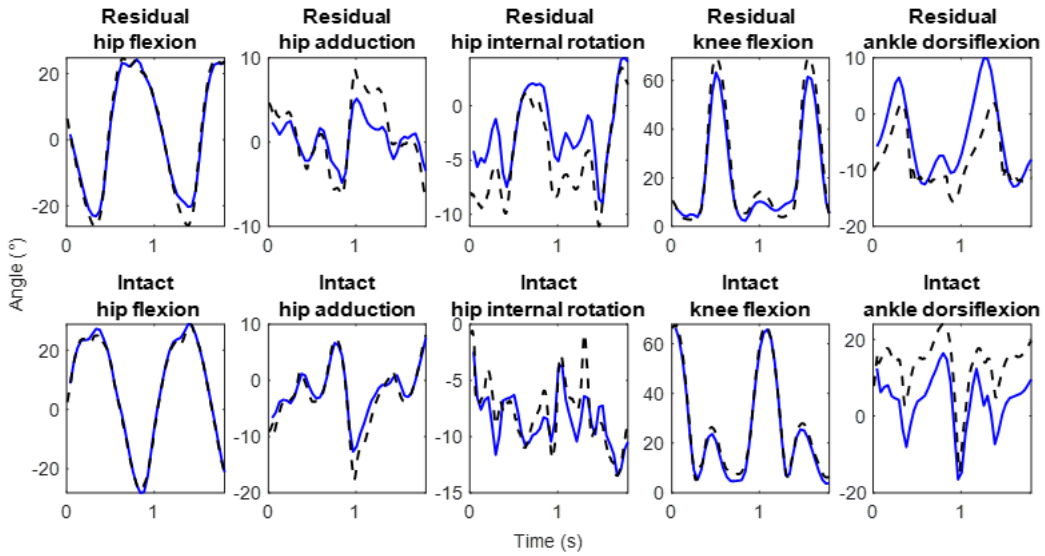


Figure 4.16: Hip, knee and ankle kinematics of the residual limb and intact limb from the tracking simulations (blue) and the inverse kinematics (black- dashed) for particpant 03

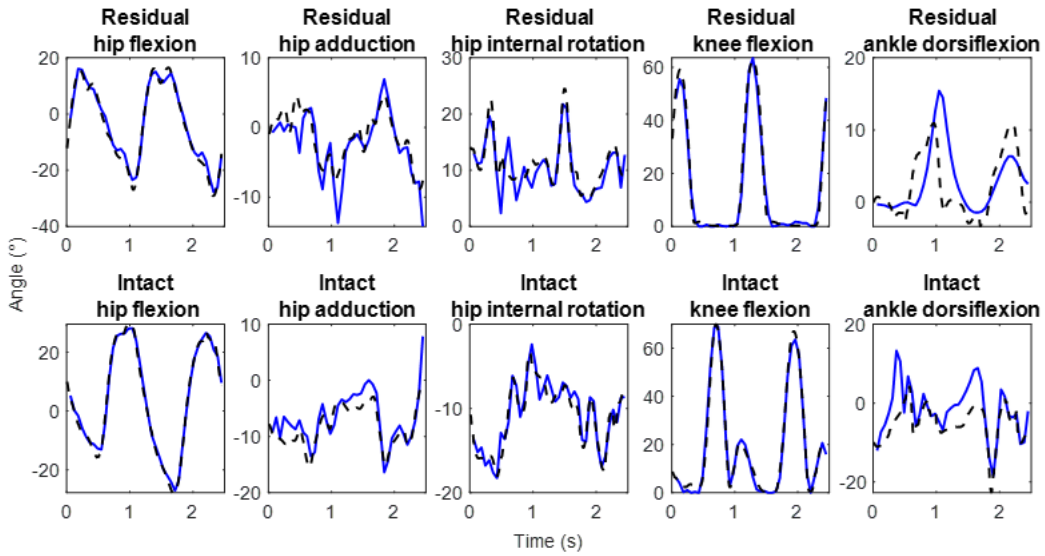


Figure 4.17: Hip, knee and ankle kinematics of the residual limb and intact limb from the tracking simulations (blue) and the inverse kinematics (black- dashed) for particpant 04

Tracking ground reaction force

The predicted ground reaction force from the tracking simulations and the recorded values from the gait trials are plotted in Figures 4.18 4.19 4.20 and 4.21 for the residual limb side and intact side of participants 01 - 04. Visually the predictions of ground reaction force were considered adequately similar to the recorded values. The average RMS error ranged from 5-7% BW across the four participants, with an average of 5.8% BW.

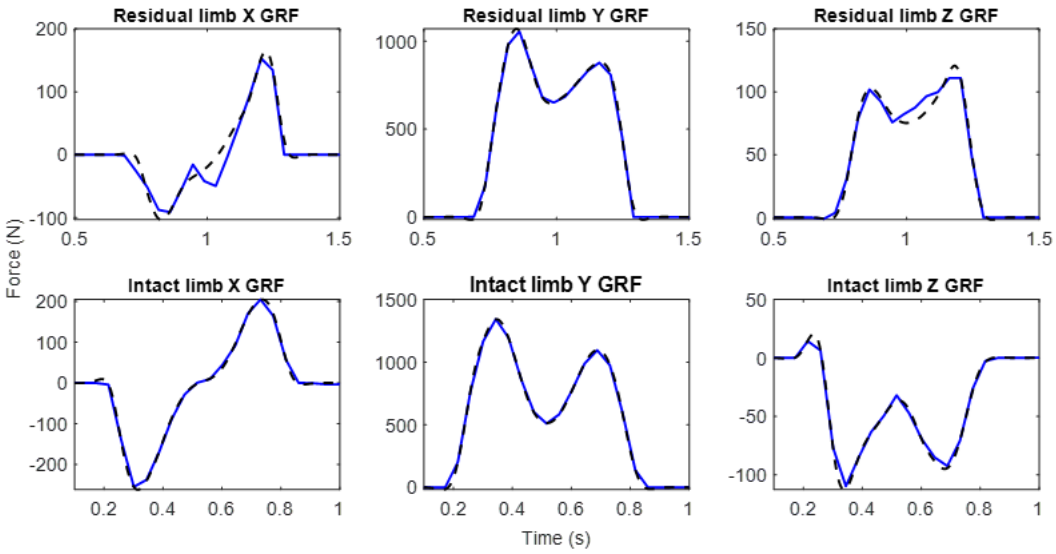


Figure 4.18: Predicted ground reaction force (blue) and recorded ground reaction force (black dashed) for participant 01

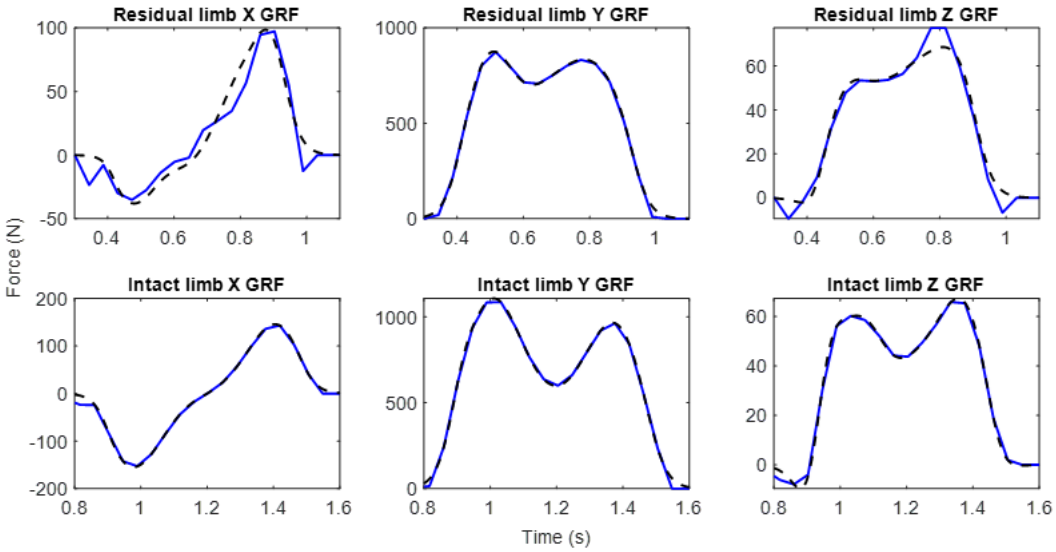


Figure 4.19: Predicted ground reaction force (blue) and recorded ground reaction force (black dashed) for participant 02

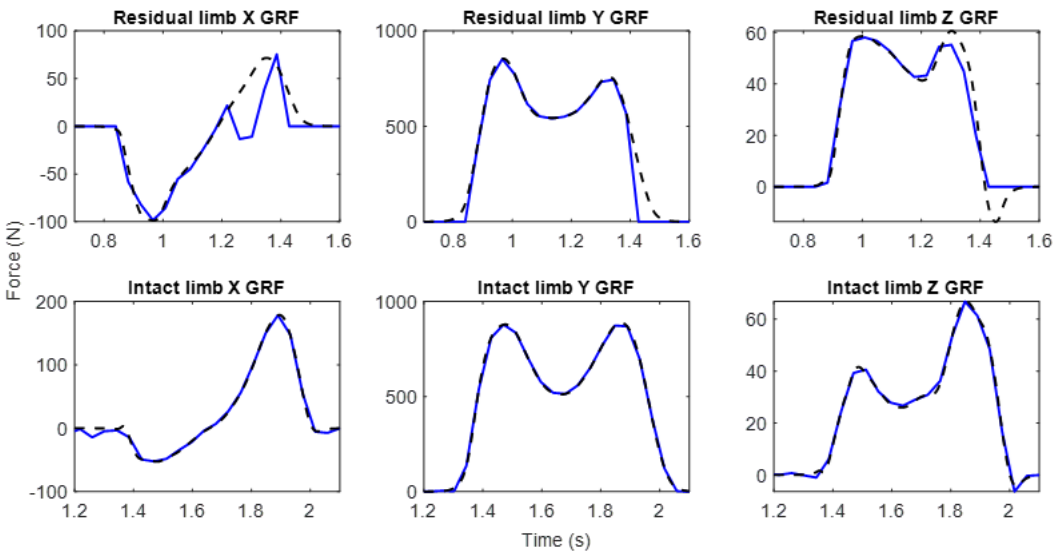


Figure 4.20: Predicted ground reaction force (blue) and recorded ground reaction force (black dashed) for participant 03

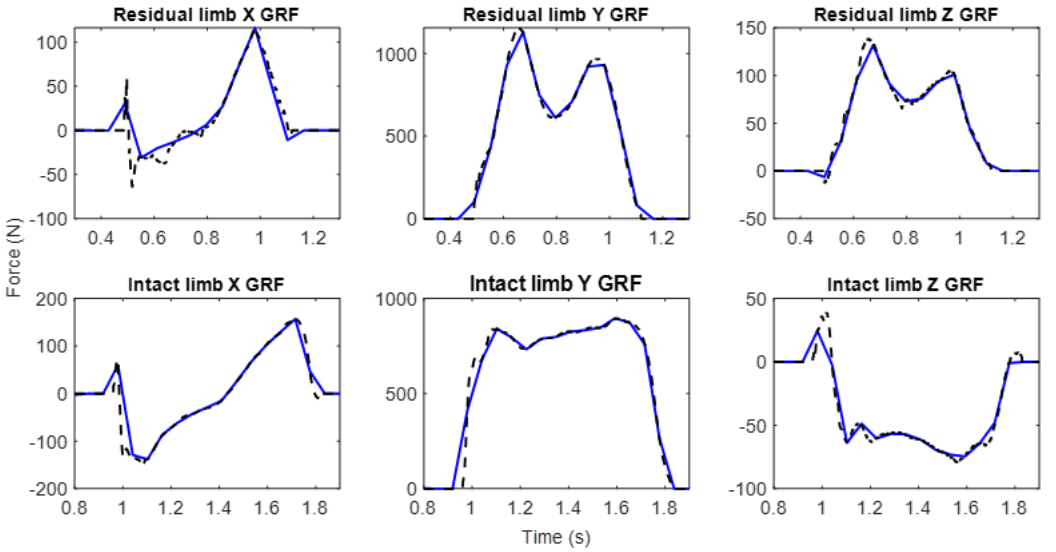


Figure 4.21: Predicted ground reaction force (blue) and recorded ground reaction force (black dashed) for participant 04

Tracking muscle activations

The muscle activations of the gluteus maximus, gluteus medius, hamstrings, iliopsoas, rectus femoris and adductor longus are plotted in Figures 4.22 4.23 4.24 and 4.25. The timing of the peak activations are comparable to previous literature of this population (Harandi et al. 2020) and the magnitude of peak activation in accordance with Chapter 3. Compared to the static optimisation results of this study, it appears that the tracking

results predict the muscles are more active, this is particularly true for the hamstring muscles group for participant 01. Tables 4.9 4.10 and 4.11 presents the combined, phase and magnitude errors from the Sprague and Geers metric between the tracking simulations and static optimisation predictions of muscle activations for participants 01-04. The errors that are above the threshold of moderate similarity (0.6) are marked with dark grey. All phase errors were excellent to moderate. Only 10 of the 48 combined and magnitude errors were excellent to moderate similarity.

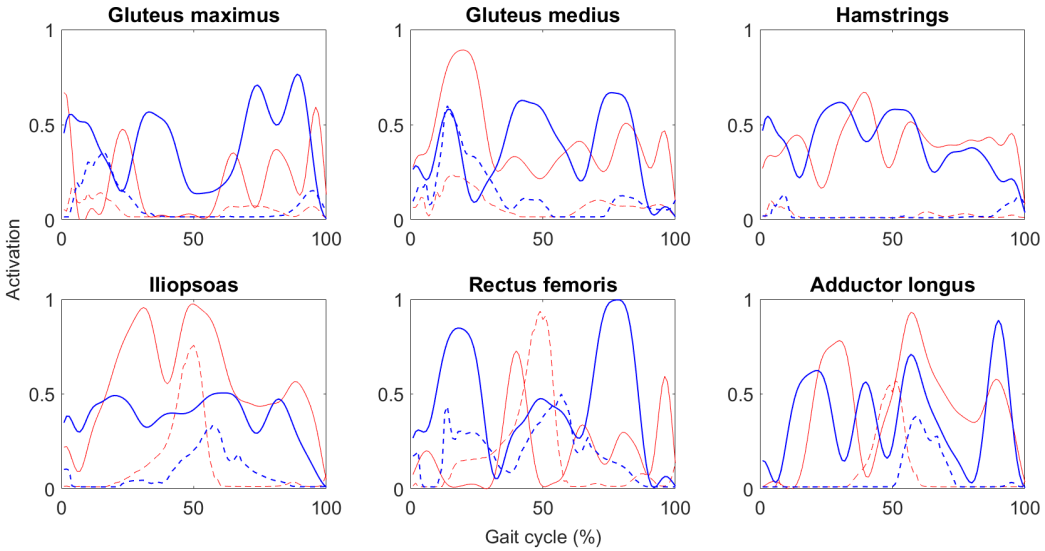


Figure 4.22: Predicted muscle activations of the gluteus maximus, the gluteus medius, hamstrings, iliopsoas, rectus femoris and adductor longus of the residual limb (red) and intact limb (blue) from the tracking simulations (solid) and static optimisations (dashed line) for participant 01

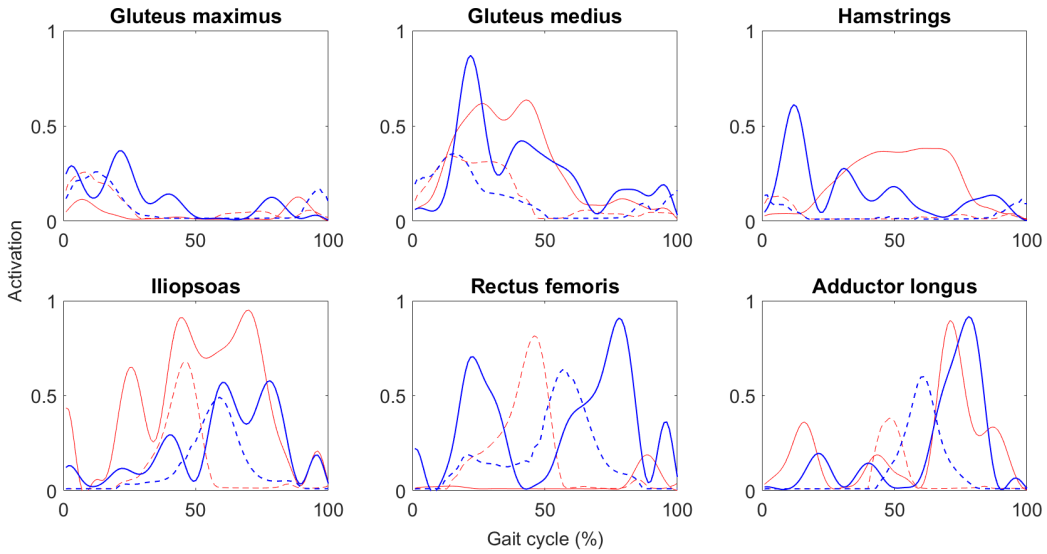


Figure 4.23: Predicted muscle activations of the gluteus maximus, the gluteus medius, hamstrings, iliopsoas, rectus femoris and adductor longus of the residual limb (red) and intact limb (blue) from the tracking simulations (solid) and static optimisations (dashed line) for participant 02

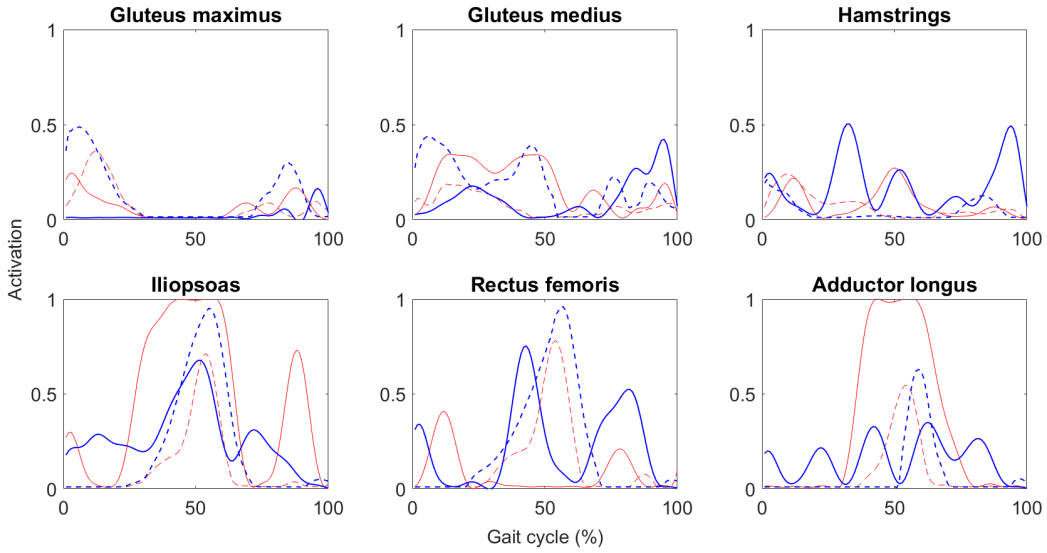


Figure 4.24: Predicted muscle activations of the gluteus maximus, the gluteus medius, hamstrings, iliopsoas, rectus femoris and adductor longus of the residual limb (red) and intact limb (blue) from the tracking simulations (solid) and static optimisations (dashed line) for participant 03

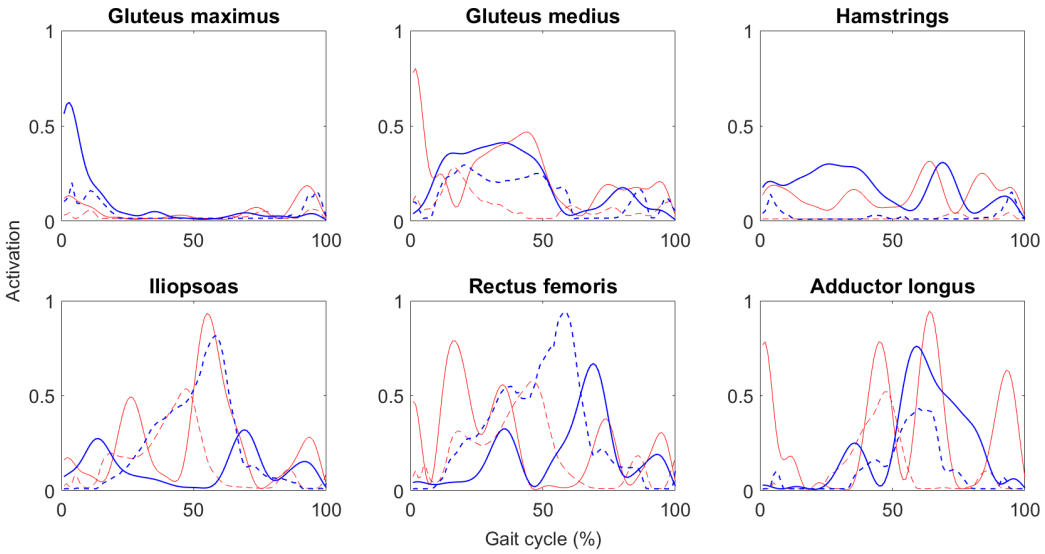


Figure 4.25: Predicted muscle activations of the gluteus maximus, the gluteus medius, hamstrings, iliopsoas, rectus femoris and adductor longus of the residual limb (red) and intact limb (blue) from the tracking simulations (solid) and static optimisations (dashed line) for participant 04

Table 4.9: Combined error for participants 01-04 for the residual (R) and intact (I) limb, where blue indicates 'excellent' similarity, green 'very good', orange 'good', yellow 'moderate' and grey 'none'

Participant	01		02		03		04	
Muscle	R	I	R	I	R	I	R	I
Gluteus maximus	3.07	5.98	0.54	0.50	0.37	0.79	1.44	4.86
Gluteus medius	3.64	3.23	1.01	0.86	1.44	0.71	1.90	1.43
Hamstrings	13.91	9.45	4.59	3.62	0.34	2.29	7.67	3.73
Iliopsoas	1.72	2.27	1.55	0.62	1.76	0.23	0.73	0.68
Rectus femoris	0.38	1.36	0.93	0.75	0.67	0.38	0.44	0.47
Adductor longus	1.96	2.65	1.79	0.82	2.12	0.32	1.34	0.91

Table 4.10: Phase error for participants 01-04 for the residual (R) and intact (I) limb, where blue indicates 'excellent' similarity, green 'very good', orange 'good', and yellow 'moderate'

Participant	01		02		03		04	
Muscle	R	I	R	I	R	I	R	I
Gluteus maximus	0.28	0.22	0.22	0.21	0.25	0.39	0.18	0.32
Gluteus medius	0.11	0.27	0.19	0.21	0.19	0.25	0.29	0.22
Hamstrings	0.24	0.33	0.39	0.31	0.29	0.33	0.23	0.32
Iliopsoas	0.26	0.23	0.28	0.23	0.21	0.20	0.32	0.38
Rectus femoris	0.37	0.22	0.45	0.30	0.48	0.35	0.29	0.27
Adductor longus	0.36	0.31	0.43	0.39	0.19	0.32	0.32	0.15

Table 4.11: Magnitude error for participants 01-04 for the residual (R) and intact (I) limb, where blue indicates 'excellent' similarity, green 'very good', orange 'good', yellow 'moderate' and grey 'none'

Participant	01		02		03		04	
Muscle	R	I	R	I	R	I	R	I
Gluteus maximus	3.06	5.97	-0.50	0.45	-0.27	-0.69	1.43	4.85
Gluteus medius	3.64	3.22	1.00	0.84	1.43	0.67	1.88	1.41
Hamstrings	13.91	9.44	4.57	3.60	0.17	2.26	7.66	3.72
Iliopsoas	1.70	2.26	1.53	0.58	1.75	-0.12	0.66	-0.56
Rectus femoris	-0.11	1.34	-0.81	0.69	-0.48	-0.15	0.32	-0.38
Adductor longus	1.93	2.63	1.74	0.71	2.11	0.04	1.30	0.90

4.3.3 'Enhanced' walking simulations

Iliospoas activation

Figures 4.26 4.27 4.28 and 4.29 display the iliopsoas muscle activation impulse for the baseline walking from the 'tracking' simulations and the iterations of 'enhanced' walking. If the 'enhanced' walking achieved a reduction in iliopsoas muscle activation, the bar is plotted in blue, if not, the bar is plotted in red. For all iterations, apart iteration 3.2 for participant 04, there was the desired effect of reduced muscle activation impulse for participants 02-04. For participant 01 only iteration 2 had the desired effect.

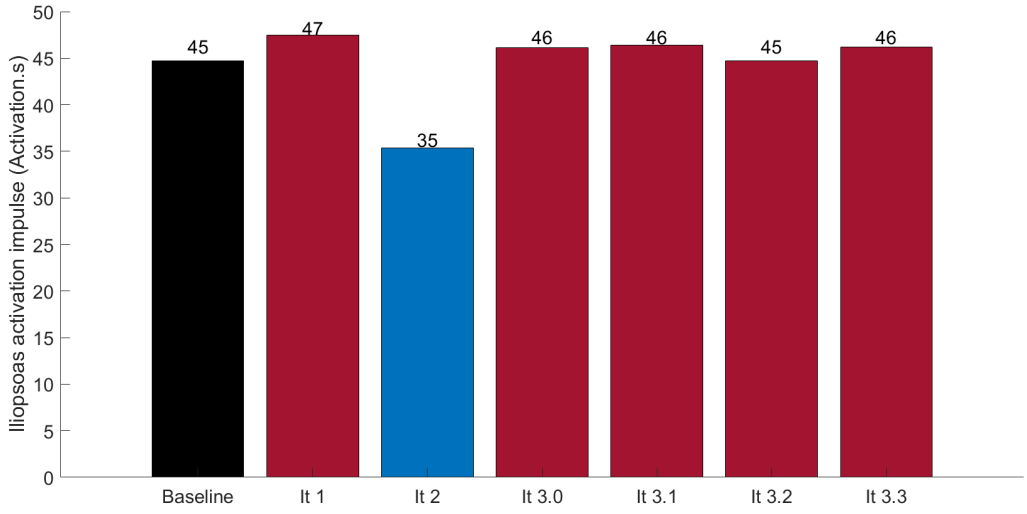


Figure 4.26: Impulse of iliopsoas muscle of the residual limb in baseline and iterations of 'enhanced walking' for participant 01

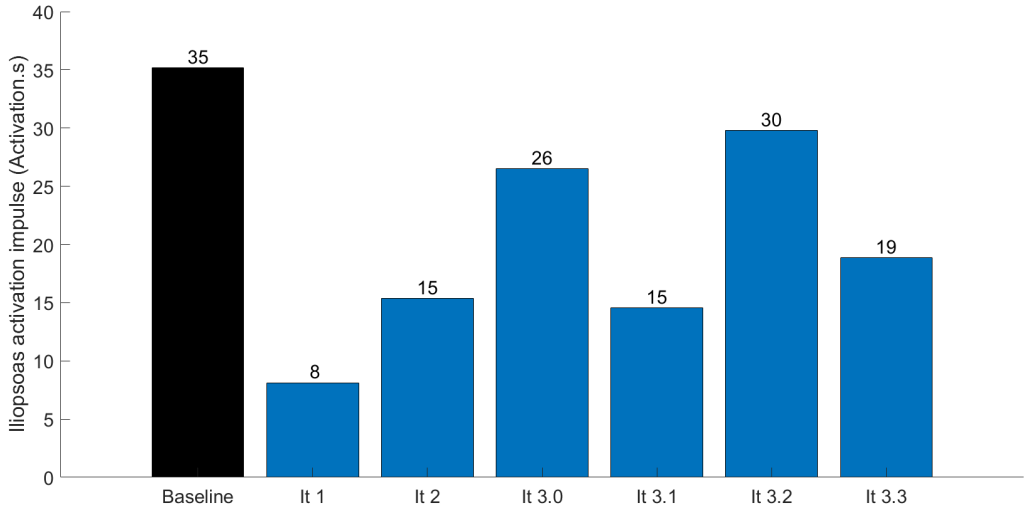


Figure 4.27: Impulse of iliopsoas muscle of the residual limb in baseline and iterations of 'enhanced walking' for participant 02

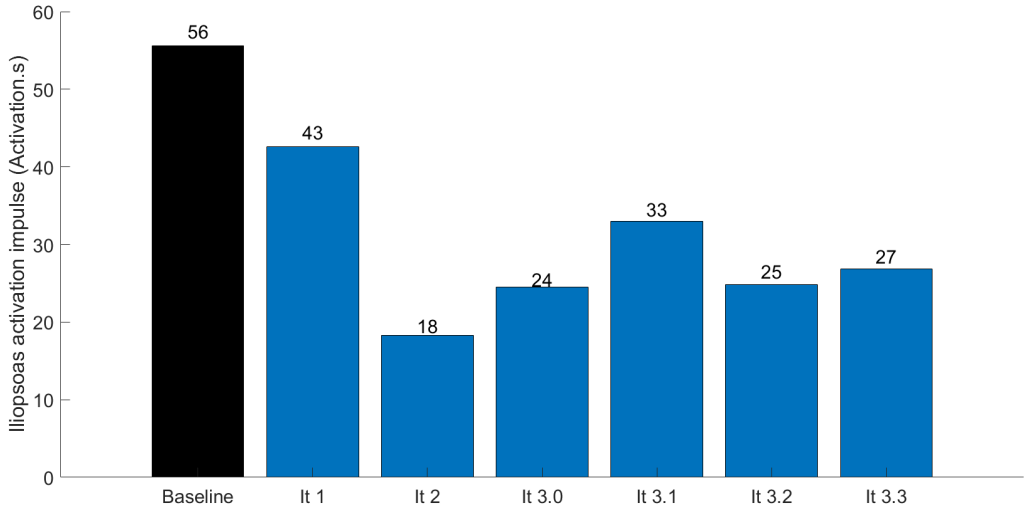


Figure 4.28: Impulse of iliopsoas muscle of the residual limb in baseline and iterations of 'enhanced walking' for participant 03

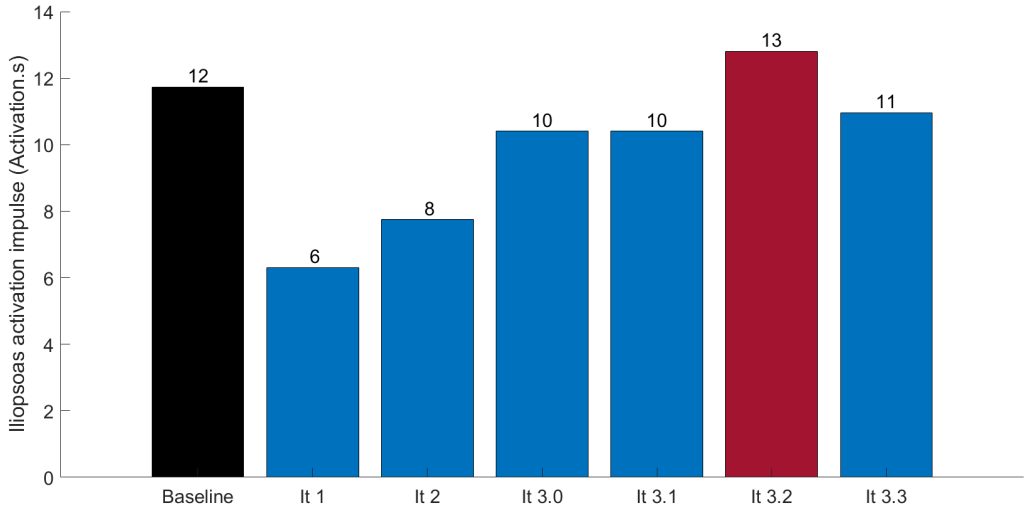


Figure 4.29: Impulse of iliopsoas muscle of the residual limb in baseline and iterations of 'enhanced walking' for participant 04

Kinematic adaptations

The kinematic modifications were observed for all solutions that achieved the desired effect of reduced activation impulse of the iliopsoas muscle.

Iteration 1

As hypothesised, the simulations from iteration 1 (Summary of objective displayed in Table 4.8) predicted abnormal walking patterns. The kinematics are presented in the Appendix A. Figures 4.30 and 4.31 demonstrate the 'abnormal' kinematics for participant 02, with baseline walking (above) and iteration 1 (below) for distinct instances in the gait cycle. The 'abnormal' kinematics here exhibit 'crouch gait' on the intact limb side with continuous knee flexion, inward pointing of the knee joints (genu valgum) position at heel strike of the intact knee, exaggerated pelvic motion in the frontal plane and increased hip abduction of the intact side during swing phase compared to baseline.

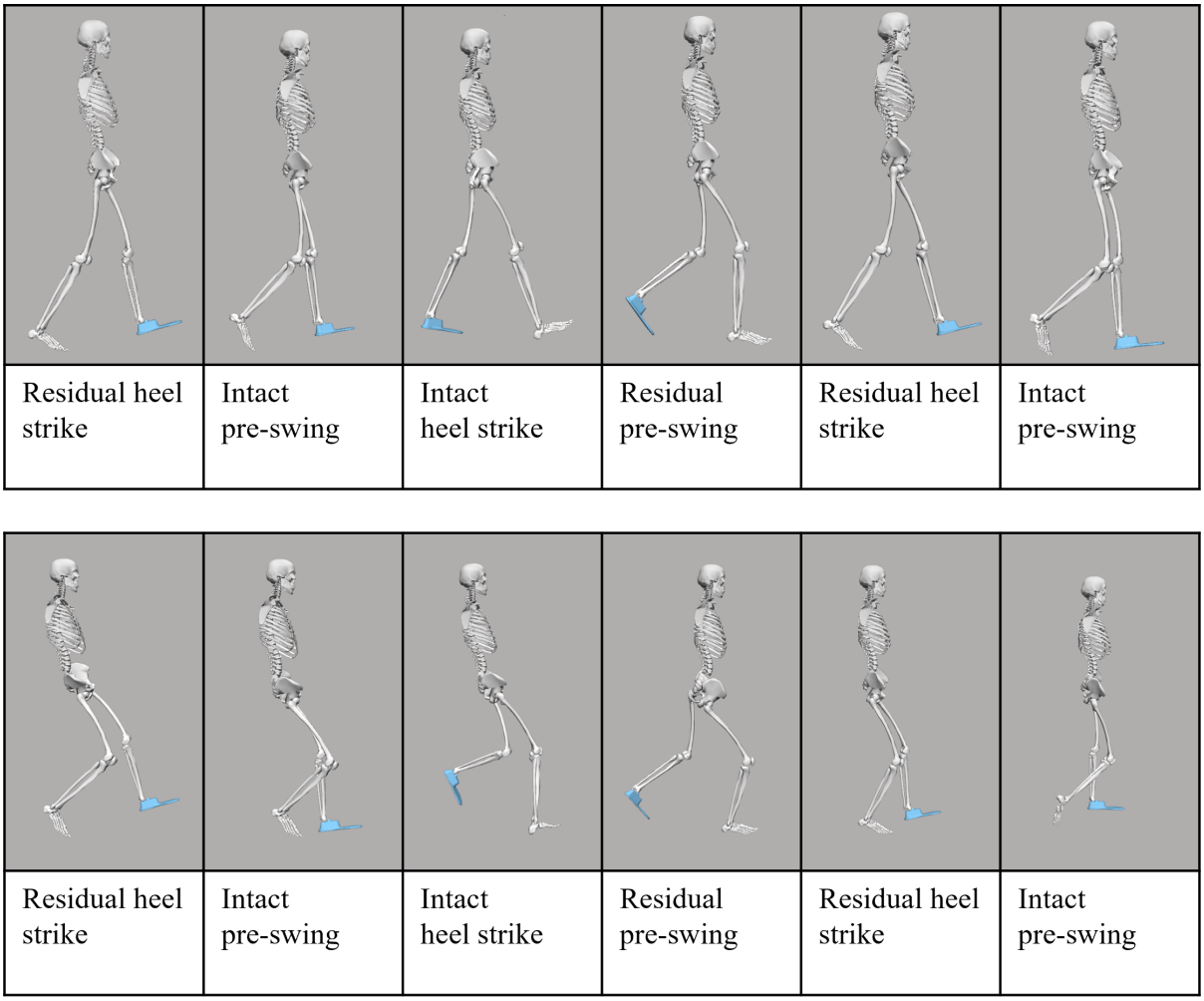


Figure 4.30: The 'normal' gait kinematics exhibited by the baseline tracking simulations (above) and the 'abnormal' gait kinematics that are displayed by kinematics of iteration 1 (below) for participant 02 in the sagittal plane

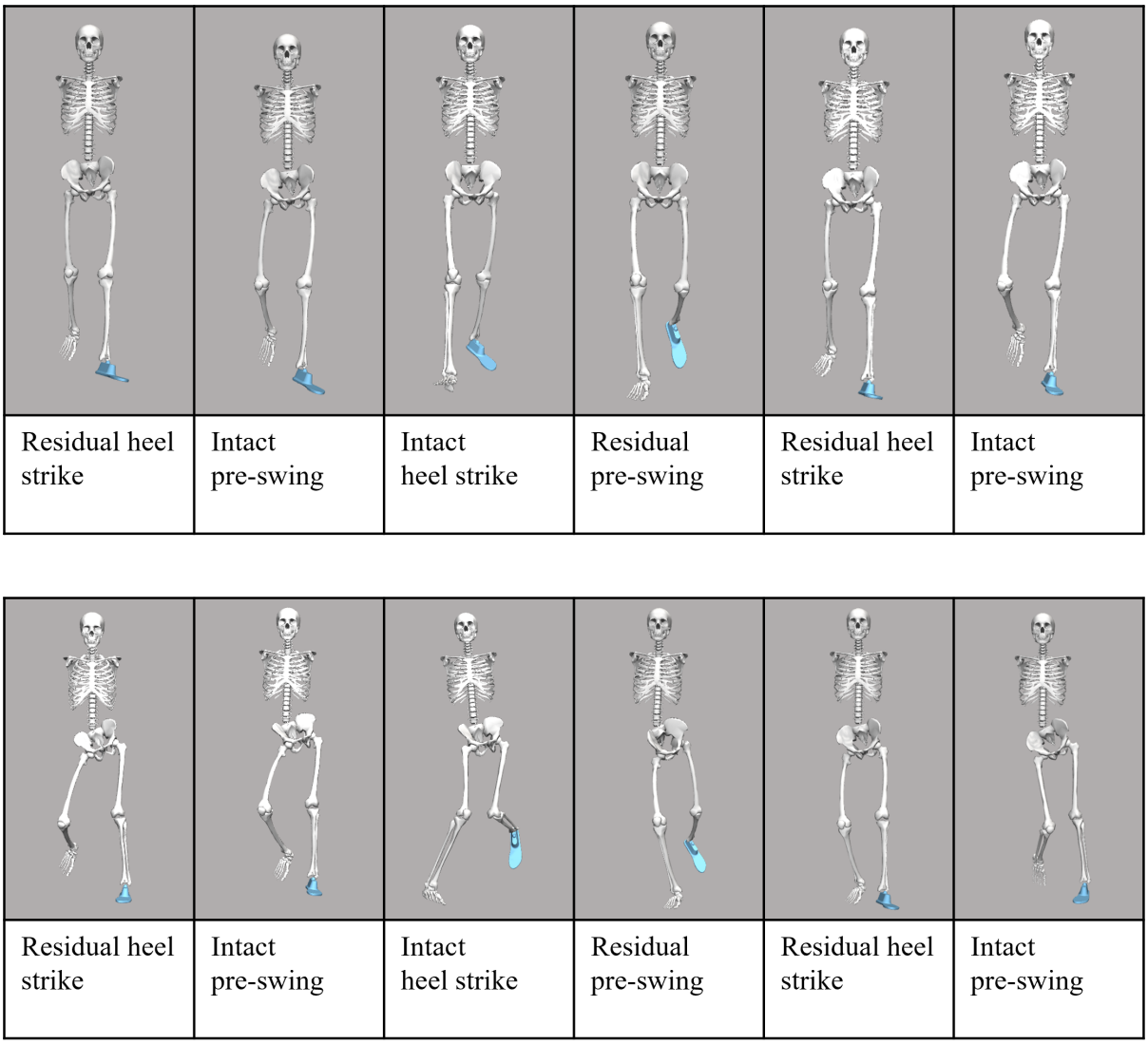


Figure 4.31: The 'normal' gait kinematics exhibited by the baseline tracking simulations (above) and the 'abnormal' gait kinematics that are displayed by kinematics of iteration 1 (below) for participant 02 in the frontal plane

Iteration 2, 3.0, 3.2, 3.3

Figures 4.32 5.36 4.34 and 4.35 present the results from the 'enhanced walking', iterations 2, 3.0, 3.1, 3.2 and 3.3 (Summary of iteration objectives found in Table 4.8) only for the simulations where the 'enhanced' walking resulted in reduced activation impulse, for the hip, knee and ankle kinematics, plotted against the baseline walking kinematics from the 'tracking' simulations for participants 01-04. For participant 02 and 03 this included all iterations of enhanced walking. For participant 01 this only included iteration 2. For participant 04 this included iteration 2, 3.0. 3.1 and 3.3.

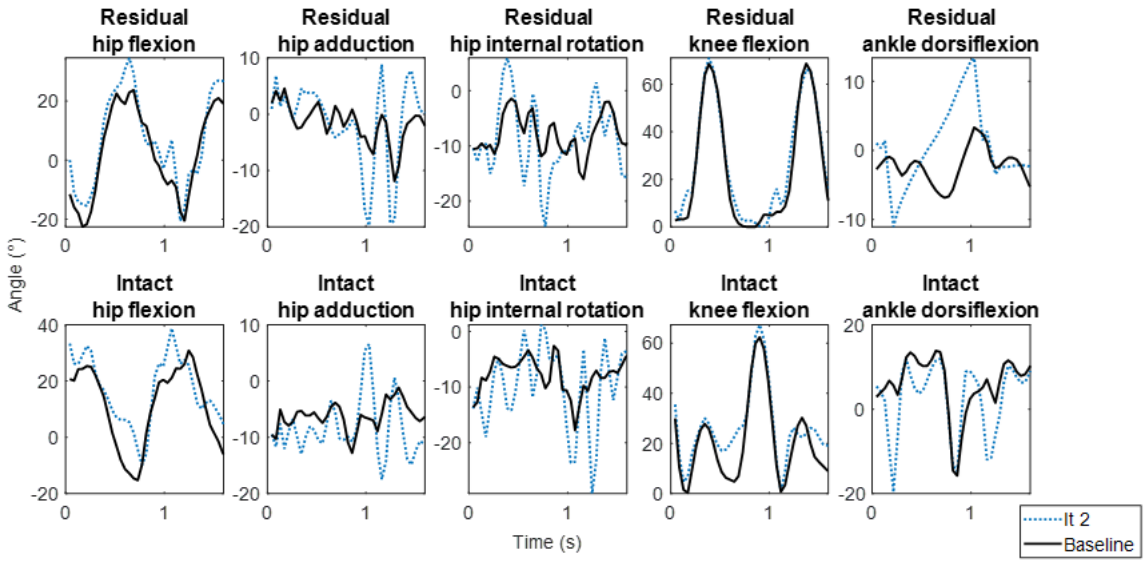


Figure 4.32: Hip, knee and ankle kinematics of the residual limb and intact limb of baseline, iteration 2 for participant 01

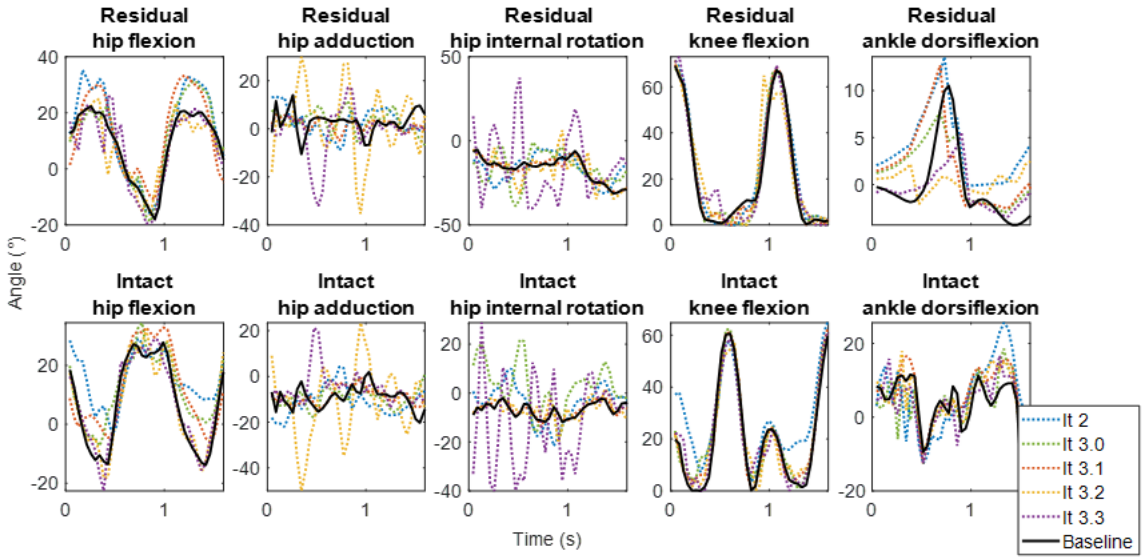


Figure 4.33: Hip, knee and ankle kinematics of the residual limb and intact limb of baseline, iteration 2, iteration 3.0 , iteration 3.1, iteration 3.2, iteration 3.3 for participant 02

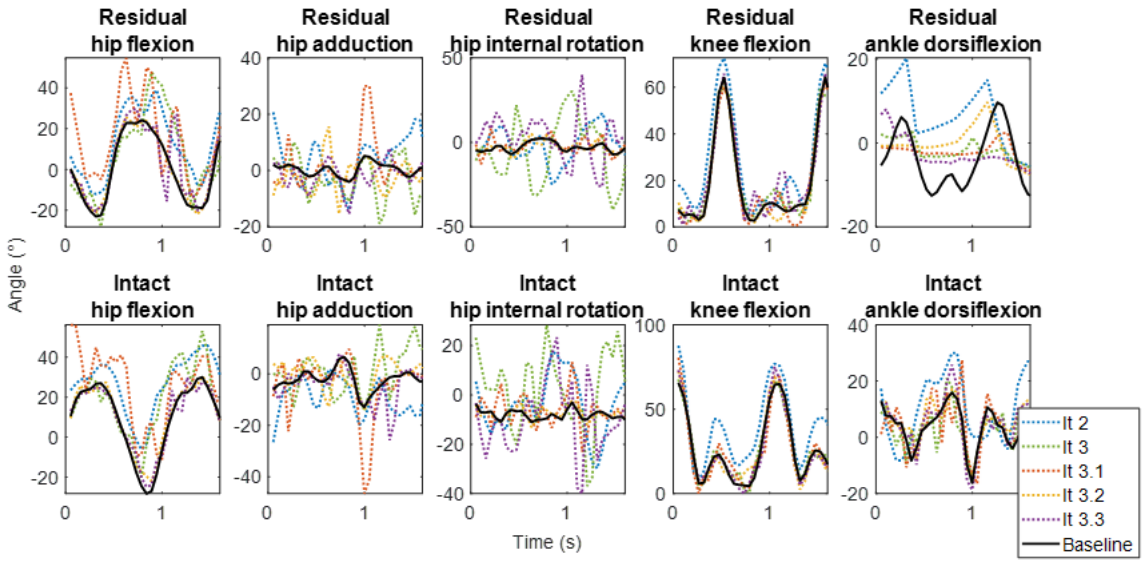


Figure 4.34: Hip, knee and ankle kinematics of the residual limb and intact limb of baseline, iteration 2, iteration 3.0, iteration 3.1, iteration 3.2, iteration 3.3 for participant 03

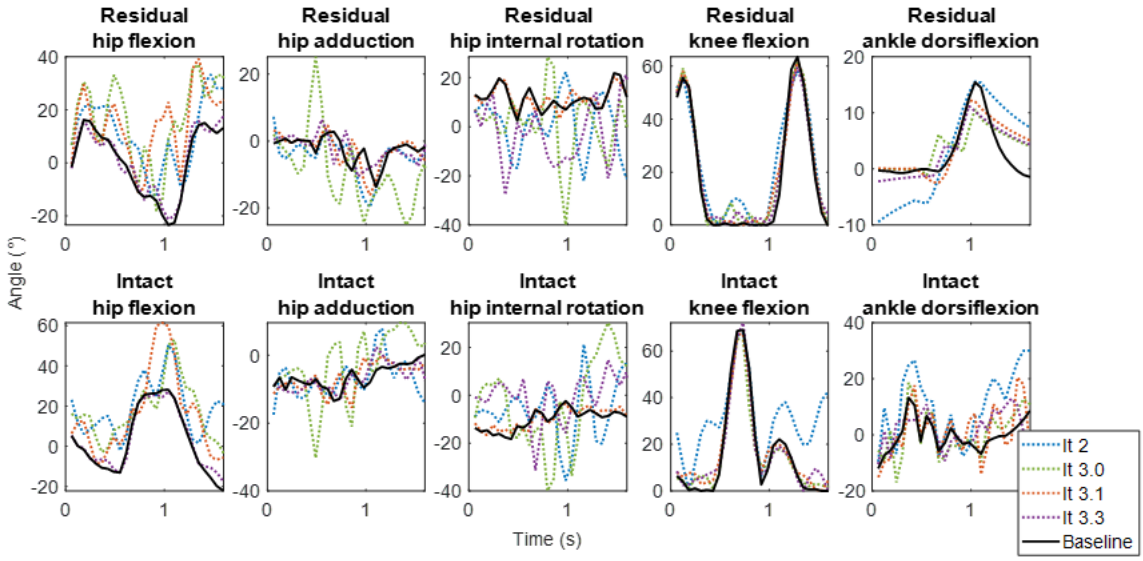


Figure 4.35: Hip, knee and ankle kinematics of the residual limb and intact limb of baseline, iteration 2, iteration 3.0, iteration 3.1, iteration 3.3 for participant 04

The kinematic modifications of iterations 2, 3.0, 3.1, 3.2 and 3.3 for the 'enhanced' walking simulations where reduced activation impulse was achieved are summarised in table 4.11. For participant 02 and 03 this included all iterations of 'enhanced' walking. For participant 01 this only included iteration 2. For participant 04 this included iteration 2, 3.0. 3.1 and 3.3.

The kinematic modifications are categorised into; changes (increased / reduced) in maximum features, changes (increased / reduced) in magnitudes of angles at certain phase of

gait or changes to range of motion (ROM) where there was a reduction / increase in joint kinematics in both directions of the plane (ie. an increase / reduction in hip abduction and adduction, or ankle dorsiflexion and planter flexion), for the residual limb and intact limb side. The changes in angles are presented in relation to baseline, ie. an increase is '+ °' from baseline. Increase is represented by a '⇑' and decrease by a '⇓'.

Table 4.12: Kinematic modifications from iterations of 2, 3.0, 3.1, 3.2 and 3.3 of enhanced walking with respect to baseline (ext = hip extension, flex = hip flexion, add = hip abduction, abd = hip abduction, int rot = internal hip rotation, ext rot = external hip rotation, k flex = knee flexion, plant flex = ankle planter flexion, dors flex = ankle dorsiflexion)

Partipcant	Iteration	Kinematic modifications (°)	
		Residual limb side	Intact limb side
01	2.0	⇓ maximum hip extension angle at first stride (-7.2 ext). ⇑ in maximum hip flexion (+10.8 flex). ⇑ frontal hip ROM (+4.3/-7.9). ⇑ transverse hip ROM (+7.3 int rot / +8.6 ext rot). ⇑ ankle ROM (+10.0 dors flex / +4.2 plant flex)	⇓ maximum hip extension (+7.2 ext). ⇑ in maximum hip flexion (+7.9 flex). ⇑ frontal hip ROM (+7.7 add / +4.7 abd). ⇑ transverse hip ROM (+3.8 int rot / +11.4 ext rot). ⇑ knee flexion during stance (+12.2 k flex). ⇑ maximum ankle plantarflexion (+3.8 plant flex).
	3.0	-	-
	3.1	-	-
	3.2	-	-
	3.3	-	-

Table 4.12 continued from previous page

02	2.0	⇑ maximum hip flexion (+12.9 flex). ⇑ maximum ankle dorsiflexion (+3 dors flex). ⇓ maximum ankle plantar flexion (+6.6 plant flex).	⇓ maximum hip extension (- 10 ext). ⇑ transverse hip ROM (+11.8 int rot / +7.9 ext rot). ⇑ knee flexion during stance (+17.8 k flex). ⇑ maximum ankle dorsiflexion (+9.0 dors flex).
	3.0	⇑ maximum hip flexion (+8.3 flex). ⇑ maximum hip external rotation (-7.5 ext rot). ⇓ maximum dorsiflexion (-3.6 dors flex).	⇓ maximum hip extension (- 6.1 ext). Increased maximum hip flexion (+7.4 flex). ⇑ maximum internal hip rotation (+23.6 int rot).
	3.1	⇑ maximum hip flexion (+10.4 flex). ⇓ maximum hip extension (-7.2 ext). ⇑ maximum ankle dorsiflexion (+2.1 dors flex).	⇓ maximum hip extension (-8.4 ext). ⇑ maximum ankle dorsiflexion (+5.6 dors flex).
	3.2	⇑ frontal hip ROM (+14 add / -22.8 abd). ⇓ ankle ROM (-7.5 dors flex / -2.22 plant flex).	⇑ frontal hip ROM (+21.6 add / +34.1 abd).
	3.3	⇑ transverse hip ROM (+42.7 int rot /+9.2 ext rot). ⇑ maximum hip abduction (+21.7 abd).	⇑ transverse hip ROM (+31.2 int rot / +29.1 ext rot). ⇑ maximum hip adduction (+19.3 add).

Table 4.12 continued from previous page

			⇓ maximum extension (-21.1 ext).
		⇓ maximum hip extension (-10.9 ext).	⇑ maximum flexion (+15.7 flex).
		⇑ maximum hip flexion (+14.7 flex).	⇑ maximum hip abduction (+6.9 abd).
	2.0	⇑ frontal hip ROM (+15.5 add/ +11.5 abd).	⇑ transverse hip ROM (-15.2 int rot / 16.4 ext rot).
03		⇑ transverse hip ROM (+9.2 int rot/ +11.9 ext rot).	⇑ knee flexion during stance (+21.2 k flex).
		⇑ maximum ankle dorsiflexion (+17.9 dors flex).	⇑ maximum ankle dorsiflexion (+14.0 dors flex).
			⇓ maximum extension (-8.4 ext).
		⇑ maximum hip flexion (+23.6 flex).	⇑ maximum flexion (+23.1 flex).
	3.0	⇑ frontal hip ROM (+4.9 add/ +16.6 abd).	⇑ maximum hip adduction (+11.2 add).
		⇓ maximum ankle dorsiflexion (-6.6 dors flex).	⇑ transverse hip ROM (+31.4 int rot / 23.5 ext rot).

Table 4.12 continued from previous page

	3.1	⇑ maximum hip flexion (+30.4 flex). ⇓ maximum hip extension (-9.3 ext). ⇑ maximum adduction (+23.5 add). ⇓ maximum ankledorsiflexion (-7.6 dors flex).	⇑ maximum hip flexion (+28.8 flex). ⇓ maximum hipextension (-13.3 ext). ⇑ maximum abduction (+33.1 abd). ⇑ maximum ankle dorsiflexion (+11.6 dors flex).
	3.2	⇑ frontal hip ROM (+19.0 add/ + 11.4 abd)	⇓ maximum hip extension (-6.3 ext).
	3.3	⇑ transverse hip ROM (+35.4 int rot/ +19.7 ext rot). ⇑ maximum hip abduction (+11.3 abd).	⇑ transverse hip ROM (+22.2 int rot / -26.7 ext rot). ⇑ maximum hip abduction (+12.8 abd).
04	2.0	⇑ maximum hip flexion (+18.8 flex). ⇓ maximum hip extension (-14.0 ext). ⇑ maximum hip abduction (+13.0 abd). ⇑ maximum external hip rotation (+19.7 ext rot). ⇑ knee flexion during stance phase (+10.2 k flex) ⇑ maximum ankle plantarflexion (+8.0 plant flex).	⇑ maximum hip flexion (+22.4 flex). ⇓ maximum hip extension (-13.3 ext). ⇑ maximum hip adduction (+7.8 add). ⇑ maximum hip external rotation (+21.6 ext rot) ⇑ knee flexion during stance phase (+20.2 k flex). ⇑ maximum ankle dorsiflexion (+16.6 dors flex).

Table 4.12 continued from previous page

3.0	⇑ maximum hip flexion (+20.9 flex). ⇓ maximum hip extension (-5.2 ext). ⇑ frontal hip ROM (+22.3 add/ +11.3 abd) ⇑ transverse hip ROM (+8.4 int rot/ +37.6 ext rot). ⇑ knee flexion during stance phase (+8.4 k flex). ⇓ maximum ankle dorsiflexion (-5.1 dors flex).	⇑ maximum hip flexion (+24.8 flex). ⇓ maximum hip extension (-19.3 ext). ⇑ frontal hip ROM (+9.0 add/ + 16.8 abd) ⇑ transverse hip ROM (+27.9 int rot/ +21.7 ext rot).
3.1	⇑ maximum hip flexion (+23.5 flex). ⇓ maximum hip extension (-12.5 ext). ⇑ maximum abduction (+2.4 abd)	⇑ maximum hip flexion (+33.5 flex). ⇓ maximum hip extension (-13.4 ext). ⇑ maximum ankle dorsiflexion (+7.16 dors flex)
3.2	-	-
3.3	⇑ maximum adduction (+6.4 add) ⇑ maximum external hip rotation (+35.6 ext rot).	⇑ frontal hip ROM (+2.4 add/ +2.9 abd) ⇑ transverse hip ROM (+17.2 int rot / 21.6 ext rot). ⇑ knee flexion during stance phase (+9.6 k flex).

Spatial features

Figures 4.36 and 4.37 display the step length and step width for baseline and iterations of 'enhanced walking' for solutions that had the desired effect of reduced iliopsoas muscle activation. The most extreme changes in these spatial features were in the solutions of iteration 1. This is to be expected, as iteration 1 encouraged the most exaggerated deviations from baseline walking. These changes were reduced step length for all participants and increase in step width for participants 02 and 03 and reduced step width in participant 04. For the other iterations there were minimal changes in step length and width, with the exception of reduced step length in the solution of iteration 3.2 for participant 02 and the solution of iteration 3.3 for participant 03.

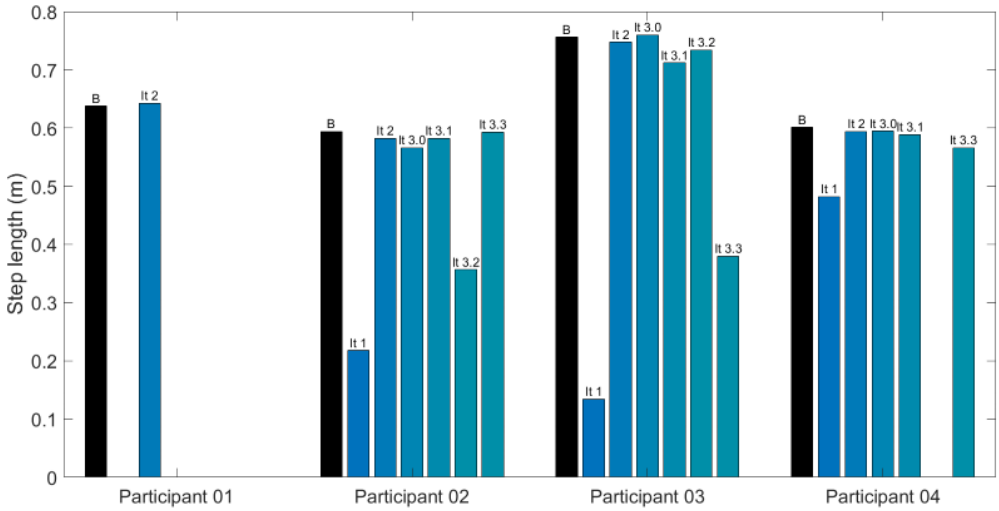


Figure 4.36: Step length in baseline (B), iteration (1), iteration 2 (It 2), iteration 3.0 (It 3.0), iteration 3.1 (It 3.1), iteration 3.2 (It 3.2) and iteration 3.3 (It 3.3)

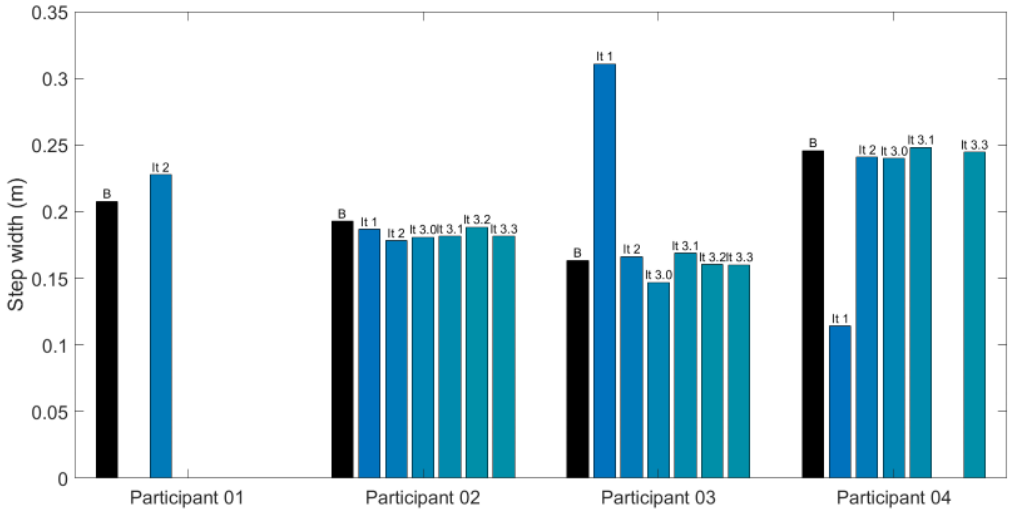


Figure 4.37: Step width in baseline (B), iteration (1), iteration 2 (It 2), iteration 3.0 (It 3.0), iteration 3.1 (It 3.1), iteration 3.2 (It 3.2) and iteration 3.3 (It 3.3)

4.4 Discussion and conclusion

4.4.1 Validation of the UTF and UTK model

The OpenSim model of an individual with UTF and UTK amputation that was developed in this chapter was validated for inverse dynamic simulations through the results of the inverse kinematics, inverse dynamics and static optimisations. This model can be used in future work for a variety of applications, including to inform rehabilitation research through MSK modelling in a methodological pipeline which is the fourth objective of this thesis. This study demonstrates how the model can be scaled and adjusted for subject specific modelling of individual with UTF and UTK amputation.

4.4.2 Baseline tracking simulations

The results of this study validate the OpenSim UTF and UTK model for optimal control tracking simulations of joint kinematics and ground reaction force, with average errors of 4.8°and 5.8 % BW. The error is slightly higher, by 2.8°and 0.8% BW, than previous studies of Moco tracking simulations of able-bodied walking (Bianco et al. 2023), however, there are arguably more sources of error when modelling the dynamics of an individual donning a prosthetic limb, particularly with the simplification of the dynamics of the MPK. Previous studies that have used Moco to model individuals donning a prosthetic limb have tracked to mean able-bodied motion data and presented their tracking results as an acceptable level of standard deviation from the mean able-bodied experimental data (Miller et al. 2023) (Miller & Esposito 2021).

The kinematic tracking was poorer at the prosthetic ankle joint on the residual limb side, particularly for participant 02. This may be due to inaccuracy in modelling the prosthetic energy return foot, as the ankle joint. The prosthetic energy return foot does not actually articulate as a pin joint, as modelled and presented in previous literature (Jarvis et al. 2021) and this study. The ankle attachment is rigid, but the energy return aspect (spring like) gives the impression of articulation. It is therefore unsurprising that modelling this as a pin joint, as commonly done in this literature, causes error. Simplification of the intact ankle joint and the prosthetic knee may also be a source of error when calculating the inverse kinematics and the tracking solution (Hicks et al. 2015). It should be noted that there is also error in inverse kinematic results which are being used as the baseline 'gold-standard' comparison. Error in inverse kinematics is unavoidable to some extent with the simplifications made with multi body dynamics (Hicks et al. 2015). In the inverse kinematics results of this study there was RMS marker error of 2cm or less for all participants. This is an 'acceptable' level of error according to the OpenSim guidelines (Hicks 2018) but should be considered when comparing the tracking to the inverse kinematic results. As outlined, the error in calculating joint kinematics via inverse kinematics and tracking simulations may be particularly expected when quantifying the kinematics of an individual donning a prosthetic limb.

The timing of the peak muscle activation of the muscle groups estimated by the tracking solutions and presented in Figures 4.22 – 4.25 was qualitatively in accordance with results from Chapter 3 and with a previous study which acquired muscle forces via static optimisation of this population and validated against EMG (Harandi et al. 2020), apart from the rectus femoris. The magnitude of activation and activation curves are qualitatively similar to the simulations of able-bodied walking with the original Rajagopal (2016) able-bodied OpenSim model, which was also validated to EMG (Rajagopal et al. 2016). However, when directly comparing the muscle activations predicted in the tracking simulations via direct collocation to the static optimisation results of this study there are differences, as demonstrated by the Sprague and Geers metric results (tables 4.8 – 4.10). The phase error was excellent to moderate for all comparisons. This signifies that the timing of the muscle activations was similar. However, the magnitude (and therefore combined) error was above 0.6 (and therefore deemed having no similarity) for 30 of the 48 comparisons. There are several potential reasons for these differences. Firstly, the differences in joint kinematics and ground reaction force between the inverse kinematic / measured values and the results of the tracking simulations, highlighted previously, will manifest as slight differences in muscle activations. Another potential reason for the differences observed, is that although this tracking method via direct collocation tracks the ground reaction force, it does not track the centre of pressure. The resultant joint torques (or skeletal dynamics) will be affected by the predicted centre of pressure. With this current method (OpenSim Moco), it is not ensured that the centre of pressure in the tracking simulations is the same as the measured centre of pressure, therefore the resultant joint torques may differ, this is a limitation of this method. The differing joint torques would lead to differing muscle activations. There is little evidence of previous studies that have directly compared results from static optimisation to direct collocation. De Groote (2016) found similar results when comparing static optimisation and direct

collocation methods of estimating muscle forces, however, in their simulations the motion was prescribed, and the skeletal dynamics were quantified with inverse dynamics for both the static optimisation and direct collocation predictions of muscle activation. This method controls for potential differences in skeletal dynamics (joint torques) that may arise from inverse and forward dynamic approaches, but allows for dynamic estimations of muscle forces, accounting for their dynamic properties (De Groote et al. 2016). An older study by Anderson & Pandy (2001) also found the results from their static and dynamic optimisations of muscle forces to be very similar, however they also used identical joint torques as inputs to their optimisations. Though Anderson & Pandy (2001) joint torques were acquired from the dynamic optimisation (Anderson & Pandy 2001). Overall the muscles appeared to be more active (increased magnitude) in the tracking simulations solved with direct collocation than predicted by the static optimisation in the results of this study. The tracking simulations predict more co-contraction.

4.4.3 Emerging walking modifications in the 'enhanced' walking iteration simulations

Iteration 1

As expected, the solution from iteration 1 (Table 4.6) which was a loose tracking simulation, so allowed large deviations from the baseline walking, produced walking simulations that prioritised reduced recruitment of the iliopsoas muscle over walking that appeared 'normal'. The simulations were visualised, and the solutions predicted motion that got the participant from start to end point, but the walking looked abnormal and like it would require high energy consumption. The 'abnormal' nature of this walking was not quantified but is visualised in Figure 4.30 – 4.31 for participant 02. It would be challenging to prescribe these walking patterns in a gait re-training protocol, and likely induce loading undesirable loading conditions as the features, crouch gait and in-turned knees, are associated with gait pathologies. The kinematic modifications predicted in the solution of iteration 1 are presented in the appendix A. However, quantifying the spatial features of the solutions from iteration 1 suggested a reduction in step length may be beneficial to reducing the activation of the iliopsoas, Figure 4.43. The reduction in step length varied from 0.12 – 0.60 m between the three participants that could achieve reduced iliopsoas activation impulse. This spatial modification could perhaps be achieved via less 'abnormal' kinematic strategies in a gait retraining protocol. It should be noted participant 01 did not achieve the reduced iliopsoas activation in iteration 1, even though large gait deviations were allowed.

Iterations 2, 3.0, 3.1, 3.2, 3.3

Though the kinematic modifications varied between participants, there were patterns in kinematic modifications that arose. For example, an increase in maximum hip flexion and reduction in maximum hip extension at residual hip, which was predicted for participant 01, 03, 04 for iteration 2, participant 04 for iteration 3,0 and participant 02, 04 for iteration 3.1. Similarly, this kinematic modification of increased maximum flexion and

reduced maximum extension was exhibited by the intact hip in the results of iteration 2 for all participants, participant 02,03, 04 for iteration 3.0 and participants 02, 03 and 04 for iteration 3.1. As the iliopsoas is a hip flexor and therefore initiates torque in the sagittal plane it is logical that an emerging gait modification involves adaptation of the hip kinematics in the sagittal hip plane for the iterations where sagittal hip kinematics were not specially tracked, as is the case with iteration 2, 3.0, 3.1. Reducing the 'extension' of the hip joint will reduce the work required of the iliopsoas hip flexion action and probably reduce the external torque in the sagittal plane. It is interesting that although the 'enhanced walking' simulations aimed to reduce the activation of the iliopsoas of the residual limb, the hip kinematic modifications in the symmetry plane for the residual and intact limb side are similar for most cases. There was no 'symmetry' term in the objective function for the forward dynamic simulations, which is sometimes included in this kind of modelling to encourage kinematic symmetry, as symmetry cannot be assumed in the walking patterns of individuals with unilateral lower limb amputations (Jarvis et al. 2021). The symmetry in kinematic modifications predicted in the 'enhanced walking' may be a result of the effort term which minmises actuator excitation per unit distance. Perhaps the enforced 'effort' term, which was weighted according to the tracking simulations and enforced in the 'enhanced walking simulations' encouraged symmetrical kinematic modifications as they may be more efficient. This would have to be investigated further to fully understand.

For iteration 2 (Table 4.6), which had no specific kinematic tracking, but achieved reduced iliopsoas impulse for all participants, it appears that the prosthetic knee kinematics were unchanged and there was increased flexion at the intact knee during stance for all of the participants. This is beneficial for the translation of these results, as an individual donning a prosthetic knee would struggle to adapt the kinematics of this joint due to a lack of control.

Another pattern that arose was an increase range of motion at the intact and residual hip in the frontal plane. For iteration 3.3 (where frontal hip plane kinematics were not tracked but the knee, ankle and two other planes of the hip were tracked) this was true for all participants, an increase in the maximum abduction and adduction in the residual and intact hip. For the other iterations, it varied between the iterations and participants whether there was an increase in maximum adduction or abduction. It would be interesting to investigate how the joint torques vary in relation to these kinematic modifications, to understand why they may lead to reduced iliopsoas muscle activation. Additionally, how frontal hip kinematic modifications relate to the moment arm of the iliopsoas muscle, which would affect the activation requirement.

In the gait modifications simulated by iteration 3.3 of the enhanced walking, which allowed deviations in the transverse plane at the hip, participant 02, 03 and 04 all exhibited an increase in maximum hip external rotation to the maximum of range of motion (40 °). This may be due to changes in the iliopsoas moment arm with external hip rotation. The ideal kinematic modifications to be predicted are the cases where there a small deviations from baseline yet result in reduced iliopsoas activation impulse as this would increase the

likelihood of implementing these in a gait retraining protocol. This was not the case for the solutions of iteration 3.3.

From spatial features plotted in Figure 4.34 and 4.35, the only pattern that arose, apart from results of iteration 1, was reduced step length for participant 02 and 03 in iteration 3.2 and 3.3 respectively.

4.4.4 Subject- specific modelling

There were variations in the kinematic strategies predicted to reduce the recruitment of the iliopsoas muscle, for example, the discrepancies in frontal modifications highlighted earlier, this compounds the need for subject-specific modelling for a study of this nature. Additionally, the reduced iliopsoas activation impulse could only be achieved by one out of five iterations of 'enhanced walking' for participant 01. This highlights how different objective functions are required for different participants to achieve the rehabilitation goals that could be predicted by this forward dynamic MSK modelling method.

4.4.5 Limitations

There are several limitations to this study such as the simplifications that were made to the model. The upper limbs were not modelled in these simulations, this was partly to reduce the complexities of the simulations (reducing the controls being solved to reduce simulation time) and due to lack of experimental upper limb data. The arms will provide propulsion, which is not provided by the model. It was assumed that normal upper limb dynamics would be preserved in the 'enhanced walking' predictions, however, this did not allow for potential modifications that could be predicted for the upper limbs. Additionally, the trunk kinematics were not tracked from experimental data, they were tracked to minimise deviations from a neutral position. This was a method presented by Miller et al (2023) who validated their model for metabolic consumption (Miller et al. 2023). There is potential that torso kinematic adaptations would be beneficial for the reduced iliopsoas conditions, and this cannot be predicted. Additionally, this may have effected the prediction pelvic kinematic modifications.

Another limitation of this study is that the residual limb and socket component was modelled as a rigid segment. This is common when modelling the individuals donning a prosthetic, but is not accurate to reality where it is known that this coupling, between the residual limb and socket, is dynamic with angular and translational degrees of freedom (Gale et al. 2020). When Miller (2021) modelled the axial 'pistoning' of the socket in individuals with transtibial amputation they found this to have minimal effect on the modelled metabolic cost which is derived from muscle force (Miller & Esposito 2021) which is the focus of this study. They found that the addition of 'pistoning' had no effect on the tracking of motion data. It should be noted that they did not include rotation when modelling the dynamic coupling of the residual limb and socket, and their study was focused on individuals with transtibial amputation which may differ from transfemoral. This dynamic relationship has been addressed in inverse dynamics modelling study of an

individual with transtibial amputation and found that modelling the residual – socket as a 6 DoF joint improved the marker errors when running inverse kinematics (LaPrè et al. 2018). Therefore, modelling the degrees of freedom of the residual limb and socket may improve the tracking results of this study and the accuracy of the forward dynamic predictions of 'enhanced walking'.

The muscle model does not account for the atrophy / hypertrophy that is known occur in this population (Jaegers et al., 1999). MRI data can be used to quantify this atrophy / hypertrophy (Suzuki 2010), and this could be represented in the muscle model by reducing / increasing the maximum force potential of the muscles accordingly. However, due to contradicting information in the literature on the patterns of this atrophy / hypertrophy and variation between individuals due to rehabilitation and surgery techniques, it was not be possible to create a 'general' pattern of atrophy and hypertrophy and therefore this was not estimated in this model (Willson et al. 2022). To include this level of detail this study would require subject specific MRI data, as presented in Chapter 2. Additionally, all the UTF residual limbs were modelled as myodesis surgery technique. This was not controlled for in the recruitment of the participants and may be an inaccurate assumption.

The MPK were modelled as generalisable spring forces. This is not an accurate representation of the variable damping that is character of MPK's. However, the specific control mechanisms of MPK remain unknown, as they are proprietary to the prosthetic manufacturer. To improve the accuracy of the model a more complex control model could be used based on the estimated control system of the MPK (Chien et al. 2014). Alternatively, to improve the method of describing the model of the knee, a data driven machine learning approach could be taken, using algorithms that do not require a prior information about the mechanical system but identify the non-linear dynamics. This approach has been taken to describe the nonlinear dynamics of the foot, ankle and shock absorbing plyon component of lower limb prosthetics using Sparse Identification of Nonlinear Dynamics with Control (SINDYc) and Extended Dynamic Mode Decomposition with control (eDMDc) algorithms (Donahue et al. 2024). However the control model is designed, the more complex the model of the control system of damping, the more computationally expensive the simulation. So, the added value of more complex model needs to be considered.

In addition to this, the intact ankle only had sagittal range of motion, this is does not account for inversion / eversion and adduction / abduction of the intact ankle kinematics, which are less significant in walking, but this may affect the results. There are some studies in the literature that have taken a fully 2D approach to the optimal control simulations of walking, for example a by Johnson et al. (2022) who simulated the asymmetry and energy lost of individuals with hemiparesis. Johnson et al. (2022) conducted their analysis with a 2-D model to reduce the confounding variables and focus on sagittal plane kinematics (Johnson et al. 2022). Although the ankle was modelled with a 2D approach, it was important that this study included the 3D kinematics of the hip to allow the possibility of predicting a range of kinematic modifications that could be implemented in a gait retraining protocol.

This model utilised the Hill-type muscle model; the limitations and assumptions of this model should be noted. The mass, fatigue, and contributions of fast and slow twitch fibres are ignored, as well as other physiological and anatomical features that may affect muscle activations (Hicks et al. 2015).

Another limitation of this chapter's methods is the simulation time. The tracking simulations, the creation of 'initial guesses' as described in the methods and 'enhanced walking' simulations took varying lengths of time to converge from 2- 10 hours. Additionally, the optimisation of spring properties took 12.4 hours to converge. These convergence times are acceptable for a study of this nature; however, they limit the translation of this method as this may be too long to be utilised in a clinical setting.

4.4.6 Future direction

The UTF and UTK model presented in this study have lots of opportunity for improvement, as highlighted in the limitations. The model could be developed to a more accurate representation, particularly of the prosthetics knee joint, though this may come at an cost of increased simulation time.

The 'enhanced' walking simulation objective function was only successful at reducing the iliopsoas activation impulse in one case for participant 01. The objective function could be refined in a more subject specific manner in future work. The objective function of the 'enhanced' walking simulations could be developed to include other features of gait, such as energy expenditure or joint loading of the intact knee, to improve the likelihood of predicting gait modifications that do not have a detrimental impact in other respects.

The future direction of this study is to validate the kinematic modifications predicted by implementing them experimentally in a laboratory. This would involve a gait retaining method, to observe whether the kinematic modifications predicted can be replicated and if so, if they have the same effect on iliopsoas activation. This is addressed in the following chapter of this thesis. This framework of forward dynamic modelling of individuals with UTF / UTK amputations could be utilised for a variety of applications with clinical relevance, for example investigating loading conditions that are associated with secondary conditions such as osteoarthritis and osteopenia (Gailey et al. 2008).

Chapter 5

A biofeedback gait retraining tool for enhanced walking in individuals with unilateral transfemoral and through-knee amputations

Addressing the third and fourth objective of this thesis, this chapter presents a feasibility study of a novel biofeedback gait retraining tool which targets muscle recruitment that may be associated with reduced walking endurance via kinematic modifications for individuals with unilateral transfemoral and through-knee amputations, based on the predictions made in Chapter 4. Chapter 3 found that there was increased recruitment (force magnitude) of the iliospoas muscle in the residual limb of individuals with unilateral transfemoral amputations compared to able bodied controls and the intact limb side. The corresponding elevated muscle activation and impulse suggest this may be a limiting factor in walking endurance for this population. The forward dynamic musculoskeletal modelling in Chapter 4 found that reducing the activations of the iliospoas while maintaining self-selected walking speed could be achieved during gait by reducing the hip extension throughout the gait cycle (increased maximum flexion and reduced maximum extension). For ease of implementation in an experimental protocol, this chapter focused on reducing the maximum extension angle of the residual limb side during terminal stance, as this is the phase of gait when flexion torque is elevated in the residual limb side compared to the intact side, leading to increased recruitment of the iliopsoas muscle according to the analysis of Chapter 3. Additionally, the forward dynamic modelling in Chapter 4 suggested that reducing step length while maintaining self-selected speed may lead to reduced iliopoas muscle activation. This chapter develops and evaluates a novel biofeedback gait retraining tool based on these two specific gait modifications: reducing the maximum extension angle and decreasing step length.

5.1 Introduction

5.1.1 Background

According to a 2010 review, bio-feedback began appearing in the literature around 40 years ago (Tate & Milner 2010). Biofeedback is the relaying of augmented physiological or biomechanical characteristics to a participant for rehabilitation purposes. This 'feedback' of information informs the participant to adapt their motion or behaviour (Tate & Milner 2010). Biofeedback allows detections of gait deviations that may not be possible with traditional gait retraining methods, which consist of verbal feedback from a physiotherapist (Quiñones et al. 2009). A review by van Gelder et al. (2018) of biofeedback in gait retraining found that visual was the most common feedback mode, the other modes being auditory, sensory (haptic), or combinations of the three. Studies found that the best results of gait retraining were obtained when combining visual and audio feedback (Hirokawa & Matsumura 1989) (Shin & Chung 2017) (Yen et al. 2014), compared to using them separately. The review found kinematic parameters were the most common parameters to be tracked and fed-back, with other parameters being kinetics, spatiotemporal, muscle activity and physiological or a combination (van Gelder et al. 2018). Most of the studies captured in this review (over half) report on just one training session with 68 % of the studies reporting positive outcomes. The majority of studies reviewed were applied to stroke patients and healthy participants. Visual biofeedback in gait re-training is becoming more common clinically when treating stroke patients (Spencer et al. 2021).

Biofeedback has been utilised in gait retraining of individuals with lower limb amputations. A 2020 review of biofeedback for gait retraining of this population found that most of the studies were implemented in laboratory settings, with both overground and treadmill gait (Escamilla-Nunez et al. 2020). A variety of gait features have been targeted in this population. For example, visual feedback has been used to increase stance time on the amputated limb of individuals with UTF / UTK amputations which achieved a 36% improvement in stance time symmetry and a 22% increase in prosthetic limb peak propulsion and 47% improvement in peak propulsion symmetry (Brandt et al. 2019). Visual feedback has also been applied to the centre of mass sway and thigh muscle activation for individuals with transtibial amputation (Russell Esposito et al. 2017), successfully reducing both parameters by 12%. Another example is knee angle which has been targeted via tactile feedback to reduce risk of falling in a pilot study of an individual with a unilateral transtibial amputation, this pilot study achieved a 17% improvement in response time during their standing task which involved the participant receiving external focus style instructions as well as the tactile feedback (Maldonado-Contreras et al. 2017).

Kinematic modifications

Chapter 4 suggested a reduction in maximum extension angle may reduce the iliacus and psoas major force during walking. A study by Lewis et al., 2010, which utilised musculoskeletal modelling to examine the mechanical conditions leading to anterior hip pain, investigated the anterior hip joint force with relation to sagittal hip range of motion

(the primary muscles contributing to anterior hip force are the iliacus and psoas major). Their model predicted there would be a 24% increase in anterior hip joint force with a 2° increase of maximum extension angle during gait. They found the timing of peak anterior hip joint force to be around the 50% of gait, where the maximum extension angle occurs. This coincides with the timing of the peak iliopsoas force in Chapter 3. This study noted reduced muscle moment arm with increasing hip extension, which would require higher activation for the same torque (Lewis et al. 2010). These results are encouraging to the rationale of this study that reducing maximum extension angle during gait may reduce the demand on the iliopsoas muscle.

Chapter 4 also suggested a reduction in step length may reduce the iliacus and psoas major force during walking. A previous study evaluated the effects of varying stride length (two successive step lengths) on knee adduction and flexion moments, which are relevant to the progression of patients with knee osteoarthritic, in a preliminary study for potential applications in gait retaining (Edd et al. 2020). This study found that a reduction of 14 cm of stride length significantly decreased knee flexion and adduction moment (Edd et al. 2020) while maintaining speed by increasing cadence. Another study found that a reduction of 10 cm and 15 cm of stride length significantly reduced the impulse of knee adduction moment in patients with medial osteoarthritis (Ulrich et al. 2023).

Motor learning in rehabilitation

Gait modification is the therapeutic aim to the optimise a specific feature of gait, a common goal in the rehabilitation of musculoskeletal disorders (Charlton et al. 2021) and the goal of this chapter. The biofeedback methods utilised in physical rehabilitation are ultimately attempting to achieve motor learning (Sawers et al. 2012). Successful motor learning of gait modifications is required for these modifications (and adopted motor skills) to be retained and have a clinical benefit long-term. Yet this motor learning process, is often not considered in studies implementing gait modifications via biofeedback (Charlton et al. 2021). In other applications, such as sports, goal setting is thought to improve learning and therefore performance (Sawers et al. 2012), and this is the nature of the biofeedback method adopted in this chapter and other studies. An understanding of motor-learning should be incorporated into the interpretation of the results of this chapter, and subsequently in the design of rehabilitation protocols for this population to achieve clinical efficacy.

5.1.2 Aims and objectives

It appears from previous studies that visual and audio biofeedback could provide effective assistance to gait retraining in individuals with UTF / UTK amputations and could be applied to implementing the gait modifications modelled in Chapter 4. The overall objective of this chapter was therefore to investigate the feasibility and effectiveness of two biofeedback tools to adapt the kinematics of individuals with UTF / UTK amputations with the purpose of reducing the peak force of the psoas major and iliacus in the

residual limb during gait. Two different biofeedback tools were tested. Both interfaces combined real-time visual and audio feedback as found effective by Gelr et al's review (2018) and implemented on a treadmill to control for walking speed. The 'extension angle goal' specifically tracked the residual limb and encouraged a reduced maximum extension angle at terminal stance. The 'step length goal' encouraged a reduction of step length for both the residual and intact limb. Both goals ultimately aimed to reduce the maximum external extension torque on the residual limb, to reduce force requirements of the residual limb's psoas major and iliacus muscles. It was hypothesised that the 'step length goal' is easier to follow and will produce more natural gait. If successful, these biofeedback tools could be incorporated into a gait retraining protocol to increase walking endurance for individuals with UTF / UTK amputation. A full breakdown of this chapters aims are listed below.

In order to investigate the feasibility and effectiveness of these biofeedback tools, two preliminary studies needed to be conducted. These were to: validate the use of treadmill gait in gait retraining biofeedback tools as a representative of overground walking for individuals with UTF / UTK amputations; and validate the use of a non-subject specific musculoskeletal model (FreeBody) for estimation of muscle activations in gait for individuals with UTF / UTK amputations. Following these two preliminary studies, three primary aims were addressed:

Aim 1: to investigate whether participants with UTF / UTK amputation donning microprocessor knee are able to follow the two novel biofeedback interfaces and adapt their kinematics accordingly.

Aim 2: to investigate whether the kinematic adaptations have the desired effect of reduced activation of the psoas major and iliacus muscles.

Aim 3: to quantify the overall kinematic strategies of achieving the kinematic modification goals.

5.2 Method

5.2.1 Participants

Six participants were included in this study (44 – 59 years), four individuals with unilateral transfemoral amputations (UTF) and two individuals with unilateral through-knee amputations (UTK). All had sustained amputation due to trauma. Five of the six participants had undergone military rehabilitation. All donned their own microprocessor prosthetic knees and energy- return prosthetic foot (Table 5.1). Ethical approval was received from the Imperial College Research Ethics Committee and written informed consent obtained from the participants.

Table 5.1: Participant information

Participant	Sex	Level	Age (years)	Years since amputation	Height (m)	Body mass with prosthetic (kg)	Residual limb length (cm)	Knee type	Foot type	Socket type
01	M	UTF	49	17.5	1.78	95	40	Genium X3	Triton	Ischial
02	M	UTK	44	19	1.77	82.2	56	Genium X3	Triton	End bearing
03	M	UTF	49	4	1.85	94	43	Genium X3	Triton	Ischial
04	M	UTF	59	20	1.78	91.8	35.5	C-leg 4	Kinterra	Ischial
05	M	UTF	54	51	1.77	90.6	27	C-leg 4	Triton	Ischial
06	F	UTK	57	2	1.72	116	55	Genium X3	Ottobock	End bearing

5.2.2 Data collection

Four walking conditions were assessed:

1. Baseline overground walking
2. Baseline treadmill walking
3. Treadmill walking following 'extension goal'
4. Treadmill walking following 'step goal'

Motion capture data collection

Reflective markers were attached to anatomical landmarks of the pelvis, the left and right lower limbs as well as marker clusters on the thighs and shanks (Table 5.2), as displayed in Figure 5.1. Initially one static and three baseline gait trials at a self-selected speed were collected in an overground motion capture laboratory which consisted of a ten camera (VICON, Oxford Metrics Group, United Kingdom) and two force plate system (Kistler Type 9286B, Kistler Instrumented AG, Winterthur, Switzerland). The marker 3D displacement and ground reaction forces were sampled at 120 Hz and 960 Hz respectively. Then the three other gait conditions (which are detailed below) were captured in a GRAIL and M-Gait system laboratory (Motek, a DIH brand, Netherlands) which consisted of 10 cameras (VICON, Oxford Metrics Group, United Kingdom) and a two-force plate instrumented treadmill (Motekforce link Force Plate, Netherlands) collected at 100 Hz and 1000 Hz respectively. As well as motion capture, the GRAIL system includes virtual reality features with a 180-degree screen for visual projection, visual floor projection, and a sound system.

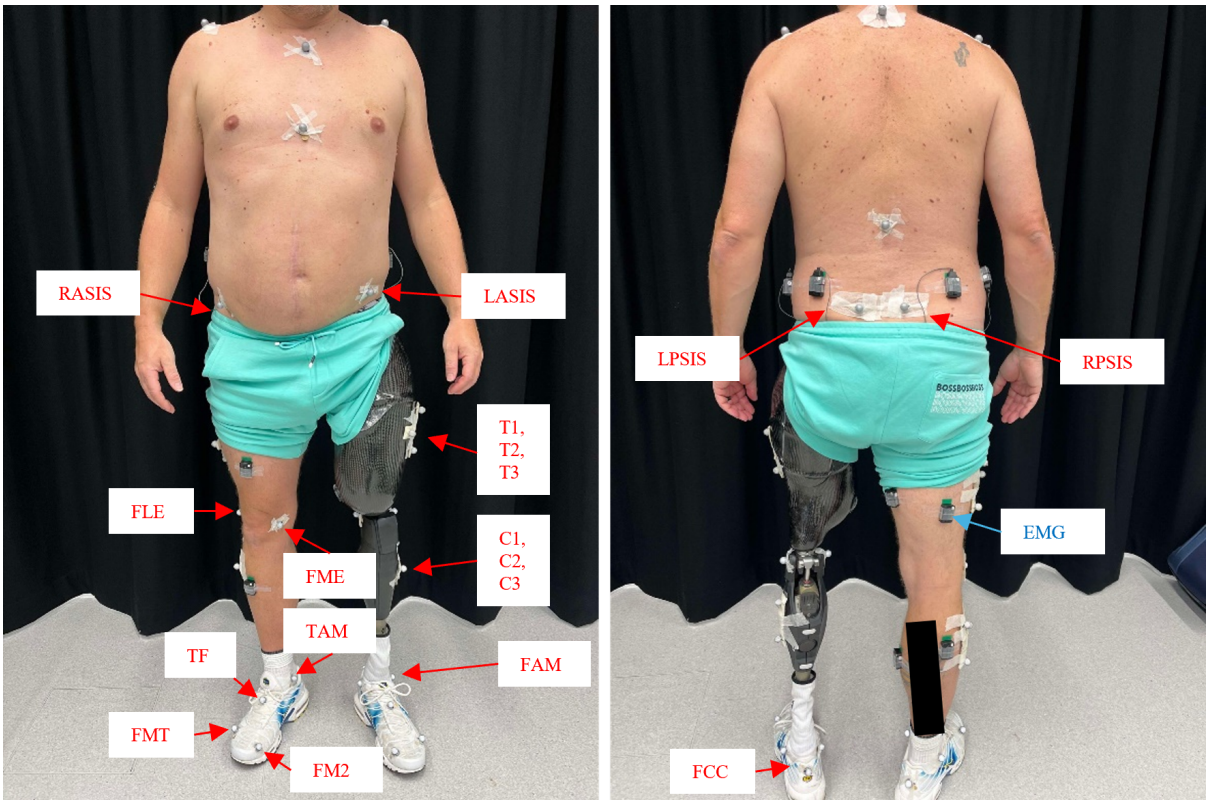


Figure 5.1: Participant with reflective markers and EMG sensors attached for data collection protocol

Table 5.2: Optical motion tracking cluster and marker positions and labels

Marker label	Anatomical location
FCC	Calcaneus
FMT	Tuberosity of the fifth metatarsal
FM2	Head of the second metatarsal
TF	Additional marker placed on foot
FAM	Apex of the lateral malleolus
TAM	Apex of the medial malleolus
C1,C2,C3 (clusters)	Additional markers placed on the shank segment
FLE	Lateral femoral epicondyle
FME	Medial femoral epicondyle
T1,T2,T3 (clusters)	Additional markers placed on the thigh segment
RASIS	Right anterior superior iliac spine
LASIS	Left anterior superior iliac spine
RPSIS	Right posterior superior iliac spine
LPSIS	Left posterior superior iliac spine

EMG data collection

Surface EMG (Delsys Incorporated, Natick, MA, USA) was collected during all the gait conditions of the tibialis anterior, semitendinosus, rectus femoris, gluteus medius, gluteus maximus, gastrocnemius medialis, gastrocnemius lateralis and biceps femoris of the intact limb for 5 of the participants, EMG was not collected for participant 06 due to difficulty identifying muscle location and adequate placement. EMG was collected of the gluteus maximus of the residual limb for participants 01, 02 and 03. EMG data collection of the residual limb was not possible for the other participants due to socket fit and scar tissue. The EMG was collected at 2000 Hz for participant 1 to 4 and 2148 Hz for participant 5. The sensors were placed over the belly of the muscles and parallel to the muscle fibres (Zipp 1982). Prior to placement the skin was cleaned with an alcohol wipe and shaved if required to reduce noise. Figure 5.1 displays EMG sensors attached to one participant ready for the data collection.

Biofeedback protocol

The GRAIL system and the Motek software D-flow (Motek, a DIH brand, Netherlands) allows for real time inverse kinematics and therefore feedback of kinematic features delivered with the visual projection and audio. D-flow was used to design two visual and audio feedback interfaces. The first encouraged a reduction in maximum hip extension angle at terminal stance phase of gait. This interface provided a visual graphical representation of real-time hip range of motion in the sagittal plane, and a 'goal' of reduced maximum extension angle was provided. When this goal was not met the participant was made aware with an audio cue. Figure 5.2 displays the visual feedback provided by this interface and indicates the conditions where the audio cue would sound. This interface will be referred to as the 'Extension goal'.

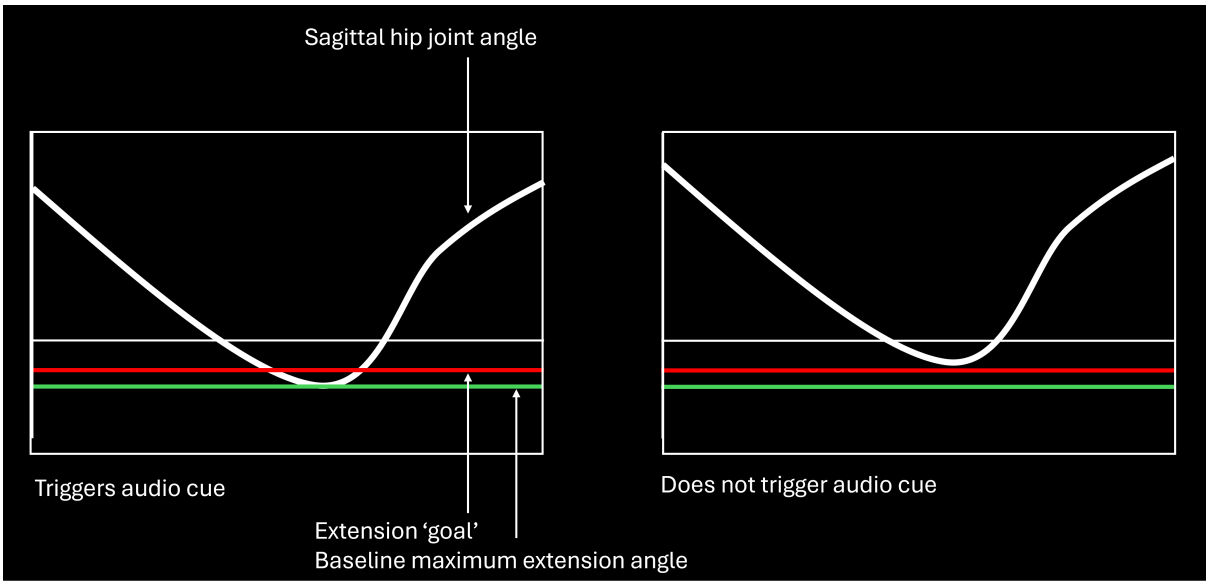


Figure 5.2: Diagram of the visual interface for the 'Extension goal'

The second interface encouraged a reduction in step length, similarly by providing a visual representation of forward foot motion (of the left and right foot) and provided a 'goal' of reduced step length, giving an audio cue when this goal was not met. Figure 5.3 displays the visual feedback of this interface and indicates the conditions where the audio cue would sound. This interface will be referred to as the 'step goal'.

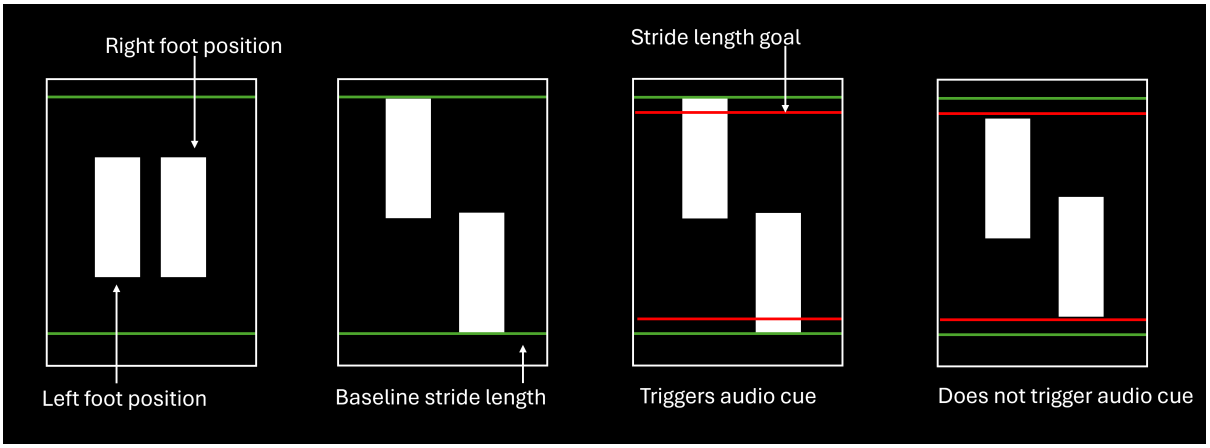


Figure 5.3: Diagram of the visual interface for the 'Step goal'

The participant wore a harness, and this harness was attached to a pulley above the treadmill to reduce the risk of falling. The participant was asked to walk on the treadmill to familiarise themselves with treadmill gait. During this period the treadmill speed was incrementally increased until a comfortable walking speed was achieved for the participant. This speed was slightly increased and then reduced, to ensure the participant felt that this comfortable walking speed was their 'baseline' walking speed. This speed was taken as their self-selected speed. This speed was maintained for all three conditions of walking in the data collections. Once this speed was selected, motion capture data (marker position and ground reaction force) was collected at baseline walking. The participant then had a rest period of 10 minutes.

During the rest period, the 'extension goal' feedback system was explained to the participant assisted with a series of diagrams, provided in Appendix B, so they knew what to expect from the interface. The participant was then asked to walk on the treadmill again, this time the visual representation of sagittal residual hip range of motion was provided. Once the participant was familiar with the real-time feedback of the visual graphical representation of the hip range of motion, the reduced maximum extension angle goal was introduced. Once the participant was familiar with the visual goal, and how their kinematics can be adapted to reach said goal, the audio cue was introduced. The participant then had a 10-minute familiarisation period with the full interface, followed by a 5-minute rest period. Motion data (marker position and ground reaction force) was then collected while the participant was walking on the treadmill while following the 'extension goal' feedback interface. After the data collection, the participant had a 10-minute rest period. During this period, they were asked to complete a perceived effort questionnaire to capture their experience of the interface (see Appendix C).

The 'step goal' feedback system was then explained to the participant with assistance of a series of diagrams (Appendix B). The same process was followed, the visual representation was introduced, then the goal and then the audio cue. The participant was given a 10-minute familiarisation period with the feedback system and a 5-minute rest period, following this, motion data was captured while walking on the treadmill following the interface. After the data collection the participant completed a perceived effort questionnaire with regards to the 'step goal' system (Appendix D).

5.2.3 Data processing and analysis

3 trials were collected and processed for the overground walking. 6 trials were collected and processed for the treadmill data collection in the three conditions (ie. a total of 18 trials per participant); this was to account for the expected increased variance in walking kinematics when following the goals.

Musculoskeletal modelling and stride length calculation

An identical method of musculoskeletal modelling as detailed in Chapter 3 was followed; the FreeBody musculoskeletal model (Cleather & Bull 2015) was used to acquire joint angles (through inverse kinematics), net joint torque (through inverse dynamics) and quantify muscle forces (through static optimisation) of the gait trials. The details of the anatomical geometries and anthropometric parameters of the FreeBody model of an individual with UTF are outlined in Chapter 3 (Toderita et al. 2021) (Ding et al. 2019). For the individuals with UTK amputations an identical method was followed in selecting the anatomical geometries, except an anatomical model of TK amputation was used.

Stride length was calculated from the position of calcaneus markers (FCC) during double support phase for the baseline treadmill walking condition and the 'step goal' walking condition for the 6 gait trials.

EMG processing

The signals were processed following a method of Amiri et al. (2015). The raw EMG signals were visually inspected, then a band pass filter (20 and 500 Hz) was applied to remove low frequency movement artefact noise (De Luca et al. 2010) and high frequency which was found negligible in EMG signals (Amiri et al. 2015). The EMG signals were then corrected for gains and bias, full wave rectified and filtered with a second order Butterworth low pass filter with a cut off frequency of 6 Hz (Winter 2009).

Data analysis and statistical testing

Preliminary Study 1 (overground versus treadmill walking): for the two-way comparison between baseline overground gait kinematics and baseline treadmill gait kinematics, the kinematics of hip, knee and ankle were normalised to gait cycle (0-100%, where 0% is

heel strike). Mean values of kinematics were calculated of the baseline overground trials (N=3) and the baseline treadmill trials (N=6) per participant, data normality was checked using the Shapiro-Wilk statistical test and then statistical parametric mapping (SPM) was used to compare the overground kinematics and treadmill kinematics with a Friedman with Wilcoxon test with significance set at 0.05 for the full group (Pataky et al., 2013). SPM was selected as an appropriate statistical method as it allows for comparison over the time series of the full gait cycle.

Preliminary Study 2 (EMG validation): the estimated muscle activations from the overground walking trials were validated against the EMG on a trial-by-trial basis. The estimated muscle activations and EMG signals were normalised to gait cycle (0-100%, where 0% is heel strike) and to the highest value reached over the gait cycle in that trial, and plotted for each muscle and each trial. The magnitude (M), phase (P) and combined (C) errors of the estimated muscle activations and the muscle activations recorded via EMG were quantified using the Sprague and Geers metric (Schwer 2007). The interpretations of these errors are defined in Table 5.3 (Klemt et al. 2019). Sprague and Geers metric was selected as an appropriate method of comparison as it incorporates the magnitude and phase over a time series quantitively, which is not true for other methods such as qualitive comparisons or binary comparisons of the muscles being 'on' and 'off'.

Table 5.3: Interpretation of error margins from the Sprague and Geers metric (Klemt et al. 2019)

Error margin	Similarity
0 – 0.15	Excellent
0.15 – 0.30	Very good
0.30 – 0.45	Good
0.45 – 0.60	Moderate
>0.60	None

Aim 1: To determine whether the participants could successfully follow the 'extension goal' and 'step goal', a full group analysis was conducted to quantify the overall effect. The mean maximum extension angle was calculated for the baseline condition and 'extension goal' condition, and mean stride length was calculated for the baseline condition and 'step goal' condition, across the six trials for all six participants. Data normality was checked using the Shapiro-Wilk statistical test and then a Wilcoxon Signed-Rank Test was then performed to compare the mean values of maximum extension angle and stride length between the baseline and the 'extension goal' and 'step goal' conditions respectively (N = 6). A Wilcoxon Signed-Rank Test was selected due to non-normal distribution.

Subsequently an individual analysis was completed to assess the participant by participant effect, where maximum extension angle and stride length was calculated for the 6 trials in the baseline and goal conditions, data normality was checked using the Shapiro-Wilk statistical test and a Wilcoxon Signed Rank Test was completed between the trials

of the baseline and goal conditions (6 baseline trial values, 6 goal condition values) for each participant. A Wilcoxon Signed-Rank Test was selected due to non-normal distribution. This was to identify any individuals who could effectively adapt their kinematics according to the 'extension goal' and 'step goal'. The participants who could reduce their maximum extension angle or stride length, while following the respective goals, to a statistically significant level were deemed able to 'successfully' adapt their kinematics or spatial features.

Aim 2: for the individuals who could successfully adapt their kinematics or spatial features according to the 'extension goal' or 'step goal', the maximum iliopsoas force (normalised to bodyweight) and force impulse (area under normalised force curve) was calculated. Data normality was checked using the Shapiro-Wilk statistical test. The maximum iliopsoas force and impulse was compared between the baseline treadmill gait trials and 'extension goal' / 'step goal' condition trials with a Student's T Test. The goal was considered to have a 'positive effect' on the participant if the iliopsoas maximum force or impulse was reduced to a statistically significant level while in the goal condition.

Aim 3: for the individuals who could successfully adapt their kinematics and spatial features according to the 'extension goal' or 'step goal', the kinematic strategies to achieve the goal were quantified by comparing the baseline kinematics to the goal kinematics. Hip, knee and ankle kinematics were normalised to gait cycle (0-100%, where 0% is heel strike), data normality was checked using the Shapiro-Wilk statistical test and SPM was used with a Friedman with Wilcoxon test to compare the baseline treadmill kinematics and the 'goal' kinematics. If the full group, all six participants, could successfully adapt their kinematics while following the 'extension' or 'step' goal, this analysis was done on the full group, ie. a mean of the 6 trials were taken per participant and the full group kinematics (in baseline and goals) were compared. If only certain participants could 'successfully' adapt their kinematics according to the 'extension' or 'step' goal, this kinematic analysis was done on an individual basis, ie. 6 trials of baseline compared to 6 trials of goal kinematics for each participant who could successfully achieve the goal. Again, SPM was selected as an appropriate statistical method as it allows for comparison over the time series of the full gait cycle.

5.3 Results

5.3.1 Preliminary Study 1: overground vs. treadmill walking kinematics

The mean and standard deviation of all participants (N=6) kinematics in baseline overground walking and baseline treadmill walking are plotted in Figure 5.4 and 5.5 for the residual limb side and the intact limb side, along with the results of the SPM comparing the overground and treadmill condition. The only significant difference found between overground and treadmill gait was in the sagittal plane of the intact hip at initial stance phase. The treadmill gait had reduced maximum flexion angle ($p = 0.001$).

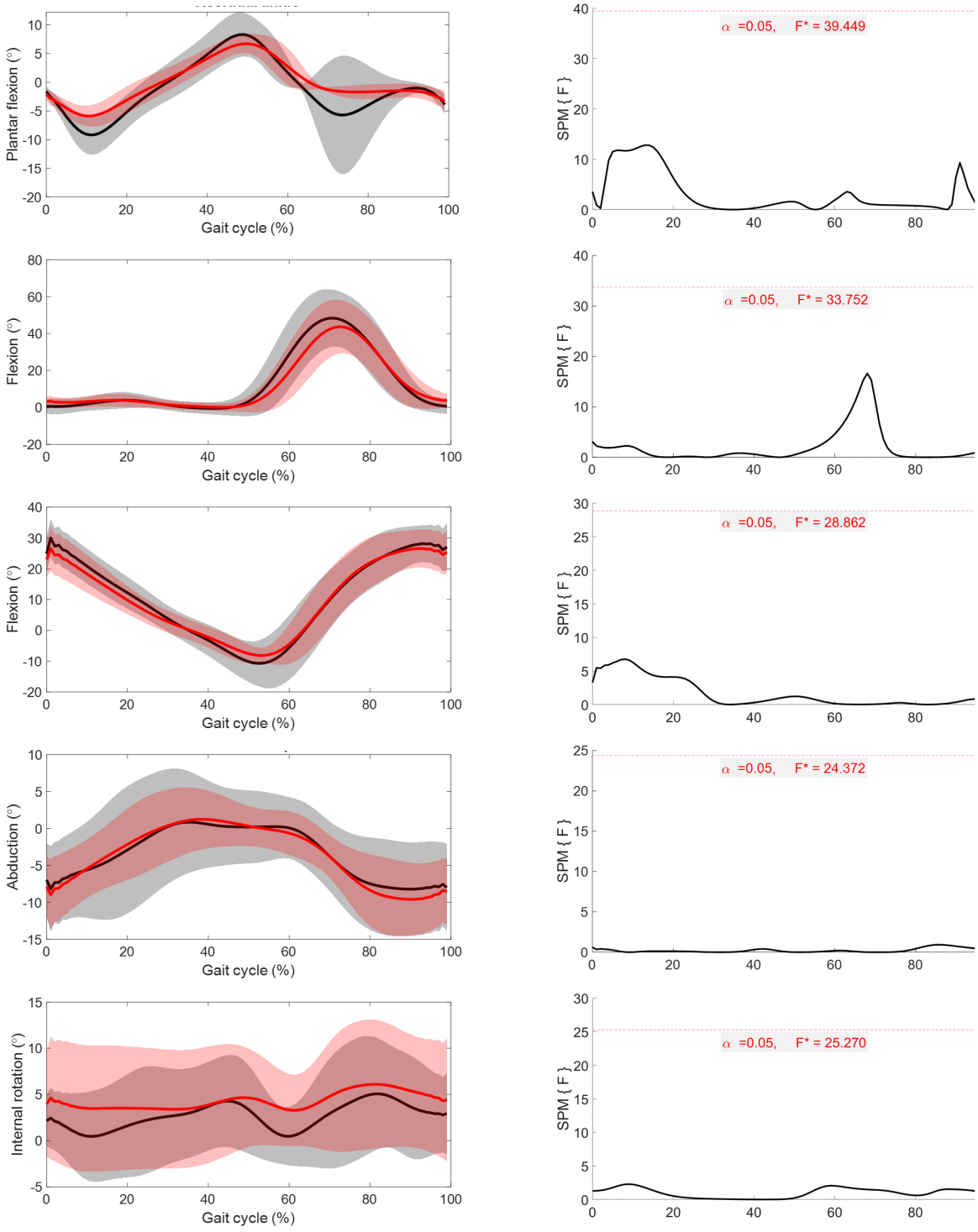


Figure 5.4: Kinematics and SPM results of overground baseline walking (black) and treadmill baseline walking (red) at self-selected speeds of the residual limb side of participants with unilateral transfemoral and through-knee amputation (N=6)

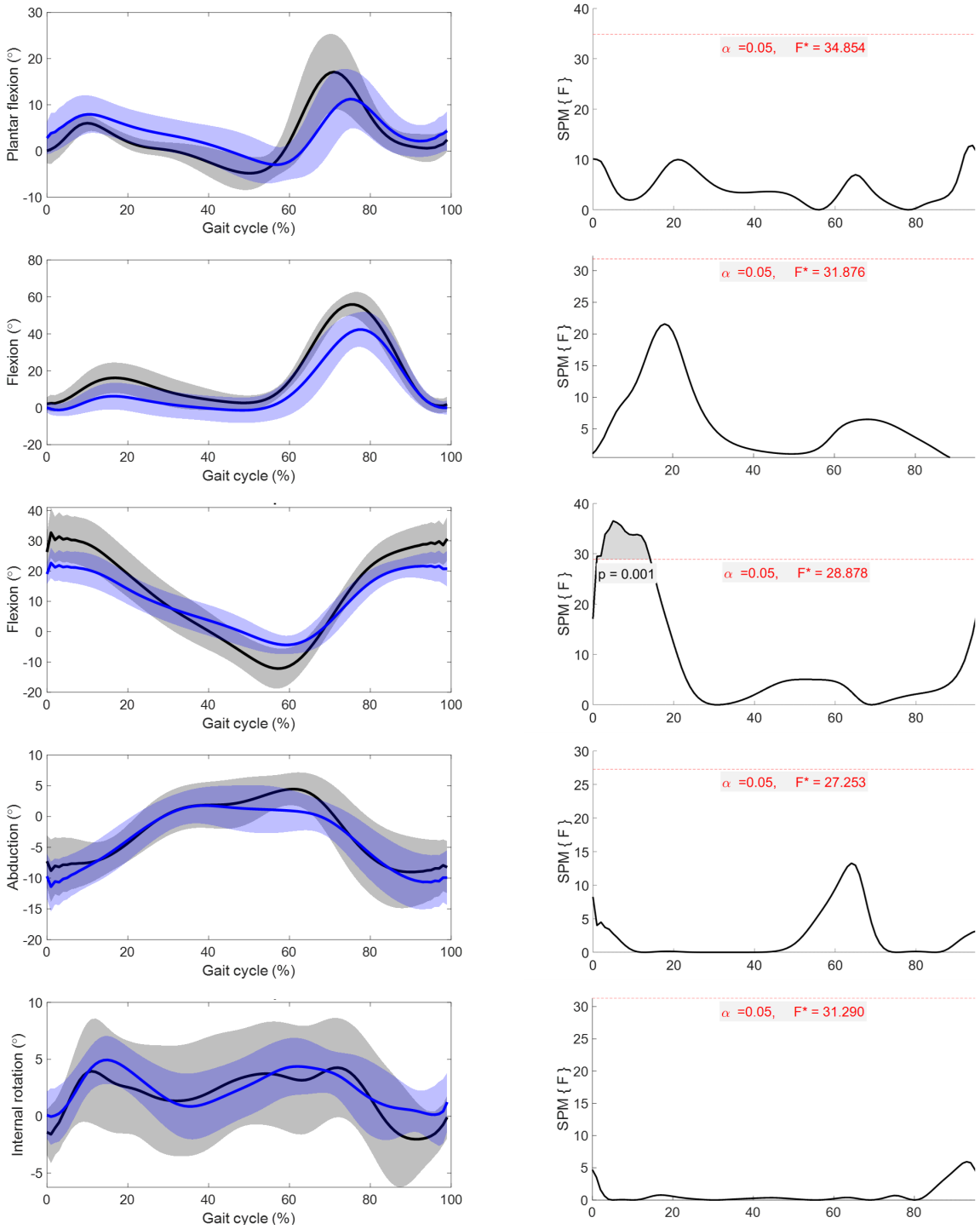


Figure 5.5: Kinematics and SPM results of overground baseline walking (black) and treadmill baseline walking (blue) at self-selected speeds of the intact limb side of participants with unilateral transfemoral and through-knee amputations (N=6)

5.3.2 Preliminary Study 2: EMG validation of Freebody for individuals with unilateral and through-knee amputations

The intact limb

Table 5.4 displays the mean and standard deviation of the combined Sprague and Geers magnitude error (M), phase error (P) and combined error (C) when comparing the EMG signals to the estimated muscle activations from the static optimisation of overground walking for the eight muscles of the 5 participants where EMG was collected. The combined Sprague and Geers value were 'good' for 7 of the 8 muscles and was 'moderate' for the rectus femoris. The normalised EMG signals and estimated muscle activations for the first trial of each participant are plotted in Figure 5.6 to 5.10. The plots of the subsequent trials can be found in Appendix E. For participant 01 there was an error in the data collection and no signal was collected for the rectus femoris and gastrocnemius medialis.

Table 5.4: Sprague and Geers measures of error of EMG signal compared to estimated muscle activations for the intact limb of participants with unilateral transfemoral and through-knee amputations (N=5)

	M (mean)	M (SD)	P (mean)	P(SD)	C (mean)	C (SD)
Tibialis anterior	0.14	0.10	0.32	0.07	0.44	0.12
Semitendinosus	0.14	0.10	0.25	0.07	0.32	0.08
Rectus femoris	0.34	0.12	0.41	0.04	0.55	0.06
Gluteus medius	0.22	0.12	0.24	0.05	0.36	0.04
Gluteus maximus	0.14	0.10	0.29	0.03	0.37	0.03
Gastrocnemius medialis	0.09	0.14	0.32	0.06	0.38	0.03
Gastrocnemius lateralis	0.12	0.28	0.29	0.09	0.42	0.13
Biceps femoris	-0.17	0.17	0.27	0.06	0.39	0.11

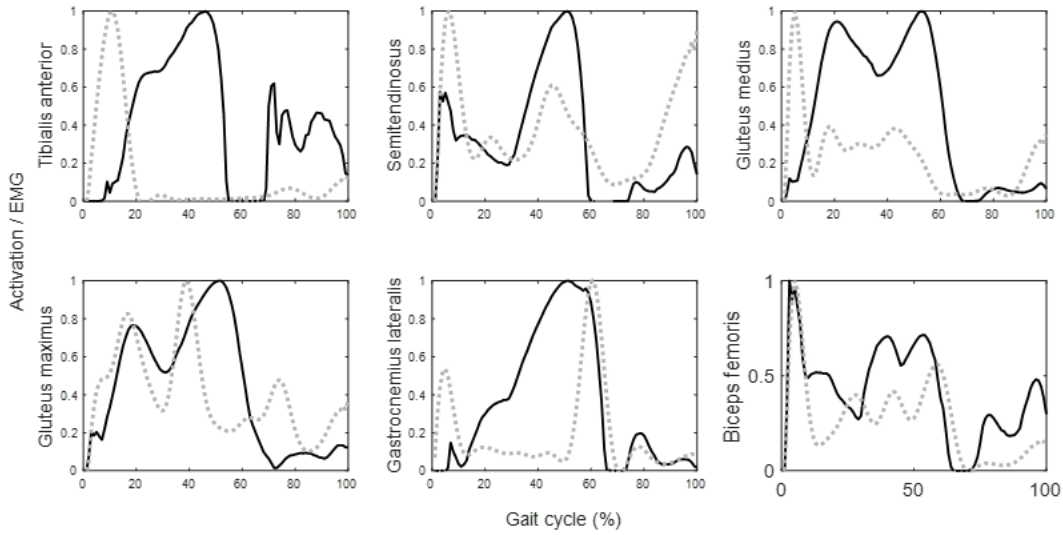


Figure 5.6: EMG (grey – dashed) and muscle activation (black – solid) of the intact limb of participant 01, trial 1

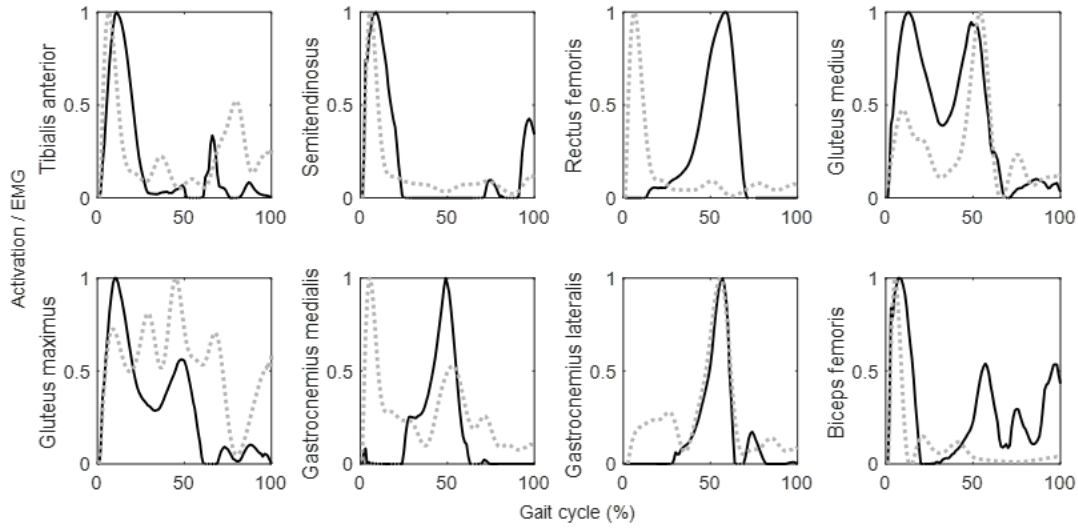


Figure 5.7: EMG (grey – dashed) and muscle activation (black – solid) of the intact limb of participant 02, trial 1

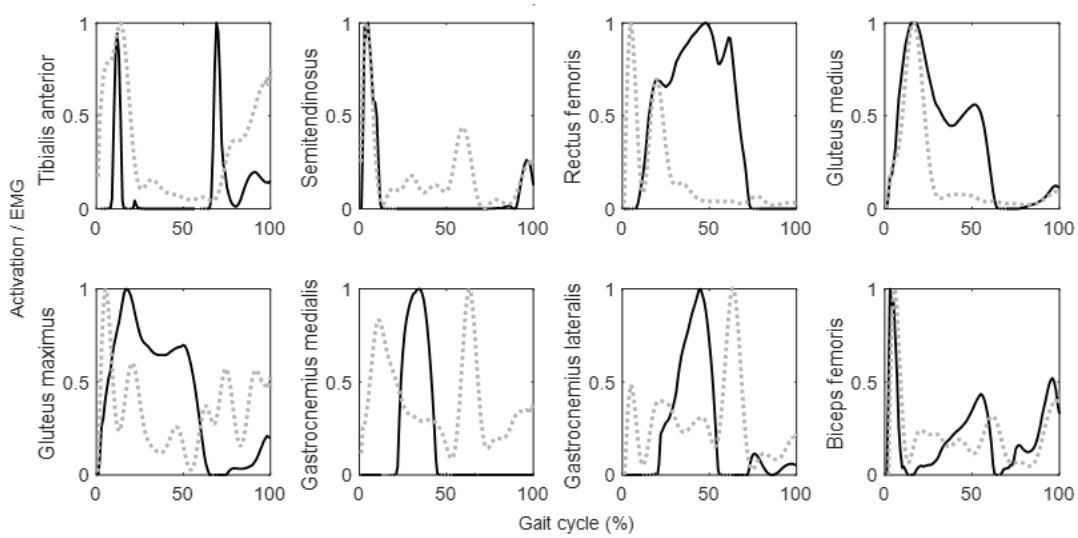


Figure 5.8: EMG (grey – dashed) and muscle activation (black – solid) of the intact limb of participant 03, trial 1

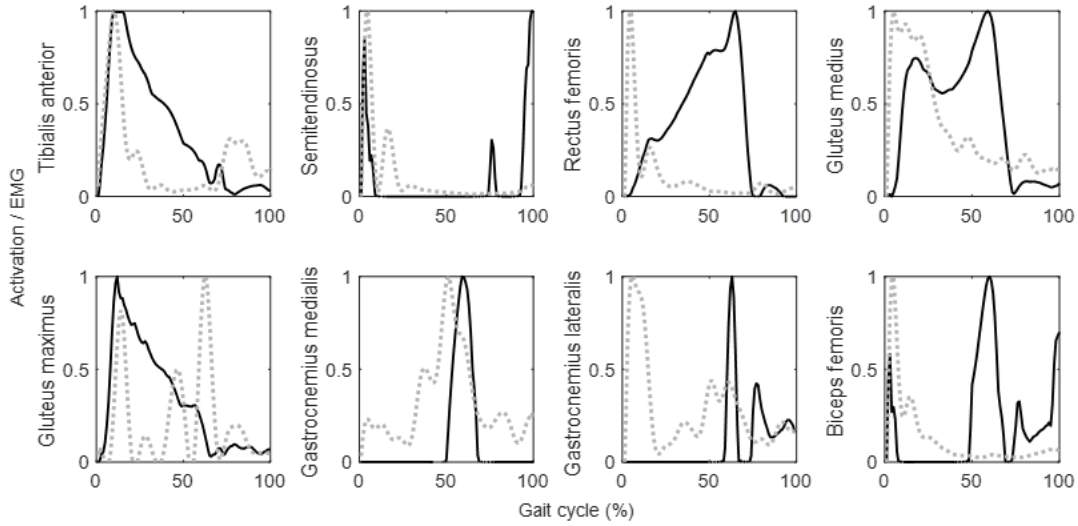


Figure 5.9: EMG (grey – dashed) and muscle activation (black – solid) of the intact limb of participant 04, trial 1

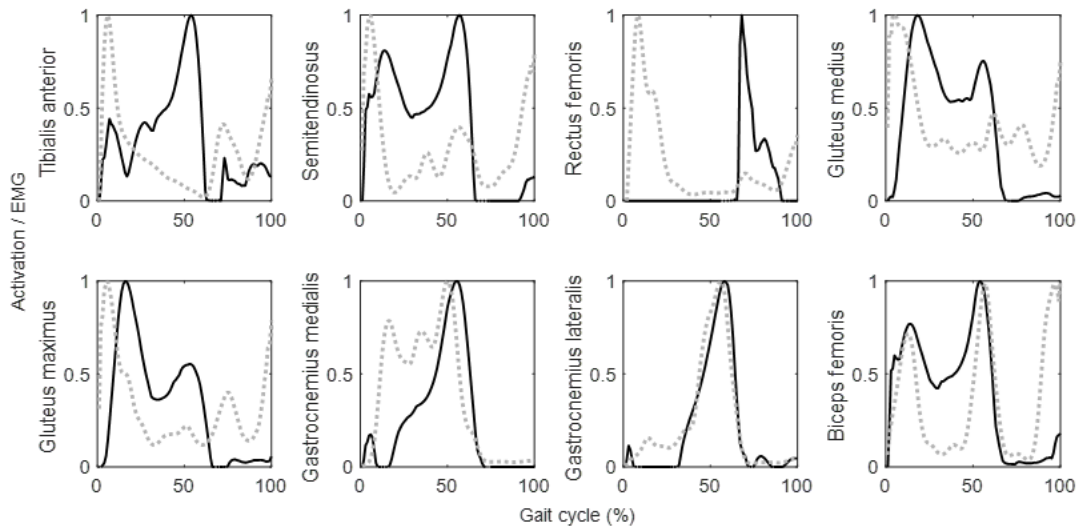


Figure 5.10: EMG (grey – dashed) and muscle activation (black – solid) of the intact limb of participant 05, trial 1

The residual limb

Table 5.5 displays the mean and standard deviation of the combined Sprague and Geers magnitude error (M), phase error (P) and combined error (C) when comparing the EMG signals to the estimated muscle activations from the static optimisation of overground walking for the gluteus maximus of the residual limb of the 3 participants where EMG was collected. The combined Sprague and Geers value was 'good' similarity. The normalised EMG signals and estimated muscle activations for the first trial of each participant are plotted in Figure 5.11 5.12 and 5.13. The plots of the subsequent trials can be found in Appendix E.

Table 5.5: Sprague and Geers measures of error of EMG signal compared to estimated muscle activations for the residual limb of participants with unilateral transfemoral and through-knee amputations (N=3)

	M (mean)	M (SD)	P (mean)	P(SD)	C (mean)	C (SD)
Gluteus maximus	0.11	0.12	0.29	0.05	0.33	0.02

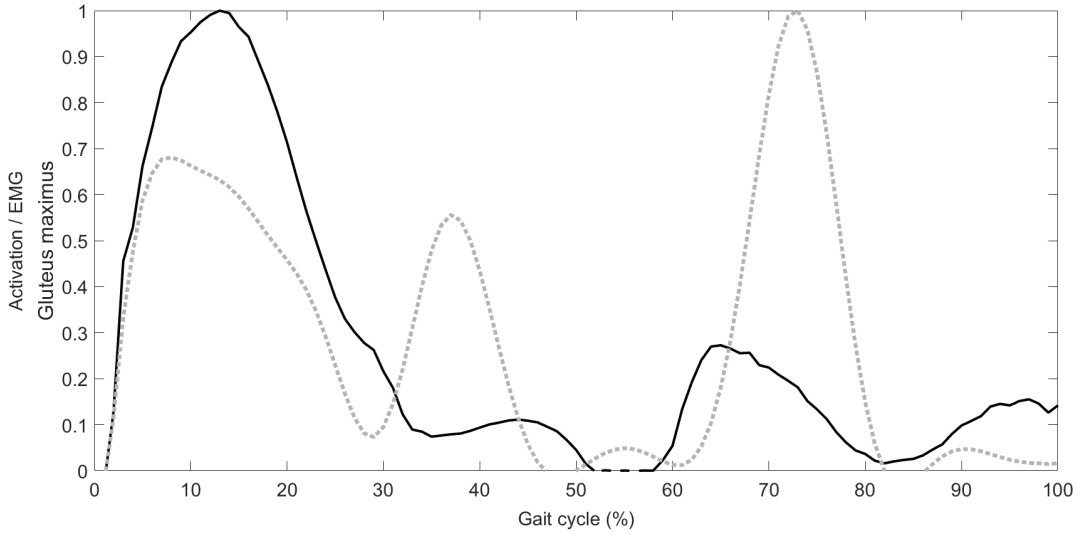


Figure 5.11: EMG (grey – dashed) and muscle activation (black – solid) of the residual limb gluteus maximus of participant 01, trial 1

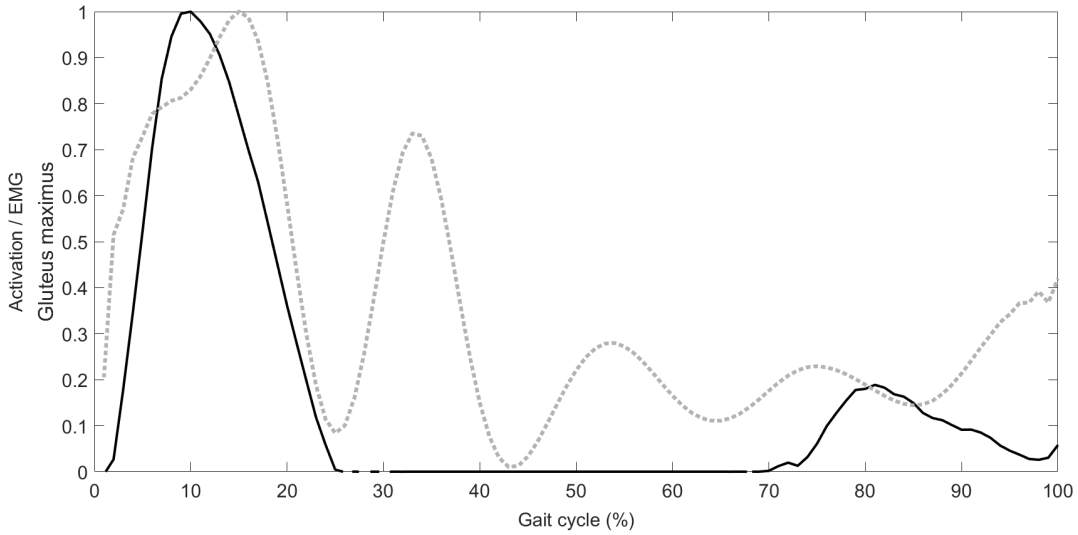


Figure 5.12: EMG (grey – dashed) and muscle activation (black – solid) of the residual limb gluteus maximus of participant 02, trial 1

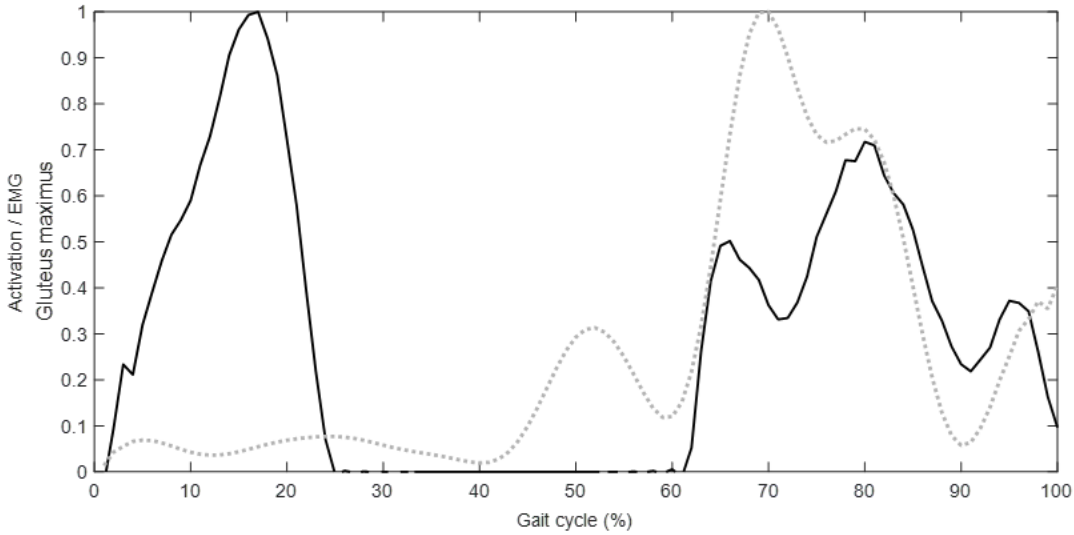


Figure 5.13: EMG (grey – dashed) and muscle activation (black – solid) of the residual limb gluteus maximus of participant 03, trial 1

5.3.3 Aim 1: could the 'extension goal' and 'step goal' be successfully followed?

Aim 1.1 Overall effect - extension goal

The maximum extension angle over a gait cycle of the residual limb hip in baseline treadmill walking and walking while following the 'extension goal' for all participants are plotted in Figure 5.14 with the results from the Wilcoxon Signed Rank Test. There was no significant difference in the overall maximum extension angle.

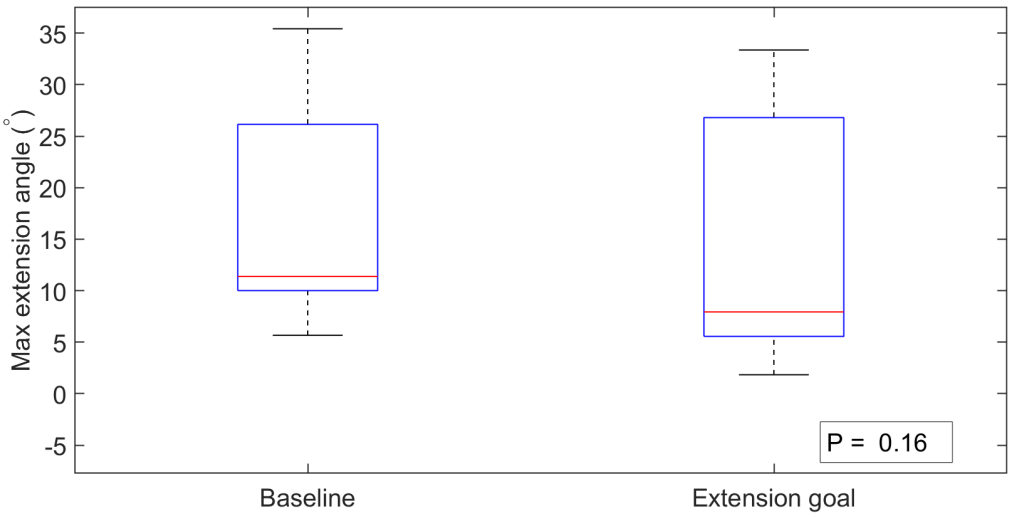


Figure 5.14: The maximum extension angle over a gait cycle for baseline treadmill gait and when following the 'extension goal' of the residual limb of participants with unilateral transfemoral and through-knee amputations (N=6)

Aim 1.1 Overall effect - step goal

The average stride length over a gait cycle in baseline treadmill walking and walking while following the 'step goal' for all participants is plotted in Figure 6.1 with the results from the Wilcoxon Signed Rank Test. There is a significant difference in average stride lengths, p = 0.03.

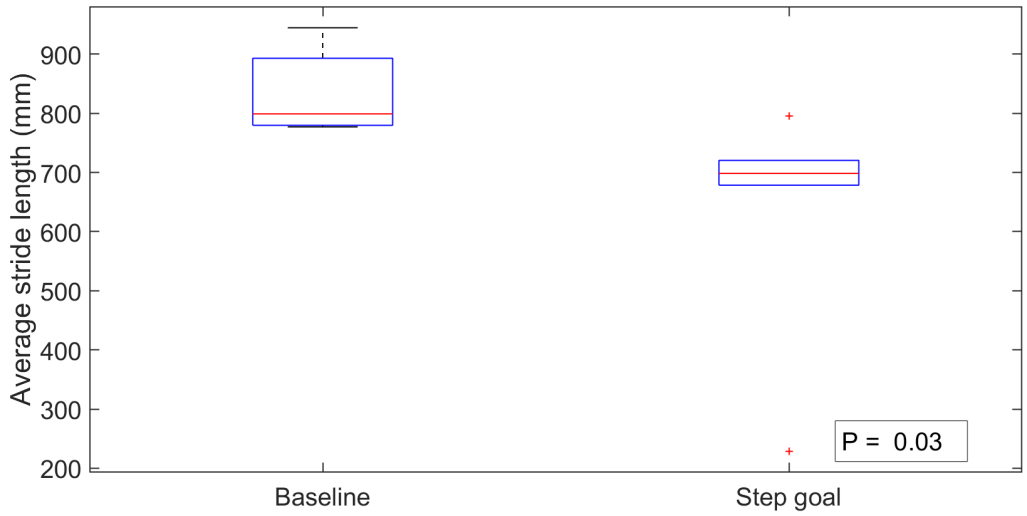


Figure 5.15: The average stride length for baseline treadmill gait and when following the 'step goal' of participants with unilateral transfemoral and through-knee amputations (N=6)

Aim 1.2 Participant by participant effect - extension goal

The mean sagittal hip kinematics of the residual limb during baseline gait and while following the 'extension goal' over 6 trials are plotted for each participant in Figure 5.16 to 5.21. The maximum extension angles are also displayed in a box plot with the results from the Wilcoxon Signed Rank Test between the trials of each condition. For participant 02, 03 and 05, there was a significant reduction in the maximum extension angle in the gait trials while following the 'extension goal' compared to baseline gait trials ($p = 0.03$), therefore it was deemed that these participants (02, 03, 05) could 'successfully' follow the 'extension goal'.

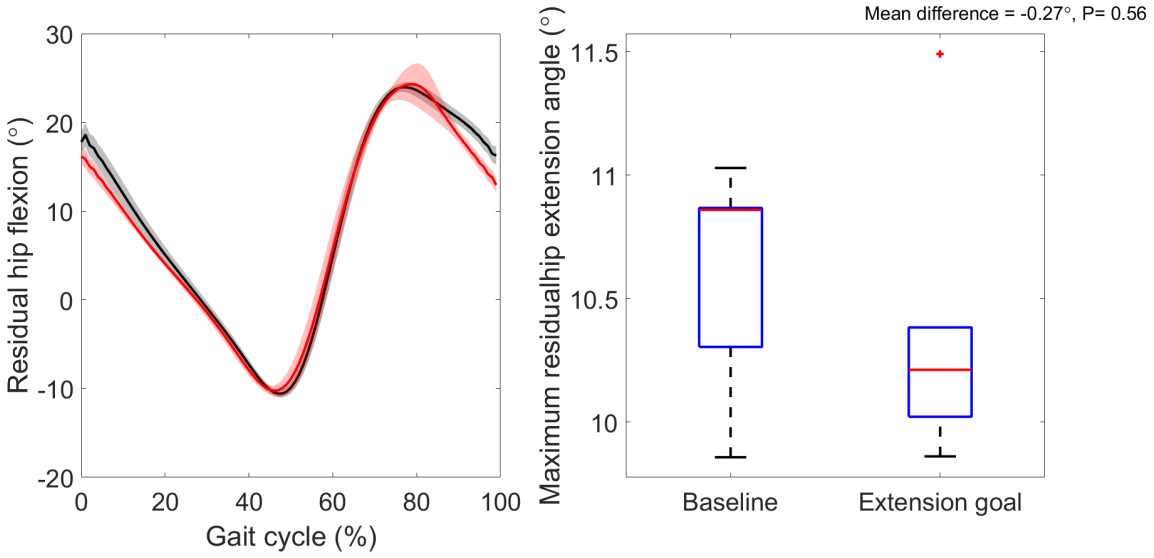


Figure 5.16: Sagittal hip kinematics of the residual limb (left) and maximum extension angle (right) for baseline treadmill walking (black) and walking while following 'extension goal' (red) over 6 trials for participant 01. P value and difference between means displayed.

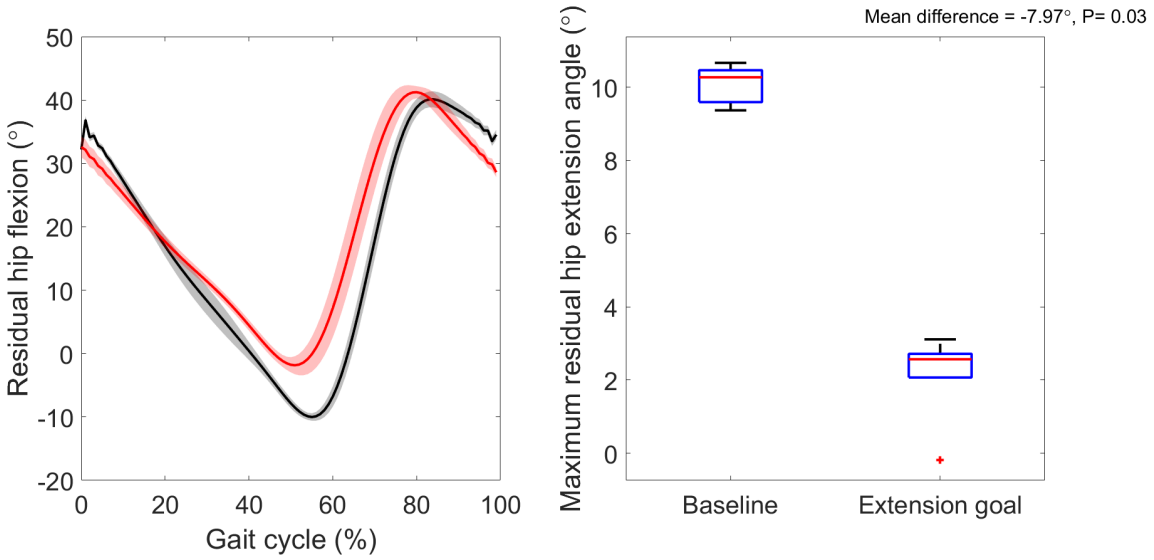


Figure 5.17: Sagittal hip kinematics of the residual limb (left) and maximum extension angle (right) for baseline treadmill walking (black) and walking while following 'extension goal' (red) over 6 trials for participant 02. P value and difference between means displayed.

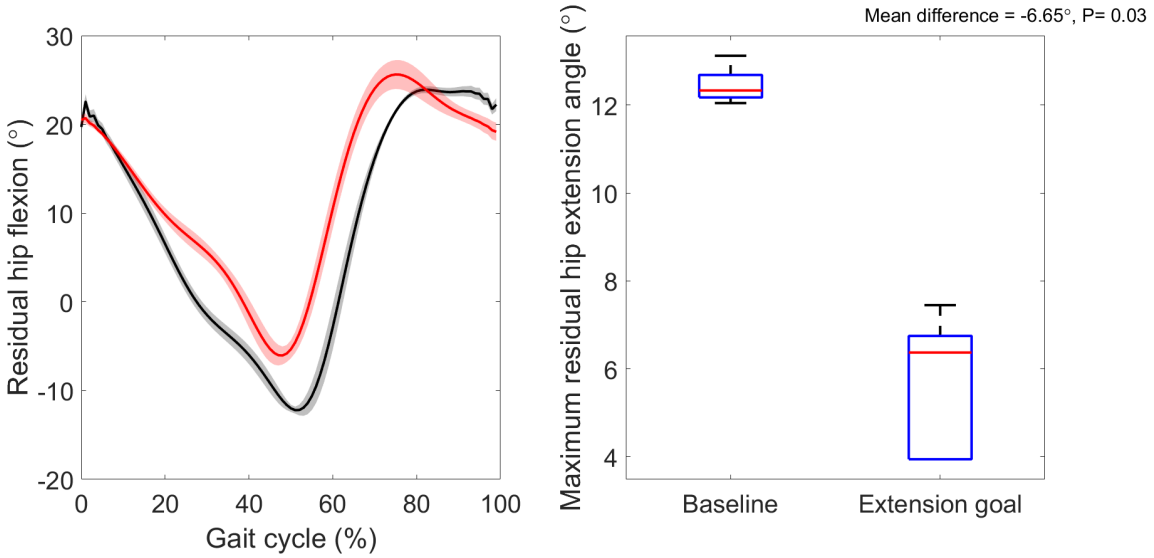


Figure 5.18: Sagittal hip kinematics of the residual limb (left) and maximum extension angle (right) for baseline treadmill walking (black) and walking while following 'extension goal' (red) over 6 trials for participant 03. P value and difference between means displayed.

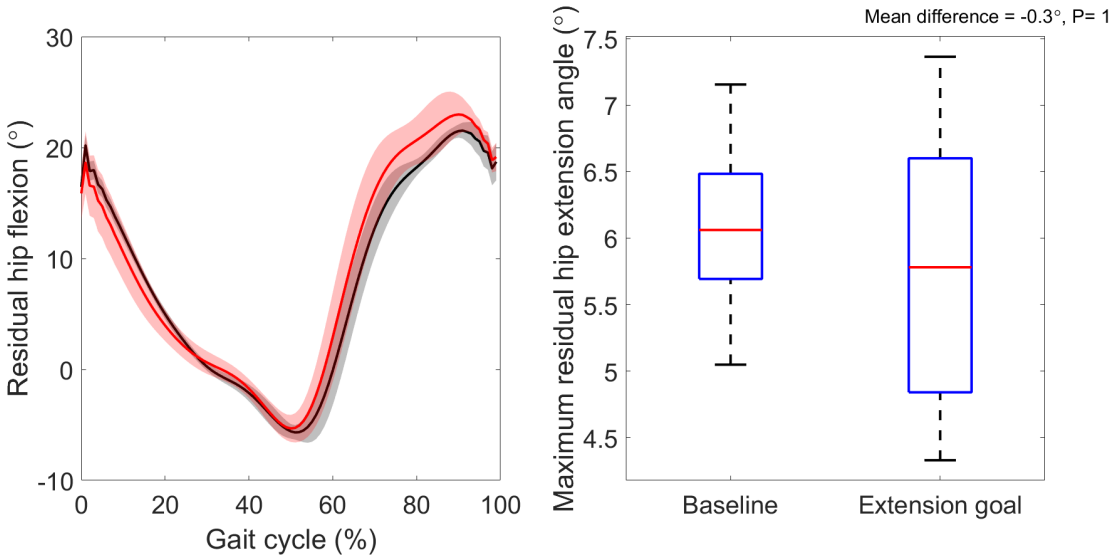


Figure 5.19: Sagittal hip kinematics of the residual limb (left) and maximum extension angle (right) for baseline treadmill walking (black) and walking while following 'extension goal' (red) over 6 trials for participant 04. P value and difference between means displayed.

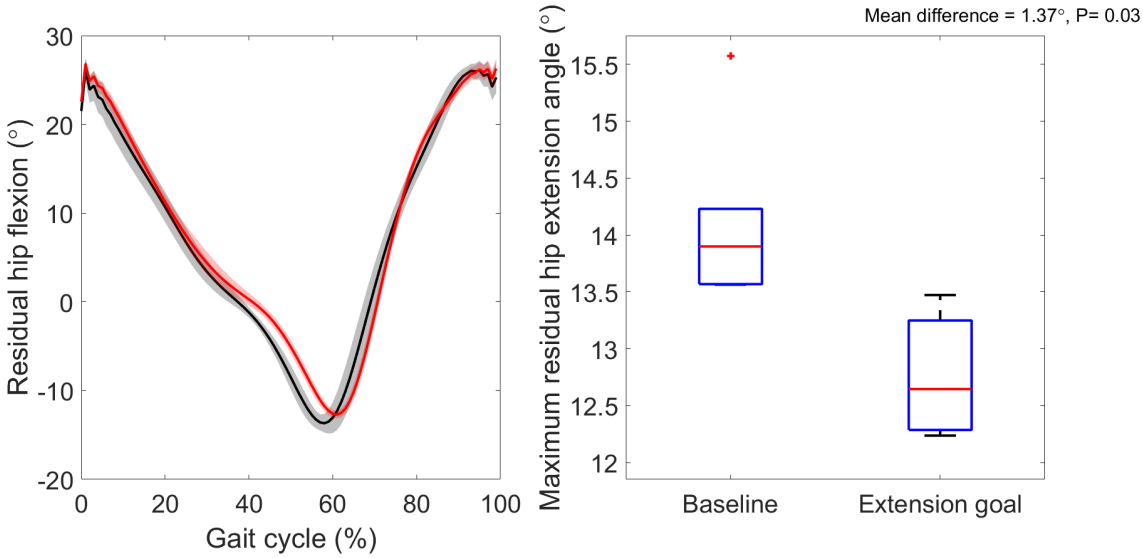


Figure 5.20: Sagittal hip kinematics of the residual limb (left) and maximum extension angle (right) for baseline treadmill walking (black) and walking while following 'extension goal' (red) over 6 trials for participant 05. P value and difference between means displayed.

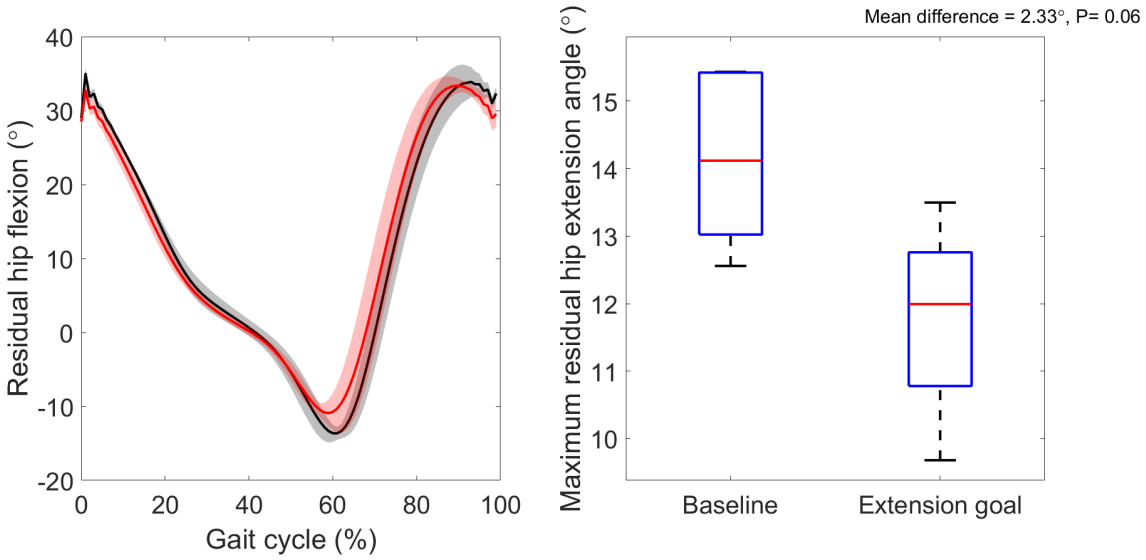


Figure 5.21: Sagittal hip kinematics of the residual limb (left) and maximum extension angle (right) for baseline treadmill walking (black) and walking while following 'extension goal' (red) over 6 trials for participant 06. P value and difference between means displayed.

Aim 1.2 Participant by participant effect – step goal

Figures 5.22 to 5.27 display the stride lengths during baseline walking and walking when following the 'step goal', along with the p values from the Wilcoxon Signed Rank Test comparing these two conditions and the difference in the means, for the 6 participants. There was a significant difference for all participants ($p = 0.03$), therefore all participants were deemed to 'successfully' be able to follow the 'step goal'.

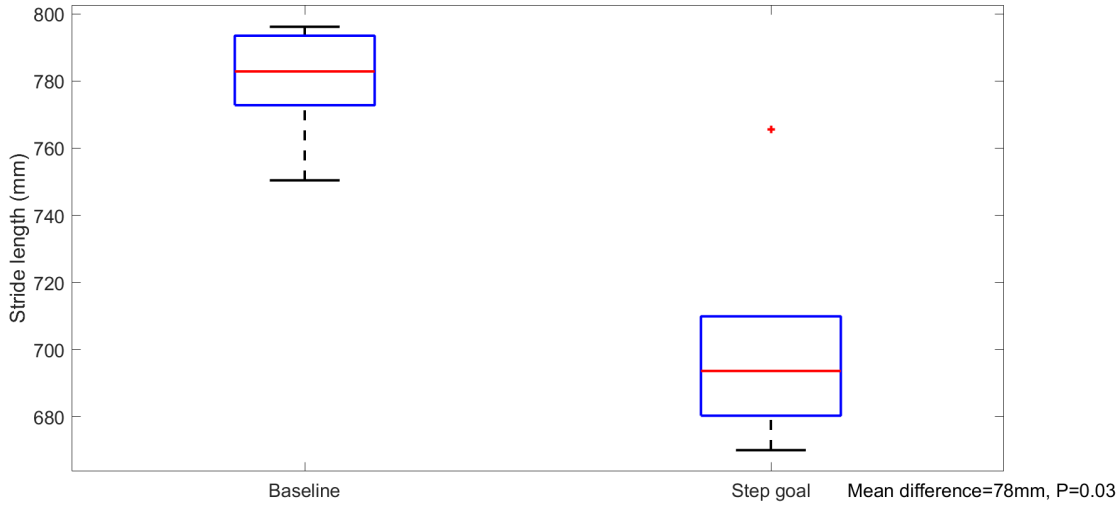


Figure 5.22: Stride length in baseline treadmill walking and walking while following 'step goal' (6 trials) for participant 01. P-value and difference between means displayed.

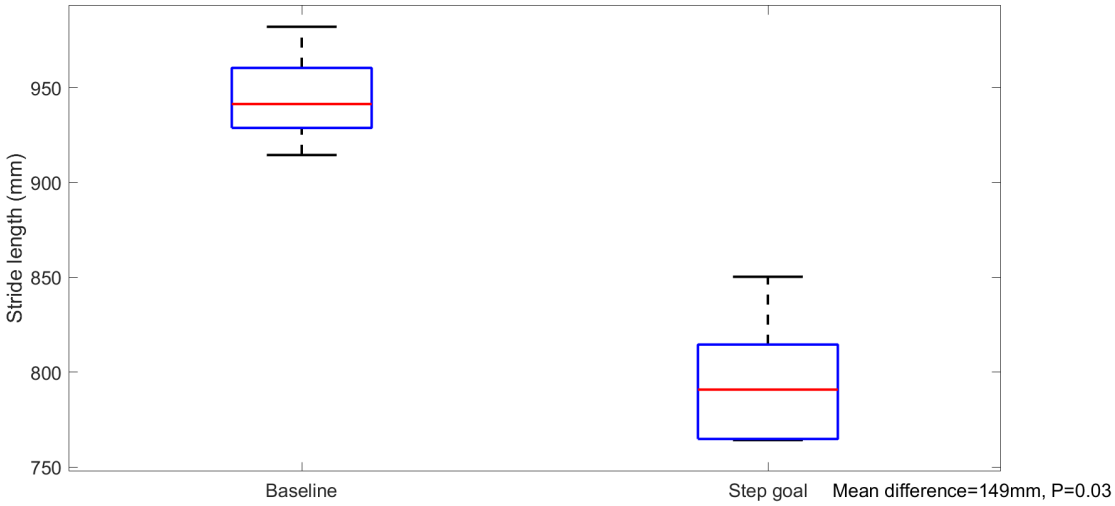


Figure 5.23: Stride length in baseline treadmill walking and walking while following 'step goal' (6 trials) for participant 02. P-value and difference between means displayed.

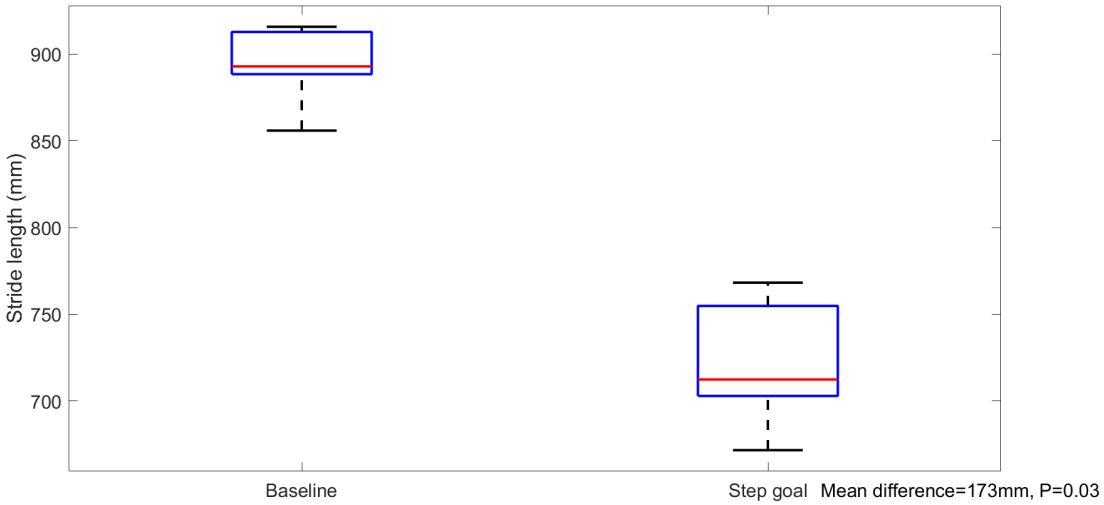


Figure 5.24: Stride length in baseline treadmill walking and walking while following 'step goal' (6 trials) for participant 03. P-value and difference between means displayed.

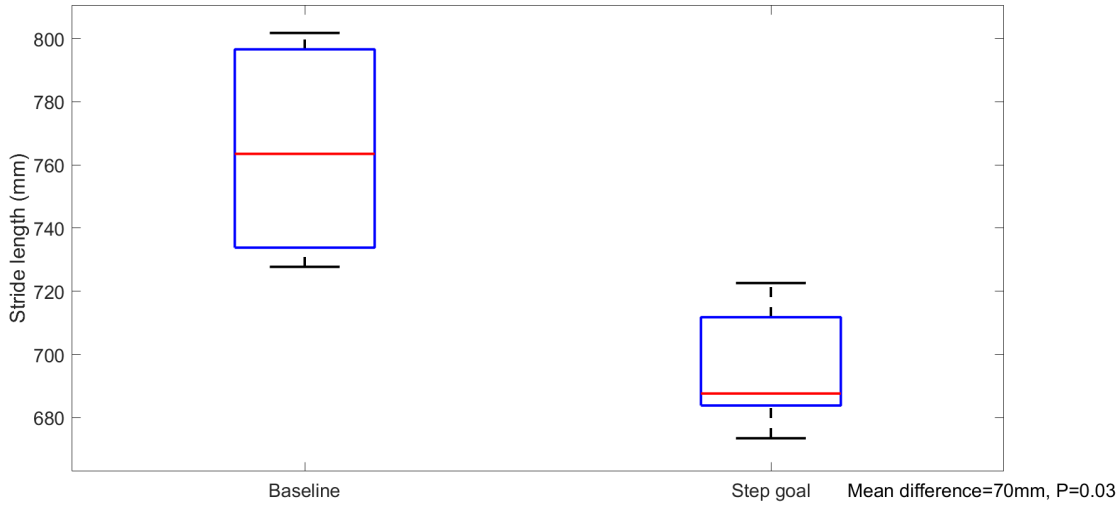


Figure 5.25: Stride length in baseline treadmill walking and walking while following 'step goal' (6 trials) for participant 04. P-value and difference between means displayed.

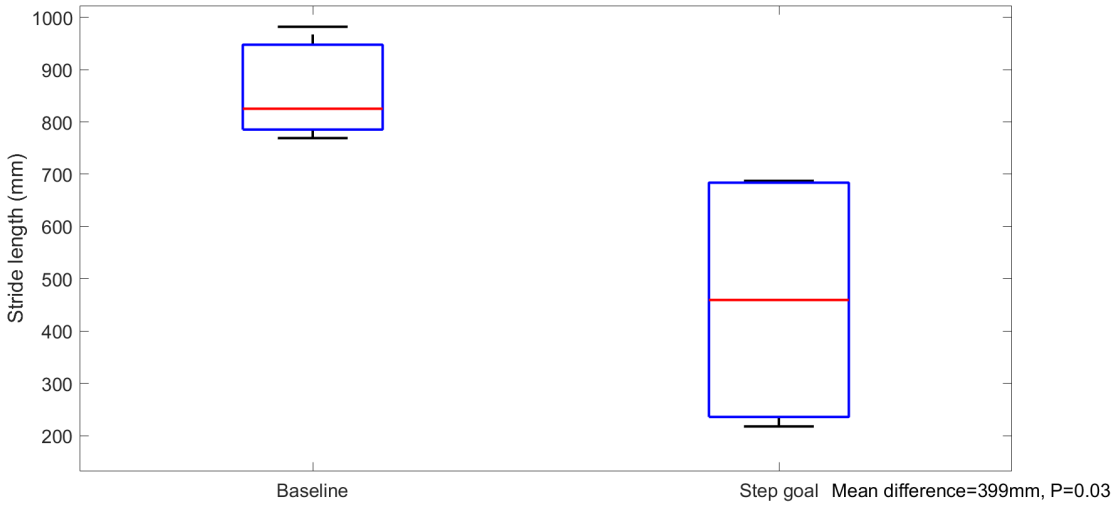


Figure 5.26: Stride length in baseline treadmill walking and walking while following 'step goal' (6 trials) for participant 05. P-value and difference between means displayed.

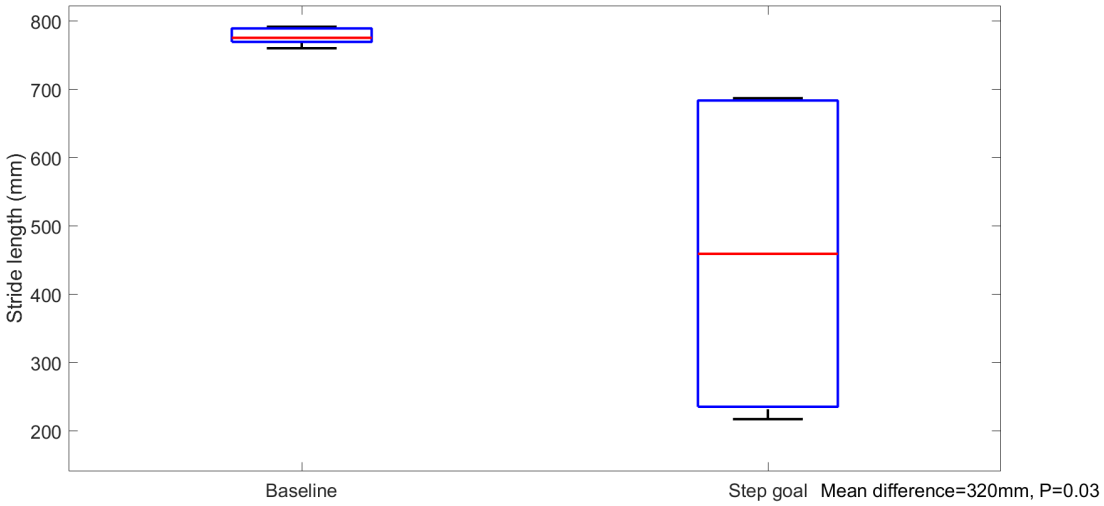


Figure 5.27: Stride length in baseline treadmill walking and walking while following 'step goal' (6 trials) for participant 06. P-value and difference between means displayed.

5.3.4 Aim 2: effect on iliopsoas recruitment

Aim 2.1: effect on iliopsoas recruitment - extension goal

Participants 02, 03 and 05 could successfully adapt their kinematics following the extension goal. While following the extension goal there was a significant increase ($p = 0.00$) in the maximum force and impulse of the iliopsoas muscle for participant 02 which was a negative effect, but no significant changes for participant 03 and 05 when compared to baseline gait. The significant change in iliopsoas muscle force, maximum muscle force and impulse for participant 02 is displayed in Figure 5.28, the same plots for participants 03 and 05 can be found in Appendix F.

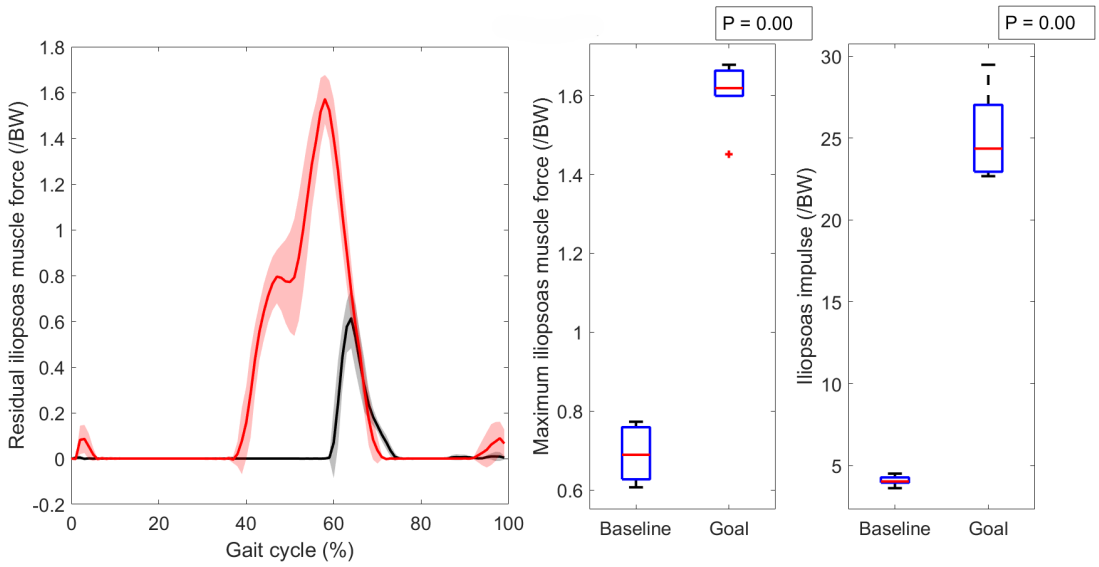


Figure 5.28: Iliopsoas force (/BW) and impulse (/BW) of the residual limb hip for participant 02, and the maximum iliopsoas force (/BW) over the six trials of baseline treadmill walking and walking while following 'extension goal'. P values displayed.

Aim 2.2: effect on iliopsoas recruitment - step goal

All participants could successfully adapt their stride length following the step goal. For participant 01 there was a significant increase in impulse of the iliopsoas force while following the 'step goal' (Figure 5.29). For participant 02 there was a significant increase in maximum force and impulse of the iliopsoas while following the 'step goal' (Figure 5.30). Both these participants therefore exhibited a negative effect while following the 'step goal'. Participant 04 had a significantly reduced value of maximum force when following the 'step goal' compared to baseline, Figure 5.31. Therefore the 'step goal' was considered the have a 'positive effect' on the iliopsoas force for participant 04. This positive effect was not reflected in participant 04's impulse, where there was no significant change between baseline and 'step goal'. For participants 03, 05 and 06 there was no significant difference in the maximum force or impulse of the iliopsoas muscle force between the baseline trials and the 'step' goal trials. The plots of iliopsoas muscle force and impulse can be found in Appendix G for participants 03, 05 and 06.

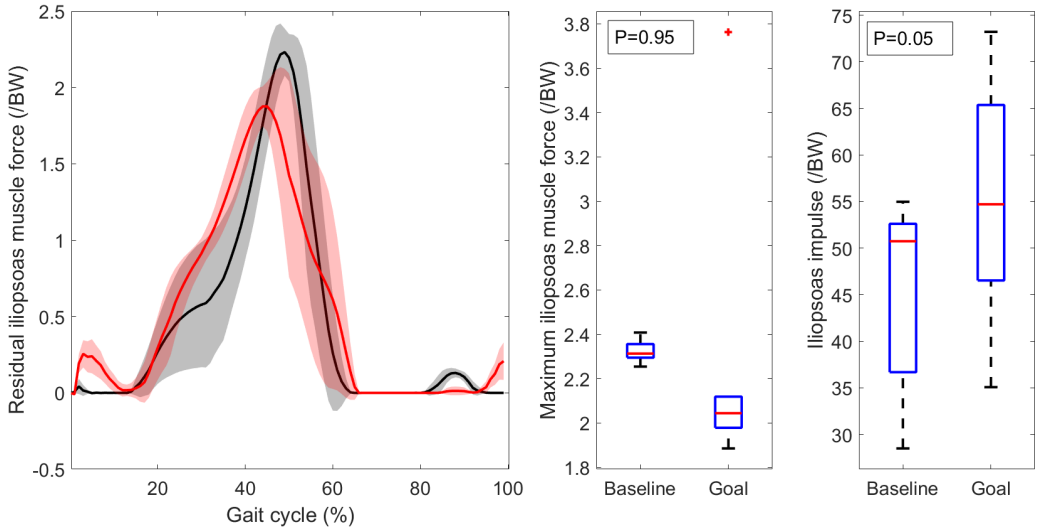


Figure 5.29: Iliopsoas force (/BW) and impulse (/BW) of the residual limb hip for participant 01, and the maximum iliopsoas force (/BW) over the six trials of baseline treadmill walking and walking while following 'step goal'. P values displayed.

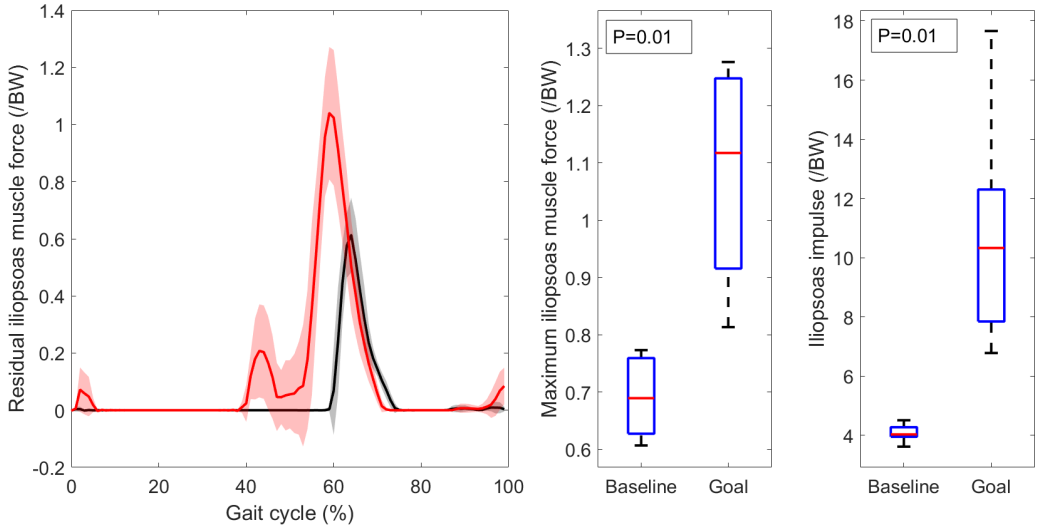


Figure 5.30: Iliopsoas force (/BW) and impulse (/BW) of the residual limb hip for participant 02, and the maximum iliopsoas force (/BW) over the six trials of baseline treadmill walking and walking while following 'step goal'. P values displayed.

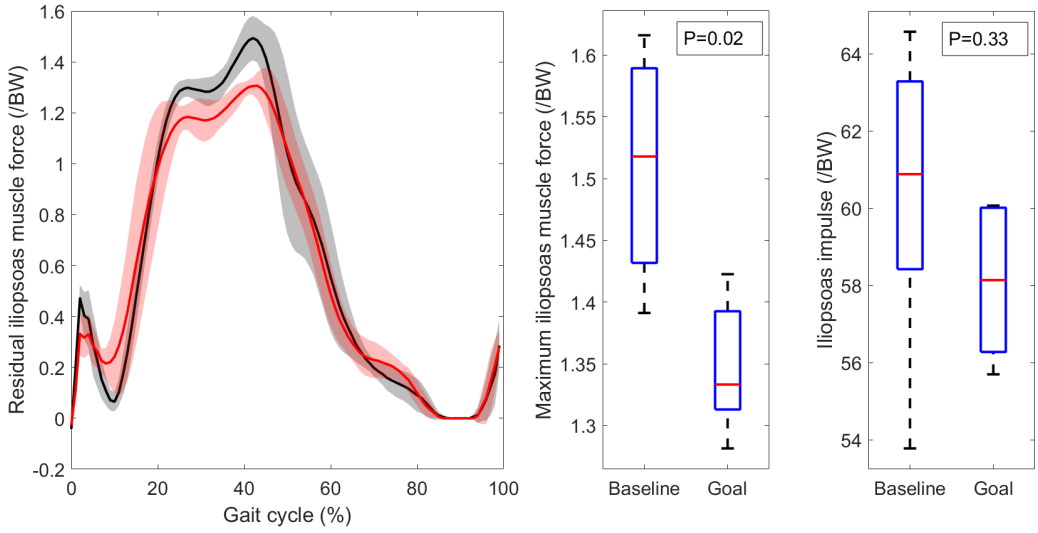


Figure 5.31: Iliopsoas force (/BW) and impulse (/BW) of the residual limb hip for participant 04, and the maximum iliopsoas force (/BW) over the six trials of baseline treadmill walking and walking while following 'step goal'. P values displayed.

5.3.5 Aim 3: kinematic strategies of achieving goals

Aim 3.1: Extension goal

The kinematics of baseline treadmill walking trials and while following the 'extension goal' are plotted along with the SPM results for participants 02, 03 and 05 in Figure 5.32 5.33 5.34 5.35 5.36 and 5.37, as these participants could 'successfully' follow the 'extension goal' and significantly reduce their maximum extension angle.

For all participants there were significant differences in their kinematics of the 'extension goal' trials compared to baseline for both the residual and intact limb side. For participants 02 and 03 this involved a reduced maximum abduction angle and reduced ankle range of motion in the residual side in the 'extension goal' condition. For 03 and 05 participants there was also an increased knee flexion angle of the residual limb side in the 'step goal' kinematics. For participant 05 there was increased external rotation the residual hip and reduced plantar flexion at the residual ankle. On the intact side of participant 02 and 03 there was also a reduced range of motion at the ankle, but increased abduction angle and increased external rotation at the hip. Participant 05 had reduced maximum flexion angle on the intact while following the 'extension goal'.

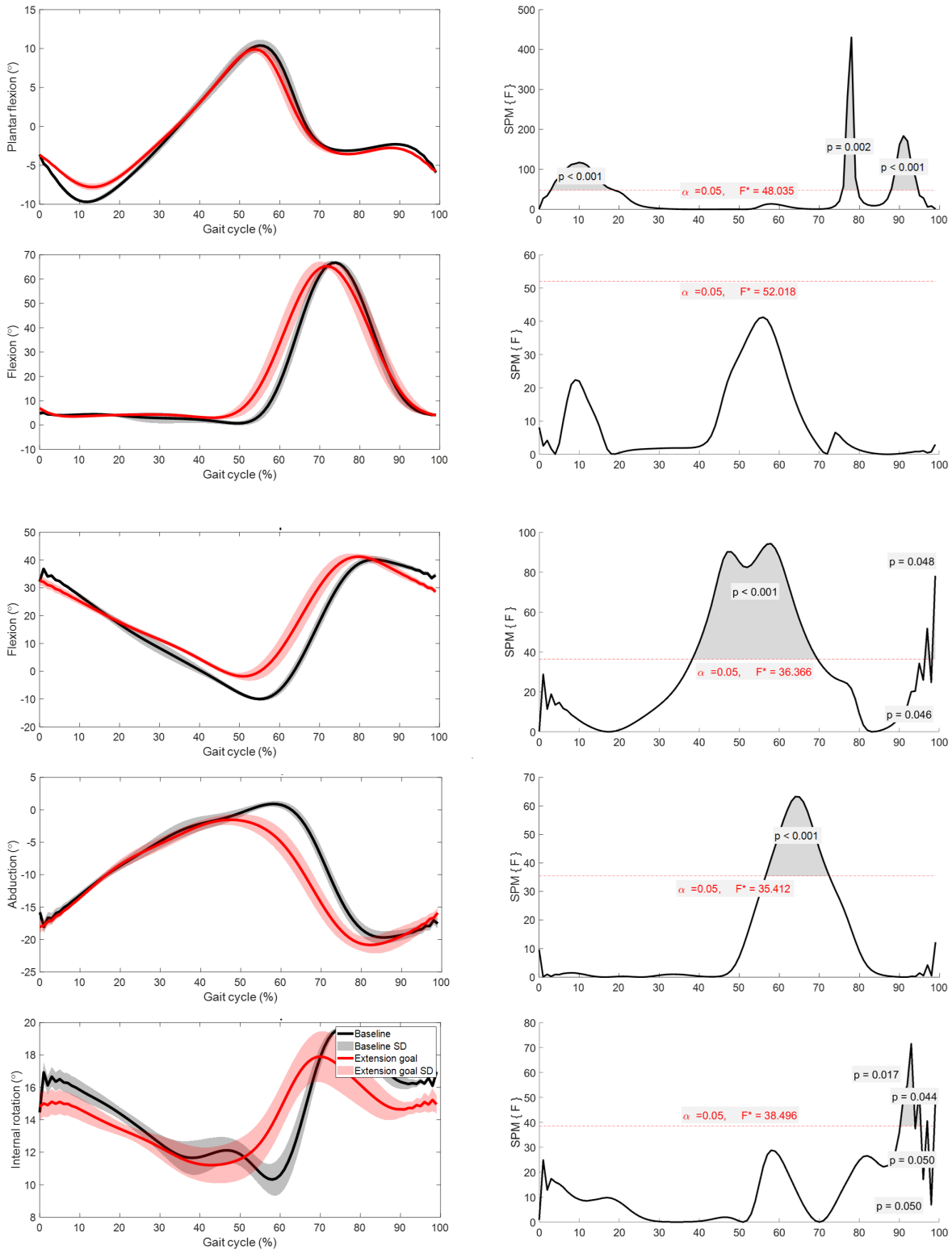


Figure 5.32: Kinematics and SPM results of baseline treadmill walking and walking while following 'extension goal' at the same self-selected speed of the residual limb side of participant 02

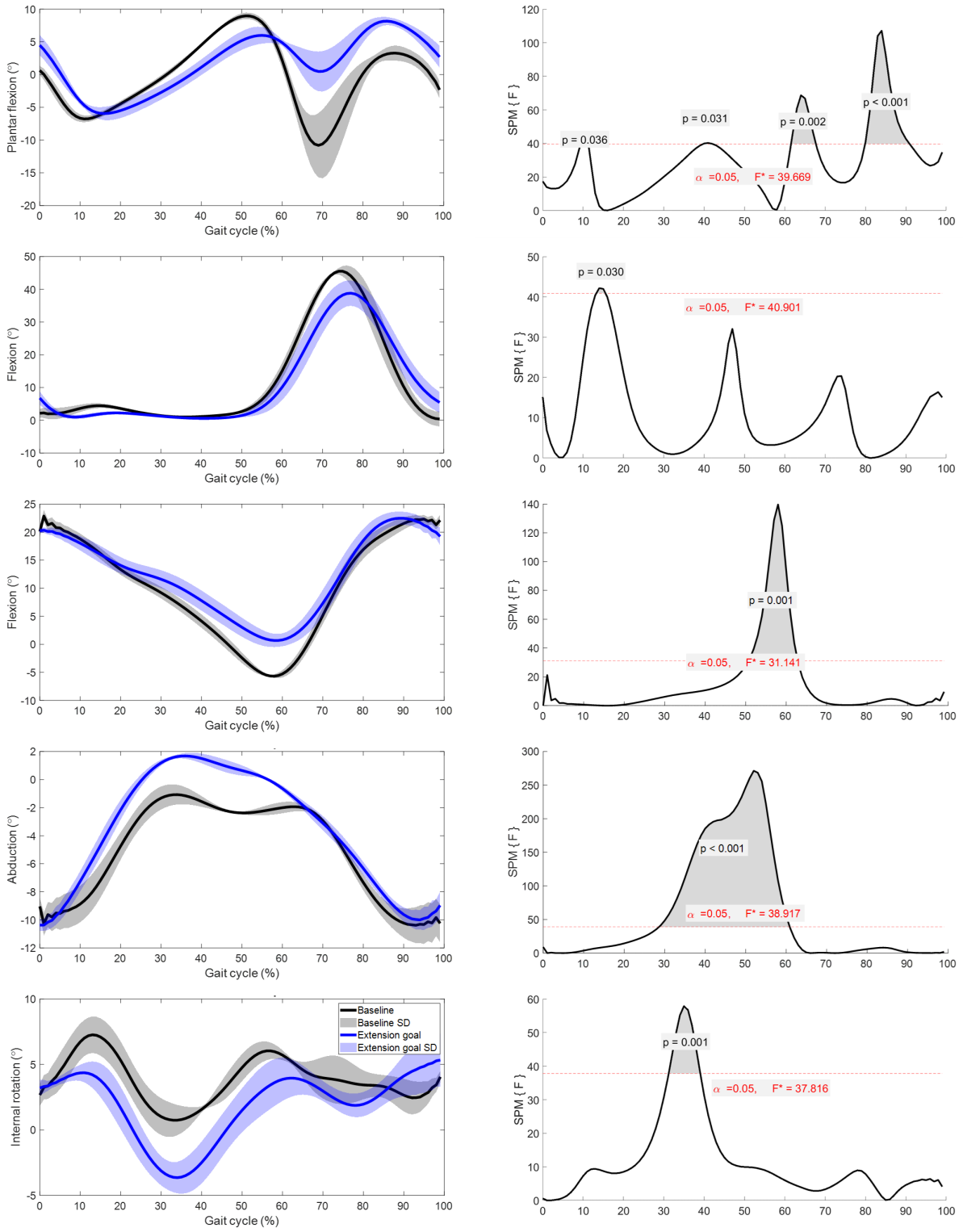


Figure 5.33: Kinematics and SPM results of baseline treadmill walking and walking while following 'extension goal' at the same self-selected speed of the intact limb side of participant 02

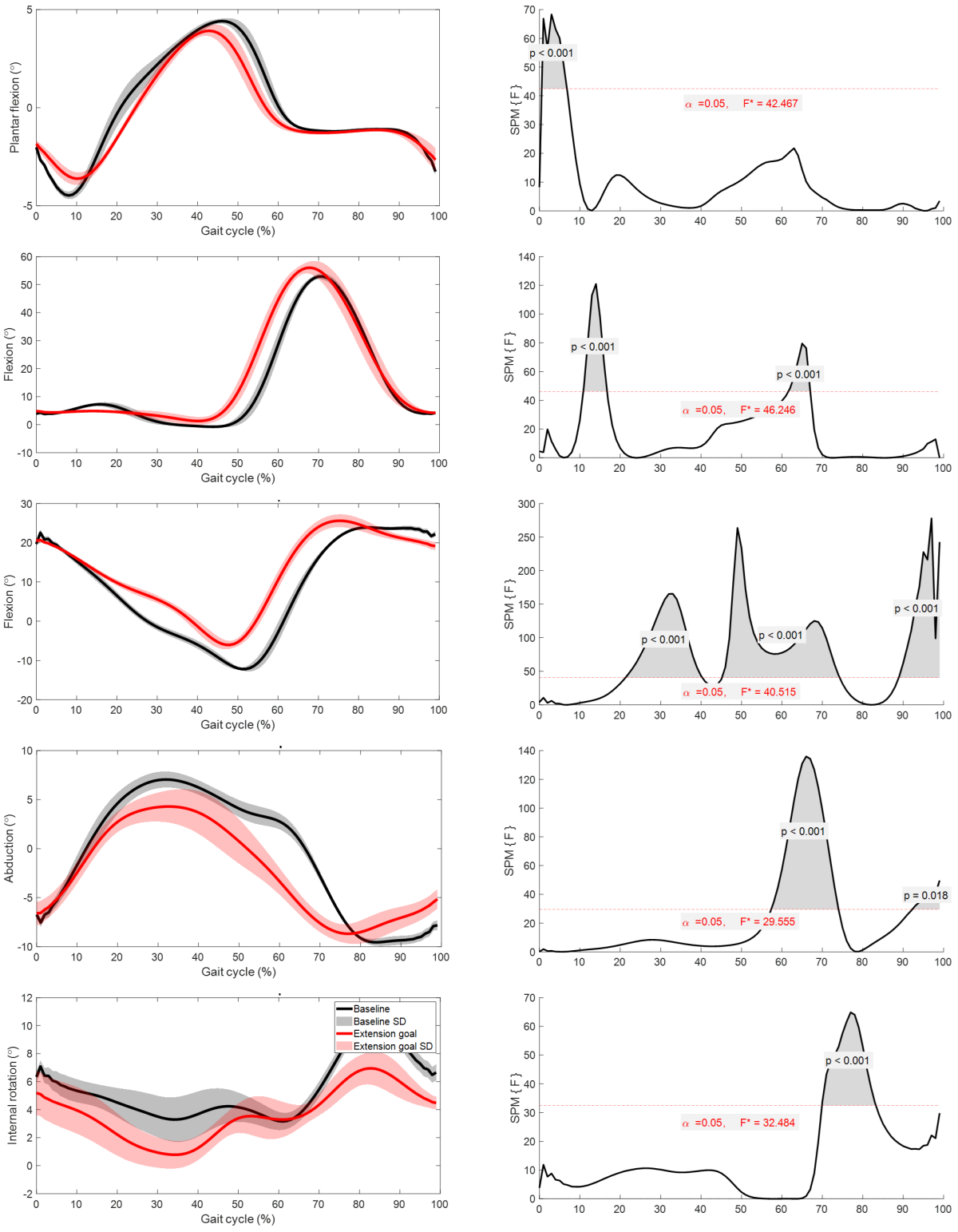


Figure 5.34: Kinematics and SPM results of baseline treadmill walking and walking while following 'extension goal' at the same self-selected speed of participant 03

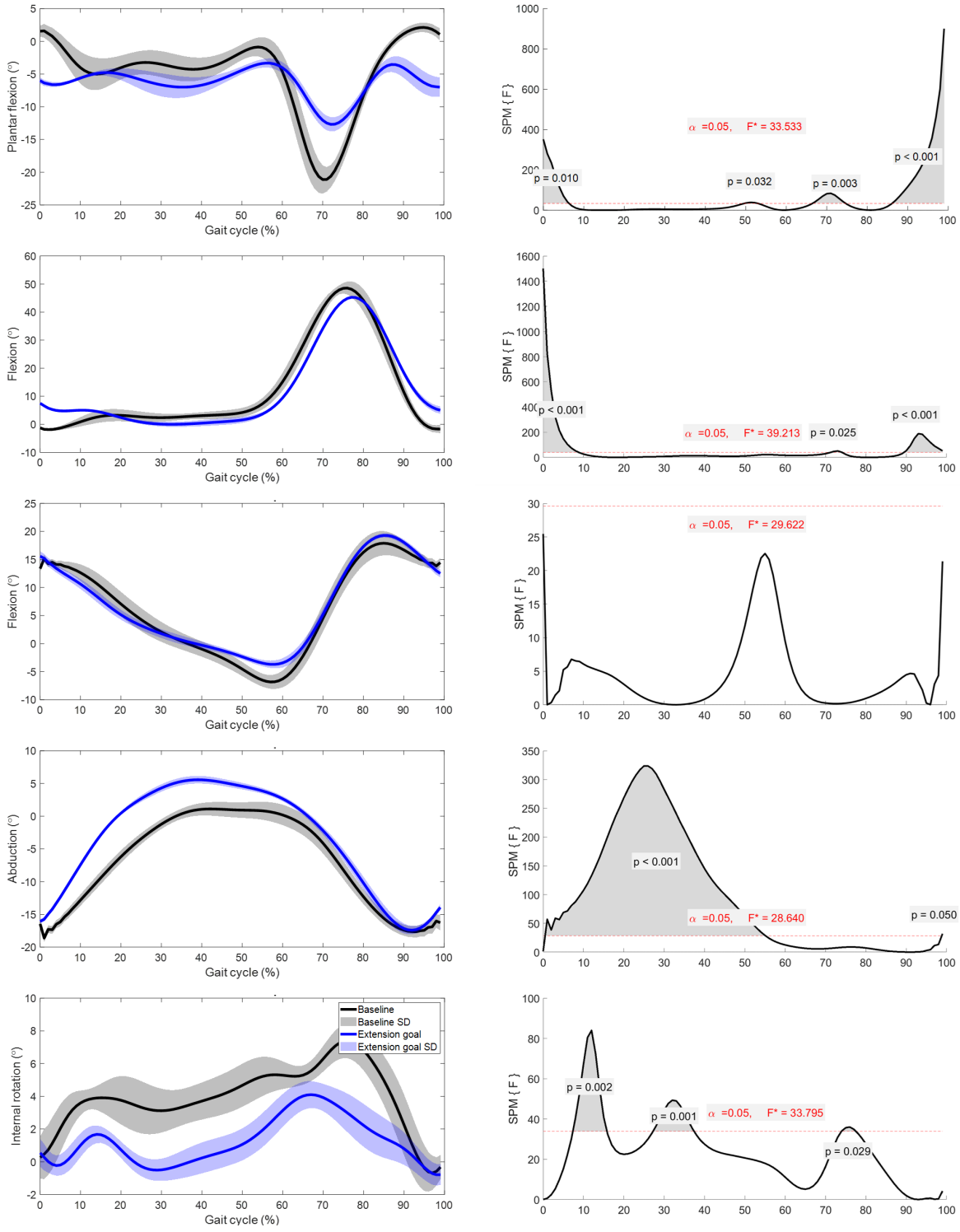


Figure 5.35: Kinematics and SPM results of baseline treadmill walking and walking while following 'extension goal' at the same self-selected speed of participant 03

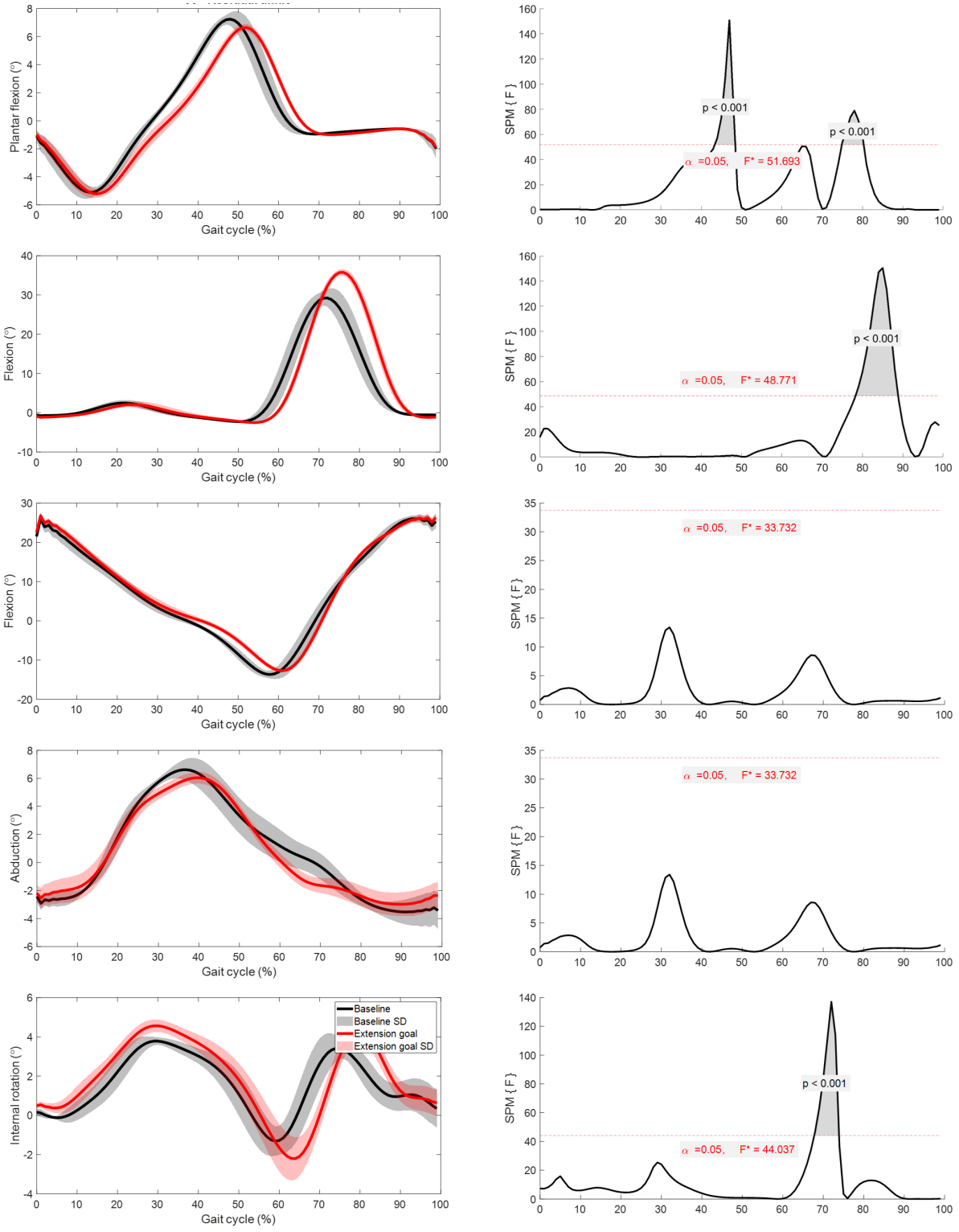


Figure 5.36: Kinematics and SPM results of baseline treadmill walking and walking while following 'extension goal' at the same self-selected speed of the residual limb side of participant 05

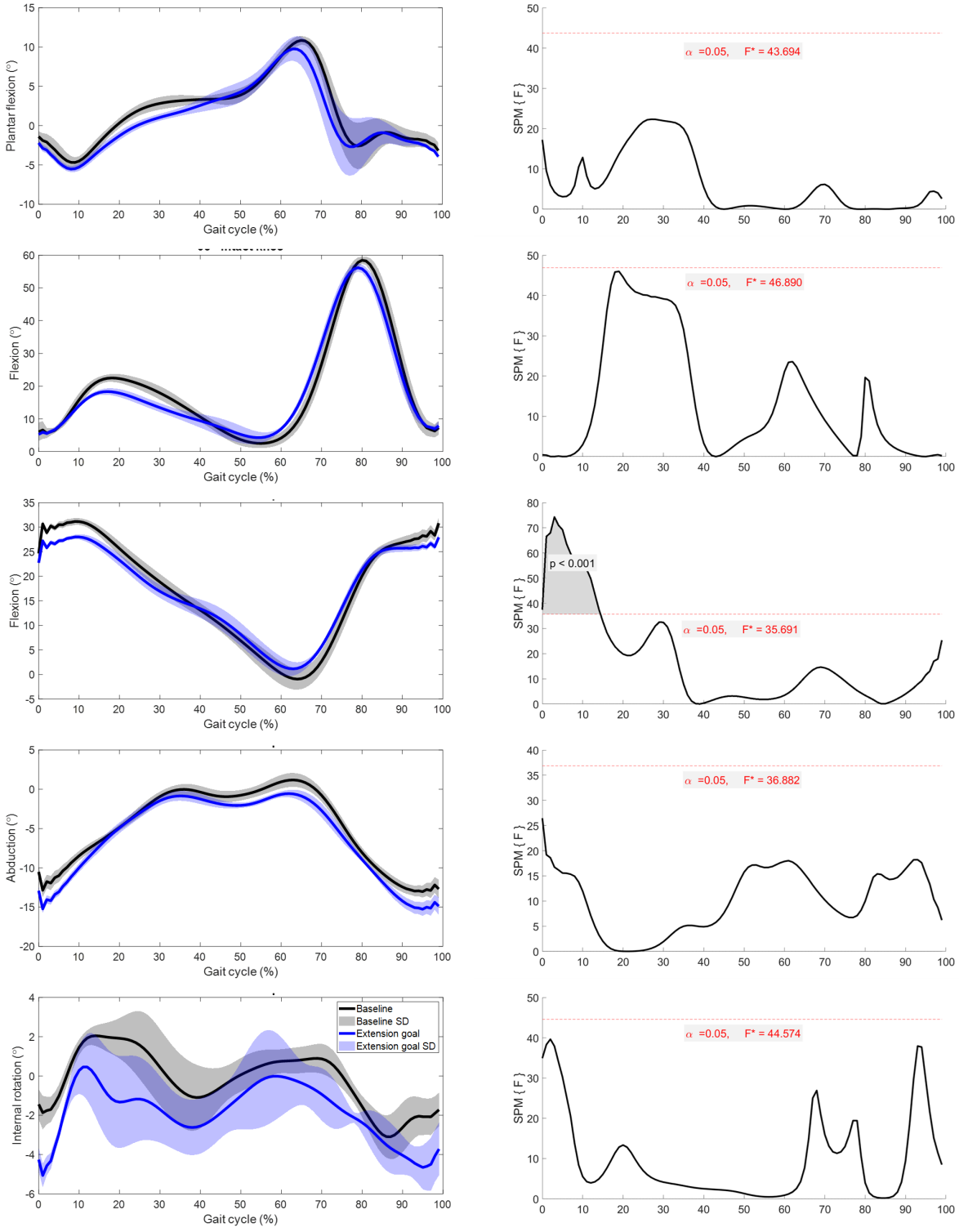


Figure 5.37: Kinematics and SPM results of baseline treadmill walking and walking while following 'extension goal' at the same self-selected speed of the intact limb side of participant 05

Aim 3.2: Step goal overall kinematic strategies

As all participants could 'successfully' follow the step goal, Figures 5.38 and 5.39 display the mean (and standard deviations) of the kinematics of all participants in baseline treadmill walking and when following the 'step goal', along with the results from the SPM test, for the residual limb and intact limb side. There are no significant differences in the kinematics between these two conditions apart from reduced intact hip flexion angle at 5-20% of gait and reduced intact knee flexion at 15-30% of gait while following the 'step goal' compared to baseline.

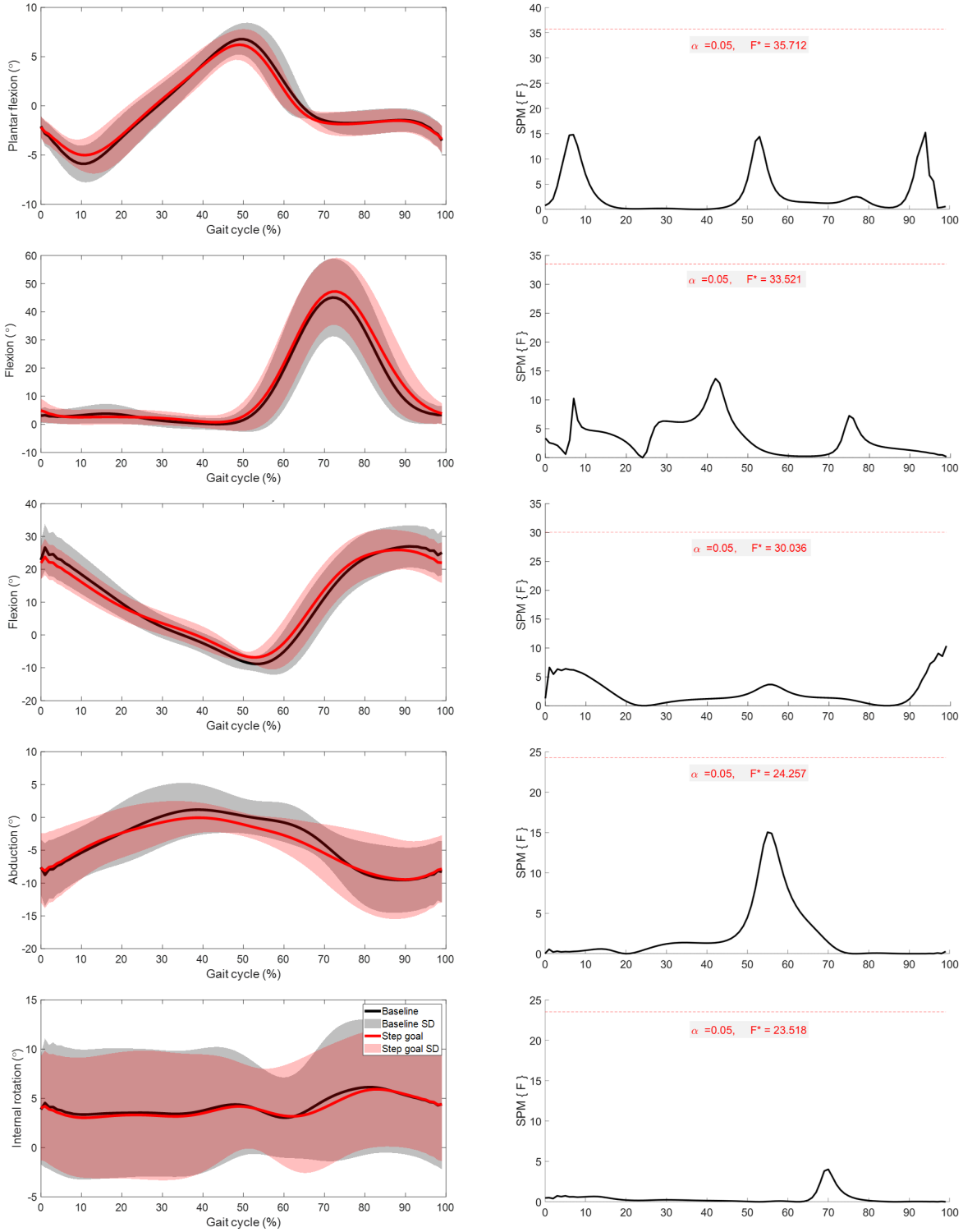


Figure 5.38: Kinematics and SPM results of baseline treadmill walking and walking while following 'step goal' at the same self-selected speed of the residual limb side of participants with unilateral transfemoral and through-knee amputations (N=6)

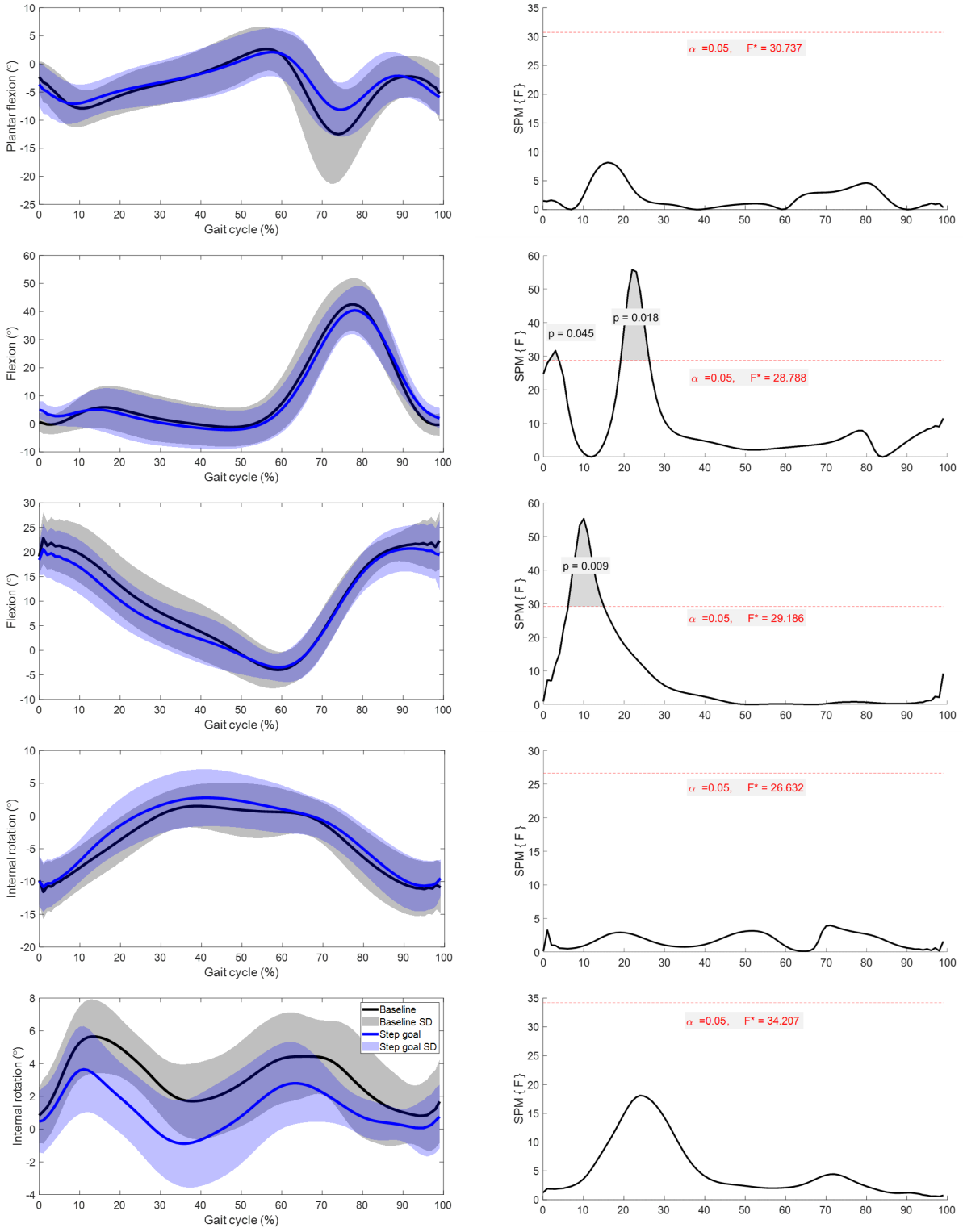


Figure 5.39: Kinematics and SPM results of baseline treadmill walking and walking while following 'step goal' at the same self-selected speed of the intact limb side of participants with unilateral transfemoral and through-knee amputatiosn (N=6)

5.3.6 Questionnaire results

Perceived effort questionnaire for the 'Extension goal'

Perceived effort questionnaire captured the participants experience of following the 'extension goal'. The results are summarised in Tables 5.6 to 5.10. Questions 5-7 were irrelevant to this study. The '*' by participant 05's answer to question 1 and 2 identify a suspected misinterpretation of the question by this participant due to discrepancy between the quantified answers given in question 1 and 2 and the qualitive comments provided in response to question 8.

For question 2 and 3 the participant's measured ability in 'successfully' adapting their kinematics is reported alongside the answers of the questionnaire, to allow for a direct comparison between reported ability / effort, and kinematic ability. For question 2, the answers in which there is a discrepancy between reported ability and measured ability are highlighted with an 'x'. Participants 04 and 06 reported that they could adapt their gait pattern, however there was no measured difference. Participant 05 reported that they couldn't adapt their kinematics, but there was a measured difference, however it is suspected question 2 was misinterpreted by participant 05 as explained above. In question 3 participants 03 and 05 reported that it required high effort to achieve the kinematic adaptations, which they were measured to be able to do 'successfully'. Participant 02 reported no effort to alter their gait which they were able to do successfully. Participant 06 reported low effort to alter their gait pattern but they were not able to do so according to their measured kinematics.

Table 5.6: Question 1

Q1. It was easy to interpret the visual biofeedback on the screen (1. Totally agree, 2. Rather agree, 3. Rather disagree, 4. Totally disagree).	
Participant	Answer
01	2. Rather agree
02	1. Totally agree
03	1. Totally agree
04	1. Totally agree
05	4. Totally disagree *
06	1. Totally agree
* This was contrasting to their comments on the day and the extra information they provided in the questionnaire (Question 8) so this may be a misinterpretation of the question.	

Table 5.7: Question 2

Q2. I was able to alter my gait pattern with the addition of biofeedback (1. Totally agree, 2. Rather agree, 3. Rather disagree, 4. Totally disagree)			
Participant	Answer	Measured success (Y = they could 'successfully' adapt extension angle, N= they could not)	Discrepancy? (x = yes)
01	3. Rather disagree	N	
02	2. Rather agree	Y	
03	1. Totally agree	Y	
04	1. Totally agree	N	x
05	4. Totally disagree*	Y	x
06	1. Totally agree	N	x
* This was contrasting to their comments on the day and the extra information they provided in the questionnaire (Question 8) so this may be a misinterpretation of the question.			

Table 5.8: Question 3

Q3. On scale of 1-10 how much perceived effort was required to alter your gait pattern (1 is no effort and 10 is maximum effort)		
Participant	Answer	Measured success (Y = they could 'successfully' adapt extension angle, N= they could not)
01	8	N
02	1 - no effort	Y
03	8	Y
04	9	N
05	7	Y
06	2	N

Table 5.9: Question 4

Q 4. If 1 is no discomfort and 10 pain, describe any changes in comfort felt with the addition of visual feedback.	
Participant	Answer
01	8
02	1 - no discomfort
03	8
04	1 - no discomfort
05	1 - no discomfort
06	1 - no discomfort

Table 5.10: Question 8

Participant	Answer
01	"Having full hip flexion extension is required for my microprocessor knee to operate"
02	-
03	"Not natural to shorten gait, if normal is ok with no pain. Not so steady on feet."
04	"Achieving the goal loaded right glute and hip. Difficult to sustain, needed a recovery stride every 3/4 steps"
05	"very easy to follow with no discomfort"
06	"The goal was easy to follow and very interesting. No discomfort or pain. The staff were excellent."

Perceived effort questionnaire for the 'Step goal'

Perceived effort questionnaire captured the participants experience of following the 'step goal'. The results are summarised in Tables 5.11 to 5.15 . Questions 5-7 were irrelevant to this study.

For question 2 and 3 the participants measured ability in 'successfully' adapting their kinematics is reported alongside the answers of the questionnaire, to allow for a direct comparison between reported ability / effort, and kinematic ability. For question 2, 'x' indicates where there was a discrepancy between reported ability and measured ability. There were no discrepancies between reported ability and measured ability. Although

participants 01, 03, 04 and 05 were able to 'successfully' reduce their stride length, this was reportedly done at high effort levels.

In the answers to question 8 '*' indicates verbal feedback that was given by the participant when reflecting on their experience of the 'step goal'.

Table 5.11: Question 1

Q1. It was easy to interpret the visual biofeedback on the screen (1. Totally agree, 2. Rather agree, 3. Rather disagree, 4. Totally disagree).	
Participant	Answer
01	2. Rather agree
02	1. Totally agree
03	1. Totally agree
04	1. Totally agree
05	1. Totally agree
06	1. Totally agree

Table 5.12: Question 2

Q2. I was able to alter my gait pattern with the addition of biofeedback (1. Totally agree, 2. Rather agree, 3. Rather disagree, 4. Totally disagree)			
Participant	Answer	Measured success (Y = they could 'successfully' adapt extension angle, N= they could not)	Discrepancy? (x = yes)
01	2. Rather agree	Y	
02	2. Rather agree	Y	
03	1. Totally agree	Y	
04	1. Totally agree	Y	
05	1. Totally agree	Y	
06	1. Totally agree	Y	

Table 5.13: Question 3

Q3. On scale of 1-10 how much perceived effort was required to alter your gait pattern (1 is no effort and 10 is maximum effort)		
Participant	Answer	Measured success (Y = they could 'successfully' adapt extension angle, N= they could not)
01	9	Y
02	2	Y
03	8	Y
04	10	Y
05	7	Y
06	4	Y

Table 5.14: Question 4

Q 4. If 1 is no discomfort and 10 pain, describe any changes in comfort felt with the addition of visual feedback.	
Participant	Answer
01	8
02	1 - no discomfort
03	8
04	1 - no discomfort
05	1 - no discomfort
06	1 - no discomfort

Table 5.15: Question 8

Participant	Answer
01	"I find it tricky to walk slow, so need to walk faster"
02	*Verbally noted it was harder than the extension goal
03	"Became painful to shorten gait, from normal possible to do so, lots of physical effort" * Verbally noted hip pain on intact side with short steps
04	"Achieving shorter stride pattern required caused foot drag and activated stumble prevention of MPK. Much more energy to achieve goal."
05	"Love this visual aid"
06	"A little harder to adjust than the first trial, but once I got the hang of it, it was easy and comfortable. Instructions given were easy to interpret.."

5.4 Discussion and conclusion

5.4.1 Validation of methods

The two preliminary studies were to validate the methods. Firstly, when implementing biofeedback, treadmill gait is much more practical than overground walking as it requires less space in a clinic, enables control of walking speed and the visual feedback can be presented on a fixed screen. Controlling walking speed was important to this study, as it allowed gait functionality (speed) to be maintained while kinematic modifications were tested. The results from preliminary Study 1 prove that treadmill gait is an adequate representation of overground walking for individuals with UTF/UTK amputations as there was only one significant difference detected, and that was in the maximum flexion angle on the intact limb side. This difference should be considered in the design of rehabilitation methods especially if the intact flexion angle is the focus of the study.

The second preliminary aim was to validate the use of the non-subject specific FreeBody musculoskeletal model when estimating muscle forces of individuals with UTF/UTK amputation. The combined Sprague and Geers errors were considered 'good' for all muscles in the intact limb apart from the rectus femoris which was 'moderate'. The EMG validation of the gluteus maximus of the residual limb, which was only completed for 3 participants, gave 'good' similarity. These results are comparable to previous study using similar methods (Ding et al. 2019). The predictions of the rectus femoris appear to be worse than for other muscles, this should be considered when evaluating results from FreeBody. It would have been ideal to validate the muscle forces of the residual limb for all participants and for more muscles, however it is difficult to collect EMG of muscles in the residual limb under the socket without causing discomfort to the participant. Future work could include EMG validation of the residual limb using embedded EMG sensors in the sockets. Overall, the FreeBody musculoskeletal can be considered good to moderate for the predictions of muscle forces in the intact and residual limb of individuals with UTF/UTK amputation.

5.4.2 Effectiveness of the interface design

The first primary aim of this study was to investigate whether it was possible for individuals with UTF/UTK amputations donning microprocessor knee to adapt their kinematics through visual and audio biofeedback. Looking at the participants as a whole group, or the 'overall' effect of the 'extension goal' and the 'step goal', the 'step goal' was successful at achieving the desired adaptations to spatial features via adapting kinematics (with a significant reduction in stride length, $p = 0.03$) but the 'extension goal' was not successful. Looking at the trials on a participant-by-participant basis, the 'extension goal' was successful for three of the six participants (achieving a statistically significant reduction in maximum extension length). As hypothesised, it appears the 'step goal' was an easier interface to follow. This may be due to it being more natural to adapt kinematics bilaterally, rather than forcing an asymmetrical adaptation. Additionally, the 'extension goal' interface involved a graphical representation of hip kinematics, perhaps this was

less intuitive for the participants to understand and follow. Interestingly, from the questionnaire data, the 'step goal' was reported to require higher levels of effort with a score of 40 / 60 (maximum effort) compared to 35 / 60 (maximum effort) for the 'extension goal'. Additionally, participant 02 verbally noted it was harder to follow the step goal, and this was reflected in answer to question 8 by participant 06 with the 'step goal' being "a little harder to follow" and participant 04 reporting that the step goal required "much more energy to achieve goal" than the extension goal.

The answers from the questionnaire can also give some insight into the effectiveness of the interface design. While following the 'extension goal', participants 04 and 06 reported false positives, meaning they were under the impression they could successfully adapt their kinematics, but this was not reflected in the measured kinematics. Perhaps the design of the goal interface needs to be adapted so that the kinematic goals are exaggerated, and this would encourage exaggerated kinematic modifications.

Overall, the results from the 'extension goal' and 'step goal' suggest that the biofeedback interfaces with combined visual and auditory cues could be effective in gait retraining methods for individuals with UTF/UTK.

5.4.3 Clinical significance of the spatial modifications

All the participants could successfully reduce their stride length. In this study the 'success' criteria of following the goals were defined as a statistically significant difference in the kinematic outcome. When considering biomechanical parameters there is the question of whether the observed statistically significant differences are clinically significant, the mean difference in stride length ranged from 7 cm to 59 cm. Previous studies by Edd et al (2020) and Ulrich et al (2023) reported that difference of 14 cm and 10 cm stride length had a beneficial effect on knee moments for patients with knee osteoarthritis, if 10 cm can be deemed 'clinically' significant, then participant 02, 03 and 05 adapted their stride length to this level. These are the same participants that could 'successfully' follow the 'extension goal'. However, these adaptions did not have a 'positive' effect on the iliopsoas muscle force in these participants, indicating this gait retraining method is ineffective for this specific purpose.

5.4.4 Effect of kinematic and spatial modifications in iliopsoas recruitment

The second primary aim of this study was to investigate the effect of the kinematic and spatial modifications, specifically whether the adaptations had the desired effect of a reduction in the force of the iliopsoas muscle of the residual limb, probably through a reduction in hip flexion moment at terminal stance phase.

For the participants (02, 03 and 05) who were able to adapt their kinematics according to the 'extension goal', it appears that these kinematic adaptions did not have the desired effect. In fact, the only significant changes in maximum muscle force of the residual

limb iliopsoas force was an increase in force in participant 02. While following the 'step goal', participant 04 reduced their stride length by 7 cm and this appears to result in a reduction of 0.20/BW of residual limb maximum iliopsoas force, however, this was not reflected in a reduced iliopsoas impulse which limits the impact of this result. This participant following the 'step goal' is the only example of the desired effect, of reduced iliopsoas force, occurring in this study.

Similarly to the 'extension goal', participant 02 exhibited a significantly increased residual limb iliopsoas force while following the 'step goal' interface, which is a negative effect. To investigate the cause of this increased iliopsoas force, the sagittal hip torque was plotted (Figure 5.40), there appears to be an increase in maximum flexion torque in the residual limb. The increased sagittal hip torque and iliopsoas force does not appear to be caused by increased external loading of the residual limb (Figure 5.41), therefore it must be induced by the kinematic strategies adopted to achieve the 'extension goal' and 'step goal'.

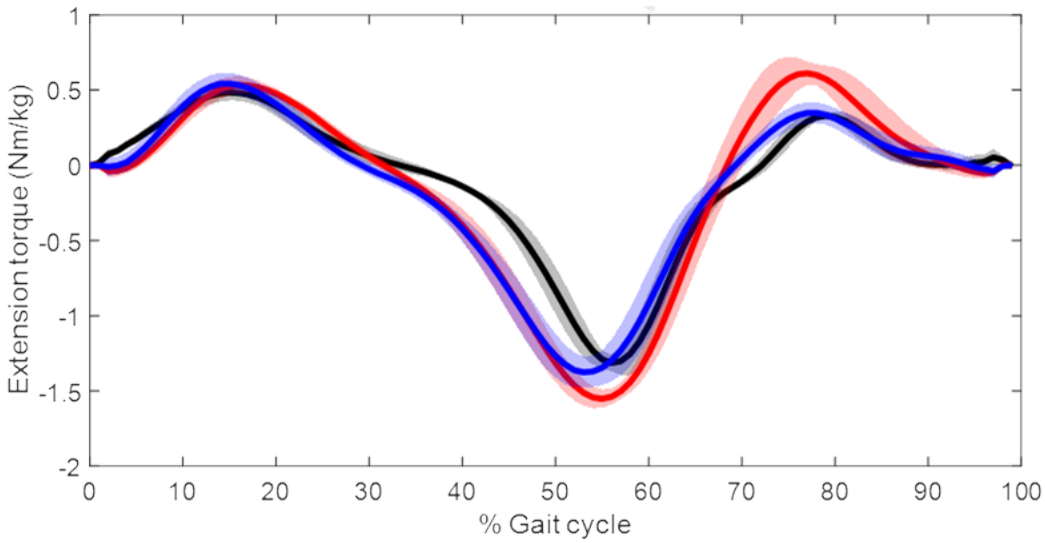


Figure 5.40: Extension torque force of the residual limb participant 02 in baseline (black), 'extension goal' (red) and 'step goal' (blue) conditions.

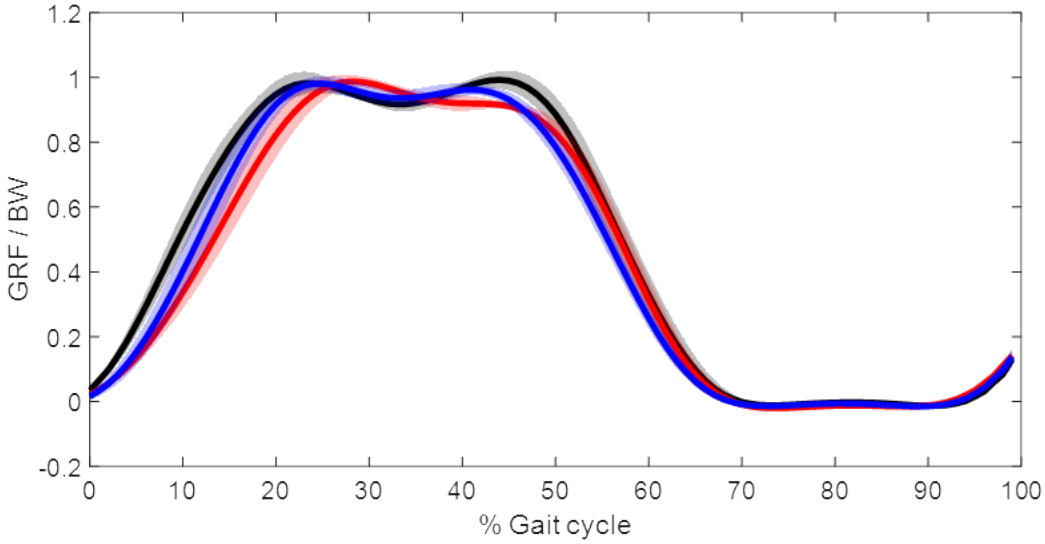


Figure 5.41: Vertical ground reaction force of the residual limb of participant 02 in baseline (black), 'extension goal' (red) and 'step goal' (blue)conditions.

The key aim of this study was to investigate whether these kinematic modifications (reduced maximum extension angle and step length) alone would reduce the maximum iliopsoas force and impulse of the residual limb during gait; this does not seem to be the case. Perhaps isolating single features in gait modifications is not effective and multiple gait features need to be considered simultaneously. This was found to be the case in a study by Edd et al (2020), where they found that modifying stride length, stride width and foot progression angle simultaneously was much more effective at reducing knee moments than modifying stride length alone, for application in patients with knee osteoarthritis.

5.4.5 Kinematic strategies to achieve goals

The 'step' goal took a bilateral approach, targeting the intact and residual limb, and was successful at reducing stride length. Figure 5.39 shows that this reduction in stride length was achieved by a reduction in maximum flexion angle at foot contact on the intact side, this is presumably why this reduction of stride did not reduce the force required of the iliopsoas muscle on the residual limb side. This does not achieve the kinematic modification that was suggested by Chapter 4, reducing extension angle (including increasing flexion angle). Although the 'step goal' was easier to follow, it appears that this goal is not targeted or specific enough, as it can be achieved without modifying kinematics on the residual limb side, which is critical for the overall objective of this study which is reducing the demand of the residual limb iliopsoas muscle.

The 'extension' goal took a unilateral approach, specifically targeting the residual limb side. As displayed in Figure 5.32 to 5.37, for the participants that were able to reduce the maximum extension angle of their residual hip following the 'extension goal' it appears that they naturally made similar adaptations of their intact side (although this is only

statistically significant for participant 02), which was not directly targeted by the goal, with a reduction of extension angle. This pattern of symmetrical gait adaptation was exhibited in the results of Chapter 4.

Participants 02 and 03, who could both successfully reduce their maximum extension angle following the 'extension goal', appear to achieve this gait adaptation with similar kinematic strategies (Figure 5.32 to 5.35). This included a reduction in hip abduction of the residual limb during terminal stance and swing phase and an increase in intact hip abduction. Additionally, both participants exhibited a reduced residual limb side (prosthetic) ankle range of motion. Ankle plantarflexion will affect the recruitment of the iliopsoas muscles, as the increased recruitment of the iliopsoas muscle in an individual with UTF/UTK may be due to the reduced plantarflexion torque in the prosthetic ankle as highlighted in Chapter 3. Though it is not statistically significant, both participants 02 and 03 appear to have increased knee flexion at around 50% of gait cycle, pre-swing, where iliopsoas muscle torque is required, perhaps this increased knee flexion counteracts the reduced hip extension angle. Increased knee flexion could potentially increase the external torque at the hip if segment speed and acceleration is preserved.

5.4.6 Interpretation of Chapter 4 results

Reducing the maximum extension angle during *terminal stance* phase of the *residual limb* was selected as the point of focus of this gait retraining biofeedback tool as *terminal stance* phase is when peak iliopsoas force occurs, and the *residual limb* is the limb of concern when considering reduced gait endurance (Chapter 3). It was believed that simplifying the gait modification to focus on a single feature would make its implementation more feasible (i.e maximum extension angle of the residual limb at terminal stance). This may have been a misguided interpretation of the predictions from Chapter 4 for two reasons. Firstly, this may have been overly reductive as there were other gait modifications that occurred simultaneously in the Chapter 4 stimulations, for example, reduced hip extension of the intact limb. However, even if not directly targeted, reduced hip extension of the intact limb did appear to occur organically as described early. Additionally, reduced maximum hip extension of the residual and intact limb was often accompanied with increased hip flexion in the predictions made by Chapter 4, increased hip flexion was not exhibited by any of the participants of this study, perhaps this is critical in the interpretation of the gait modification. Secondly, perhaps it is not effective to attempt to generalise the learning from predictions made across 4 participants in Chapter 4. It may have been more effective to do a fully comprehensive subject- specific pipeline of inverse dynamic analysis of muscle forces, forward dynamic predictions to suggest gait modification and implementation with biofeedback tools. There were three recurring participants across Chapters 4 and 5. These included Participants 02, 03, and 04 from Chapter 4, who corresponded to Participants 01, 02, and 04 in Chapter 5, respectively. The data collection of the two chapters was completed over a year apart, so it cannot be assumed that the walking patterns remained the same between follow-ups.

5.4.7 Future direction

The overall objective of this study was to achieve reduced recruitment of the iliopsoas muscle of the residual limb through kinematic adaptions guided by biofeedback. The results of this study suggest that the mode of feedback (combined audio and visual) could potentially be effective, however, the information that is being relayed (kinematic and spatial features) is not effective at achieving this goal of reduced residual limb iliopsoas. The current method is fundamentally an indirect method, and evidently sensitive to a variety of biomechanical parameters, compared to directly quantifying the muscle activation of the residual limbs iliopsoas and using this information in the feedback. EMG sensors have been used to quantify muscle activity in real time to guide biofeedback, such as a study by Jonsdottir (2010) which used EMG to feedback activity of the gastrocnemius lateralis via acoustic cues when the participant reached the activation goal. This system achieved its intended purpose of increased push off force at the ankle for the participants who had chronic mild to moderate hemiparesis (Jonsdottir et al. 2010). Another study used EMG guided feedback to reduce the activation the plantar flexors with the goal of offloading the knee (Uhlrich et al. 2022). This demonstrates how EMG can be used directly to influence biomechanical parameters. Perhaps this method could be used to either reduce the recruitment of the iliopsoas or increase the recruitment of the muscle which may lead to a reduced iliopsoas recruitment. The latter would require further computational modelling to design, but the former may be challenging due to the position of the iliopsoas and inaccessibility for the EMG sensors, though it has been shown to be possible (Katsavrias et al. 2005). Alternatively, with real-time inverse dynamics, which is possible with the GRAIL system and D-flow (Motek, a DIH brand, Netherlands), the sagittal hip torque could have been directly tracked and this information could have been used in the feedback. This could be used to directly attempt to reduce the flexion torque of the residual hip during terminal stance. The kinematic strategies adopted to achieve the goals could guide future biofeedback methods if a kinematic approach is still taken. For example, as previously highlighted, it appears that reduced hip abduction on the residual limb side and increased abduction on the intact side was adopted by participants 02 and 03 who could effectively reduce their maximum extension angle. Perhaps the frontal hip kinematics either need to be controlled, via tracking and feedback, or used indirectly to reduce hip extension angle if this is easier for the participants to adopt via a biofeedback system either physically or conceptually.

In the future development of this tool another approach could be taken when improving the feedback method. As described in the introduction, an understanding of motor learning should ideally be incorporated when designing rehabilitation protocols. This is true for the information feedback itself, for example, it has been found that the focus of the goal impacts the success of learning (Sawers et al. 2012) (Wulf et al. 2002). 'External' goals are goals that draw the focus of the individual to the effects of the motion, as opposed to 'internal' goals which instead draw the individual's focus to the motion of their body. External goals are thought to enhance motor learning as they induce an unconscious and automatic adaptation of motion, whereas internal goals induce a conscious control in the attempt to adapt motion. It is thought that this conscious control

intervenes with automatic control, and detrimental to the overall performance of the motion (Wulf et al. 2002). Similarly, verbal instructions (or audio feedback) in rehabilitation have been categorised into 'explicit' and 'implicit', where explicit rely on an understanding of the desired motion and implicit give an analogy which encourages the individual to adapt their motion in a certain way without explicitly citing the desired adaption. It has been found, similarly to 'external' goals, that implicit instructions lead to an automatic or unconscious adaptation in motion (Lam et al. 2009) (Jie et al. 2018) which may enhance rehabilitation potential. Both 'goals' in this study visualised direct features of the individuals body position, this is an internal focus and explicit feedback. It may have been more effective to adapt these goals, so they are removed from the individual's consciousness of their own body and the explicit adaptation, but ultimately aim to achieve the same adaptations in motion.
Furthermore, this was a proof-of-concept feasibility study, but for this biofeedback tool to be part of a clinical effective protocol, the motor-learning potential of the gait modification should be considered. Future work should incorporate understanding of motor learning, using this biofeedback tool in a protocol with consideration of feedback timing, length of training and the mode of feedback, to achieve improved walking performance long-term, and not just momentarily in the laboratory setting (Charlton et al. 2021).

5.4.8 Limitations

There were several limitations to this study, firstly the biofeedback interfaces encouraged a change in kinematics, but it did not quantify the 'goals'. A more precise protocol would have quantified the difference in maximum extension angle and step length that is communicated through the goals. Another limitation was that this study only gave a 10-minute familiarisation period. When this study was designed, it was designed as a feasibility study of implementing kinematic modifications through visual and audio feedback in this population and to observe whether the kinematic modifications had the desired effect on the iliopsoas recruitment. Future work would utilise this biofeedback gait retraining tool but with a comprehensive training period to investigate whether these changes could be achieved and crucially sustained. There are limitations of musculoskeletal modelling, outlined in Chapter 3, and specifically limitations when using a non-subject specific model as there are increased errors when not using subject specific anatomical geometry in the model (Ding et al. 2019) (Toderita et al. 2021). Another limitation of this study was the participant demographics, which included only one female participant and two individuals with through-knee amputations. Ideally, the groups (female and through-knee amputation) would have been evenly represented. However, these individuals were included as there was no evidence to suggest that their characteristics would affect the effectiveness of the biofeedback intervention. Additionally, the inclusion of a female participant introduces further limitations with respect to musculoskeletal modelling methods. The anatomical dataset for the female participant's residual limb was derived from a male individual, potentially overlooking sex-based differences in muscular anatomy that could influence the estimations of muscle force.

5.4.9 Conclusion

From the preliminary studies it appears it may be valid to use treadmill walking and the FreeBody musculoskeletal model to implement and quantify the effects of biofeedback gait training tools. It is possible to use visual and audio biofeedback to adapt the kinematics of individuals with unilateral and transfemoral amputations donning microprocessor knees. This tool could be used to develop a gait training tool; consideration of motor learning should be taken when developing a gait modification protocol for long term benefits. It appears that solely reducing maximum extension angle or stride length momentarily does not reduce the recruitment of the iliopsoas muscle during gait for individuals with UTF/UTK amputations. This chapter addresses the third and fourth objective of this thesis by using the forward dynamic predictions from Chapter 4 to design and implement a novel gait retraining method for individuals with unilateral TF and TK amputation.

Chapter 6

Conclusion

This chapter discusses the results, limitations and impact of the thesis in a wider context.

6.1 Summary of thesis results

Addressing the first objective of this thesis, Chapter 2 and 3 quantified the muscle recruitment and function during walking in individuals with bilateral and unilateral transfemoral and through-knee amputation due to trauma. The findings of Chapter 2 and 3 highlight how reduced muscular capacity following a TF / TK amputation increases the functional burden on the residual limb. Specifically, for individuals who have had bilateral and unilateral TF and TK, it appears muscles with flexor action are in relatively high demand during walking. Chapter 2 highlights how the relatively high recruitment of the psoas major and adductor longus muscles could become a limiting factor for walking if their functional capacity were reduced due to diminished muscular endurance as a result of the high intensity contractions required by baseline walking. This is evident from the study findings, where actuating the kinematics and kinetics of the collected gait trials was not possible for 5 of the 12 cases of simulated reduced muscular endurance of the psoas major and adductor longus ie. when their maximum force capacity was limited to 50% its original. Building on this, Chapter 3 highlights that the abnormally high (significantly higher than the able-bodied control group, $p = 0.00$) activation, an estimate of contraction intensity, and impulse, representing energy expenditure, of the iliopsoas, adductor longus, tensor fasciae latae, and pectineus muscles may contribute to reduced walking endurance in individuals with UTF. Furthermore, Chapter 3 demonstrates how compensatory gait strategies manifest in the intact limb of individuals with UTF, characterized by increased recruitment of the plantar flexors compared to able-bodied controls ($p = 0.01$).

Progressing on from the analysis of Chapter 2 and 3, it was evident that it may be beneficial to walking endurance for individuals with TF / TK amputation to relieve the demand on the hip flexors. The iliopsoas muscle remains intact in the residual limb following a TF and TK surgery. As a key hip flexor, the iliopsoas evidently compensates for the loss of plantar flexor's forward propulsion in actuating the hip flexion torque at terminal stance. Chapter 3 found hip flexion torque at terminal stance to be significantly higher ($p = 0.00$) in the residual limb side than to the intact limb side for individuals with UTF amputations. This results in the iliopsoas muscle producing a significantly higher magnitude of force ($p = 0.00$) and activation ($p = 0.00$) than the iliospoas muscle of the intact side (Chapter 3). Therefore, the primary focus for the remainder of the thesis was established as reducing the activation of the iliopsoas muscle in the residual limb during walking. In order to address this rehabilitation goal and in turn the second and fourth objective of this thesis, a forward dynamics musculoskeletal model was developed of an individual with unilateral TF and TK amputation. The unilateral condition was selected as the starting point due to the increased global prevalence (Yuan et al., 2023). The forward dynamics model, which enables the synthesis of non-captured motion, has the potential to be used for a broad range of rehabilitation applications. In Chapter 4 it was utilised to predict walking kinematics that reduced the activation of the iliopsoas muscle. Common kinematic modifications that emerged from the forward dynamic simulations of gait that achieved the goal of reduced iliopsoas activation, was increased hip flexion and reduced hip extension, and reduced step length. This was interpreted as 'minimising hip

extension reduces the demand on the hip flexors'.

The third and fourth objective of this thesis were to test predictions of the forward dynamic MSK model utilising biofeedback methods for a potential gait retraining tool and in turn demonstrate a methodological framework where MSK modelling inform experimental rehabilitation methods. To address these objectives and building on from the rationale established in Chapter 4, that reducing hip extension during walking may decrease the activation of the iliopsoas in the residual limb for individuals with TF and TK amputations, Chapter 5 introduced a rehabilitation tool designed to achieve these gait modifications. Biofeedback is a emerging rehabilitation method in rehabilitation of individuals with lower limb amputations. Biofeedback enables targeted gait retraining on specific biomechanical parameters that may be difficult to achieve using traditional rehabilitation methods. The real time feedback, in this case delivered with a combination of audio and visual cues, gives the participant an augmented sense of these biomechanical parameters. A Biofeedback intervention was developed via two methods, one targeting the maximum extension angle and the other reducing the stride length of both limbs. Both methods aimed to reduce the demand on the residual limb iliopsoas muscle during walking for individuals with UTF and UTK amputation. Chapter 5 presents a feasibility study testing the novel biodfeedback tool answering two key questions: is the biofeedback tool effective at modifying the walking patterns? And if so, do these kinematic modifications have the desired effect on the recruitment of the iliopsoas muscle of the residual limb of individuals with unilateral TF and TK amputations? Chapter 5 concludes that kinematic modifications are possible with this biofeedback method exhibited by significant changes in maximum extension angle for half the participants ($p \leq 0.03$) and stride length for all participants ($P \leq 0.03$), but these kinematic modifications did not have the desired effect on the iliospsoas recruitment. This chapter will explore the significance and context of these findings, the methods employed, and the next steps for future research.

6.2 Thesis discussion

6.2.1 Discussion of methods

Chapter 4 and 5 discussion – modelling to experimental implementation

A significant feature of this thesis was the methodological pipeline of designing a biofeedback gait retraining tool from predictions made by a forward dynamic MSK model. There is limited evidence of this being completed in the literature. This pipeline demonstrates how MSK modelling can be enabled to develop novel rehabilitation methods and in turn potentially validate the MSK model itself with experimental data. However, the progression from forward dynamic MSK modelling predictions to designing a experimental protocol, involved interpretation of the results into a generalisable gait feature that could be implemented. For example, one of the 'gait modifications' that was extracted from the forward dynamic's simulations, was reduced maximum extension angle. This feature was selected as a point of focus as maximum extension angle occurs at terminal stance phase of gait, which is when there is elevated flexion torque and recruitment of the il-

iopsoas muscle of the residual limb compared to the intact side according to the results of Chapter 3. Theoretically, reducing the maximum extension angle of the hip could reduce the external hip extension moment arm of the ground reaction force. The focus on reducing maximum extension was possibly a misinterpretation. Instead of focusing on one gait feature, or modification, it may have been more effective to have designed a biofeedback tool that implemented the gait modifications predicted in Chapter 4 in a more comprehensive manner.

Subject-specific modelling to experimental implementation would have been the ideal method. Due to computational time of the forward dynamic simulations and challenges in participant recruitment this was not completely possible. Participants 02, 03, and 04 in Chapter 4 correspond respectively to Participants 01, 02, and 04 in Chapter 5. Notably participant 04 was the only participant who could achieve a reduced maximum force of the iliopsoas muscle with the biofeedback tool. This may be coincidental or may be confirming the value of subject-specific modelling. However, the gait trials utilised in Chapter 4 were collected over a year before the data collection of Chapter 5, there was no verification that the gait kinematics had been preserved in this time. Due to the lack of a full subject specific pipeline, from forward dynamics modelling to biofeedback gait retraining tool design, this thesis attempted to generalise learning from Chapter 4. Generalising kinematic modifications has been effective in gait retraining interventions for other populations. For example, reducing step width and length to reduce knee moments for individuals with knee osteoarthritis (Edd et al. 2020) (Ulrich et al. 2023). However, this may not be the case for individuals with UTF / UTK amputations. Reducing computational time of the forward dynamics MSK modelling would improve the potential for clinical translation by potentially allowing subject specific prescription of gait retraining goals.

MSK modelling

Validation of FreeBody for individuals with UTF / UTK amputations

The EMG analysis completed in Chapter 5 validates the use of non-subject specific FreeBody MSK model, where the intact limb anatomical geometry was derived from MRI scans of able-bodied limbs and the residual limb from MRI's of BTF residual limbs, for predictions of muscle activations. Subsequently, this work validates the results of Chapter 3 as the same method was used.

Limitation of the models

Error is the difference between measured (or assumed value) and true value. Errors create uncertainty to the solutions (the amount of error in the solution). There are inherent sources of error in any study of motion. Inverse dynamics will include errors from skin movement artefacts, error in identification of centres of joint rotation, and error in the estimation of mass and inertia properties of the segments. Additionally, the inverse dynamic calculations will propagate any error that exists in the data collection equipment

(cameras and force plates) (Riemer et al. 2008). Marker error in motion capture systems tend to be between 1 – 5 mm and increase to 10 mm when propagated with soft tissue motion (Hicks et al. 2015). Measure of the ground reaction force and marker positions both have some level of inaccuracies, which may lead to inconsistency in the inverse dynamic calculations (Hicks et al. 2015). These fundamental limitations of motion analysis should be considered.

A core element of this thesis involved using musculoskeletal modelling to quantify and predict the internal forces within the MSK system. This approach was essential for the research, as muscle forces cannot be measured non-invasively. However, as a 'model', this method relies on certain assumptions and simplifications.

A key feature of the methods used in Chapter 2 – 5 is the estimation of muscle properties, particularly the maximum force potential which is derived from PCSA and maximum muscle stress / tension. Maximum muscle stress has been estimated by calculating the ratio between PCSA and measured muscle tension, but the value of maximum muscle stress varies in the literature ranges from 11-100 N/cm^2 (Hicks et al. 2015) (Rajagopal et al. 2016). The FreeBody model in this study uses a maximum muscle stress of 31.39 N/cm^2 (Cleather & Bull 2015) and the OpenSim model $60N/cm^2$ (Rajagopal et al. 2016). However, if the estimation of maximum muscle force is consistent in the model when completing static optimisation, the force sharing / muscle contribution should give valuable insight and not be sensitive to these modelling details.

Some of the simplifications of MSK modelling that are specific to this thesis are highlighted in the discussion sections of Chapter 2,3, and 4. For example; non-subject specific or MRI derived muscle anatomy used in Chapter 3, 4, 5, the lack of control for surgical technique in Chapter 2, 4 and 5, the simplified model of MPK prosthetic knee dynamics in Chapter 4 and the assumption that the socket-residual limb segment acts as a rigid segment, where in reality it is dynamically coupled (Gale et al. 2020) in Chapters 2, 3, 4 and 5.

Particular assumptions are made when modelling the anatomy and prosthetic anatomy of individuals with lower limb amputations. Beyond those previously mentioned, the loading dynamics at the socket-residual limb interface represent another area of simplification. One feature that is overlooked is the socket design. A majority of the participants in this study donned ischial containment sockets. In this design, the ischial containment of the socket fits snugly to the ischial tuberosity and ramus. This fit allows loading through the ischium as shown in Figure 6.1, edited from (Lee et al. 1997). This contact force acting on the thigh segment will create a moment about the centre of hip rotation, however, this contact force is mostly ignored in the musculoskeletal models of transfemoral socket wearers apart from a couple of examples found in the literature of the same author (Fougeron et al. 2020) (Fougeron et al. 2022). Both these studies by Fougeron (2020, 2022) simply reduce the hip moment in the frontal plane by varying amounts after performing inverse dynamics, before solving for muscle forces with static optimisation. This method was based on estimates in older literature (Pritham 1990) (Radcliffe 1955). The reduction

in frontal torque was based on the estimated percentage of body weight transferred through the pelvis to the ischial containment. This estimate ranges from 50 to 83%. This method by Fougeron et al. (2020) is not based on experimental measures of contact force and does not consider the inevitable variation in contact force during the stance phase of gait. This interaction is challenging to model in inverse dynamic methods, without direct measurement, but this contact force could be modelled in the MSK model for forward dynamics methods. This may be challenging to do accurately as the geometry would be sensitive to variations in socket fit. The ignoring of this ischial containment contact force is a potential limitation of the methods used in this thesis. However, incorporating this feature would not change the main findings, that the hip flexors are in high demand during gait, as this contact force primarily affects frontal plane torques, as highlighted by Pritham (1990) and Fougeron et al. (2020) .

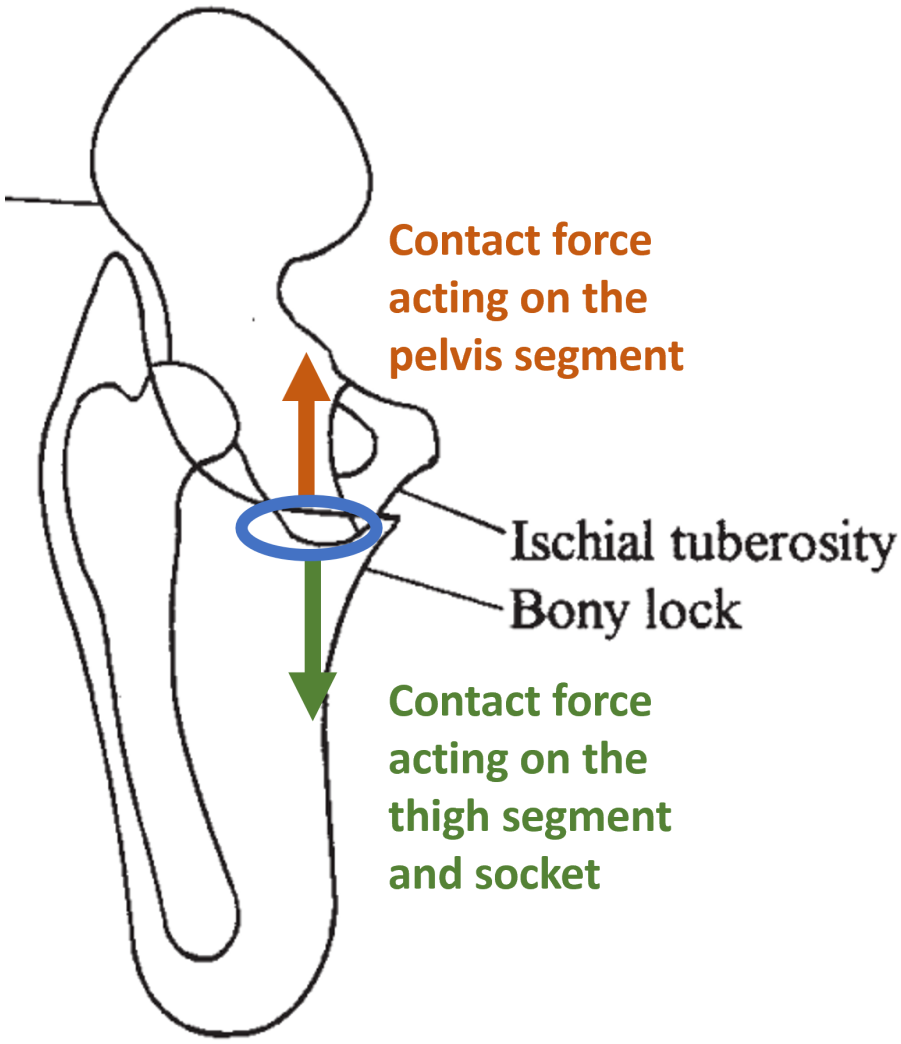


Figure 6.1: Schematic of the contact force provided by ischial containment sockets, edited from (Lee et al. 1997)

Adding additional force components (ie. modelling the ischial compartment) or joints (ie. modelling the dynamic coupling of the socket and residual limb) to models that are to be used for forward dynamic modelling adds variables to the optimal control simulations and the added complexity is likely to add computational time. A sensitivity analysis should therefore be conducted to assess whether these features would impact the predictions of muscle forces to determine whether they are worthwhile additions to the model. Miller (2022) found that adding positioning of the residual limb in the socket of their model of an individual with transtibial amputation had little effect on predicted metabolic cost which was derived from muscle forces (Miller & Esposito 2021).

Future of MSK modelling

Forward dynamics MSK modelling that is accessible for laboratories of non-experts in optimal control programming with usual research computer power is a promising development for biomechanical research, with the opportunity to help answer a variety of rehabilitation challenges. This thesis has used OpenSim Moco which is a method of optimal control solved by direct collocation. Other forward dynamic models are available, for example Simulated Controller Optimization Environment (SCONE) (Geijtenbeek 2019). SCONE uses shooting-based optimisation methods to solve optimal control problems. Shooting methods are where the model makes an initial guess (of initial states) and then simulates a trajectory (or shoots) with forward integration for states and controls. The solution is then fed through an optimiser (covariance matrix adaptation (CMA)) which evaluates the results, ie. has the goal been met and to what cost, and if not, to inform the next guess. The simulation is a black box, so the optimiser does not see the simulated trajectory, only the result. At each iteration a new simulation (guess of the trajectory) needs to be generated. Model simplifications are often used to limit the number of variables as these SCONE simulations tend to be very slow compared to direct collocation (De Groote et al. 2016). However, more recently SCONE has been combined with a physics based engine, MuJoCo (Todorov et al. 2012), to create HYFYDY (high fidelity dynamics) models (Geijtenbeek 2021). HYFYDY models can be implemented in SCONE, using the same OpenSim MSK model of muscle and contact dynamics as utilised in this thesis. HYFYDY models are designed for forward dynamic simulations and allow for fast solving, still solving through CMA (Waterval et al. 2023). This HYFYDY model could be utilised to increase the speed and therefore clinical translation of the forward dynamic simulation to rehabilitation design pipeline as demonstrated in this thesis.

The integration of physics-based modelling with machine learning is an emerging trend in biomechanical research (Uhlrich et al., 2023). Reinforcement learning, a method where a model learns to make decisions based on feedback from its environment, is now being applied to simulate human walking (Schumacher et al., 2023). Deep reinforcement learning, which combines reinforcement learning with deep learning, neural network models based on the human brain to recognise pattern and relationships in data, has been used for the forward dynamic modelling of walking in individuals with TF amputation (De Vree & Carloni 2021) (Ogum et al. 2024). This development in biomechanical research may bring opportunity for a wide range of modelling methods with rehabilitation application

in this population as this method integrates the feature of feedback.

Validation and clinical impact of MSK modelling

Validating inverse dynamic models that predict muscle forces is challenging because, aside from using animal models, directly measuring muscles forces is difficult (Wakeling et al. 2023) (Hicks et al. 2015). Validating with EMG signals of muscle activation and instrumented implant measures of joint loading, while ensuring dynamic consistencies, is the gold standard for inverse dynamic MSK modelling (Hicks et al. 2015). However, validating forward dynamic predictions is even more challenging. There are examples of studies which have used the model to validate itself with comparison from data extracted from the literature. For example, Pariser & Higginson (2022) simulated walking on a treadmill (using OpenSim Moco) and validated their model by varying the simulated 'treadmill' speed and comparing the observed (predicted) changes in kinematics, GRF and spatiotemporal values to reported experimental data (Pariser & Higginson 2022). Similarly Miller & Esposito (2021) validated their metabolic cost predictions of their model of an individual with transtibial amputation (developed in OpenSim Moco) by adding weights of varying magnitude to the feet of their model and comparing the changes in modelled metabolic cost when walking with these added weights to reported experimental values of changes in metabolic cost due to the addition of the same weights (Miller & Esposito 2021).

This thesis attempts to validate predictions made with forward dynamic modelling experimentally. This is a key feature of this thesis and is rare in current literature. There is a slight exception of a study by Uhlrich (2022), this study successfully predicted that the reduction in the activity of two plantarflexes could offload the knee and validated these predictions by using EMG biofeedback (with a single session) (Uhlrich et al. 2022). However, unlike the methods of this thesis these predictions were made with inverse dynamic static optimisation methods of one subject. They name this pipeline 'simulation informed coordination retraining'. It is important that the pipeline of forward dynamic MSK modelling to experimental validation is done more frequently to improve models (Uhlrich et al. 2023*b*). This research would assist in MSK models being used as clinically robust tools, where the findings can translate into rehabilitation practise. The current use of MSK modelling in clinical practise is rare as it requires an interdisciplinary team (Smith et al. 2021) (Killen et al. 2020) (Uhlrich et al. 2023*b*), however, the potential applications in rehabilitation research are significant.

6.2.2 Biofeedback development

As demonstrated in Chapter 5, modifying gait of individuals with UTF / UTK amputation is possible with biofeedback, but the information being relayed needs to be adapted to have the desired effect on muscle recruitment and therefore gait endurance. As mentioned in the discussion of Chapter 5, the biofeedback system could incorporate EMG to directly measure iliopsoas activation, though this may be challenging due to the position of the muscle group. Alternatively, the biofeedback system could make use of recent

developments in real-time MSK modelling (Uhlrich et al. 2023*b*) (Killen et al. 2020), as provided by the 'Human Body Model' (Motek 2024) which facilitates real-time MSK modelling. Potential increased error of real-time MSK modelling should be considered (Falisse et al. 2018), and perhaps real-time MSK modelling should only be used to estimate the information feedback and not used to quantify the effects of the biofeedback itself. The analysis of the effect of the biofeedback system could be done in a post-hoc manner as demonstrated by Chapter 5.

6.2.3 Implication on prosthetic design

Both Chapter 2 and 3 quantified and highlighted the increased demand on the hip flexors in the TF and TK amputation condition, which was partly associated to the loss of power and forward propulsion provided by the ankle planter flexors and Achilles tendon in the intact anatomy. Although this thesis took the approach of enhancing walking with the current rehabilitation and state-of-the-art prosthetics, an alternative route would have been to quantify and model potential prosthetic device development. It would seem that the demand on the hip flexors, in individuals with both BTF / BTK and UTF / UTK, could be solved by adding power to the MSK system with a powered ankle prosthetic, potentially in combination with a powered prosthetic knee. Ottobock, a key prosthetics manufacturer, currently have the Empower powered prosthetic ankle and the Power knee (Ottobock, Germany). Currently, powered prosthetics are heavier than MPK's and energy return feet due to the additional battery requirements, sensors and actuators. This weight would increase the cost of walking and would be particularly troublesome when donning a powered ankle as the weight of the ankle is distally positioned and would create a pendulum effect during swing phase (Gehlhar et al. 2023). Knight et al. (2023) reported some evidence that powered ankle-knee prosthetics induce exaggerated compensatory strategies, compared to MPK and energy return feet, in a study investigating a small group of military personnel. These exaggerated compensatory strategies may lead to the development of secondary conditions (ie. lower back pain) if not addressed in rehabilitation (Knight et al. 2023). Powered knees have been found to improve functional ability during sit to stand task (reduced asymmetry, demand on the intact vastus medialis and duration) for individuals with UTF (Hunt et al. 2022). A case series of individuals with UTF found reduced power and work at the residual hip while donning a powered knee-ankle prosthetic, compared their usual prosthetics, which may reduce fatigue and 'over-use' injuries (Elery et al. 2020). Development of lighter powered prosthetics is required to benefit the rehabilitation of individuals with TK and TF amputation.

6.2.4 Alternative methods for rehabilitation improvement

Fundamentally this thesis aimed to improve walking endurance for individuals with TF / TK amputation through the analysis of muscle recruitment. This method of in-depth analysis of a smaller group of individuals provides important insights but is also much more feasible than a study design of alternative methods of a larger participant group, such as an randomised control trial, due to the relatively small population of individuals with lower limb amputations due to trauma in the U.K (Moxey et al. 2010), with an

estimated 3 - 13 % amputations in the UK being related to trauma (NHS-England 2016).

Aside from an in-depth analysis of muscle recruitment with MSK modelling, another approach would have been to quantify walking endurance (through a 6-minute walking test) in individuals, and to have done a post-hoc analysis to identify any correlations between walking endurance and gait features (muscle coordinate, spatiotemporal, kinematics) to identify any desirable characteristics, which could be used as rehabilitation goals.

This thesis concluded that the hip flexors of the residual limb were highly active during gait of individuals with TK / TF amputations, which may be a source of reduced muscular endurance during walking. Instead of adapting walking kinematics to reduce the recruitment of the flexors, which was the approach taken by this thesis, a more direct method of modifying muscle recruitment could have been taken. For example, botulinum toxin injections have been used to manage muscle over-activity by inducing temporary denervation (Cullen et al. 2007) in the lower limb of patients following stroke (Gracies et al. 2007). Perhaps this method could be applied to individuals with TF / TK amputation. Alternatively, functional electrical stimulation (FES), a method of artificially activating muscles for a functional purpose, could be employed to manipulate muscle co-ordination. FES has been used to increase the activity of the gluteus medius in order to unload the medial compartment of the knee which is significant to knee osteoarthritis (Rane & Bull 2016). Similar work was done by Xu et al. (2019) in stimulating the biceps femoris for reduced knee medial compartment loading. This research demonstrates how FES can be utilised to manipulate the internal loading of the MSK system. Theoretically, MSK modelling could be implemented to model desirable muscle recruitment of surrounding muscles for reduced iliopsoas activity. FES could then be employed to achieve this muscle co-ordination.

Another feature of rehabilitation for individuals with TF and TK amputations that may affect muscle recruitment but has not been considered in this thesis is prosthetic alignment. Previous research has shown that prosthetic alignment affects energy consumption during walking for individuals with transfemoral amputation due to trauma, additionally they identified changes to the saggital hip plane torques with changes in prosthetic knee alignment (Schmalz et al. 2002). Similar work could be conducted with a focus on iliopsoas muscle activity using MSK modelling or EMG data collection.

6.2.5 Broader context - demographic and access

A review by Kaur (2021) highlighted the lack of studies analysing the functional outcomes of individuals with lower-limb amputation due to trauma that included female, civilian and patients from low to middle income countries (Kaur et al. 2021). This thesis only included one female participant, this is due to participant recruitment and data availability, however, it is essential that an effort is made to include more female participants in this research area. Additionally, this research focused on individuals donning state-of-the art prosthetics (MPK and dynamic response feet). With the current conflicts, there will be a rise in individuals sustaining traumatic amputations. Many of these individuals are likely

to be physically fit at the time of injury and have a right to a long, active life. However, they may not access to the state-of-the-art prosthetics that are analysed and modelled in this thesis. The WHO estimate that globally only 5 - 15 % of people who require assistive products (including prosthetics) have access to them (World-Health-Organisation 2017), let alone state-of-the-art prosthetics. MPK's are too expensive for many people living in lower to middle income countries (Narang et al. 2015). Additionally, in the UK MPK prescription on the NHS is dependent on the activity and mobility level of the patient, as well as other attributes such as cognitive reasoning and commitment to rehabilitation. Furthermore, the NHS MPK commissioning policy advises on prioritising patients dependent on clinical need within the patient group who are eligible, due to the lack of resources (NHS-England 2016). MPK's are not available to all individuals with TF / TK amputations due to trauma, and therefore the focus on state-of-the-art prosthetics in this research is limiting to the broader translation. It is crucial to continue research focused on improving rehabilitation for individuals with traumatic transfemoral and through-knee amputations, ensuring it addresses a broader demographic and represents those who do not use state-of-the-art prosthetics for daily ambulation.

6.2.6 Future work

Below summarises the potential future work of this thesis, some of which has been previously mentioned, that would continue the research of enhancing walking for individuals with transfemoral and through-knee amputation.

- To develop a muscle model of the anatomical geometry of the residual limb and intact of individuals with unilateral TF amputations from MRI data, to be implemented in inverse dynamics and forward dynamics simulation. Currently this thesis only used anatomical geometry derived from MRI scans of individuals with bilateral TF / TK for the residual limb and able-bodied individuals for the intact limb.

- To develop a forward dynamic model of individuals with bilateral TF / TK amputations to be used as a tool to propose rehabilitation solutions in this population, as was completed for unilateral TF / TK population in this thesis.

- Use the current forward dynamic model to predict the enhancement of a variety of phenomena which are associated with secondary conditions such as asymmetrical joint loading or the increased anterior pelvic tilt in individuals with unilateral TF / TK amputations.

- Use the current forward dynamic model to predict an array of loading conditions from non-recorded motion. This information could be used in studies of MSK system on a tissue level. For example, loading conditions could be predicted of certain gait patterns, or compensatory strategies, and these predicted loads (muscle forces, tendon and joint loading) could be fed into finite element models which have the algorithms to predict changes in bone remodelling (osteopenia) or tissue health (tendonitis).

- To continue this work for a broader demographic, for example more females, individuals who have been less active, a range of different ages (including paediatrics). The MSK models would have to be developed and validated to accurately represent this wider range of demographics.

- To complete a longitudinal study looking at ageing in this population of individuals who sustained an amputation due to trauma at an age where they tend to be fit and want to maintain their active lifestyles, which is demanding on their residual MSK system. We are living in a period where people are living longer and maintaining active later into life. This means that regenerative MSK medicine is a growing research area. How this research relates to individuals with TF / TK amputations with their specific loading conditions and secondary health conditions is significant to rehabilitation outcomes.

- This research on enhancing walking, therefore improving social inclusion and quality of life, in individuals with TF / TK amputations should be translated for individuals who do not have access to state-of-the-art prosthetics and are donning mechanical prosthetic knees and non-articulating prosthetic feet.

6.2.7 Closing remarks

This thesis has used inverse dynamic and forward dynamic approaches to musculoskeletal modeling to provide an in-depth analysis of the muscle recruitment compensatory strategies adopted for walking by individuals who have sustained bilateral and unilateral transfemoral and through-knee amputations due to trauma. It has demonstrated how these approaches can be utilised in a methodological pipeline for rehabilitation research in this population to improve quality of life for all living with traumatic lower limb amputations.

Appendices

Appendix A

Chapter 4: Iteration 1 results

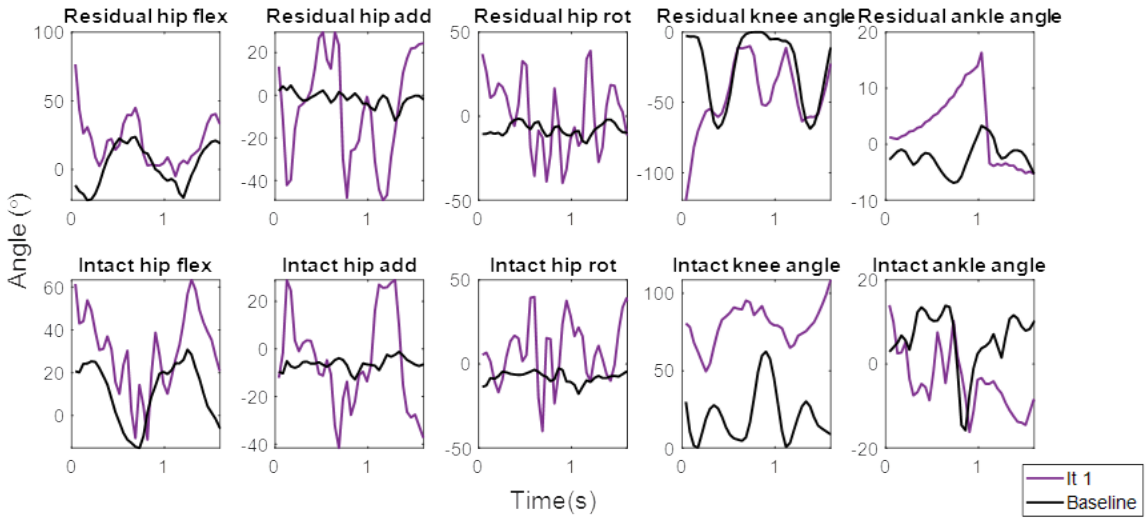


Figure A.1: Iteration 1 results participant 01 for the residual and intact limbs

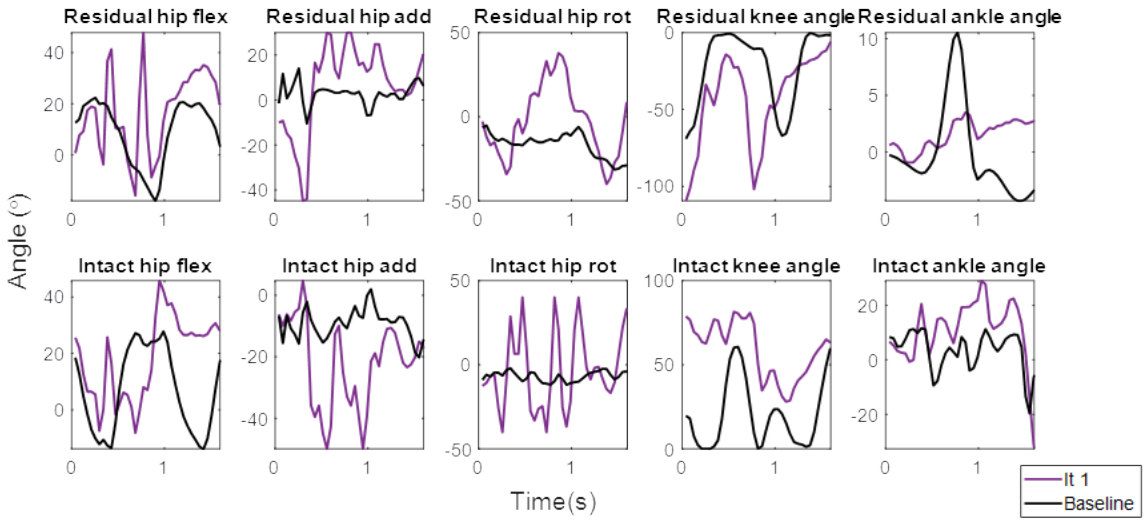


Figure A.2: Iteration 1 results participant 02 for the residual and intact limbs

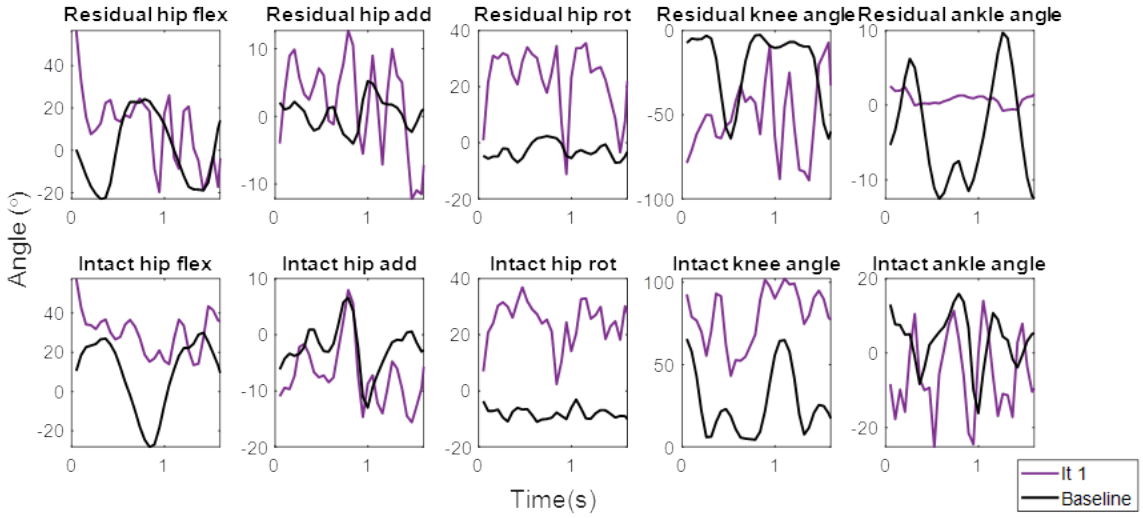


Figure A.3: Iteration 1 results participant 03 for the residual and intact limbs

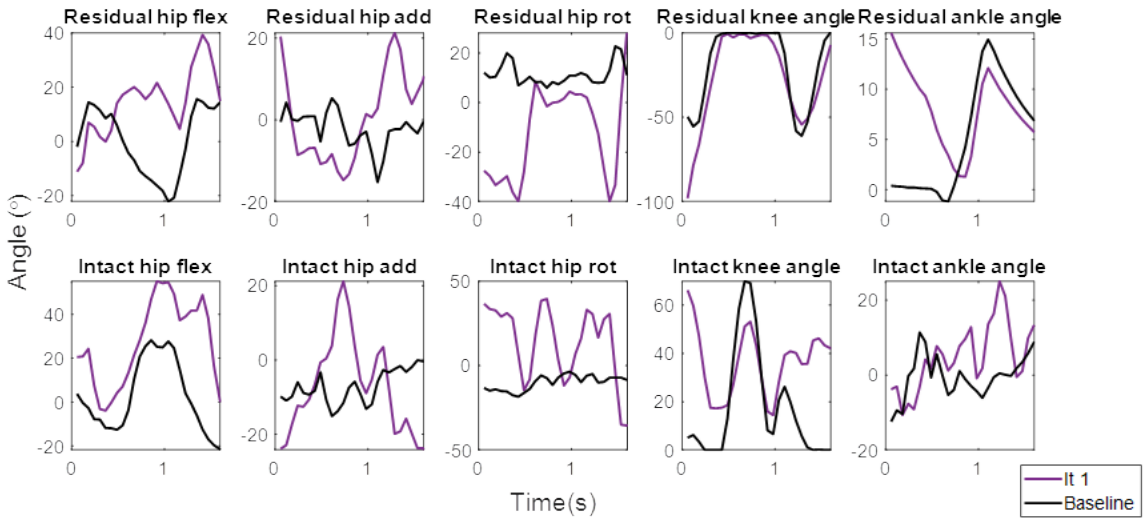


Figure A.4: Iteration 1 results participant 04 for the residual and intact limbs

Appendix B

Chapter 5: Biofeedback demonstration slide deck

The following slide deck was used in Chapter 5 to demonstrate the visual feedback provided by the biofeedback system. This was to assist the participants in understanding the interface.

The images in the slide deck were sourced from:

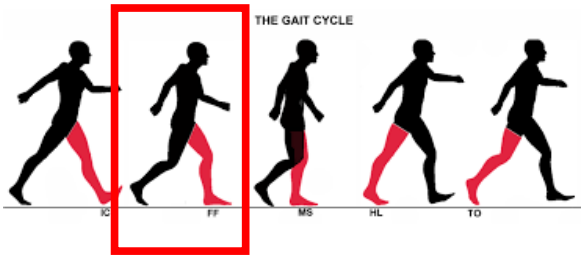
Porter, S. ed., 2013. Tidy's Physiotherapy E-Book: Tidy's Physiotherapy E-Book. Elsevier Health Sciences.

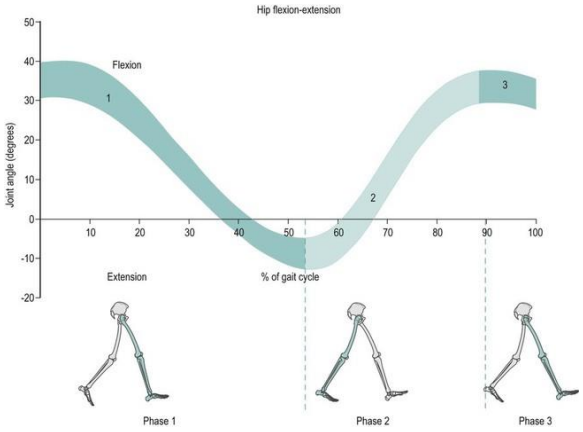
Bhongade, A., Gupta, R., Gandhi, T.K. and Ap, P., 2024. Intelligent Single IMU Sensor Module for Gait Temporal Parameter Estimation. Authorea Preprints.

Visual feedback demonstration

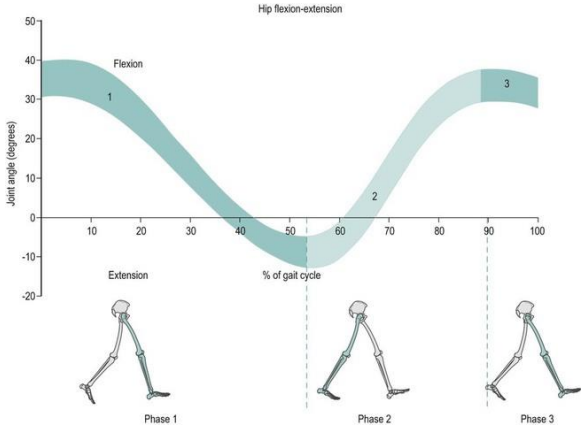
Description for participants

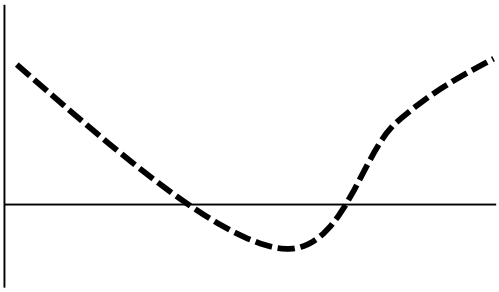
Extension angle goal



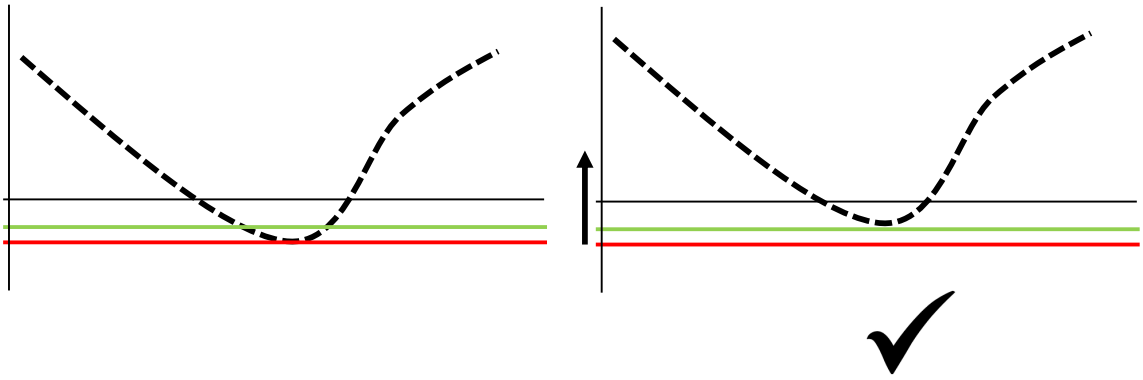


Extension angle goal

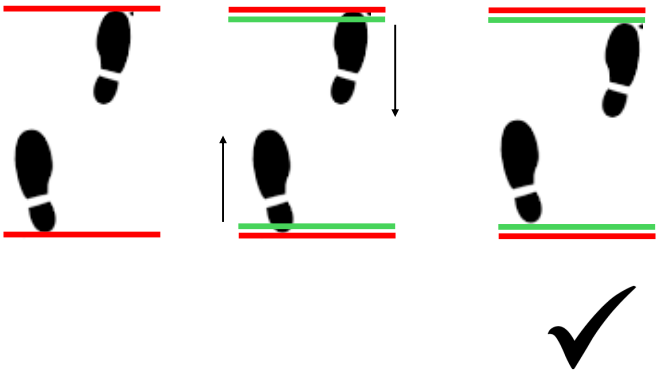




Extension angle goal



Step length goal



Appendix C

Chapter 5: Perceived effort questionnaire - extension goal

Visual feedback – hip extension angle

Date:

Participant ID number:

PERCEIVED EFFORT QUESTIONNAIRE

For each question, please **circle the number** that best describes your satisfaction with your prosthesis.

1. It was easy to interpret the visual biofeedback on the screen.
    1) Totally agree
    2) Rather agree
    3) Rather disagree
    4) Totally disagree

2. I was able to alter my gait pattern with the addition of visual biofeedback.
    1) Totally agree
    2) Rather agree
    3) Rather disagree
    4) Totally disagree

3. On a scale of 1-10, how much perceived effort was required to alter your gait pattern.

    1 2 3 4 5 6 7 8 9 10

4. If 1 is no discomfort and 10 is pain, describe any changes in comfort felt with the addition of visual feedback.

    1 2 3 4 5 6 7 8 9 10

5. I did not feel any pain or discomfort due the use of functional electrical stimulation.
    1) Totally agree
    2) Rather agree
    3) Rather disagree
    4) Totally disagree

6. If 1 is no discomfort and 10 is pain, describe any changes in comfort felt with the addition of functional electrical stimulation.

    1 2 3 4 5 6 7 8 9 10

7. Changes in my gait reduced discomfort felt.
    1) Totally agree
    2) Rather agree
    3) Neutral
    4) Rather disagree
    5) Totally disagree

8. Any other comments?

END OF QUESTIONNAIRE

Appendix D

Chapter 5: Perceived effort questionnaire - step goal

Visual feedback – step length

Date:

Participant ID number:

PERCEIVED EFFORT QUESTIONNAIRE

For each question, please **circle the number** that best describes your satisfaction with your prosthesis.

1. It was easy to interpret the visual biofeedback on the screen.
    1) Totally agree
    2) Rather agree
    3) Rather disagree
    4) Totally disagree

2. I was able to alter my gait pattern with the addition of visual biofeedback.
    1) Totally agree
    2) Rather agree
    3) Rather disagree
    4) Totally disagree

3. On a scale of 1-10, how much perceived effort was required to alter your gait pattern.

    1 2 3 4 5 6 7 8 9 10

4. If 1 is no discomfort and 10 is pain, describe any changes in comfort felt with the addition of visual feedback.

    1 2 3 4 5 6 7 8 9 10

5. I did not feel any pain or discomfort due the use of functional electrical stimulation.
    1) Totally agree
    2) Rather agree
    3) Rather disagree
    4) Totally disagree

6. If 1 is no discomfort and 10 is pain, describe any changes in comfort felt with the addition of functional electrical stimulation.

    1 2 3 4 5 6 7 8 9 10

7. Changes in my gait reduced discomfort felt.
    1) Totally agree
    2) Rather agree
    3) Neutral
    4) Rather disagree
    5) Totally disagree

8. Any other comments?

END OF QUESTIONNAIRE

Appendix E

Chapter 5: EMG validation - trial 2-3

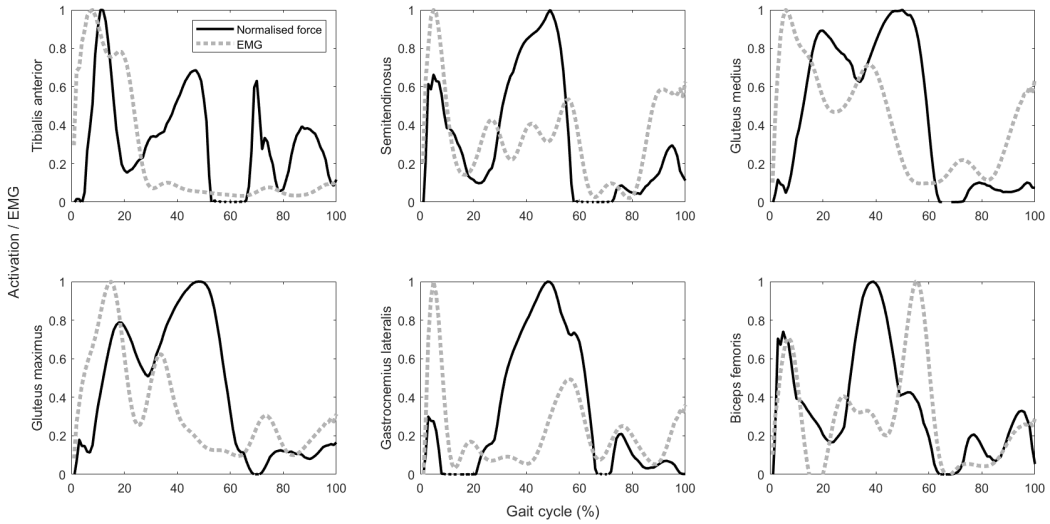


Figure E.1: EMG validation intact limb participant 01 trial 02

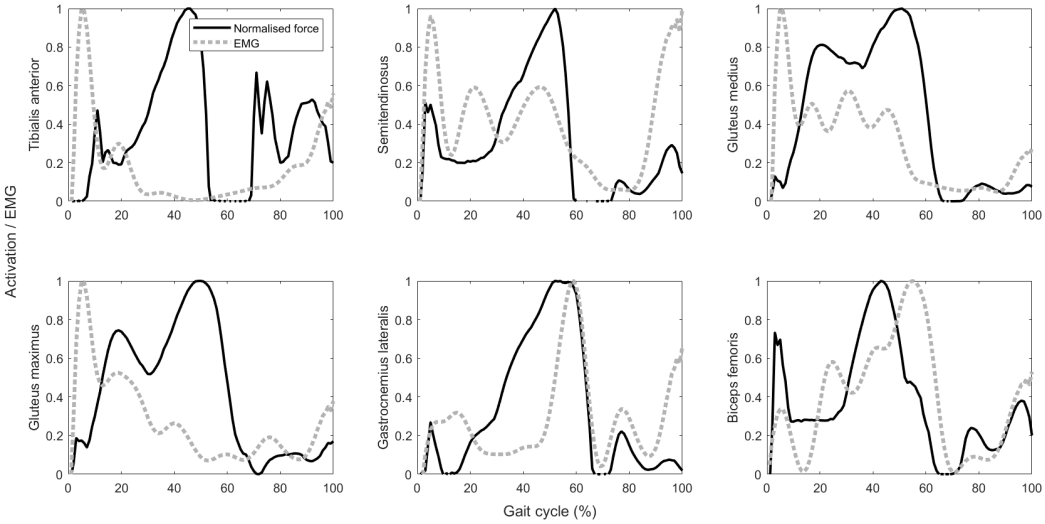


Figure E.2: EMG validation intact limb participant 01 trial 03

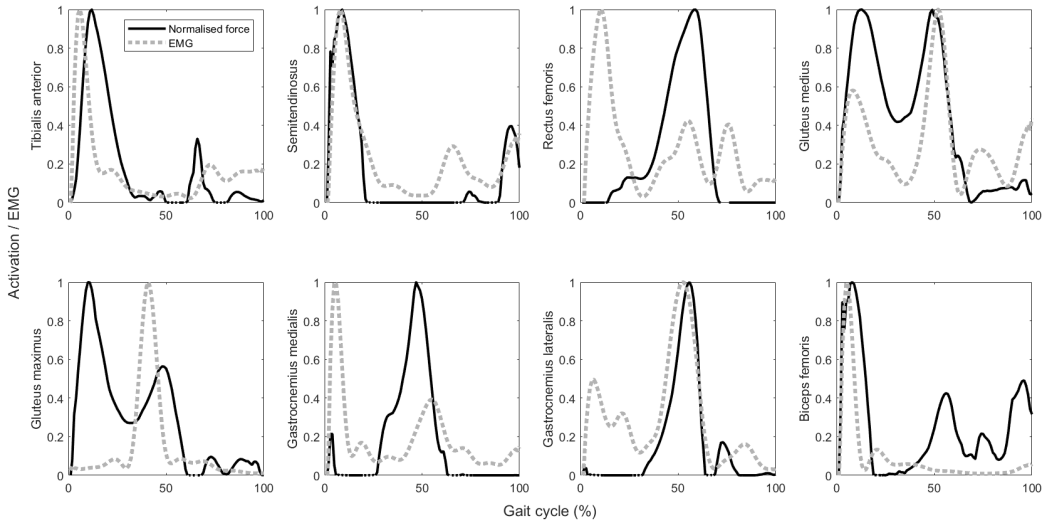


Figure E.3: EMG validation intact limb participant 02 trial 02

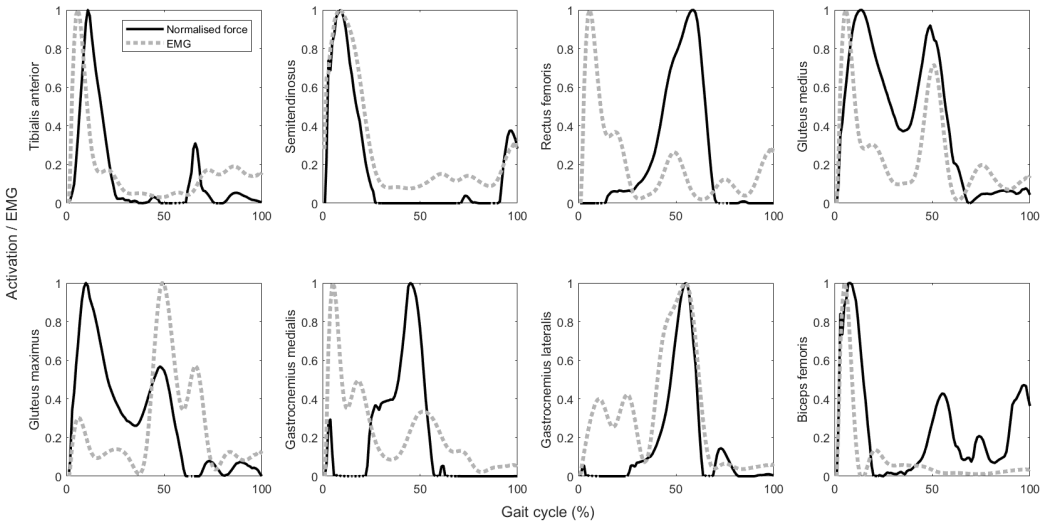


Figure E.4: EMG validation intact limb participant 02 trial 03

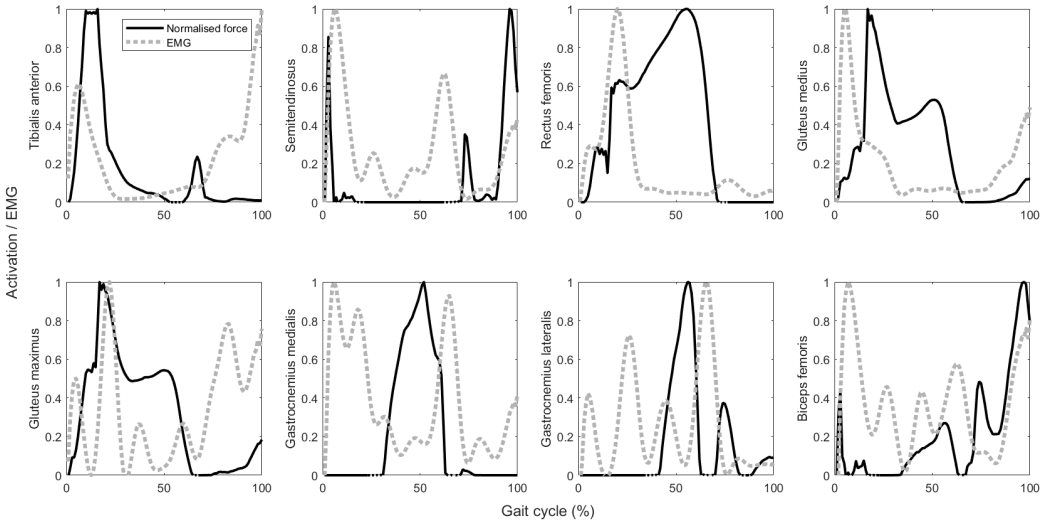


Figure E.5: EMG validation intact limb participant 03 trial 02

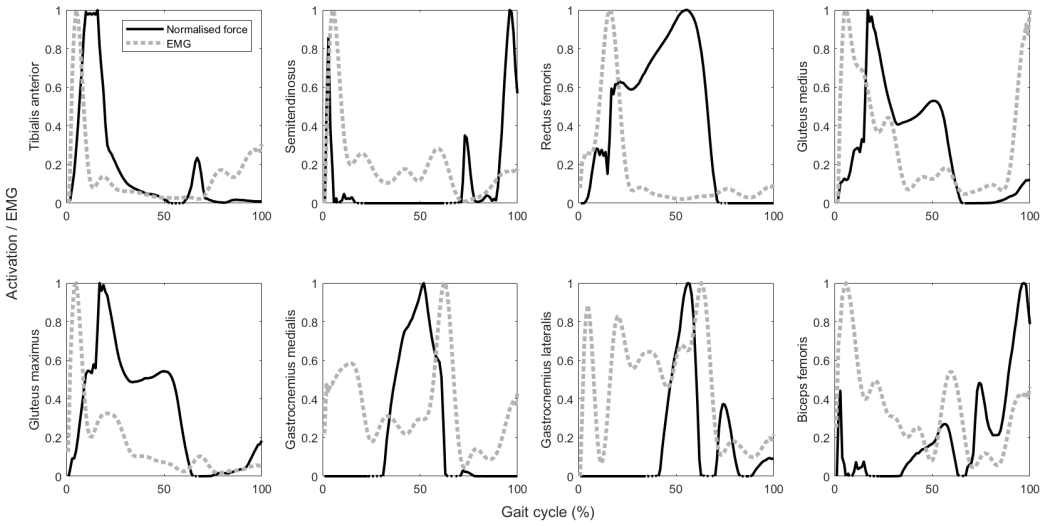


Figure E.6: EMG validation intact limb participant 03 trial 03

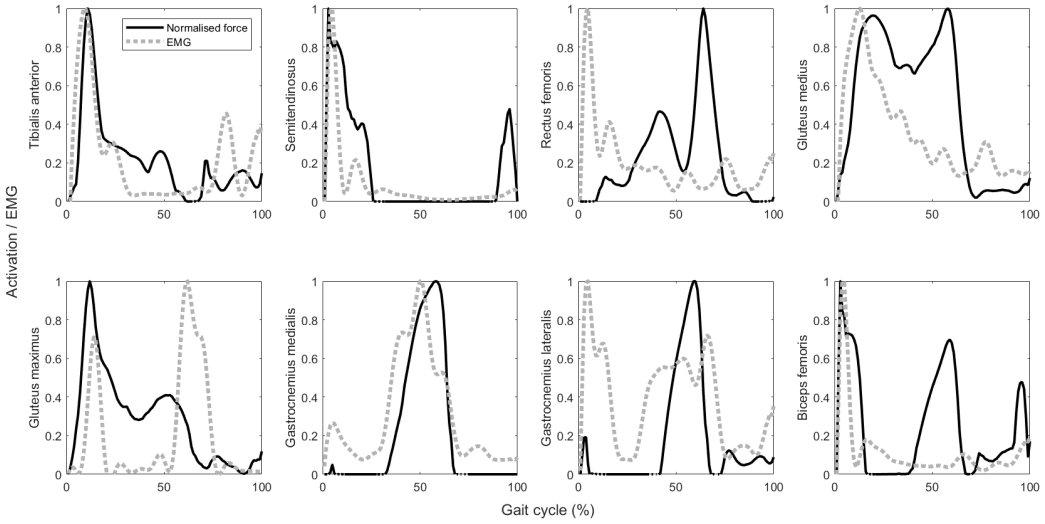


Figure E.7: EMG validation intact limb participant 04 trial 02

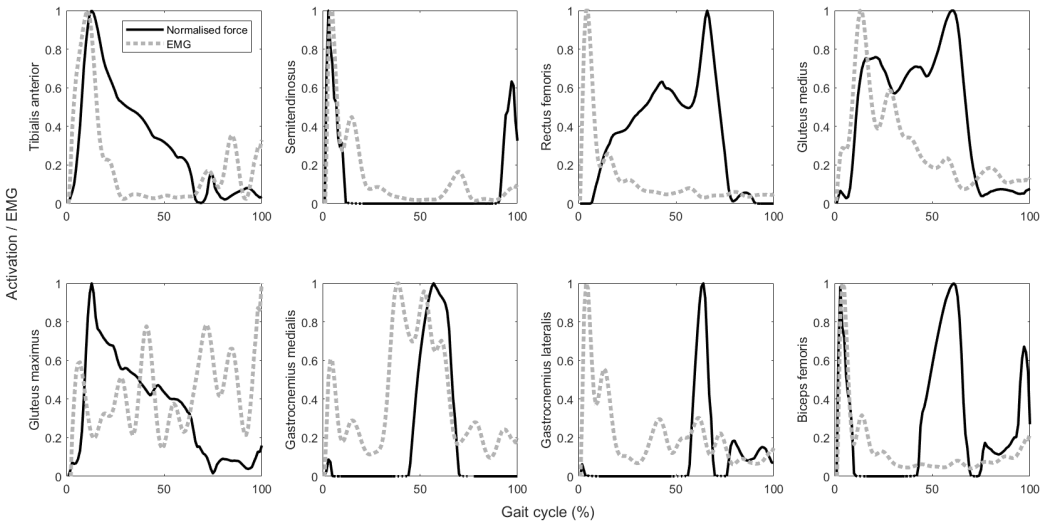


Figure E.8: EMG validation intact limb participant 04 trial 03

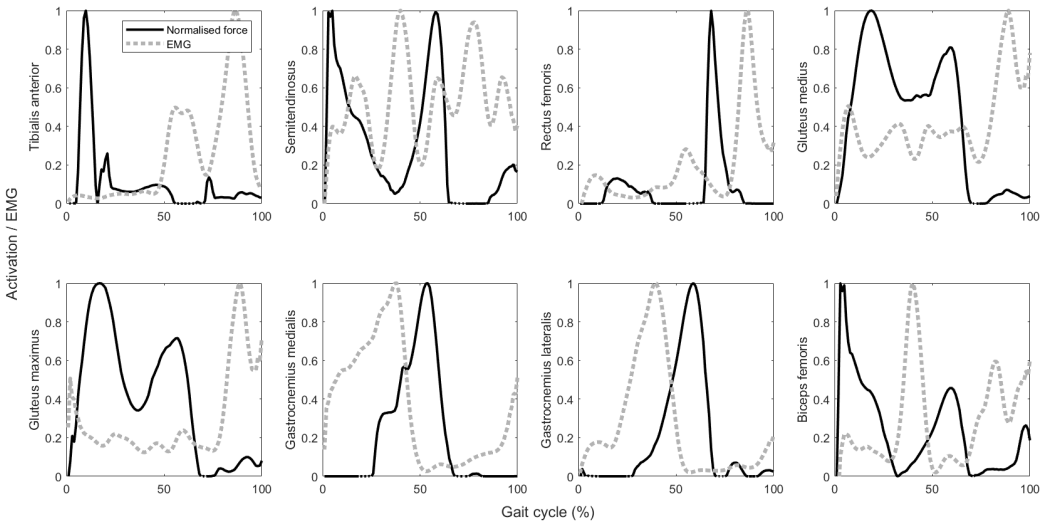


Figure E.9: EMG validation intact limb participant 05 trial 02

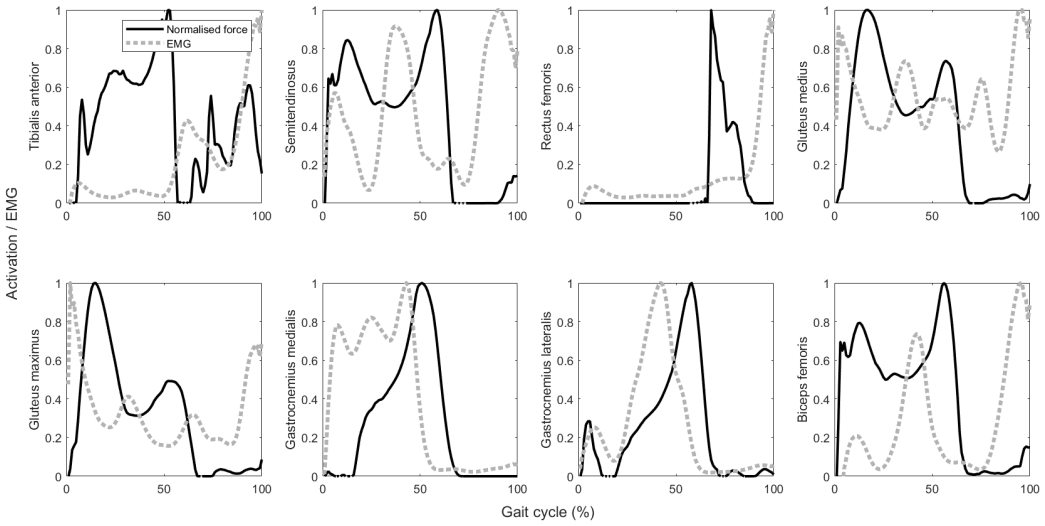


Figure E.10: EMG validation intact limb participant 05 trial 03

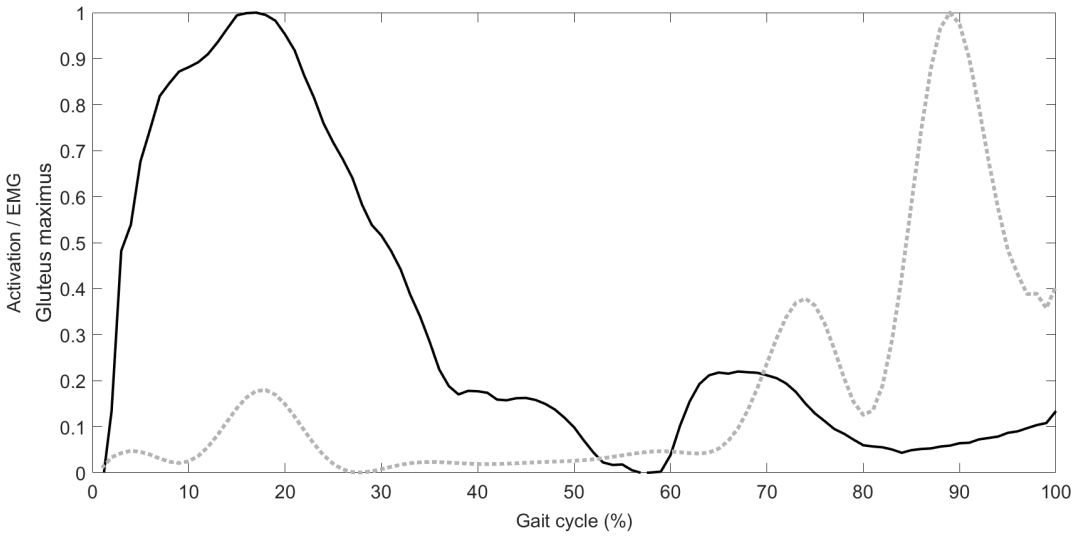


Figure E.11: EMG validation residual limb participant 01 trial 02

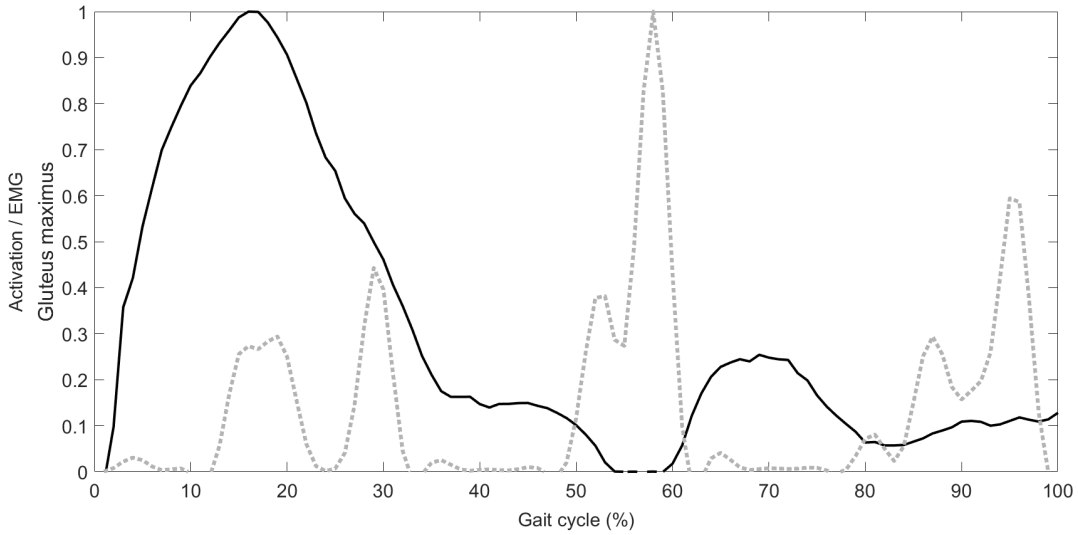


Figure E.12: EMG validation residual limb participant 01 trial 03

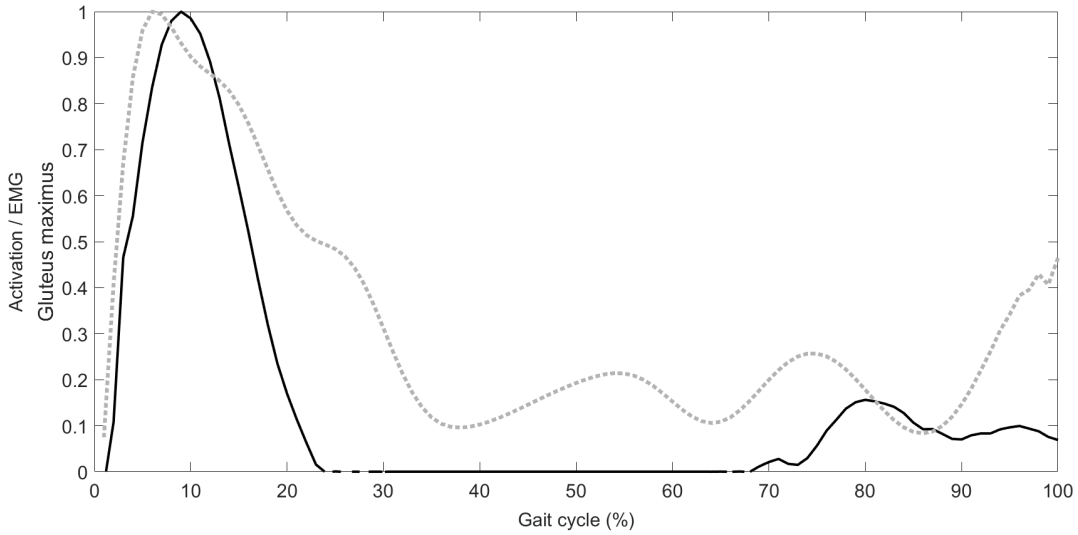


Figure E.13: EMG validation residual limb participant 02 trial 02

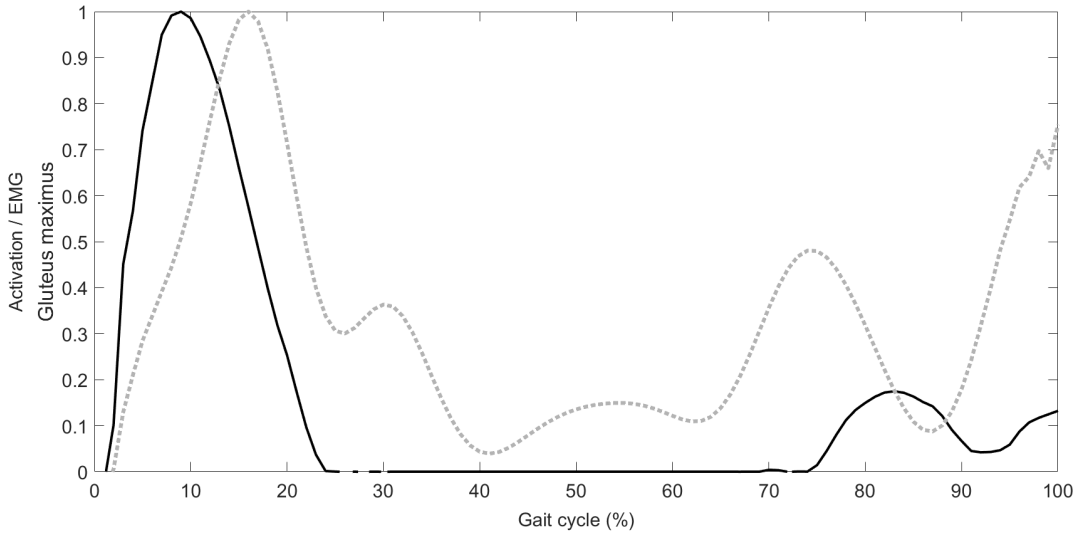


Figure E.14: EMG validation residual limb participant 02 trial 03

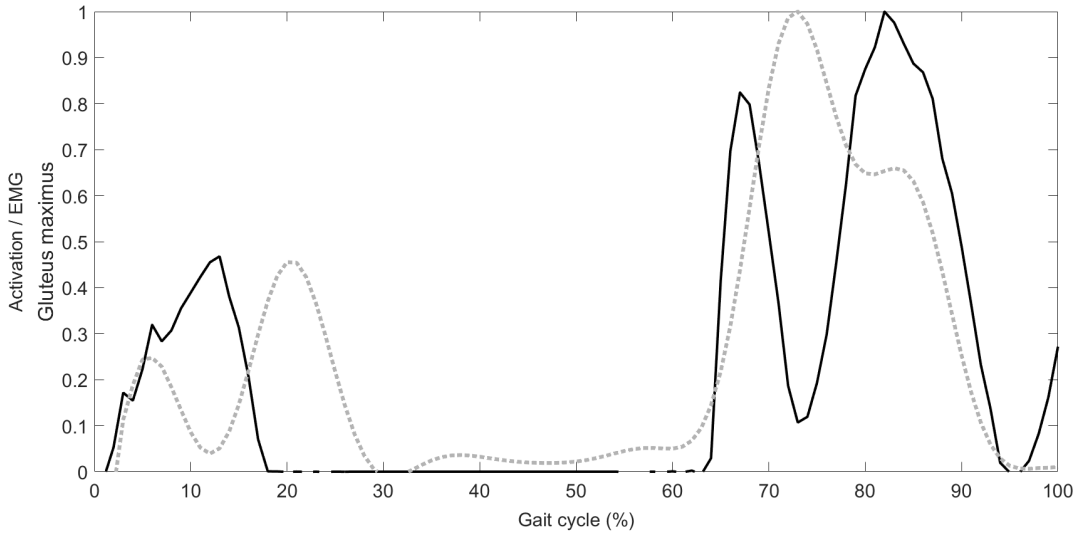


Figure E.15: EMG validation residual limb participant 03 trial 02

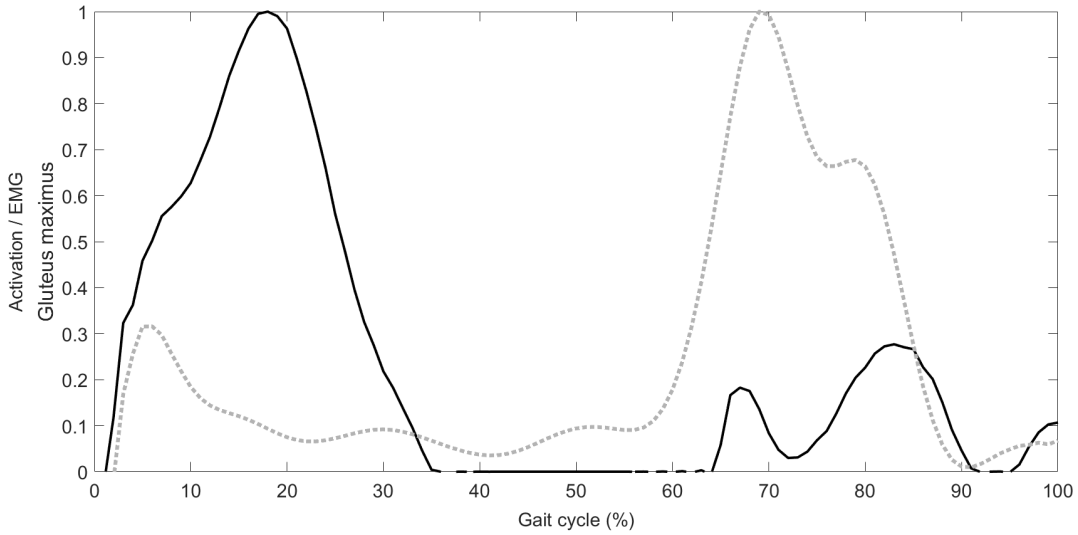


Figure E.16: EMG validation residual limb participant 03 trial 03

Appendix F

Chapter 5: Iliospoas force following 'extension goal' - participants 03 and 05

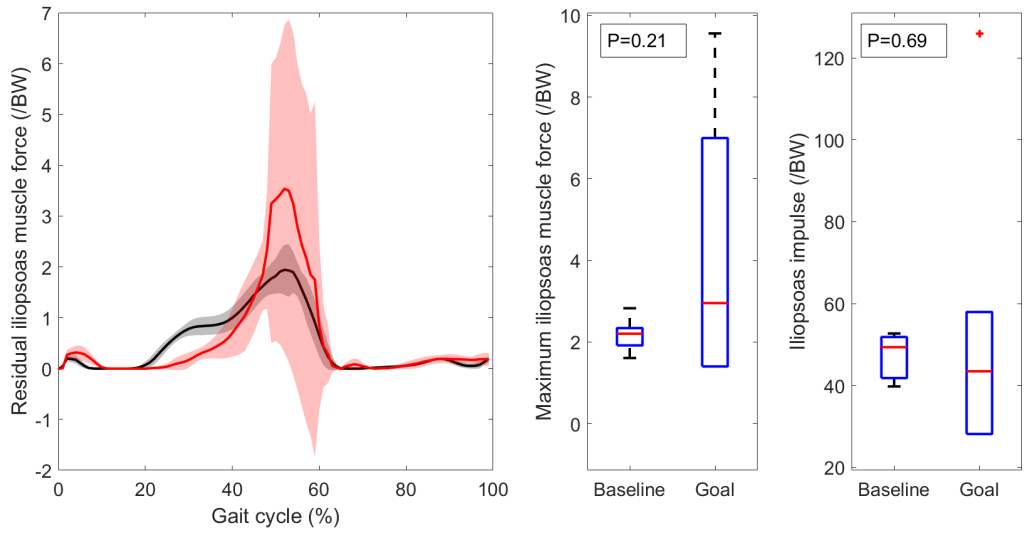


Figure F.1: Iliopsoas force (/BW) and impulse (/BW) of the residual limb hip for an individual with through-knee amputation (participant 03), and the maximum iliopsoas force (/BW) over the six trials of baseline treadmill walking and walking while following 'extension goal'. P values displayed.

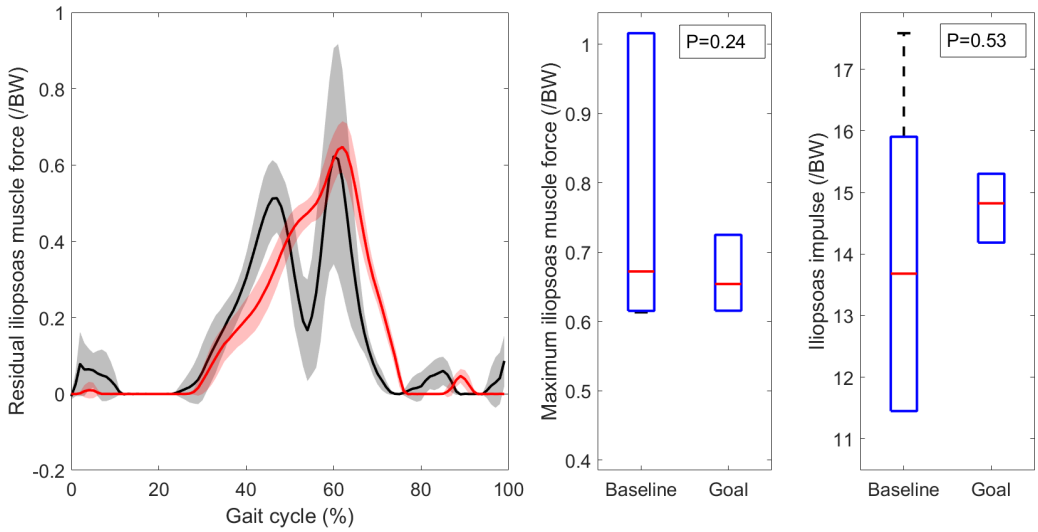


Figure F.2: Iliopsoas force (/BW) and impulse (/BW) of the residual limb hip for an individual with through-knee amputation (participant 05), and the maximum iliopsoas force (/BW) over the six trials of baseline treadmill walking and walking while following 'extension goal'. P values displayed.

Appendix G

Chapter 5: Iliospoas force following 'step goal' - participants 03, 05 and 06

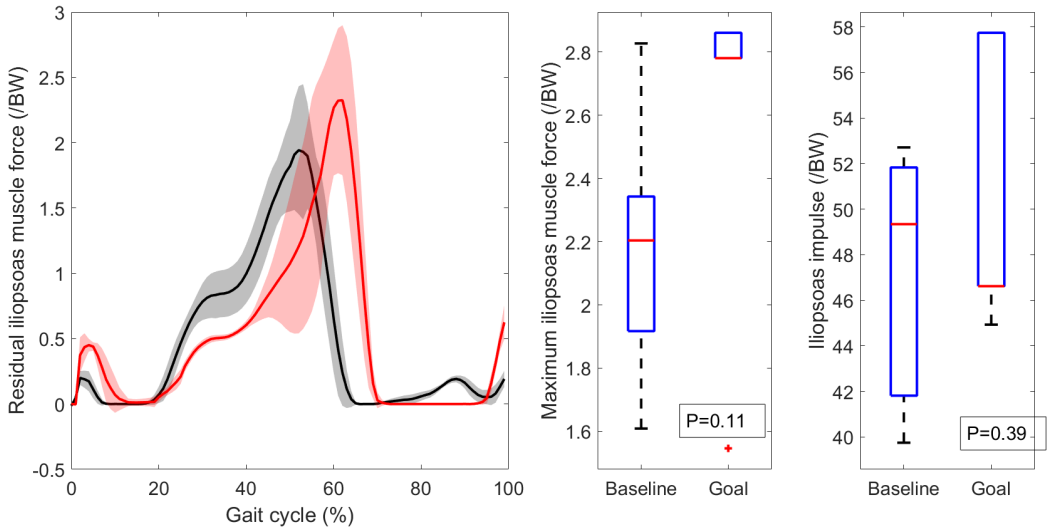


Figure G.1: Iliopsoas force (/BW) and impulse (/BW) of the residual limb hip for an individual with through-knee amputation (participant 03), and the maximum iliopsoas force (/BW) over the six trials of baseline treadmill walking and walking while following 'step goal'. P values displayed.

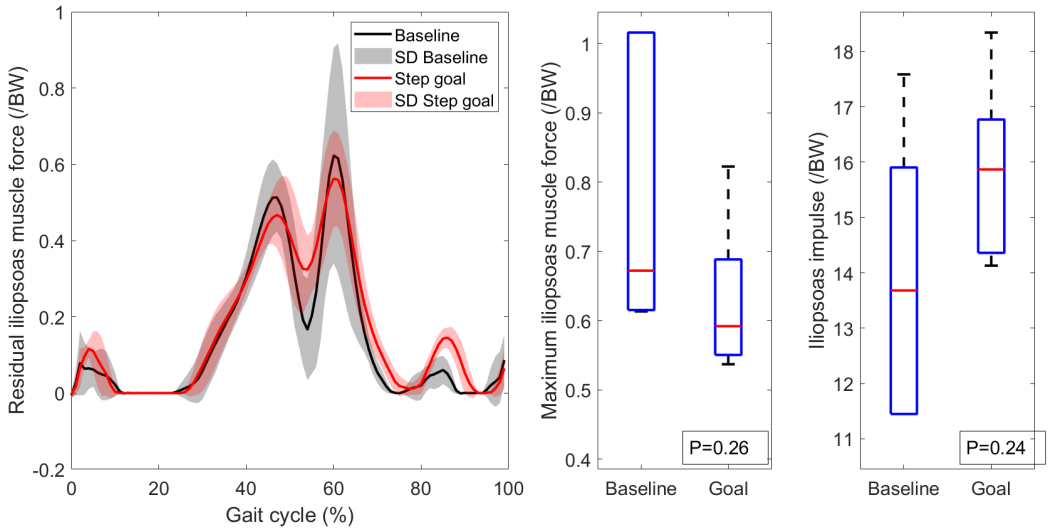


Figure G.2: Iliopsoas force (/BW) and impulse (/BW) of the residual limb hip for an individual with through-knee amputation (participant 05), and the maximum iliopsoas force (/BW) over the six trials of baseline treadmill walking and walking while following 'step goal'. P values displayed.

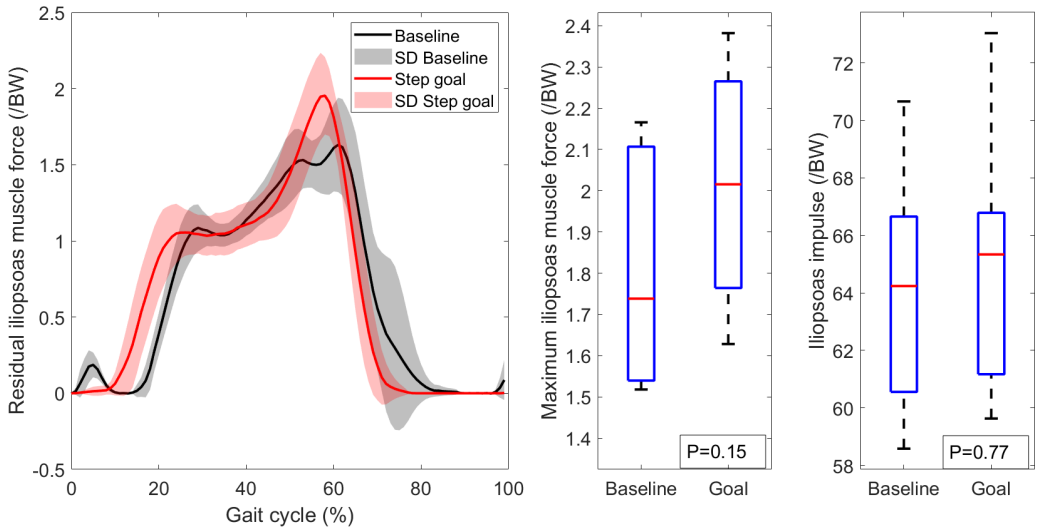


Figure G.3: Iliopsoas force (/BW) and impulse (/BW) of the residual limb hip for an individual with through-knee amputation (participant 06), and the maximum iliopsoas force (/BW) over the six trials of baseline treadmill walking and walking while following 'step goal'. P values displayed.

Appendix H

List of publications and conference presentations

H.1 List of publications

Benton, A. M., Amiri, P., Henson, D. P., Sivapuratharasu, B., Mcgregor, A. H. & Bull, A. M. 2023. Characterization of muscle recruitment during gait of bilateral transfemoral and through-knee persons with limb loss. Frontiers in bioengineering and biotechnology, 11, 438.

Benton, A. M., Toderita, D., Egginton, N. L., Liu, S., Amiri, P., Sherman, K., Bennett, A. N. & Bull, A. M. 2024. Muscle recruitment during gait in individuals with unilateral transfemoral amputation due to trauma compared to able-bodied controls. Frontiers in bioengineering and biotechnology, 12, 1429574.

H.2 List of conference presentations

Gait requires elevated muscle activation of the hip flexors in the residual limb of unilateral transfemoral and through-knee amputees. A M Benton, P Amiri, A. M J Bull. International Society of Prosthetics and Orthotics (ISPO) Congress, Mexico, 2023.

Characterization of the muscular overloading experienced by bilateral trans-femoral/ through-knee amputees during gait to inform the development of a functional electrical stimulation-based rehabilitation intervention. A M Benton, P Amiri, A. M J Bull. BioMedEng22, London, 2022 (presented on my behalf).

Characterizing the overloading of the residual musculoskeletal system during gait of bilateral transfemoral and through-knee amputees. A M Benton, P Amiri, A. M J Bull. The World Congress of Biomechanics (WCB), Taiwan, 2022.

References

Aerts, P. & Clercq, D. D. (1993), 'Deformation characteristics of the heel region of the shod foot during a simulated heel strike: the effect of varying midsole hardness', *Journal of Sports Sciences* **11**(5), 449–461.

Amann, M. & Dempsey, J. A. (2008), 'Locomotor muscle fatigue modifies central motor drive in healthy humans and imposes a limitation to exercise performance', *The Journal of Physiology* **586**(1), 161–173.

Amiri, P. & Bull, A. M. (2022), 'Prediction of in vivo hip contact forces during common activities of daily living using a segment-based musculoskeletal model', *Frontiers in Bioengineering and Biotechnology* **10**.

Amiri, P., Hubley-Kozey, C., Landry, S., Stanish, W. & Wilson, J. A. (2015), 'Obesity is associated with prolonged activity of the quadriceps and gastrocnemii during gait', *Journal of Electromyography and Kinesiology* **25**(6), 951–958.

Amudhan, K., Vasanthanathan, A. & Anish Jafrin Thilak, J. (2022), 'An insight into transfemoral prostheses: Materials, modelling, simulation, fabrication, testing, clinical evaluation and performance perspectives', *Expert Review of Medical Devices* **19**(2), 123–140.

Anderson, D. E. & Madigan, M. L. (2014), 'Healthy older adults have insufficient hip range of motion and plantar flexor strength to walk like healthy young adults', *Journal of Biomechanics* **47**(5), 1104–1109.

Anderson, F. C. & Pandy, M. G. (2001), 'Static and dynamic optimization solutions for gait are practically equivalent', *Journal of Biomechanics* **34**(2), 153–161.

Au, S. K. & Herr, H. M. (2008), 'Powered ankle-foot prosthesis', *IEEE Robotics & Automation Magazine* **15**(3), 52–59.

Barbieri, F. A., dos Santos, P. C. R., Vitório, R., van Dieën, J. H. & Gobbi, L. T. B. (2013), 'Effect of muscle fatigue and physical activity level in motor control of the gait of young adults', *Gait & Posture* **38**(4), 702–707.

Bell, J. C., Wolf, E. J., Schnall, B. L., Tis, J. E. & Potter, B. K. (2014), 'Transfemoral amputations: is there an effect of residual limb length and orientation on energy expenditure?', *Clinical Orthopaedics and Related Research®* **472**(10), 3055–3061.

Bemben, M. G., Massey, B. H., Bemben, D. A., Misner, J. E. & Boileau, R. A. (1996), 'Isometric intermittent endurance of four muscle groups in men aged 20-74 yr', *Medicine and Science in Sports and Exercise* **28**(1), 145–154.

Bianco, N. A., Collins, S. H., Liu, K. & Delp, S. L. (2023), 'Simulating the effect of ankle plantarflexion and inversion-eversion exoskeleton torques on center of mass kinematics during walking', *PLoS Computational Biology* **19**(8), e1010712.

Bishop, D. J. (2012), 'Fatigue during intermittent-sprint exercise', *Clinical and Experimental Pharmacology and Physiology* **39**(9), 836–841.

Bogdanis, G. C. (2012), 'Effects of physical activity and inactivity on muscle fatigue', *Frontiers in Physiology* **3**, 142.

Bovi, G., Rabuffetti, M., Mazzoleni, P. & Ferrarin, M. (2011), 'A multiple-task gait analysis approach: kinematic, kinetic and emg reference data for healthy young and adult subjects', *Gait & Posture* **33**(1), 6–13.

Brandt, A., Riddick, W., Stallrich, J., Lewek, M. & Huang, H. H. (2019), 'Effects of extended powered knee prosthesis stance time via visual feedback on gait symmetry of individuals with unilateral amputation: a preliminary study', *Journal of Neuroengineering and Rehabilitation* **16**, 1–12.

Brodie, M., Murray, L. & McGarry, A. (2022), 'Transfemoral prosthetic socket designs: a review of the literature', *JPO: Journal of Prosthetics and Orthotics* **34**(2), e73–e92.

Burden, A., Trew, M. & Baltzopoulos, V. (2003), 'Normalisation of gait emgs: a re-examination', *Journal of Electromyography and Kinesiology* **13**(6), 519–532.

Carloni, R., Luinge, R. & Raveendranathan, V. (2024), 'The gait1415+ 2 opensim musculoskeletal model of transfemoral amputees with a generic bone-anchored prosthesis', *Medical Engineering & Physics* **123**, 104091.

Carse, B., Scott, H., Brady, L. & Colvin, J. (2020), 'A characterisation of established unilateral transfemoral amputee gait using 3d kinematics, kinetics and oxygen consumption measures', *Gait & Posture* **75**, 98–104.

Charlton, J. M., Eng, J. J., Li, L. C. & Hunt, M. A. (2021), 'Learning gait modifications for musculoskeletal rehabilitation: applying motor learning principles to improve research and clinical implementation', *Physical therapy* **101**(2), pzaa207.

Chien, M. C.-H., Erdemir, A., van den Bogert, A. J. & Smith, W. A. (2014), 'Development of dynamic models of the mauch prosthetic knee for prospective gait simulation', *Journal of Biomechanics* **47**(12), 3178–3184.

Chin, T., Sawamura, S., Shiba, R., Oyabu, H., Nagakura, Y., Takase, I., Machida, K. & Nakagawa, A. (2003), 'Effect of an intelligent prosthesis (ip) on the walking ability of young transfemoral amputees: comparison of ip users with able-bodied people', *American Journal of Physical Medicine & Rehabilitation* **82**(6), 447–451.

Chui, K. K., Jorge, M., Yen, S.-C. & Lusardi, M. M. (2019), *Orthotics and Prosthetics in Rehabilitation E-Book: Orthotics and Prosthetics in Rehabilitation E-Book*, Elsevier Health Sciences. ISBN: 0323610188.

Cleather, D. J. & Bull, A. M. (2011), 'An optimization-based simultaneous approach to the determination of muscular, ligamentous, and joint contact forces provides insight into musculoligamentous interaction', *Annals of Biomedical Engineering* **39**(7), 1925–1934.

Cleather, D. J. & Bull, A. M. (2015), 'The development of a segment-based musculoskeletal model of the lower limb: introducing freebody', *Royal Society open science* **2**(6), 140449.

Crowninshield, R. D. & Brand, R. A. (1981), 'A physiologically based criterion of muscle force prediction in locomotion', *Journal of Biomechanics* **14**(11), 793–801.

Cullen, D., Boyle, J., Silbert, P., Singer, B. & Singer, K. (2007), 'Botulinum toxin injection to facilitate rehabilitation of muscle imbalance syndromes in sports medicine', *Disability and Rehabilitation* **29**(23), 1832–1839.

De Groote, F., Kinney, A. L., Rao, A. V. & Fregly, B. J. (2016), 'Evaluation of direct collocation optimal control problem formulations for solving the muscle redundancy problem', *Annals of Biomedical Engineering* **44**(10), 2922–2936.

De Leva, P. (1996), 'Adjustments to zatsiorsky-seluyanov's segment inertia parameters', *Journal of Biomechanics* **29**(9), 1223–1230.

De Luca, C. J., Gilmore, L. D., Kuznetsov, M. & Roy, S. H. (2010), 'Filtering the surface emg signal: Movement artifact and baseline noise contamination', *Journal of Biomechanics* **43**(8), 1573–1579.

De Vree, L. & Carloni, R. (2021), 'Deep reinforcement learning for physics-based musculoskeletal simulations of healthy subjects and transfemoral prostheses' users during normal walking', *IEEE Transactions on Neural Systems and Rehabilitation Engineering* **29**, 607–618.

Dembia, C. L., Bianco, N. A., Falisse, A., Hicks, J. L. & Delp, S. L. (2020), 'Opensim moco: musculoskeletal optimal control', *PLOS Computational Biology* **16**(12), e1008493.

Detrembleur, C., Vanmarsenille, J.-M., De Cuyper, F. & Dierick, F. (2005), 'Relationship between energy cost, gait speed, vertical displacement of centre of body mass and efficiency of pendulum-like mechanism in unilateral amputee gait', *Gait & Posture* **21**(3), 333–340.

Devan, H., Hendrick, P., Ribeiro, D. C., Hale, L. A. & Carman, A. (2014), 'Asymmetrical movements of the lumbopelvic region: is this a potential mechanism for low back pain in people with lower limb amputation?', *Medical hypotheses* **82**(1), 77–85.

Ding, Z., Henson, D., Sivapuratharasu, B., McGregor, A. & Bull, A. (2023), 'The effect of muscle atrophy in people with unilateral transtibial amputation for three activities: gait alone does not tell the whole story', *Journal of Biomechanics* p. 111484.

Ding, Z., Jarvis, H. L., Bennett, A. N., Baker, R. & Bull, A. M. (2021), 'Higher knee contact forces might underlie increased osteoarthritis rates in high functioning amputees: A pilot study', *Journal of Orthopaedic Research®* **39**(4), 850–860.

Ding, Z., Nolte, D., Kit Tsang, C., Cleather, D. J., Kedgley, A. E. & Bull, A. M. (2016), 'In vivo knee contact force prediction using patient-specific musculoskeletal geometry in a segment-based computational model', *Journal of Biomechanical Engineering* **138**(2), 021018.

Ding, Z., Tsang, C. K., Nolte, D., Kedgley, A. E. & Bull, A. M. (2019), 'Improving musculoskeletal model scaling using an anatomical atlas: the importance of gender and anthropometric similarity to quantify joint reaction forces', *IEEE Transactions on Biomedical Engineering* **66**(12), 3444–3456.

Donahue, S., Kingsbury, T., Takahashi, K. & Major, M. J. (2024), 'Data-driven modeling of the nonlinear dynamics of passive lower-limb prosthetic systems', *Journal of Mechanisms and Robotics* **16**(8), 081012.

Dumas, R., Aissaoui, R. & de Guise, J. A. (2004), 'A 3d generic inverse dynamic method using wrench notation and quaternion algebra', *Computer methods in Biomechanics and Biomedical engineering* **7**(3), 159–166.

Edd, S. N., Bennour, S., Ulrich, B., Jolles, B. M. & Favre, J. (2020), 'Modifying stride length in isolation and in combination with foot progression angle and step width can improve knee kinetics related to osteoarthritis; a preliminary study in healthy subjects', *Journal of Biomechanical Engineering* **142**(7), 074505.

Edwards, D., Phillip, R. D., Bosanquet, N., Bull, A. M. & Clasper, J. C. (2015), 'What is the magnitude and long-term economic cost of care of the british military afghanistan amputee cohort?', *Clinical Orthopaedics and Related Research®* **473**(9), 2848–2855.

Elery, T., Rezazadeh, S., Reznick, E., Gray, L. & Gregg, R. D. (2020), 'Effects of a powered knee-ankle prosthesis on amputee hip compensations: A case series', *IEEE Transactions on Neural Systems and Rehabilitation Engineering* **28**(12), 2944–2954.

Elsais, W. M., Preece, S. J., Jones, R. K. & Herrington, L. (2020), 'Between-day repeatability of lower limb emg measurement during running and walking', *Journal of Electromyography and Kinesiology* **55**, 102473.

Escamilla-Nunez, R., Michelini, A. & Andrysek, J. (2020), 'Biofeedback systems for gait rehabilitation of individuals with lower-limb amputation: a systematic review', *Sensors* **20**(6), 1628.

Fabre, I., Thompson, D., Gwilym, B., Jones, K., Pinzur, M., Geertzen, J. H., Twine, C. & Bosanquet, D. (2024), 'Surgical techniques of, and outcomes after, distal muscle stabilization in transfemoral amputation: A systematic review and narrative synthesis', *Annals of Vascular Surgery* **98**, 182–193.

Falisse, A., Van Rossom, S., Gijsbers, J., Steenbrink, F., van Basten, B. J., Jonkers, I., van den Bogert, A. J. & De Groote, F. (2018), 'Opensim versus human body model: a comparison study for the lower limbs during gait', *Journal of Applied Biomechanics* **34**(6), 496–502.

Fang, L., Jia, X. & Wang, R. (2007), 'Modeling and simulation of muscle forces of trans-tibial amputee to study effect of prosthetic alignment', *Clinical Biomechanics* **22**(10), 1125–1131.

Farrokhi, S., Mazzone, B., Eskridge, S., Shannon, K. & Hill, O. T. (2018), 'Incidence of overuse musculoskeletal injuries in military service members with traumatic lower limb amputation', *Archives of Physical Medicine and Rehabilitation* **99**(2), 348–354. e1.

Fidalgo-Herrera, A., Miangolarra-Page, J. & Carratalá-Tejada, M. (2022), 'Traces of muscular fatigue in the rectus femoris identified with surface electromyography and wavelets on normal gait', *Physiotherapy Theory and Practice* **38**(1), 211–225.

Fougeron, N., Bonnet, X., Panhelleux, B., Rose, J.-L., Rohan, P.-Y. & Pillet, H. (2020), 'Prediction of muscle forces in residual limb during walking: comparison of transfemoral and gritti–stokes amputations', *Computer Methods in Biomechanics and Biomedical Engineering* **23**(sup1), S107–S109.

Fougeron, N., Rohan, P.-Y., Rose, J.-L., Bonnet, X. & Pillet, H. (2022), 'Finite element analysis of the stump-ischial containment socket interaction: a technical note', *Medical Engineering & Physics* **105**, 103829.

Fraisse, N., Martinet, N., Kpadonou, T., Paysant, J., Blum, A. & André, J. (2008), Les muscles de l'amputé tibial muscles of the below-knee amputees, *in* 'Annales de réadaptation et de médecine physique', Vol. 51, pp. 218–227.

Franz, J. R. & Kram, R. (2013), 'How does age affect leg muscle activity/coactivity during uphill and downhill walking?', *Gait & Posture* **37**(3), 378–384.

Gaffney, B. M., Davis-Wilson, H. C., Christiansen, C. L., Awad, M. E., Lev, G., Tracy, J. & Stoneback, J. W. (2023), 'Osseointegrated prostheses improve balance and balance confidence in individuals with unilateral transfemoral limb loss', *Gait & Posture* **100**, 132–138.

Gailey, R., Allen, K., Castles, J., Kucharik, J. & Roeder, M. (2008), 'Review of secondary physical conditions associated with lower-limb amputation and long-term prosthesis use', *Journal of Rehabilitation Research & Development* **45**(1).

Gale, T., Yang, S., McGough, R., Fiedler, G. & Anderst, W. (2020), 'Motion of the residual femur within the socket during gait is associated with patient-reported problems in transfemoral amputees', *Journal of Biomechanics* **112**, 110050.

Gehlhar, R., Tucker, M., Young, A. J. & Ames, A. D. (2023), 'A review of current state-of-the-art control methods for lower-limb powered prostheses', *Annual Reviews in Control* .

Geijtenbeek, T. (2019), 'Scone: Open source software for predictive simulation of biological motion', *Journal of Open Source Software* **4**(38), 1421.

Geijtenbeek, T. (2021). Last accessed November 2024.
URL: *https://hyfydy.com/*

Gottschalk, F. (1999), 'Transfemoral amputation: biomechanics and surgery', *Clinical Orthopaedics and Related Research®* **361**, 15–22.

Gottschalk, F. & Stills, M. (1994), 'The biomechanics of trans-femoral amputation', *Prosthetics and Orthotics International* **18**(1), 12–17.

Gracies, J.-M., Singer, B. J. & Dunne, J. W. (2007), 'The role of botulinum toxin injections in the management of muscle overactivity of the lower limb', *Disability and Rehabilitation* **29**(23), 1789–1805.

Griffin, T. M., Roberts, T. J. & Kram, R. (2003), 'Metabolic cost of generating muscular force in human walking: insights from load-carrying and speed experiments', *Journal of Applied Physiology* **95**(1), 172–183.

Guan, X., Kuai, S., Song, L., Liu, W., Liu, Y., Ji, L. & Wang, R. (2019), 'Effects of ankle joint motion on pelvis-hip biomechanics and muscle activity patterns of healthy individuals in knee immobilization gait', *Journal of Healthcare Engineering* **2019**.

Gupta, D., Donnelly, C. J. & Reinbolt, J. A. (2022), 'Finding emergent gait patterns may reduce progression of knee osteoarthritis in a clinically relevant time frame', *Life* **12**(7), 1050.

Göktepe, A. S., Cakir, B., Yilmaz, B. & Yazicioglu, K. (2010), 'Energy expenditure of walking with prostheses: comparison of three amputation levels', *Prosthetics and orthotics international* **34**(1), 31–36.

Hahn, M. E., Lee, H.-J. & Chou, L.-S. (2005), 'Increased muscular challenge in older adults during obstructed gait', *Gait & Posture* **22**(4), 356–361.

Handsfield, G. G., Meyer, C. H., Hart, J. M., Abel, M. F. & Blemker, S. S. (2014), 'Relationships of 35 lower limb muscles to height and body mass quantified using mri', *Journal of Biomechanics* **47**(3), 631–638.

Harandi, V. J., Ackland, D. C., Haddara, R., Lizama, L. E. C., Graf, M., Galea, M. P. & Lee, P. V. S. (2020), 'Gait compensatory mechanisms in unilateral transfemoral amputees', *Medical Engineering & Physics* **77**, 95–106.

Henson, D. P., Edgar, C., Ding, Z., Sivapuratharasu, B., Le Feuvre, P., Finnegan, M. E., Quest, R., McGregor, A. H. & Bull, A. M. (2021), 'Understanding lower limb muscle volume adaptations to amputation', *Journal of Biomechanics* **125**, 110599.

Hicks, J. L. (2018), 'Getting started with inverse kinematics'. Last accessed November 2024.
URL: *https://opensimconfluence.atlassian.net/wiki/spaces/OpenSim/pages/53090032/Getting+Started+with+Inverse+Kinematics*

Hicks, J. L., Uchida, T. K., Seth, A., Rajagopal, A. & Delp, S. L. (2015), 'Is my model good enough? best practices for verification and validation of musculoskeletal models and simulations of movement', *Journal of Biomechanical Engineering* **137**(2).

Hirokawa, S. & Matsumura, K. (1989), 'Biofeedback gait training system for temporal and distance factors', *Medical and Biological Engineering and Computing* **27**, 8–13.

Hoffman, M. D., Sheldahl, L. M., Buley, K. J. & Sandford, P. R. (1997), 'Physiological comparison of walking among bilateral above-knee amputee and able-bodied subjects, and a model to account for the differences in metabolic cost', *Archives of physical medicine and rehabilitation* **78**(4), 385–392.

Horsman, M. K., Koopman, H. F., van der Helm, F. C., Prosé, L. P. & Veeger, H. (2007), 'Morphological muscle and joint parameters for musculoskeletal modelling of the lower extremity', *Clinical Biomechanics* **22**(2), 239–247.

Hortobágyi, T., Finch, A., Solnik, S., Rider, P. & DeVita, P. (2011), 'Association between muscle activation and metabolic cost of walking in young and old adults', *Journals of Gerontology Series A: Biomedical Sciences and Medical Sciences* **66**(5), 541–547.

Hortobágyi, T., Mizelle, C., Beam, S. & DeVita, P. (2003), 'Old adults perform activities of daily living near their maximal capabilities', *The Journals of Gerontology Series A: Biological Sciences and Medical Sciences* **58**(5), M453–M460.

Hunt, G. R., Hood, S., Gabert, L. & Lenzi, T. (2022), 'Effect of increasing assistance from a powered prosthesis on weight-bearing symmetry, effort, and speed during stand-up in individuals with above-knee amputation', *IEEE Transactions on Neural Systems and Rehabilitation Engineering* **31**, 11–21.

Ishmael, M. K., Archangeli, D. & Lenzi, T. (2021), 'Powered hip exoskeleton improves walking economy in individuals with above-knee amputation', *Nature Medicine* **27**(10), 1783–1788.

Jaegers, S. M., Arendzen, J. H. & de Jongh, H. J. (1995), 'Changes in hip muscles after above-knee amputation', *Clinical Orthopaedics and Related Research®* **319**, 276–284.

Jarvis, H. L., Bennett, A. N., Twiste, M., Phillip, R. D., Etherington, J. & Baker, R. (2017), 'Temporal spatial and metabolic measures of walking in highly functional individuals with lower limb amputations', *Archives of Physical Medicine and Rehabilitation* **98**(7), 1389–1399.

Jarvis, H. L., Reeves, N. D., Twiste, M., Phillip, R. D., Etherington, J. & Bennett, A. N. (2021), 'Can high-functioning amputees with state-of-the-art prosthetics walk normally? a kinematic and dynamic study of 40 individuals', *Annals of Physical and Rehabilitation Medicine* **64**(1), 101395.

Jie, L.-J., Kleynen, M., Meijer, K., Beurskens, A. & Braun, S. (2018), 'The effects of implicit and explicit motor learning in gait rehabilitation of people after stroke: protocol for a randomized controlled trial', *JMIR research protocols* **7**(5), e9595.

Johnson, R. T., Bianco, N. A. & Finley, J. M. (2022), 'Patterns of asymmetry and energy cost generated from predictive simulations of hemiparetic gait', *PLoS Computational Biology* **18**(9), e1010466.

Jonsdottir, J., Cattaneo, D., Recalcati, M., Regola, A., Rabuffetti, M., Ferrarin, M. & Casiraghi, A. (2010), 'Task-oriented biofeedback to improve gait in individuals with chronic stroke: motor learning approach', *Neurorehabilitation and Neural Repair* **24**(5), 478–485.

Jorge, M. (2020), *Orthotics and prosthetics in rehabilitation*, Elsevier.

Katsavrias, E., Primetis, E. & Karandreas, N. (2005), 'Iliopsoas: a new electromyographic technique and normal motor unit action potential values', *Clinical Neurophysiology* **116**(11), 2528–2532.

Kaur, Y., Cimino, S. R., Albarico, M., Mayo, A. L., Guilcher, S. J., Robinson, L. R., Hanada, E. & Hitzig, S. L. (2021), 'Physical function outcomes in patients with lower-limb amputations due to trauma: a systematic review', *JPO: Journal of Prosthetics and Orthotics* **33**(2), 88–95.

Keeves, J., Hutchison, A., D'Cruz, K. & Anderson, S. (2023), 'Social and community participation following traumatic lower limb amputation: an exploratory qualitative study', *Disability and Rehabilitation* **45**(26), 4404–4412.

Kell, R. T., Bell, G. & Quinney, A. (2001), 'Musculoskeletal fitness, health outcomes and quality of life', *Sports Medicine* **31**(12), 863–873.

Kelly, M. (2017), 'An introduction to trajectory optimization: How to do your own direct collocation', *SIAM Review* **59**(4), 849–904.

Killen, B. A., Falisse, A., De Groote, F. & Jonkers, I. (2020), 'In silico-enhanced treatment and rehabilitation planning for patients with musculoskeletal disorders: can musculoskeletal modelling and dynamic simulations really impact current clinical practice?', *Applied Sciences* **10**(20), 7255.

Klemt, C., Nolte, D., Ding, Z., Rane, L., Quest, R. A., Finnegan, M. E., Walker, M., Reilly, P. & Bull, A. M. (2019), 'Anthropometric scaling of anatomical datasets for subject-specific musculoskeletal modelling of the shoulder', *Annals of Biomedical Engineering* **47**, 924–936.

Knight, A. D., Jayaraman, C., Elrod, J. M., Schnall, B. L., McGuire, M. S., Sleeman, T. J., Hoppe-Ludwig, S., Dearth, C. L., Hendershot, B. D. & Jayaraman, A. (2023), 'Functional performance outcomes of a powered knee–ankle prosthesis in service members with unilateral transfemoral limb loss', *Military Medicine* **188**(11-12), 3432–3438.

Komura, T., Prokopow, P. & Nagano, A. (2004), 'Evaluation of the influence of muscle deactivation on other muscles and joints during gait motion', *Journal of Biomechanics* **37**(4), 425–436.

Kumar, S. (2001), 'Theories of musculoskeletal injury causation', *Ergonomics* **44**(1), 17–47.

Ladlow, P., Phillip, R., Etherington, J., Coppack, R., Bilzon, J., McGuigan, M. P. & Bennett, A. N. (2015), 'Functional and mental health status of united kingdom military amputees postrehabilitation', *Archives of Physical Medicine and rehabilitation* **96**(11), 2048–2054.

Lam, W., Maxwell, J. & Masters, R. (2009), 'Analogy versus explicit learning of a modified basketball shooting task: Performance and kinematic outcomes', *Journal of sports sciences* **27**(2), 179–191.

LaPrè, A., Price, M., Wedge, R., Umberger, B. & Sup IV, F. C. (2018), 'Approach for gait analysis in persons with limb loss including residuum and prosthesis socket dynamics', *International Journal for Numerical Methods in Biomedical Engineering* **34**(4), e2936.

Lee, V., Solomonidis, S. & Spence, W. (1997), 'Stump-socket interface pressure as an aid to socket design in prostheses for trans-femoral amputees—a preliminary study', *Proceedings of the Institution of Mechanical Engineers, Part H: Journal of Engineering in Medicine* **211**(2), 167–180.

Lewis, C. L., Sahrmann, S. A. & Moran, D. W. (2010), 'Effect of hip angle on anterior hip joint force during gait', *Gait & posture* **32**(4), 603–607.

Lieber, R. L., Loren, G. J. & Friden, J. (1994), 'In vivo measurement of human wrist extensor muscle sarcomere length changes', *Journal of Neurophysiology* **71**(3), 874–881.

Lin, Y.-C. & Pandy, M. G. (2017), 'Three-dimensional data-tracking dynamic optimization simulations of human locomotion generated by direct collocation', *Journal of Biomechanics* **59**, 1–8.

Linberg, A. A., Roach, K. E., Campbell, S. M., Stoneman, P. D., Gaunaurd, I. A., Raya, M. A., Gomez-Orozco, C. & Gailey, R. S. (2013), 'Comparison of 6-minute walk test performance between male active duty soldiers and servicemembers with and without traumatic lowerlimb loss', *Journal of Rehabilitation Research & Development* **50**(7).

Lindner, H., Montgomery, S. & Hiyoshi, A. (2020), 'Risk of depression following traumatic limb amputation—a general population-based cohort study', *Scandinavian Journal of Public health* **48**(3), 289–293.

Long, M. J., Papi, E., Duffell, L. D. & McGregor, A. H. (2017), 'Predicting knee osteoarthritis risk in injured populations', *Clinical biomechanics* **47**, 87–95.

Maldonado-Contreras, J., Marayong, P., Khoo, I.-H., Rivera, R., Ruhe, B. & Wu, W. (2017), Proprioceptive improvements of lower-limb amputees under training with a vibrotactile device—a pilot study, *in* '2017 IEEE Healthcare Innovations and Point of Care Technologies (HI-POCT)', IEEE, pp. 229–232.

Mazzone, B., Farrokhi, S., Hendershot, B. D., McCabe, C. T. & Watrous, J. R. (2020), 'Prevalence of low back pain and relationship to mental health symptoms and quality of life after a deployment-related lower limb amputation', *Spine* **45**(19), 1368–1375.

McDonald, C. L., Westcott-McCoy, S., Weaver, M. R., Haagsma, J. & Kartin, D. (2021), 'Global prevalence of traumatic non-fatal limb amputation', *Prosthetics and Orthotics international* p. 0309364620972258.

Mckechnie, P. & John, A. (2014), 'Anxiety and depression following traumatic limb amputation: a systematic review', *Injury* **45**(12), 1859–1866.

McMenemy, L., Behan, F. P., Kaufmann, J., Cain, D., Bennett, A. N., Boos, C. J., Fear, N. T., Cullinan, P., Bull, A. M. & Phillips, A. T. (2023), 'Association between combat-related traumatic injury and skeletal health: Bone mineral density loss is localized and correlates with altered loading in amputees: the armed services trauma rehabilitation outcome (advance) study', *Journal of Bone and Mineral Research* **38**(9), 1227–1233.

McNealy, L. L. & Gard, S. (2008), 'Effect of prosthetic ankle units on the gait of persons with bilateral trans-femoral amputations', *Prosthetics and Orthotics international* **32**(1), 111–126.

Mehryar, P., Shourijeh, M. S., Rezaeian, T., Khandan, A. R., Messenger, N., O'Connor, R., Farahmand, F. & Dehghani-Sanij, A. (2021), 'Muscular activity comparison between non-amputees and transfemoral amputees during normal transient-state walking speed', *Medical Engineering & Physics* **95**, 39–44.

Miller, R. H., Bell, E. M. & Russell Esposito, E. (2023), 'Transfemoral limb loss modestly increases the metabolic cost of optimal control simulations of walking', *bioRxiv* p. 2023.06. 26.546515.

Miller, R. H. & Esposito, E. R. (2021), 'Transtibial limb loss does not increase metabolic cost in three-dimensional computer simulations of human walking', *PeerJ* **9**, e11960.

Milosevic, S., Strange, H., Morgan, M., Ambler, G. K., Bosanquet, D. C., Waldron, C.-A., Thomas-Jones, E., Harris, D., Twine, C. P. & Brookes-Howell, L. (2024), 'Rehabilitation experiences following major lower limb amputation due to complications of vascular disease: a uk qualitative study', *Disability and Rehabilitation* pp. 1–10.

Mohd Safee, M. K. & Abu Osman, N. A. (2021), 'Effect of lower limb muscle fatigue on fall risk for transfemoral amputee: a pilot study', *Occupational therapy international* **2021**.

Motek (2024). Last accessed Novemeber 2024.
URL: *https://www.motekmedical.com/software/hbm/get-inspired*

Moxey, P. W., Hofman, D., Hinchliffe, R., Jones, K., Thompson, M. & Holt, P. (2010), 'Epidemiological study of lower limb amputation in england between 2003 and 2008', *Journal of British Surgery* **97**(9), 1348–1353.

Narang, Y. S., Arelekatti, V. M. & Winter, A. G. (2015), 'The effects of prosthesis inertial properties on prosthetic knee moment and hip energetics required to achieve able-bodied kinematics', *IEEE Transactions on Neural Systems and Rehabilitation Engineering* **24**(7), 754–763.

Neumann, D. A. (2010), 'Kinesiology of the hip: a focus on muscular actions', *Journal of Orthopaedic & Sports Physical Therapy* **40**(2), 82–94.

NHS-England (2016), Clinical commissioning policy: Microprocessor controlled prosthetic knees, Report, NHS England.

Nishijima, Y., Kato, T., Yoshizawa, M., Miyashita, M. & Iida, H. (2010), 'Application of the segment weight dynamic movement method to the normalization of gait emg amplitude', *Journal of Electromyography and Kinesiology* **20**(3), 550–557.

Ogum, B. N., Schomaker, L. R. & Carloni, R. (2024), 'Learning to walk with deep reinforcement learning: Forward dynamic simulation of a physics-based musculoskeletal model of an osseointegrated transfemoral amputee', *IEEE Transactions on Neural Systems and Rehabilitation Engineering* .

Ostraich, B. & Riemer, R. (2024), 'Rethinking exoskeleton simulation-based design: The effect of using different cost functions', *IEEE Transactions on Neural Systems and Rehabilitation Engineering* .

Pariser, K. M. & Higginson, J. S. (2022), 'Development and validation of a framework for predictive simulation of treadmill gait', *Journal of Biomechanical Engineering* **144**(11), 114505.

Pataky, T. C., Robinson, M. A. & Vanrenterghem, J. (2013), 'Vector field statistical analysis of kinematic and force trajectories', *Journal of Biomechanics* **46**(14), 2394–2401.

Pickle, N. T., Grabowski, A. M., Jeffers, J. R. & Silverman, A. K. (2017), 'The functional roles of muscles, passive prostheses, and powered prostheses during sloped walking in people with a transtibial amputation', *Journal of Biomechanical Engineering* **139**(11), 111005.

Porsa, S., Lin, Y.-C. & Pandy, M. G. (2016), 'Direct methods for predicting movement biomechanics based upon optimal control theory with implementation in opensim', *Annals of Biomedical Engineering* **44**(8), 2542–2557.

Pritham, C. (1990), 'Biomechanics and shape of the above-knee socket considered in light of the ischial containment concept', *Prosthetics and orthotics international* **14**(1), 9–21.

Putz, C., Block, J., Gantz, S., Heitzmann, D., Dreher, T., Lehner, B., Alimusaj, M., Wolf, S. & Müller, S. (2017), 'Structural changes in the thigh muscles following trans-femoral amputation', *European Journal of Orthopaedic Surgery & Traumatology* **27**(6), 829–835.

Quiñones, I., Vela, E., Pérez, A., Alessi, A., Urrusti, J. & Cepeda, D. (2009), Biofeedback system for transfemoral amputees rehabilitation, *in* '2009 Pan American Health Care Exchanges', IEEE, pp. 148–152.

Radcliffe, C. W. (1955), *Functional considerations in the fitting of above-knee prostheses*, Biomechanics Laboratory, University of California.

Rajagopal, A., Dembia, C. L., DeMers, M. S., Delp, D. D., Hicks, J. L. & Delp, S. L. (2016), 'Full-body musculoskeletal model for muscle-driven simulation of human gait', *IEEE transactions on biomedical engineering* **63**(10), 2068–2079.

Rane, L. & Bull, A. M. J. (2016), 'Functional electrical stimulation of gluteus medius reduces the medial joint reaction force of the knee during level walking', *Arthritis Research & Therapy* **18**(1), 1–11.

Ranz, E. C., Wilken, J. M., Gajewski, D. A. & Neptune, R. R. (2017), 'The influence of limb alignment and transfemoral amputation technique on muscle capacity during gait', *Computer methods in BiomeChaniCs and BiomediCal engineering* **20**(11), 1167–1174.

Raveendranathan, V., Kooiman, V. G. & Carloni, R. (2023), 'Musculoskeletal model of osseointegrated transfemoral amputees in opensim', *Plos one* **18**(9), e0288864.

Requiao, L., Nadeau, S., Milot, M., Gravel, D., Bourbonnais, D. & Gagnon, D. (2005), 'Quantification of level of effort at the plantarflexors and hip extensors and flexor muscles in healthy subjects walking at different cadences', *Journal of Electromyography and Kinesiology* **15**(4), 393–405.

Riemer, R., Hsiao-Wecksler, E. T. & Zhang, X. (2008), 'Uncertainties in inverse dynamics solutions: a comprehensive analysis and an application to gait', *Gait & Posture* **27**(4), 578–588.

Russell Esposito, E., Choi, H. S., Darter, B. J. & Wilken, J. M. (2017), 'Can real-time visual feedback during gait retraining reduce metabolic demand for individuals with transtibial amputation?', *PLoS One* **12**(2), e0171786.

Sangeux, M. (2019), *Biomechanics of the Hip During Gait*, Springer, pp. 53–71.

Sawers, A. & Fatone, S. (2023), 'After scaling to body size hip strength of the residual limb exceeds that of the intact limb among unilateral lower limb prosthesis users', *Journal of NeuroEngineering and Rehabilitation* **20**(1), 1–12.

Sawers, A., Hahn, M. E., Kelly, V. E., Czerniecki, J. M. & Kartin, D. (2012), 'Beyond componentry: How principles of motor learning can enhance locomotor rehabilitation of individuals with lower limb loss-a review', *Journal of rehabilitation research and development* **49**(10), 1431.

Schmalz, T., Blumentritt, S. & Jarasch, R. (2002), 'Energy expenditure and biomechanical characteristics of lower limb amputee gait:: The influence of prosthetic alignment and different prosthetic components', *Gait & Posture* **16**(3), 255–263.

Schwartzman, G. & Ramamurti, P. (2021), 'Visible body human anatomy atlas: innovative anatomy learning', *Journal of Digital Imaging* **34**(5), 1328–1330.

Schwer, L. E. (2007), 'Validation metrics for response histories: perspectives and case studies', *Engineering with Computers* **23**(4), 295–309.

Seroussi, R. E., Gitter, A., Czerniecki, J. M. & Weaver, K. (1996), 'Mechanical work adaptations of above-knee amputee ambulation', *Archives of Physical Medicine and Rehabilitation* **77**(11), 1209–1214.

Sherk, V. D., Bemben, M. G. & Bemben, D. A. (2010), 'Interlimb muscle and fat comparisons in persons with lower-limb amputation', *Archives of Physical Medicine and Rehabilitation* **91**(7), 1077–1081.

Sherman, M. A., Seth, A. & Delp, S. L. (2011), 'Simbody: multibody dynamics for biomedical research', *Procedia Iutam* **2**, 241–261.

Shin, J. & Chung, Y. (2017), 'Influence of visual feedback and rhythmic auditory cue on walking of chronic stroke patient induced by treadmill walking in real-time basis', *NeuroRehabilitation* **41**(2), 445–452.

Sibley, A. R., Strike, S., Moudy, S. C. & Tillin, N. A. (2020), 'The effects of long-term muscle disuse on neuromuscular function in unilateral transtibial amputees', *Experimental Physiology* **105**(3), 408–418.

Silverman, A. K., Hendershot, B. D. & Mcgregor, A. H. (2023), *Musculoskeletal Health After Blast Injury*, Springer, pp. 489–497.

Sivapuratharasu, B., Bull, A. M. & McGregor, A. H. (2019), 'Understanding low back pain in traumatic lower limb amputees: a systematic review', *Archives of Rehabilitation Research and Clinical Translation* **1**(1-2), 100007.

Slater, L., Finucane, S. & Hargrove, L. J. (2022), 'Knee extensor power predicts six-minute walk test performance in people with transfemoral amputations', *PM&R* **14**(4), 445–451.

Smith, J. D., Ferris, A. E., Heise, G. D., Hinrichs, R. N. & Martin, P. E. (2014), 'Oscillation and reaction board techniques for estimating inertial properties of a below-knee prosthesis', *JoVE (Journal of Visualized Experiments)* **1**(87), e50977.

Smith, S. H., Coppack, R. J., van den Bogert, A. J., Bennett, A. N. & Bull, A. M. (2021), 'Review of musculoskeletal modelling in a clinical setting: Current use in rehabilitation design, surgical decision making and healthcare interventions', *Clinical Biomechanics* **83**, 105292.

Spencer, J., Wolf, S. L. & Kesar, T. M. (2021), 'Biofeedback for post-stroke gait retraining: a review of current evidence and future research directions in the context of emerging technologies', *Frontiers in Neurology* **12**, 637199.

Su, P.-F., Gard, S. A., Lipschutz, R. D. & Kuiken, T. A. (2007), 'Gait characteristics of persons with bilateral transtibial amputations', *Journal of rehabilitation research & development* **44**(4).

Suzuki, Y. (2010), 'Dynamic optimization of transfemoral prosthesis during swing phase with residual limb model', *Prosthetics and Orthotics International* **34**(4), 428–438.

Tatarelli, A., Serrao, M., Varrecchia, T., Fiori, L., Silvetti, A., De Marchis, C., Ranaldi, S., Draicchio, F., Conforto, S. & Ranavolo, A. (2020), Global lower limb muscle coactivation during walking in trans-femoral and trans-tibial amputees, *in* '2020 IEEE International Symposium on Medical Measurements and Applications (MeMeA)', IEEE, pp. 1–6.

Tate, J. J. & Milner, C. E. (2010), 'Real-time kinematic, temporospatial, and kinetic biofeedback during gait retraining in patients: a systematic review', *Physical therapy* **90**(8), 1123–1134.

Toderita, D., Henson, D., Klemt, C., Ding, Z. & Bull, A. M. (2021), 'An anatomical atlas-based scaling study for quantifying muscle and hip joint contact forces in above and through-knee amputees using validated musculoskeletal modelling', *IEEE Transactions on Biomedical Engineering* .

Todorov, E., Erez, T. & Tassa, Y. (2012), Mujoco: A physics engine for model-based control, *in* '2012 IEEE/RSJ international conference on intelligent robots and systems', IEEE, pp. 5026–5033.

Tzamaloukas, A. H., Patron, A. & Malhotra, D. (1994), 'Body mass index in amputees', *Journal of Parenteral and Enteral Nutrition* **18**(4), 355–358.

Uhlrich, S. D., Jackson, R. W., Seth, A., Kolesar, J. A. & Delp, S. L. (2022), 'Muscle coordination retraining inspired by musculoskeletal simulations reduces knee contact force', *Scientific reports* **12**(1), 9842.

Uhlrich, S. D., Uchida, T. K., Lee, M. R. & Delp, S. L. (2023*a*), 'Ten steps to becoming a musculoskeletal simulation expert: a half-century of progress and outlook for the future', *Journal of Biomechanics* **154**, 111623.

Uhlrich, S. D., Uchida, T. K., Lee, M. R. & Delp, S. L. (2023*b*), 'Ten steps to becoming a musculoskeletal simulation expert: a half-century of progress and outlook for the future', *Journal of Biomechanics* **154**, 111623.

Ulrich, B., Pereira, L. C., Jolles, B. M. & Favre, J. (2023), 'Walking with shorter stride length could improve knee kinetics of patients with medial knee osteoarthritis', *Journal of Biomechanics* **147**, 111449.

van den Bogert, A. J., Samorezov, S., Davis, B. L. & Smith, W. A. (2012), 'Modeling and optimal control of an energy-storing prosthetic knee', *Journal of Biomechanical engineering* **134**(5).

van der Kruk, E., Silverman, A. K., Koizia, L., Reilly, P., Fertleman, M. & Bull, A. M. (2021), 'Age-related compensation: Neuromusculoskeletal capacity, reserve & movement objectives', *Journal of Biomechanics* **122**, 110385.

Van Geel, F., Hvid, L. G., Van Noten, P., Eijnde, B. O., Dalgas, U. & Feys, P. (2021), 'Is maximal muscle strength and fatigability of three lower limb muscle groups associated with walking capacity and fatigability in multiple sclerosis? an exploratory study', *Multiple Sclerosis and Related Disorders* **50**, 102841.

van Gelder, L. M., Barnes, A., Wheat, J. S. & Heller, B. W. (2018), 'The use of biofeedback for gait retraining: A mapping review', *Clinical Biomechanics* **59**, 159–166.

Vandenberg, N. W., Stoneback, J. W., Davis-Wilson, H., Christiansen, C. L., Awad, M. E., Melton, D. H. & Gaffney, B. M. (2023), 'Unilateral transfemoral osseointegrated prostheses improve joint loading during walking', *Journal of Biomechanics* p. 111658.

Visser, J., McCarthy, I., Marks, L. & Davis, R. (2011), 'Is hip muscle strength the key to walking as a bilateral amputee, whatever the level of the amputations?', *Prosthetics and Orthotics International* **35**(4), 451–458.

Wakeling, J. M., Febrer-Nafría, M. & De Groote, F. (2023), 'A review of the efforts to develop muscle and musculoskeletal models for biomechanics in the last 50 years', *Journal of Biomechanics* **155**, 111657.

Wang, M. (2014), 'Generalized estimating equations in longitudinal data analysis: a review and recent developments', *Advances in Statistics* **2014**.

Ward, S. R., Eng, C. M., Smallwood, L. H. & Lieber, R. L. (2009), 'Are current measurements of lower extremity muscle architecture accurate?', *Clinical Orthopaedics and Related Research* **467**(4), 1074–1082.

Waterval, N., van der Krogt, M., Veerkamp, K., Geijtenbeek, T., Harlaar, J., Nollet, F. & Brehm, M. (2023), 'The interaction between muscle pathophysiology, body mass, walking speed and ankle foot orthosis stiffness on walking energy cost: a predictive simulation study', *Journal of Neuroengineering and Rehabilitation* **20**(1), 117.

Wei Tech, A. (2023), Investigation of modeling differences between opensim and visual3d for gait analysis of healthy gait, *in* 'Proceedings of the 16th International Convention on Rehabilitation Engineering and Assistive Technology', pp. 42–46.

Wentink, E. C., Prinsen, E. C., Rietman, J. S. & Veltink, P. H. (2013), 'Comparison of muscle activity patterns of transfemoral amputees and control subjects during walking', *Journal of neuroengineering and rehabilitation* **10**(1), 1–11.

West, W., Hicks, A., Clements, L. & Dowling, J. (1995), 'The relationship between voluntary electromyogram, endurance time and intensity of effort in isometric hand-grip exercise', *European journal of applied Physiology and Occupational Physiology* **71**(4), 301–305.

Westerblad, H. & Allen, D. G. (2002), 'Recent advances in the understanding of skeletal muscle fatigue', *Current Opinion in Rheumatology* **14**(6), 648–652.

White, D., Woodard, H. & Hammond, S. (1987), 'Average soft-tissue and bone models for use in radiation dosimetry', *The British Journal of Radiology* **60**(717), 907–913.

Willson, A. M., Anderson, A. J., Richburg, C. A., Muir, B. C., Czerniecki, J., Steele, K. M. & Aubin, P. M. (2022), 'Full body musculoskeletal model for simulations of gait in persons with transtibial amputation', *Computer Methods in Biomechanics and Biomedical Engineering* pp. 1–12.

Winter, D. A. (2009), *Biomechanics and Motor Control of Human Movement*, John wiley & sons. ISBN = 0470398183.

Wong, D. W.-C., Lam, W. K., Yeung, L. & Lee, W. C. (2015), 'Does long-distance walking improve or deteriorate walking stability of transtibial amputees?', *Clinical Biomechanics* **30**(8), 867–873.

World-Health-Organisation (2017), 'Standards for prosthetics and orthotics'.

Wright, D., Marks, L. & Payne, R. (2008), 'A comparative study of the physiological costs of walking in ten bilateral amputees', *Prosthetics and Orthotics International* **32**(1), 57–67.

Wulf, G., McConnel, N., Gärtner, M. & Schwarz, A. (2002), 'Enhancing the learning of sport skills through external-focus feedback', *Journal of motor behavior* **34**(2), 171–182.

Xu, R., Ming, D., Ding, Z. & Bull, A. M. J. R. S. o. s. (2019), 'Extra excitation of biceps femoris during neuromuscular electrical stimulation reduces knee medial loading', *Royal Society Open Science* **6**(3), 181545.

Yamaguchi, G. T. (2005), *Dynamic modeling of musculoskeletal motion: a vectorized approach for biomechanical analysis in three dimensions*, Springer Science & Business Media. ISBN = 0387287043.

Yen, S.-C., Landry, J. M. & Wu, M. (2014), 'Augmented multisensory feedback enhances locomotor adaptation in humans with incomplete spinal cord injury', *Human Movement Science* **35**, 80–93.

Yuan, B., Hu, D., Gu, S., Xiao, S. & Song, F. (2023), 'The global burden of traumatic amputation in 204 countries and territories', *Frontiers in Public Health* **11**, 1258853.

Zajac, F. E. (1989), 'Muscle and tendon: properties, models, scaling, and application to biomechanics and motor control', *Critical Reviews in Biomedical Engineering* **17**(4), 359–411.

Zipp, P. (1982), 'Recommendations for the standardization of lead positions in surface electromyography', *European Journal of Applied Physiology and Occupational Physiology* **50**(1), 41–54.